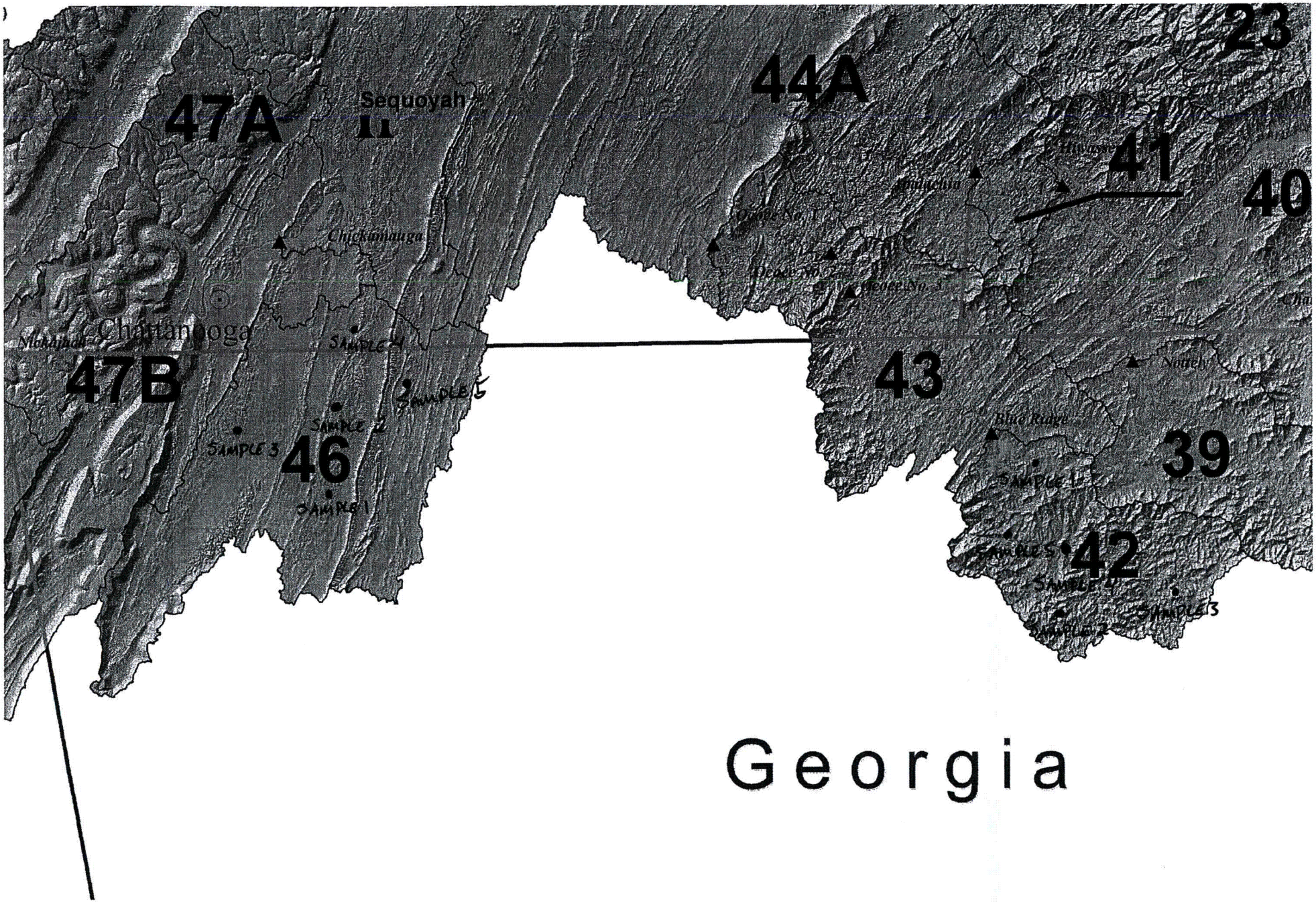
47A
Sequoyah
44A
23
41
40
Chickamauga
Chattanooga
47B
SAMPLE 4
SAMPLE 5
43
Nantahala
SAMPLE 2
SAMPLE 3
46
Blue Ridge
39
SAMPLE 1
SAMPLE 5
42
SAMPLE 3
Georgia

CDQ000020080052 API and Rain Runoff Relationship for TN River Watershed Attachment 12

Hydrologic Soil Group—Catoosa County, Georgia, and Murray and Whitfield Counties, Georgia
(South Chickamauga Sample 1)

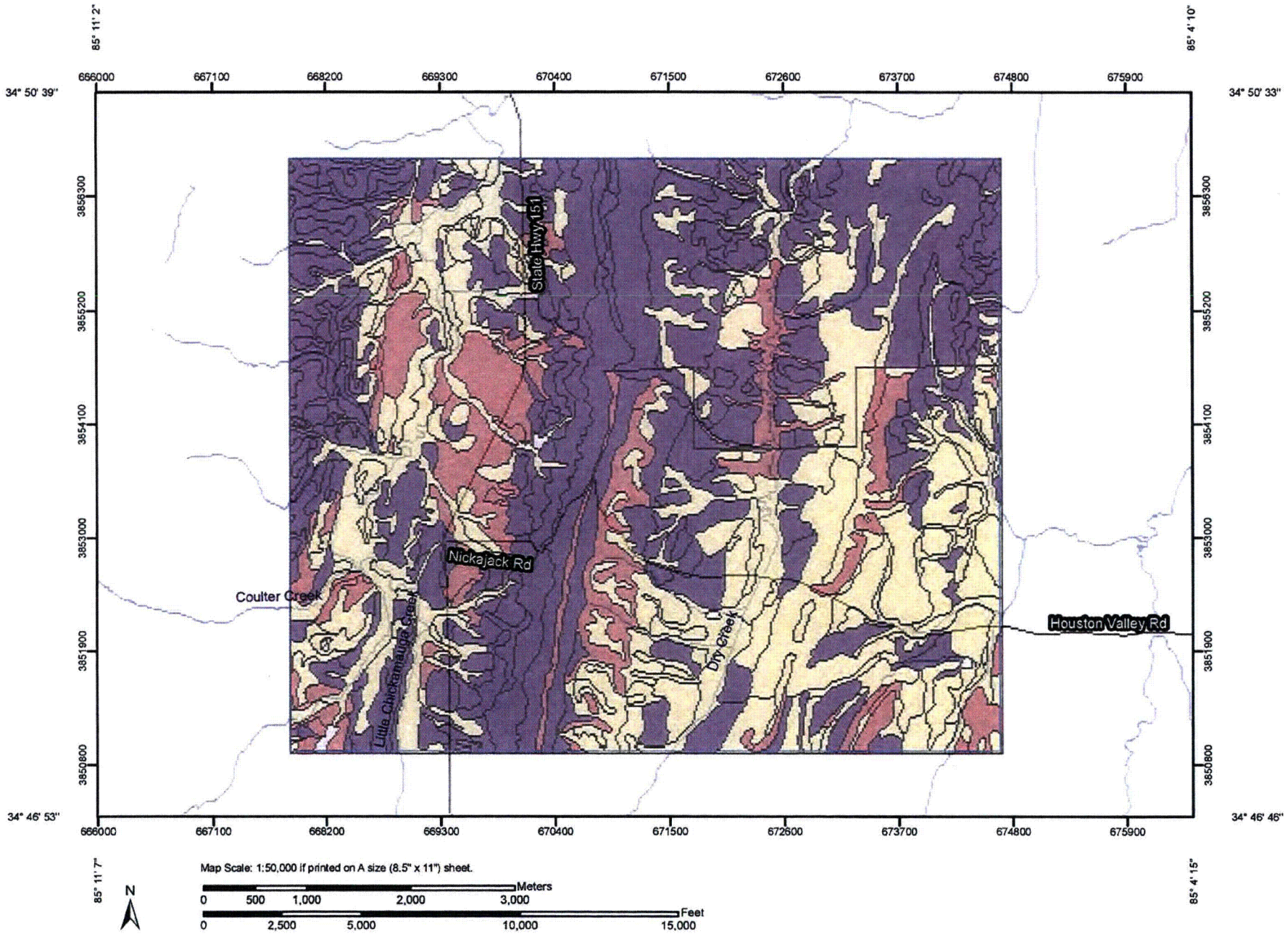

USDA Natural Resources Conservation Service

Web Soil Survey 2.1
National Cooperative Soil Survey

12/19/2008
Page 1 of 7

Hydrologic Soil Group–Catoosa County, Georgia, and Murray and Whitfield Counties, Georgia
(South Chickamauga Sample 1)

MAP LEGEND

Area of Interest (AOI)

- Area of Interest (AOI)

Soils

Soil Ratings

- A
- A/D
- B
- B/D
- C
- C/D
- D
- Not rated or not available

Water Features

- Oceans
- Streams and Canals

Transportation

- Interstate Highways
- US Routes
- Major Roads

MAP INFORMATION

Map Scale: 1:50,000 if printed on A size (8.5" × 11") sheet.

The soil surveys that comprise your AOI were mapped at scales ranging from 1:12,000 to 1:20,000.

Please rely on the bar scale on each map sheet for accurate map measurements.

Source of Map: Natural Resources Conservation Service
Web Soil Survey URL: http://websoilsurvey.nrcs.usda.gov
Coordinate System: UTM Zone 16N NAD83

This product is generated from the USDA-NRCS certified data as of the version date(s) listed below.

Soil Survey Area: Catoosa County, Georgia
Survey Area Data: Version 7, Apr 21, 2008

Soil Survey Area: Murray and Whitfield Counties, Georgia
Survey Area Data: Version 8, Jan 3, 2008

Your area of interest (AOI) includes more than one soil survey area. These survey areas may have been mapped at different scales, with a different land use in mind, at different times, or at different levels of detail. This may result in map unit symbols, soil properties, and interpretations that do not completely agree across soil survey area boundaries.

Hydrologic Soil Group

Hydrologic Soil Group—Summary by Map Unit — Catoosa County, Georgia				
Map unit symbol	Map unit name	Rating	Acres in AOI	Percent of AOI
AnB	Allen silt loam, 2 to 6 percent slopes	B	53.4	0.6%
AnC	Allen silt loam, 6 to 10 percent slopes	B	84.1	0.9%
AnD	Allen silt loam, 10 to 15 percent slopes	B	154.3	1.6%
AnE	Allen silt loam, 15 to 25 percent slopes	B	53.6	0.6%
AoC2	Allen clay loam, 6 to 10 percent slopes, eroded	B	37.7	0.4%
ApB	Apison loam, 2 to 6 percent slopes	B	84.2	0.9%
ApC	Apison loam, 6 to 10 percent slopes	B	200.3	2.1%
ArC	Armuchee channery silt loam, 6 to 10 percent slopes	C	64.2	0.7%
BoE	Bodine cobbly silt loam, 10 to 25 percent slopes, stony	B	3.4	0.0%
Cb	Cedarbluff loam, occasionally flooded	C	279.9	2.9%
Ce	Chenneby silt loam, occasionally flooded	C	423.5	4.4%
CoB	Conasauga silt loam, 1 to 6 percent slopes	C	74.1	0.8%
CoC	Conasauga silt loam, 6 to 10 percent slopes	C	1.7	0.0%
CuB	Cunningham silt loam, 2 to 6 percent slopes	C	32.6	0.3%
CuC	Cunningham silt loam, 6 to 10 percent slopes	C	37.9	0.4%
CuD	Cunningham silt loam, 10 to 15 percent slopes	C	64.9	0.7%
CxD2	Cunningham silty clay loam, 6 to 15 percent slopes, eroded	C	0.2	0.0%
DaB	Decatur silt loam, 2 to 6 percent slopes	B	38.5	0.4%
DaC	Decatur silt loam, 6 to 10 percent slopes	B	11.9	0.1%
DcD2	Decatur silty clay loam, 10 to 15 percent slopes, eroded	B	12.4	0.1%
DeC	Dewey silt loam, 6 to 10 percent slopes	B	7.3	0.1%
Em	Emory silt loam	B	13.6	0.1%
Es	Ennis gravelly silt loam, 0 to 3 percent slopes, occasionally flooded	B	105.1	1.1%
EtB	Etowah loam, 2 to 6 percent slopes	B	129.6	1.3%
EtC	Etowah loam, 6 to 10 percent slopes	B	19.0	0.2%
FeB	Fullerton gravelly silt loam, 2 to 6 percent slopes	B	2.5	0.0%
FeC	Fullerton gravelly silt loam, 6 to 10 percent slopes	B	69.0	0.7%

Hydrologic Soil Group—Summary by Map Unit — Catoosa County, Georgia				
Map unit symbol	Map unit name	Rating	Acres in AOI	Percent of AOI
FeD	Fullerton gravelly silt loam, 10 to 15 percent slopes	B	31.7	0.3%
FeE	Fullerton gravelly silt loam, 15 to 40 percent slopes	B	8.2	0.1%
FrE2	Fullerton gravelly silty clay loam, 10 to 25 percent slopes, eroded	B	37.7	0.4%
HoB	Holston fine sandy loam, 2 to 6 percent slopes	B	111.7	1.2%
HoC	Holston fine sandy loam, 6 to 10 percent slopes	B	82.2	0.9%
LeB	Lyerly silty clay loam, 2 to 6 percent slopes	D	439.0	4.6%
LeC	Lyerly silty clay loam, 6 to 10 pecent slopes	D	64.2	0.7%
LrC	Lyerly-Rock outcrop complex, 2 to 10 percent slopes	D	71.8	0.7%
MsC	Minvale-Shack gravelly silt loams, 6 to 10 percent slopes	B	155.3	1.6%
MsD	Minvale-Shack gravelly silt loams, 10 to 15 percent slopes	B	190.5	2.0%
MsE	Minvale-Shack gravelly silt loams, 15 to 25 percent slopes	B	43.2	0.4%
NaD	Nauvoo fine sandy loam, 10 to 15 percent slopes	B	28.6	0.3%
NaE	Nauvoo fine sandy loam, 15 to 35 percent slopes	B	183.0	1.9%
NeF	Nella stony fine sandy loam, 25 to 45 percent slopes, very stony	B	300.7	3.1%
RoA	Rome silt loam, 0 to 2 percent slopes, occasionally flooded	B	22.7	0.2%
RoB	Rome silt loam, 2 to 6 percent slopes	B	269.2	2.8%
SmB	Shack-Minvale gravelly silt loams, 2 to 6 percent slopes	B	39.4	0.4%
TaB	Talbott silt loam, 2 to 6 percent slopes	C	57.6	0.6%
TaC	Talbott silt loam, 6 to 10 percent slopes	C	72.4	0.8%
TbC2	Talbott silty clay loam, 6 to 10 percent slopes, eroded	C	83.3	0.9%
TbD2	Talbott silty clay loam, 10 to 15 percent slopes, eroded	C	108.0	1.1%
TgG	Tidings-Gorgas complex, 45 to 70 percent slopes	B	244.1	2.5%
TmD	Tidings-Townley complex, 10 to 25 percent slopes	B	173.5	1.8%
TmF	Tidings-Townley complex, 25 to 45 percent slopes	B	604.7	6.3%
TnC	Townley silt loam, 2 to 10 percent slopes	C	92.0	1.0%

Hydrologic Soil Group—Summary by Map Unit — Catoosa County, Georgia				
Map unit symbol	Map unit name	Rating	Acres in AOI	Percent of AOI
TnE	Townley silt loam, 10 to 25 percent slopes	C	166.6	1.7%
ToC2	Townley silty clay loam, 2 to 10 percent slopes, eroded	C	23.5	0.2%
ToE2	Townley silty clay loam, 10 to 25 percent slopes, eroded	C	0.2	0.0%
TpA	Tupelo silt loam, 0 to 2 percent slopes, rarely flooded	D	36.4	0.4%
TuA	Tupelo silt loam, 0 to 2 percent slopes, frequently flooded	D	116.5	1.2%
UpF	Udorthents-Pits complex, gently sloping to steep		0.3	0.0%
W	Water		20.1	0.2%
WaA	Wax loam, 0 to 2 percent slopes, occasionally flooded	C	151.0	1.6%
WaB	Wax loam, 2 to 6 percent slopes, rarely flooded	C	15.2	0.2%
WhA	Whitwell loam, 1 to 3 percent slopes, occasionally flooded	C	53.5	0.6%
Subtotals for Soil Survey Area			**6,156.6**	**63.8%**
Totals for Area of Interest			**9,646.6**	**100.0%**

Hydrologic Soil Group—Summary by Map Unit — Murray and Whitfield Counties, Georgia				
Map unit symbol	Map unit name	Rating	Acres in AOI	Percent of AOI
AbB	Albertville silt loam, 2 to 6 percent slopes	C	78.5	0.8%
AbD	Albertville silt loam, 6 to 15 percent slopes	C	51.8	0.5%
AnB	Allen loam, 2 to 6 percent slopes	B	73.8	0.8%
AnD	Allen loam, 6 to 15 percent slopes	B	121.2	1.3%
AnE	Allen loam, 15 to 30 percent slopes	B	26.2	0.3%
AuA	Arkabutla silt loam, 0 to 2 percent slopes, occasionally flooded	C	64.5	0.7%
CaA	Capshaw silt loam, 0 to 2 percent slopes	C	41.8	0.4%
CaB	Capshaw silt loam, 2 to 6 percent slopes	C	8.0	0.1%
CnA	Chenneby silt loam, 0 to 2 percent slopes, occasionally flooded	C	267.7	2.8%
CsC	Conasauga silt loam, 6 to 10 percent slopes	C	3.2	0.0%
CxB	Cunningham silt loam, 2 to 6 percent slopes	C	2.2	0.0%
CxD	Cunningham silt loam, 6 to 15 percent slopes	C	394.9	4.1%
CxE	Cunningham silt loam, 15 to 30 percent slopes	C	53.4	0.6%
CxF	Cunningham silt loam, 30 to 60 percent slopes	C	360.9	3.7%

Hydrologic Soil Group—Summary by Map Unit — Murray and Whitfield Counties, Georgia				
Map unit symbol	Map unit name	Rating	Acres in AOI	Percent of AOI
DoA	Docena silt loam, 0 to 2 percent slopes, occasionally flooded	C	15.7	0.2%
DsB	Docena-Conasauga complex, 2 to 6 percent slopes	C	110.3	1.1%
EnD	Enders silt loam, 6 to 15 percent slopes	C	82.1	0.9%
HrF	Hector-Townley-Rock outcrop complex, 5 to 35 percent slopes	D	56.3	0.6%
HsB	Holston fine sandy loam, 2 to 6 percent slopes	B	146.9	1.5%
HsD	Holston fine sandy loam, 6 to 15 percent slopes	B	62.7	0.7%
KtA	Ketona silt loam, 0 to 2 percent slopes, frequently flooded	D	27.7	0.3%
MoF	Montevallo very channery loam, 30 to 60 percent slopes	D	169.9	1.8%
MtD	Montevallo-Townley complex, 6 to 15 percent slopes	D	18.8	0.2%
MtE	Montevallo-Townley complex, 15 to 30 percent slopes	D	220.0	2.3%
NaD	Nauvoo fine sandy loam, 6 to 15 percent slopes	B	48.3	0.5%
NaE	Nauvoo fine sandy loam, 15 to 35 percent slopes	B	72.6	0.8%
NeF	Nella gravelly fine sandy loam, 30 to 60 percent slopes	B	143.8	1.5%
SaA	Sequatchie loam, 0 to 2 percent slopes, occasionally flooded	B	7.9	0.1%
SaB	Sequatchie loam, 2 to 6 percent slopes	B	11.9	0.1%
SpD	Sipsey fine sandy loam, 4 to 15 percent slopes	B	144.5	1.5%
SpE	Sipsey fine sandy loam, 15 to 30 percent slopes	B	75.2	0.8%
TnB	Townley silt loam, 2 to 6 percent slopes	C	11.4	0.1%
TnD	Townley silt loam, 6 to 15 percent slopes	C	265.6	2.8%
TnE	Townley silt loam, 15 to 30 percent slopes	C	115.0	1.2%
TnF	Townley silt loam, 30 to 45 percent slopes	C	73.8	0.8%
W	Water		4.2	0.0%
WaA	Wax fine sandy loam, 0 to 2 percent slopes, occasionally flooded	C	6.2	0.1%
WtA	Whitwell silt loam, 0 to 2 percent slopes, occasionally flooded	C	28.3	0.3%
WtB	Whitwell silt loam, 2 to 6 percent slopes	C	22.3	0.2%
Subtotals for Soil Survey Area			3,490.0	36.2%
Totals for Area of Interest			9,646.6	100.0%

Description

Hydrologic soil groups are based on estimates of runoff potential. Soils are assigned to one of four groups according to the rate of water infiltration when the soils are not protected by vegetation, are thoroughly wet, and receive precipitation from long-duration storms.

The soils in the United States are assigned to four groups (A, B, C, and D) and three dual classes (A/D, B/D, and C/D). The groups are defined as follows:

Group A. Soils having a high infiltration rate (low runoff potential) when thoroughly wet. These consist mainly of deep, well drained to excessively drained sands or gravelly sands. These soils have a high rate of water transmission.

Group B. Soils having a moderate infiltration rate when thoroughly wet. These consist chiefly of moderately deep or deep, moderately well drained or well drained soils that have moderately fine texture to moderately coarse texture. These soils have a moderate rate of water transmission.

Group C. Soils having a slow infiltration rate when thoroughly wet. These consist chiefly of soils having a layer that impedes the downward movement of water or soils of moderately fine texture or fine texture. These soils have a slow rate of water transmission.

Group D. Soils having a very slow infiltration rate (high runoff potential) when thoroughly wet. These consist chiefly of clays that have a high shrink-swell potential, soils that have a high water table, soils that have a claypan or clay layer at or near the surface, and soils that are shallow over nearly impervious material. These soils have a very slow rate of water transmission.

If a soil is assigned to a dual hydrologic group (A/D, B/D, or C/D), the first letter is for drained areas and the second is for undrained areas. Only the soils that in their natural condition are in group D are assigned to dual classes.

Rating Options

Aggregation Method: Dominant Condition

Component Percent Cutoff: None Specified

Tie-break Rule: Lower

CDQ000020080052 API and Rain Runoff Relationship for TN River Watershed Attachment 12

Hydrologic Soil Group—Catoosa County, Georgia
(South Chickamauga Sample 2)

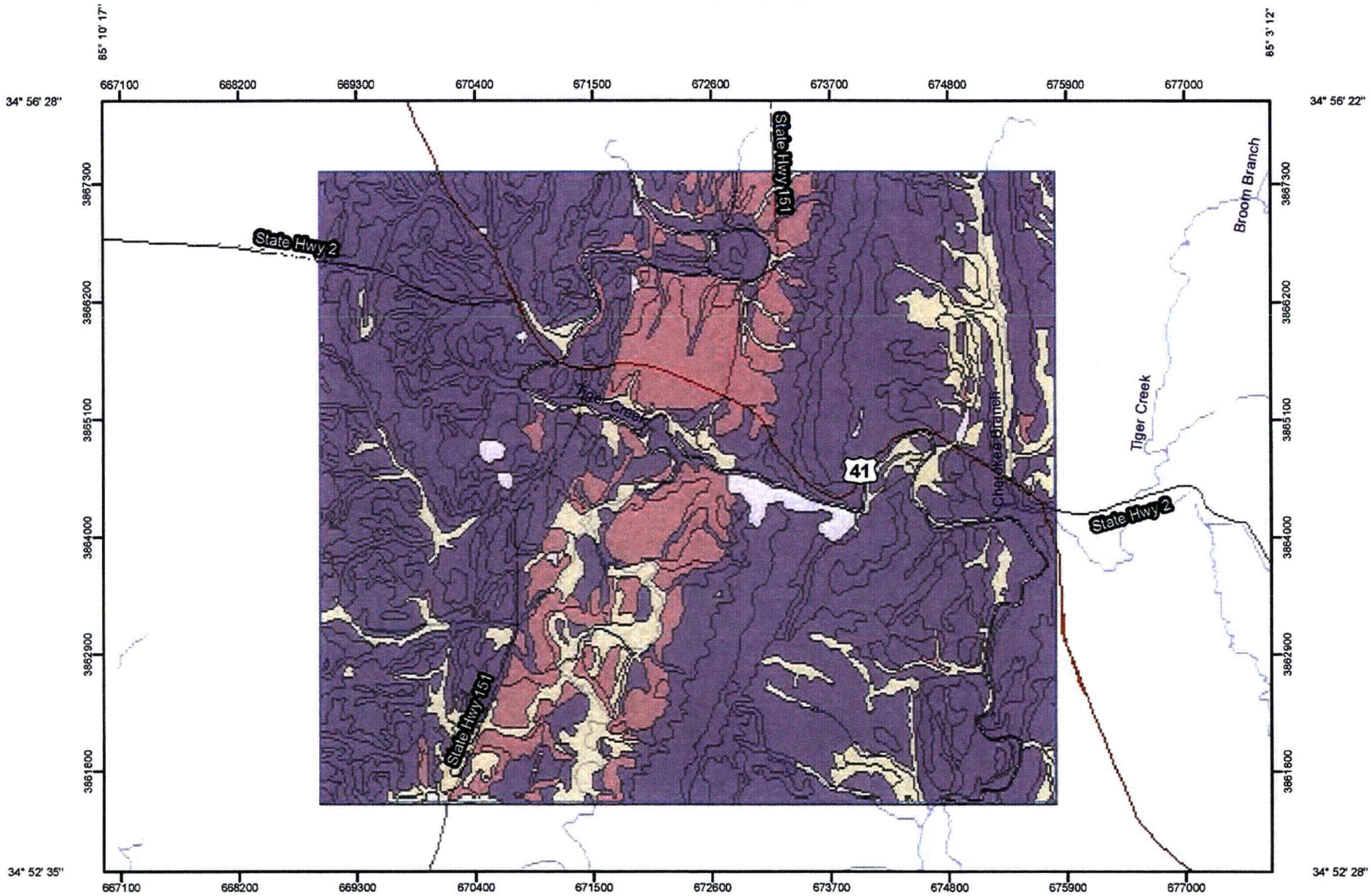

Hydrologic Soil Group–Catoosa County, Georgia
(South Chickamauga Sample 2)

MAP LEGEND

Area of Interest (AOI)

- Area of Interest (AOI)

Soils

Soil Ratings

- A
- A/D
- B
- B/D
- C
- C/D
- D
- Not rated or not available

Water Features

- Oceans
- Streams and Canals

Transportation

- Interstate Highways
- US Routes
- Major Roads

MAP INFORMATION

Map Scale: 1:51,500 if printed on A size (8.5" × 11") sheet.

The soil surveys that comprise your AOI were mapped at 1:20,000.

Please rely on the bar scale on each map sheet for accurate map measurements.

Source of Map: Natural Resources Conservation Service
Web Soil Survey URL: http://websoilsurvey.nrcs.usda.gov
Coordinate System: UTM Zone 16N NAD83

This product is generated from the USDA-NRCS certified data as of the version date(s) listed below.

Soil Survey Area: Catoosa County, Georgia
Survey Area Data: Version 7, Apr 21, 2008

Hydrologic Soil Group

Hydrologic Soil Group—Summary by Map Unit — Catoosa County, Georgia				
Map unit symbol	Map unit name	Rating	Acres in AOI	Percent of AOI
AnB	Allen silt loam, 2 to 6 percent slopes	B	53.7	0.5%
AnC	Allen silt loam, 6 to 10 percent slopes	B	77.5	0.8%
AnD	Allen silt loam, 10 to 15 percent slopes	B	115.0	1.2%
AnE	Allen silt loam, 15 to 25 percent slopes	B	34.5	0.3%
ApC	Apison loam, 6 to 10 percent slopes	B	38.4	0.4%
BoE	Bodine cobbly silt loam, 10 to 25 percent slopes, stony	B	17.2	0.2%
BoF	Bodine cobbly silt loam, 25 to 60 percent slopes, stony	B	115.5	1.2%
Cb	Cedarbluff loam, occasionally flooded	C	146.1	1.5%
Ce	Chenneby silt loam, occasionally flooded	C	588.4	5.9%
CuB	Cunningham silt loam, 2 to 6 percent slopes	C	13.9	0.1%
CuC	Cunningham silt loam, 6 to 10 percent slopes	C	80.6	0.8%
CuD	Cunningham silt loam, 10 to 15 percent slopes	C	83.4	0.8%
CxD2	Cunningham silty clay loam, 6 to 15 percent slopes, eroded	C	12.4	0.1%
DaB	Decatur silt loam, 2 to 6 percent slopes	B	118.4	1.2%
DaC	Decatur silt loam, 6 to 10 percent slopes	B	67.7	0.7%
DcC2	Decatur silty clay loam, 6 to 10 percent slopes, eroded	B	15.0	0.2%
DcD2	Decatur silty clay loam, 10 to 15 percent slopes, eroded	B	59.7	0.6%
DeB	Dewey silt loam, 2 to 6 percent slopes	B	19.0	0.2%
Em	Emory silt loam	B	24.8	0.2%
Es	Ennis gravelly silt loam, 0 to 3 percent slopes, occasionally flooded	B	392.8	4.0%
EtB	Etowah loam, 2 to 6 percent slopes	B	177.8	1.8%
EtC	Etowah loam, 6 to 10 percent slopes	B	32.3	0.3%
FeB	Fullerton gravelly silt loam, 2 to 6 percent slopes	B	24.5	0.2%
FeC	Fullerton gravelly silt loam, 6 to 10 percent slopes	B	140.9	1.4%
FeD	Fullerton gravelly silt loam, 10 to 15 percent slopes	B	33.6	0.3%
FeE	Fullerton gravelly silt loam, 15 to 40 percent slopes	B	51.3	0.5%

Hydrologic Soil Group— Summary by Map Unit — Catoosa County, Georgia				
Map unit symbol	Map unit name	Rating	Acres in AOI	Percent of AOI
FrE2	Fullerton gravelly silty clay loam, 10 to 25 percent slopes, eroded	B	119.5	1.2%
HoB	Holston fine sandy loam, 2 to 6 percent slopes	B	101.2	1.0%
HoC	Holston fine sandy loam, 6 to 10 percent slopes	B	41.5	0.4%
Ke	Ketona silty clay loam, frequently flooded	D	21.7	0.2%
LeB	Lyerly silty clay loam, 2 to 6 percent slopes	D	403.2	4.1%
LeC	Lyerly silty clay loam, 6 to 10 pecent slopes	D	123.6	1.2%
LrC	Lyerly-Rock outcrop complex, 2 to 10 percent slopes	D	420.8	4.2%
LuC	Lyerly-Urban land complex, 2 to 10 percent slopes	D	283.5	2.9%
MsC	Minvale-Shack gravelly silt loams, 6 to 10 percent slopes	B	767.7	7.7%
MsD	Minvale-Shack gravelly silt loams, 10 to 15 percent slopes	B	735.4	7.4%
MsE	Minvale-Shack gravelly silt loams, 15 to 25 percent slopes	B	572.6	5.8%
NaD	Nauvoo fine sandy loam, 10 to 15 percent slopes	B	63.1	0.6%
NaE	Nauvoo fine sandy loam, 15 to 35 percent slopes	B	261.3	2.6%
NeF	Nella stony fine sandy loam, 25 to 45 percent slopes, very stony	B	277.7	2.8%
RoA	Rome silt loam, 0 to 2 percent slopes, occasionally flooded	B	454.8	4.6%
RoB	Rome silt loam, 2 to 6 percent slopes	B	338.9	3.4%
SmB	Shack-Minvale gravelly silt loams, 2 to 6 percent slopes	B	111.6	1.1%
TaB	Talbott silt loam, 2 to 6 percent slopes	C	12.8	0.1%
TaC	Talbott silt loam, 6 to 10 percent slopes	C	56.0	0.6%
TbC2	Talbott silty clay loam, 6 to 10 percent slopes, eroded	C	10.0	0.1%
TbD2	Talbott silty clay loam, 10 to 15 percent slopes, eroded	C	27.4	0.3%
TgG	Tidings-Gorgas complex, 45 to 70 percent slopes	B	323.3	3.3%
TmD	Tidings-Townley complex, 10 to 25 percent slopes	B	638.0	6.4%
TmF	Tidings-Townley complex, 25 to 45 percent slopes	B	838.6	8.4%
TnC	Townley silt loam, 2 to 10 percent slopes	C	8.3	0.1%
TnE	Townley silt loam, 10 to 25 percent slopes	C	57.4	0.6%

Hydrologic Soil Group— Summary by Map Unit — Catoosa County, Georgia				
Map unit symbol	Map unit name	Rating	Acres in AOI	Percent of AOI
ToC2	Townley silty clay loam, 2 to 10 percent slopes, eroded	C	0.6	0.0%
TpA	Tupelo silt loam, 0 to 2 percent slopes, rarely flooded	D	16.4	0.2%
TuA	Tupelo silt loam, 0 to 2 percent slopes, frequently flooded	D	4.3	0.0%
UpF	Udorthents-Pits complex, gently sloping to steep		95.1	1.0%
W	Water		117.0	1.2%
WaA	Wax loam, 0 to 2 percent slopes, occasionally flooded	C	8.8	0.1%
WaB	Wax loam, 2 to 6 percent slopes, rarely flooded	C	5.7	0.1%
WhA	Whitwell loam, 1 to 3 percent slopes, occasionally flooded	C	90.7	0.9%
Totals for Area of Interest			9,943.0	100.0%

Rating Options

Aggregation Method: Dominant Condition

Component Percent Cutoff: None Specified

Tie-break Rule: Lower

Hydrologic Soil Group—Catoosa County, Georgia
(South Chickamauga Sample 3)

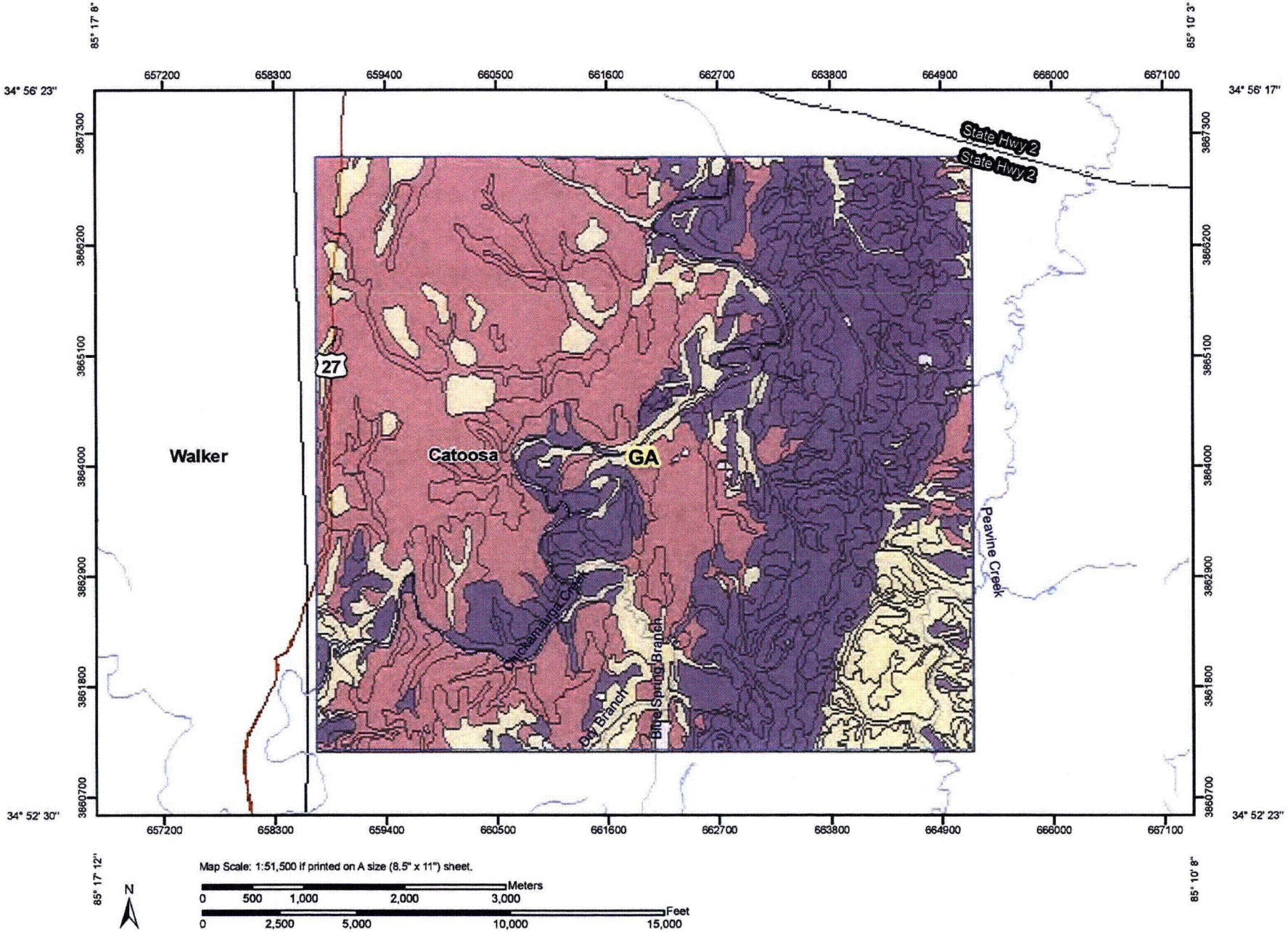

USDA Natural Resources Conservation Service

Web Soil Survey 2.1
National Cooperative Soil Survey

12/19/2008
Page 1 of 5

Hydrologic Soil Group–Catoosa County, Georgia
(South Chickamauga Sample 3)

MAP LEGEND

Area of Interest (AOI)

- Area of Interest (AOI)

Soils

Soil Ratings

- A
- A/D
- B
- B/D
- C
- C/D
- D
- Not rated or not available

Political Features

- States
- Counties

Water Features

- Oceans
- Streams and Canals

Transportation

- Interstate Highways
- US Routes
- Major Roads

MAP INFORMATION

Map Scale: 1:51,500 if printed on A size (8.5" × 11") sheet.

The soil surveys that comprise your AOI were mapped at 1:20,000.

Please rely on the bar scale on each map sheet for accurate map measurements.

Source of Map: Natural Resources Conservation Service
Web Soil Survey URL: http://websoilsurvey.nrcs.usda.gov
Coordinate System: UTM Zone 16N NAD83

This product is generated from the USDA-NRCS certified data as of the version date(s) listed below.

Soil Survey Area: Catoosa County, Georgia
Survey Area Data: Version 7, Apr 21, 2008

Hydrologic Soil Group

Hydrologic Soil Group—Summary by Map Unit—Catoosa County, Georgia				
Map unit symbol	Map unit name	Rating	Acres in AOI	Percent of AOI
BoF	Bodine cobbly silt loam, 25 to 60 percent slopes, stony	B	63.3	0.7%
CaB	Capshaw silt loam, 2 to 6 percent slopes	C	137.7	1.5%
Cb	Cedarbluff loam, occasionally flooded	C	172.6	1.8%
Ce	Chenneby silt loam, occasionally flooded	C	450.6	4.8%
CoB	Conasauga silt loam, 1 to 6 percent slopes	C	98.9	1.0%
CoC	Conasauga silt loam, 6 to 10 percent slopes	C	141.4	1.5%
CuB	Cunningham silt loam, 2 to 6 percent slopes	C	49.8	0.5%
CxD2	Cunningham silty clay loam, 6 to 15 percent slopes, eroded	C	27.0	0.3%
DaB	Decatur silt loam, 2 to 6 percent slopes	B	22.6	0.2%
DcD2	Decatur silty clay loam, 10 to 15 percent slopes, eroded	B	13.4	0.1%
DeB	Dewey silt loam, 2 to 6 percent slopes	B	50.3	0.5%
DeC	Dewey silt loam, 6 to 10 percent slopes	B	50.1	0.5%
Em	Emory silt loam	B	10.0	0.1%
Es	Ennis gravelly silt loam, 0 to 3 percent slopes, occasionally flooded	B	177.0	1.9%
EtB	Etowah loam, 2 to 6 percent slopes	B	212.6	2.3%
EtC	Etowah loam, 6 to 10 percent slopes	B	95.4	1.0%
FeB	Fullerton gravelly silt loam, 2 to 6 percent slopes	B	15.9	0.2%
FeC	Fullerton gravelly silt loam, 6 to 10 percent slopes	B	87.6	0.9%
FeD	Fullerton gravelly silt loam, 10 to 15 percent slopes	B	122.3	1.3%
FeE	Fullerton gravelly silt loam, 15 to 40 percent slopes	B	92.1	1.0%
FrE2	Fullerton gravelly silty clay loam, 10 to 25 percent slopes, eroded	B	12.9	0.1%
HoB	Holston fine sandy loam, 2 to 6 percent slopes	B	30.1	0.3%
HoC	Holston fine sandy loam, 6 to 10 percent slopes	B	3.4	0.0%
Ke	Ketona silty clay loam, frequently flooded	D	41.2	0.4%
LeB	Lyerly silty clay loam, 2 to 6 percent slopes	D	2,614.2	27.7%

Hydrologic Soil Group—Summary by Map Unit — Catoosa County, Georgia				
Map unit symbol	Map unit name	Rating	Acres in AOI	Percent of AOI
LeC	Lyerly silty clay loam, 6 to 10 pecent slopes	D	556.7	5.9%
LrC	Lyerly-Rock outcrop complex, 2 to 10 percent slopes	D	469.7	5.0%
MsC	Minvale-Shack gravelly silt loams, 6 to 10 percent slopes	B	438.7	4.6%
MsD	Minvale-Shack gravelly silt loams, 10 to 15 percent slopes	B	379.1	4.0%
MsE	Minvale-Shack gravelly silt loams, 15 to 25 percent slopes	B	725.2	7.7%
RoA	Rome silt loam, 0 to 2 percent slopes, occasionally flooded	B	383.9	4.1%
RoB	Rome silt loam, 2 to 6 percent slopes	B	378.8	4.0%
SmB	Shack-Minvale gravelly silt loams, 2 to 6 percent slopes	B	79.7	0.8%
TaB	Talbott silt loam, 2 to 6 percent slopes	C	215.5	2.3%
TaC	Talbott silt loam, 6 to 10 percent slopes	C	128.1	1.4%
TbC2	Talbott silty clay loam, 6 to 10 percent slopes, eroded	C	37.5	0.4%
TbD2	Talbott silty clay loam, 10 to 15 percent slopes, eroded	C	15.2	0.2%
TnC	Townley silt loam, 2 to 10 percent slopes	C	40.9	0.4%
TnE	Townley silt loam, 10 to 25 percent slopes	C	2.5	0.0%
ToC2	Townley silty clay loam, 2 to 10 percent slopes, eroded	C	22.4	0.2%
ToE2	Townley silty clay loam, 10 to 25 percent slopes, eroded	C	134.6	1.4%
TpA	Tupelo silt loam, 0 to 2 percent slopes, rarely flooded	D	304.0	3.2%
TuA	Tupelo silt loam, 0 to 2 percent slopes, frequently flooded	D	119.9	1.3%
UpF	Udorthents-Pits complex, gently sloping to steep		3.4	0.0%
W	Water		110.5	1.2%
WaA	Wax loam, 0 to 2 percent slopes, occasionally flooded	C	47.7	0.5%
WaB	Wax loam, 2 to 6 percent slopes, rarely flooded	C	33.4	0.4%
WhA	Whitwell loam, 1 to 3 percent slopes, occasionally flooded	C	18.8	0.2%
Totals for Area of Interest			9,438.9	100.0%

Rating Options

Aggregation Method: Dominant Condition

Component Percent Cutoff: None Specified

Tie-break Rule: Lower

Hydrologic Soil Group—Hamilton County, Tennessee
(South Chickamauga Sample 4)

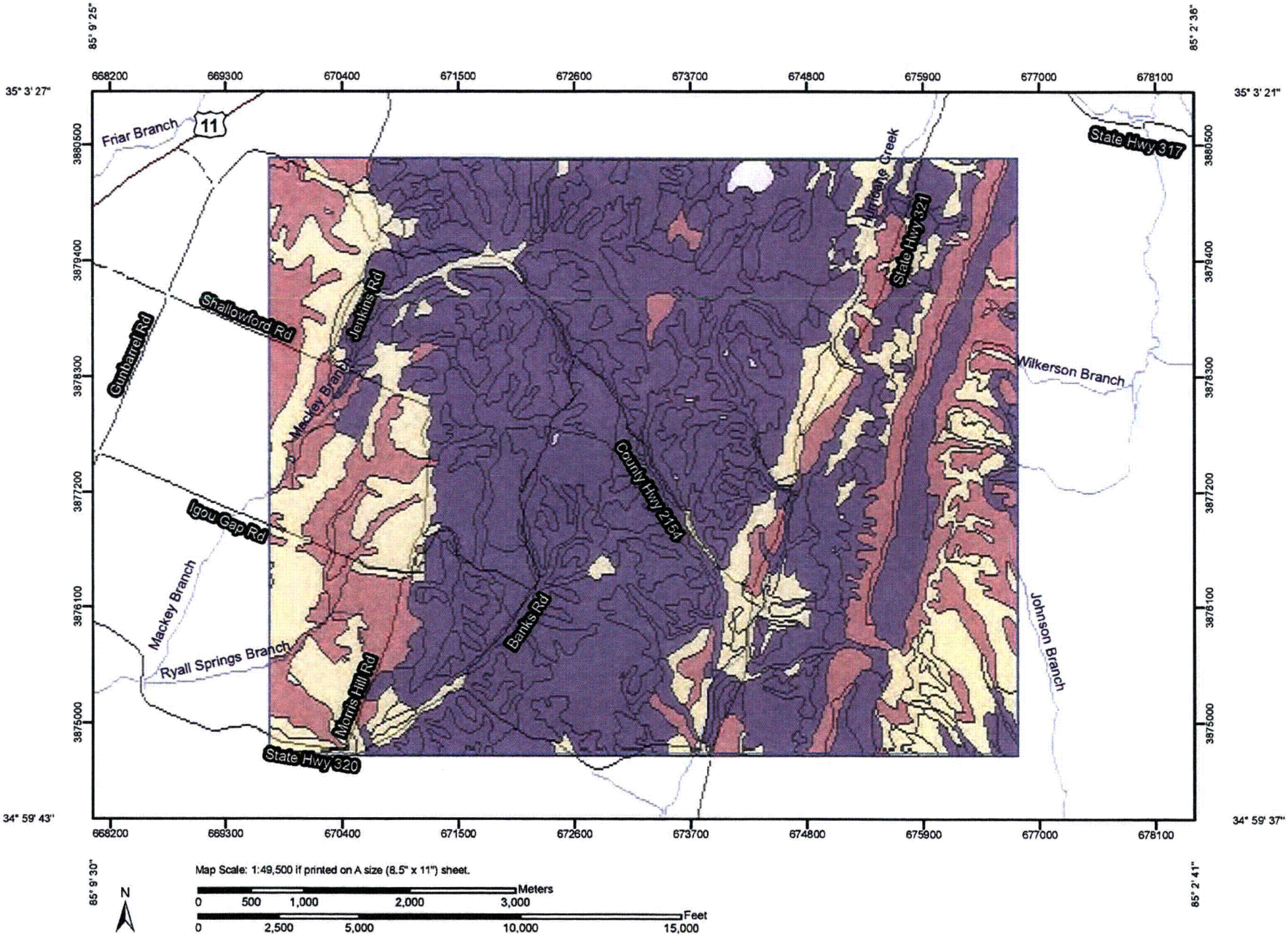

USDA Natural Resources Conservation Service

Web Soil Survey 2.1
National Cooperative Soil Survey

12/19/2008
Page 1 of 5

Hydrologic Soil Group–Hamilton County, Tennessee
(South Chickamauga Sample 4)

MAP LEGEND

Area of Interest (AOI)

- Area of Interest (AOI)

Soils

Soil Ratings

- A
- A/D
- B
- B/D
- C
- C/D
- D
- Not rated or not available

Water Features

- Oceans
- Streams and Canals

Transportation

- Interstate Highways
- US Routes
- Major Roads

MAP INFORMATION

Map Scale: 1:49,500 if printed on A size (8.5" × 11") sheet.

The soil surveys that comprise your AOI were mapped at 1:15,840.

Please rely on the bar scale on each map sheet for accurate map measurements.

Source of Map: Natural Resources Conservation Service
Web Soil Survey URL: http://websoilsurvey.nrcs.usda.gov
Coordinate System: UTM Zone 16N NAD83

This product is generated from the USDA-NRCS certified data as of the version date(s) listed below.

Soil Survey Area: Hamilton County, Tennessee
Survey Area Data: Version 6, Sep 25, 2008

Hydrologic Soil Group

Hydrologic Soil Group— Summary by Map Unit — Hamilton County, Tennessee				
Map unit symbol	Map unit name	Rating	Acres in AOI	Percent of AOI
AeC	Allen loam, 3 to 12 percent slopes	B	53.0	0.5%
AeD	Allen loam, 12 to 25 percent slopes	B	132.2	1.3%
AeE	Allen loam, 25 to 40 percent slopes	B	72.7	0.7%
ArB	Arents		27.0	0.3%
AuD	Armuchee silt loam, 10 to 25 percent slopes	C	297.6	3.0%
AuE	Armuchee silt loam, 25 to 40 percent slopes	C	155.0	1.6%
BoC	Bodine cherty silt loam, 5 to 12 percent slopes	B	1,425.0	14.4%
BoD	Bodine cherty silt loam, 12 to 25 percent slopes	B	111.3	1.1%
BoE	Bodine cherty silt loam, 25 to 45 percent slopes	B	1,045.2	10.6%
BuF	Bouldin-Gilpin complex, 20 to 60 percent slopes	B	17.6	0.2%
CaB	Capshaw silt loam, 2 to 6 percent slopes	C	237.7	2.4%
CbC	Colbert silt loam, 2 to 12 percent slopes	D	788.2	8.0%
CcD	Colbert-Rock outcrop complex, 5 to 20 percent slopes	D	1.2	0.0%
CoC	Collegedale silt loam, 2 to 12 percent slopes	C	81.4	0.8%
CoD	Collegedale silt loam, 12 to 25 percent slopes	C	39.0	0.4%
DeB	Dewey silt loam, 2 to 6 percent slopes	B	156.2	1.6%
DeD	Dewey silt loam, 12 to 25 percent slopes	B	127.8	1.3%
Ec	Emory silt loam	B	2.4	0.0%
EdC	Enders silt loam, 2 to 12 percent slopes	C	59.3	0.6%
EeD	Enders silty clay loam, 12 to 25 percent slopes, eroded	C	24.9	0.3%
En	Ennis cherty silt loam	B	186.5	1.9%
EtB	Etowah silt loam, 2 to 5 percent slopes	B	413.3	4.2%
EtD	Etowah silt loam, 12 to 20 percent slopes	B	9.5	0.1%
FuB	Fullerton cherty silt loam, 3 to 7 percent slopes	B	723.7	7.3%

Hydrologic Soil Group—Summary by Map Unit — Hamilton County, Tennessee				
Map unit symbol	Map unit name	Rating	Acres in AOI	Percent of AOI
FuD	Fullerton cherty silt loam, 12 to 25 percent slopes	B	674.5	6.8%
FuE	Fullerton cherty silt loam, 25 to 40 percent slopes	B	325.8	3.3%
Gu	Guthrie silt loam	D	34.6	0.4%
Ha	Hamblen silt loam	C	39.5	0.4%
HcD	Hanceville loam, 12 to 25 percent slopes	B	20.5	0.2%
HcE	Hanceville loam, 25 to 40 percent slopes	B	313.5	3.2%
HuB	Humphreys cherty silt loam, 1 to 6 percent slopes	B	0.0	0.0%
Lo	Lobelville cherty silt loam	C	21.7	0.2%
MnB	Minvale cherty silt loam, 3 to 12 percent slopes	B	98.5	1.0%
MoE	Montevallo shaly silt loam, 20 to 45 percent slopes	D	657.0	6.6%
NsB	Nesbitt silt loam, 2 to 6 percent slopes	B	7.4	0.1%
RaD	Ramsey loam, 8 to 25 percent slopes	D	10.5	0.1%
RcF	Ramsey-Rock outcrop complex, 15 to 70 percent slopes	D	63.8	0.6%
RoB	Roane cherty silt loam, 2 to 6 percent slopes	C	176.7	1.8%
SeB	Sequatchie loam, 2 to 7 percent slopes	B	35.9	0.4%
St	Staser loam	B	33.0	0.3%
TaC	Talbott silt loam, 2 to 12 percent slopes	C	866.8	8.8%
TaD	Talbott silt loam, 12 to 25 percent slopes	C	47.3	0.5%
TrD	Talbott-Rock outcrop complex, 5 to 25 percent slopes	C	24.5	0.2%
Tu	Tupelo silt loam, 0 to 3 percent slopes	D	183.9	1.9%
W	NRI 1982 water		16.6	0.2%
WaB	Waynesboro loam, 3 to 8 percent slopes	B	28.3	0.3%
WaD	Waynesboro loam, 12 to 25 percent slopes	B	1.7	0.0%
Wh	Whitwell loam	C	11.5	0.1%
Wo	Woodmont silt loam	C	4.9	0.0%
Totals for Area of Interest			9,686.2	100.0%

Rating Options

Aggregation Method: Dominant Condition

Component Percent Cutoff: None Specified

Tie-break Rule: Lower

Hydrologic Soil Group—Catoosa County, Georgia
(South Chickamauga Sample 5)

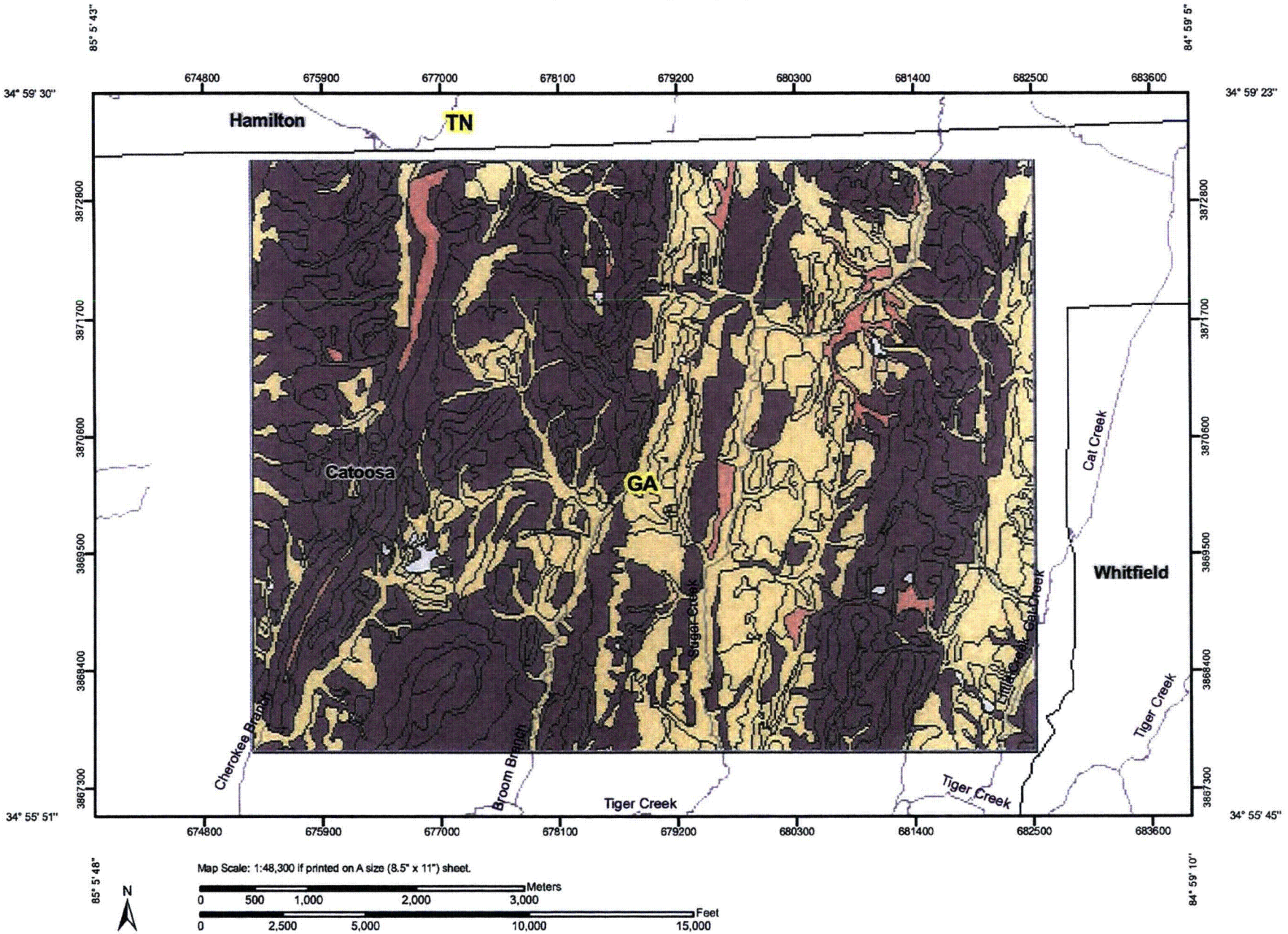

Hydrologic Soil Group–Catoosa County, Georgia
(South Chickamauga Sample 5)

MAP LEGEND

Area of Interest (AOI)
- Area of Interest (AOI)

Soils

Soil Ratings
- A
- A/D
- B
- B/D
- C
- C/D
- D
- Not rated or not available

Political Features
- States
- Counties
- Cities

Water Features
- Oceans
- Streams and Canals

Transportation
- Rails
- Interstate Highways
- US Routes
- Major Roads

MAP INFORMATION

Map Scale: 1:48,300 if printed on A size (8.5" × 11") sheet.

The soil surveys that comprise your AOI were mapped at 1:20,000.

Please rely on the bar scale on each map sheet for accurate map measurements.

Source of Map: Natural Resources Conservation Service
Web Soil Survey URL: http://websoilsurvey.nrcs.usda.gov
Coordinate System: UTM Zone 16N NAD83

This product is generated from the USDA-NRCS certified data as of the version date(s) listed below.

Soil Survey Area: Catoosa County, Georgia
Survey Area Data: Version 7, Apr 21, 2008

Hydrologic Soil Group

Hydrologic Soil Group—Summary by Map Unit — Catoosa County, Georgia				
Map unit symbol	Map unit name	Rating	Acres in AOI	Percent of AOI
AnB	Allen silt loam, 2 to 6 percent slopes	B	74.7	0.8%
AnC	Allen silt loam, 6 to 10 percent slopes	B	130.5	1.3%
AnD	Allen silt loam, 10 to 15 percent slopes	B	99.0	1.0%
AnE	Allen silt loam, 15 to 25 percent slopes	B	163.3	1.6%
AoC2	Allen clay loam, 6 to 10 percent slopes, eroded	B	72.3	0.7%
ApB	Apison loam, 2 to 6 percent slopes	B	48.0	0.5%
ApC	Apison loam, 6 to 10 percent slopes	B	134.2	1.4%
ArC	Armuchee channery silt loam, 6 to 10 percent slopes	C	328.1	3.3%
BoF	Bodine cobbly silt loam, 25 to 60 percent slopes, stony	B	227.9	2.3%
CaB	Capshaw silt loam, 2 to 6 percent slopes	C	4.2	0.0%
Cb	Cedarbluff loam, occasionally flooded	C	36.4	0.4%
Ce	Chennaby silt loam, occasionally flooded	C	827.1	8.3%
CoB	Conasauga silt loam, 1 to 6 percent slopes	C	27.4	0.3%
CoC	Conasauga silt loam, 6 to 10 percent slopes	C	8.3	0.1%
CuB	Cunningham silt loam, 2 to 6 percent slopes	C	155.7	1.6%
CuC	Cunningham silt loam, 6 to 10 percent slopes	C	244.6	2.5%
CuD	Cunningham silt loam, 10 to 15 percent slopes	C	62.0	0.6%
CxD2	Cunningham silty clay loam, 6 to 15 percent slopes, eroded	C	24.0	0.2%
DaB	Decatur silt loam, 2 to 6 percent slopes	B	36.6	0.4%
DaC	Decatur silt loam, 6 to 10 percent slopes	B	4.2	0.0%
DcC2	Decatur silty clay loam, 6 to 10 percent slopes, eroded	B	34.3	0.3%
DcD2	Decatur silty clay loam, 10 to 15 percent slopes, eroded	B	80.9	0.8%
DeC	Dewey silt loam, 6 to 10 percent slopes	B	0.4	0.0%
Em	Emory silt loam	B	23.2	0.2%
Es	Ennis gravelly silt loam, 0 to 3 percent slopes, occasionally flooded	B	162.0	1.6%
EtB	Etowah loam, 2 to 6 percent slopes	B	125.7	1.3%
FeB	Fullerton gravelly silt loam, 2 to 6 percent slopes	B	6.0	0.1%

Hydrologic Soil Group—Summary by Map Unit — Catoosa County, Georgia				
Map unit symbol	Map unit name	Rating	Acres in AOI	Percent of AOI
FeC	Fullerton gravelly silt loam, 6 to 10 percent slopes	B	46.4	0.5%
FeD	Fullerton gravelly silt loam, 10 to 15 percent slopes	B	80.7	0.8%
FeE	Fullerton gravelly silt loam, 15 to 40 percent slopes	B	92.8	0.9%
FrE2	Fullerton gravelly silty clay loam, 10 to 25 percent slopes, eroded	B	12.6	0.1%
HoB	Holston fine sandy loam, 2 to 6 percent slopes	B	150.6	1.5%
HoC	Holston fine sandy loam, 6 to 10 percent slopes	B	61.6	0.6%
LeB	Lyerly silty clay loam, 2 to 6 percent slopes	D	3.0	0.0%
LrC	Lyerly-Rock outcrop complex, 2 to 10 percent slopes	D	79.4	0.8%
MsC	Minvale-Shack gravelly silt loams, 6 to 10 percent slopes	B	484.0	4.9%
MsD	Minvale-Shack gravelly silt loams, 10 to 15 percent slopes	B	453.0	4.6%
MsE	Minvale-Shack gravelly silt loams, 15 to 25 percent slopes	B	409.7	4.1%
NaC	Nauvoo fine sandy loam, 6 to 10 percent slopes	B	183.2	1.8%
NaD	Nauvoo fine sandy loam, 10 to 15 percent slopes	B	429.8	4.3%
NaE	Nauvoo fine sandy loam, 15 to 35 percent slopes	B	103.1	1.0%
NeF	Nella stony fine sandy loam, 25 to 45 percent slopes, very stony	B	215.1	2.2%
RoA	Rome silt loam, 0 to 2 percent slopes, occasionally flooded	B	45.5	0.5%
RoB	Rome silt loam, 2 to 6 percent slopes	B	77.2	0.8%
SmB	Shack-Minvale gravelly silt loams, 2 to 6 percent slopes	B	185.8	1.9%
TaB	Talbott silt loam, 2 to 6 percent slopes	C	23.1	0.2%
TaC	Talbott silt loam, 6 to 10 percent slopes	C	35.2	0.4%
TbC2	Talbott silty clay loam, 6 to 10 percent slopes, eroded	C	25.4	0.3%
TbD2	Talbott silty clay loam, 10 to 15 percent slopes, eroded	C	57.8	0.6%
TmD	Tidings-Townley complex, 10 to 25 percent slopes	B	281.8	2.8%
TmF	Tidings-Townley complex, 25 to 45 percent slopes	B	1,115.1	11.2%
TnC	Townley silt loam, 2 to 10 percent slopes	C	642.4	6.5%

Hydrologic Soil Group—Summary by Map Unit — Catoosa County, Georgia				
Map unit symbol	Map unit name	Rating	Acres in AOI	Percent of AOI
TnE	Townley silt loam, 10 to 25 percent slopes	C	721.9	7.3%
TnF	Townley silt loam, 25 to 45 percent slopes	C	190.7	1.9%
ToC2	Townley silty clay loam, 2 to 10 percent slopes, eroded	C	14.5	0.1%
ToE2	Townley silty clay loam, 10 to 25 percent slopes, eroded	C	16.6	0.2%
TpA	Tupelo silt loam, 0 to 2 percent slopes, rarely flooded	D	34.7	0.3%
TuA	Tupelo silt loam, 0 to 2 percent slopes, frequently flooded	D	129.7	1.3%
UpF	Udorthents-Pits complex, gently sloping to steep		2.4	0.0%
W	Water		44.6	0.4%
WaA	Wax loam, 0 to 2 percent slopes, occasionally flooded	C	233.1	2.3%
WaB	Wax loam, 2 to 6 percent slopes, rarely flooded	C	57.6	0.6%
WhA	Whitwell loam, 1 to 3 percent slopes, occasionally flooded	C	42.4	0.4%
Totals for Area of Interest			9,923.6	100.0%

Rating Options

Aggregation Method: Dominant Condition

Component Percent Cutoff: None Specified

Tie-break Rule: Lower

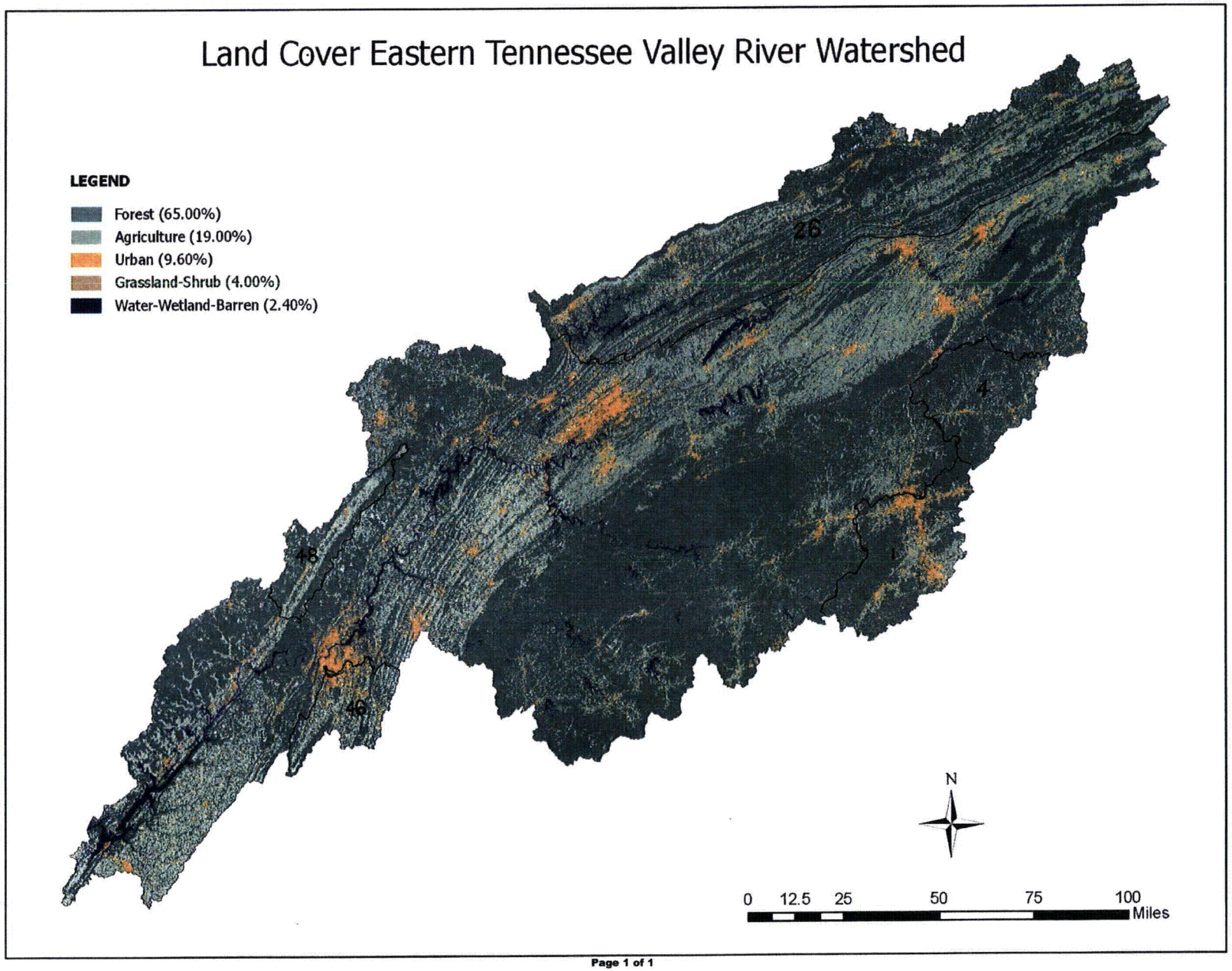
Land Cover Eastern Tennessee Valley River Watershed
LEGEND
Forest (65.00%)
Agriculture (19.00%)
Urban (9.60%)
Grassland-Shrub (4.00%)
Water-Wetland-Barren (2.40%)
26
4
48
46
N
0 12.5 25 50 75 100
Miles

U. S. DEPARTMENT OF COMMERCE
CHARLES SAWYER, *Secretary*
WEATHER BUREAU
F. W. REICHELDERFER, *Chief*

RESEARCH PAPER NO. 34

PREDICTING THE RUNOFF FROM STORM RAINFALL

by
M. A. KOHLER and R. K. LINSLEY

WASHINGTON
September 1951

For sale by the Superintendent of Documents, U. S. Government Printing Office, Washington 25, D. C. - Price 5 cents

PREDICTING THE RUNOFF FROM STORM RAINFALL[1]

M. A. Kohler and R. K. Linsley[2]

Division of Climatological and Hydrologic Services, U. S. Weather Bureau, Washington, D. C.

ABSTRACT

The estimation of the volume of runoff to be expected from a given volume of rainfall is a fundamental problem in flood forecasting. Such estimates are necessary before the unit hydrograph [1] or other techniques can be used to predict the streamflow hydrograph. The authors describe the technique now used at the River Forecast Centers of the U. S. Weather Bureau for evaluating the effect of season, antecedent conditions, duration of rainfall and rainfall amount in determining the portion of the rainfall contributing to storm runoff [2]. Special problems encountered in flood forecasting are emphasized. The technique, developed and tested over several years, yields a high degree of accuracy in estimated runoff. Although prepared by empirical procedures, the close agreement between relations for basins of similar hydrologic characteristics suggests that rational parameters have been adopted. The similarity between relations also simplifies the work required for their preparation.

METHOD OF APPROACH

Many articles have appeared in the technical literature describing the application of infiltration theory to the problem of estimating storm runoff [3]. This is considered by many hydrologists to be the rational approach and, when considering heavy, intense rainfall over a small homogeneous area, it can be used to advantage for some specialized purposes. However, the hydrologic characteristics of a natural basin exceeding a few acres in area are so variable as to make such a rational approach exceedingly complex. When the usual variations in storm characteristics are superimposed, the solution becomes virtually impossible unless an unusually dense network of precipitation stations exists. Moreover, the direct application of the infiltration theory can be utilized to determine only the surface-runoff component of the flood hydrograph. River forecasting requires that the total flow, including interflow and groundwater flow, be estimated and these two latter components constitute a major portion of the flood hydrographs for some basins. An even more important consideration in forecasting, however, is speed. Time is not available for the detailed consideration of large basins by the rational infiltration approach.

The difficulties encountered in treating large natural basins in strict accordance with the infiltration theory have led to the use of infiltration indices such as the ϕ- and W-indices [3]. Since these indices must be correlated empirically to factors representing moisture deficiency of the basin, their use cannot be considered rational. There is no advantage in the use of such indices over a direct correlation of runoff with appropriate factors. The use of such arbitrary indices for computing runoff complicates the solution without enhancing the accuracy or rationalizing the approach. After extensive study the Weather Bureau has adopted a graphical correlation of runoff with selected parameters as the most satisfactory approach for forecasting purposes.

SELECTION OF PARAMETERS

The most important problem in developing a technique for forecasting runoff is the selection of the proper parameters to be used. Runoff is the factor which is required in the preparation of river forecasts. However, since runoff is the residual after the demands of interception, infiltration, and depression storage have been satisfied, there is some logic in using the difference between rainfall and runoff as the dependent variable. This difference is often called the "loss," but because of the ambiguity of this term the authors prefer the term "basin recharge." Knowing the basin recharge

[1] Paper presented at the 30th Annual Meeting of the American Geophysical Union, Washington, D. C., April 21, 1949.

[2] Now with Dept. of Civil Engineering, Stanford University, Palo Alto, Calif.

and the rainfall, runoff can be computed by direct subtraction.

For the purpose of forecasting, runoff is assumed to fall into two classes—(1) base or groundwater flow, and (2) direct runoff. Many methods have been suggested for the separation of these two components in the hydrograph. The selection of method is not as important as the consistent use of a single method throughout the study.

The method used by the Weather Bureau is shown in figure 1. The curve AB represents an extension of the recession existing prior to the storm, point B being directly under the peak. The straight line BC intersects the hydrograph at a point n-days after the crest or after the end of runoff-producing rainfall. The value of n is assumed constant for any basin, but is varied according to drainage area. While basin slope and other factors should be considered, the value of n is not particularly critical. If the derived relation is to be used in conjunction with a unit graph, then the same time base should, of course, be used in both analyses. The area bounded by the hydrograph and ABC converted to inches depth over the basin is considered to be the storm runoff. The basin recharge data are computed by direct subtraction of runoff from rainfall.

The amount of basin recharge resulting from a given storm depends upon (1) the moisture deficiency of the basin at the beginning of rainfall, and (2) the storm characteristics such as rainfall amount, intensity, etc. While storm characteristics can be determined from an adequate network of precipitation stations, the direct determination of moisture conditions throughout a basin is extremely difficult. Reliable point-observations of soil moisture are possible, but an integrated value (over area and throughout depth) is required in a medium recognized for its marked physical discontinuities, further emphasized by cultivation and vegetal cover. Moreover, conditions above the soil surface must be considered, i. e., storage capacity of depressions and vegetal cover (interception).

Numerous measureable factors have been used as indices to moisture conditions, notably (1) days since last rain, (2) discharge at beginning of the storm, and (3) antecedent precipitation. The first of these is obviously insensitive and should not be used if accurate results are required. The second, base flow, is a reasonably good index in humid and sub-humid regions, but it is affected by season and it does not necessarily reflect changes caused by rains during the previous week. Antecedent precipitation is universally applicable and yields good results provided the index is properly derived and is used in conjunction with season of the year or temperature.

The antecedent precipitation index is generally defined by an equation of the type

$$I=b_1P_1+b_2P_2+b_3P_3+\ldots+b_iP_i \qquad (1)$$

Where P_i is the amount of precipitation which occurred i days prior to the storm under consideration, b_i is a constant which is assumed to be some function of time such as $b_i=1/i$, and the number of terms is arbitrarily selected. If a day-to-day value of the index I is required, as is the case in river forecasting, there is considerable advantage in assuming that b_i decreases with time (prior to the storm of interest) according to a logarithmic recession rather than as a reciprocal. In other words, during periods of no precipitation,

$$I_t=I_0k^t \qquad (2)$$

where t is the number of days between I_t and the initial index I_0. Letting t equal unity,

$$I_1=kI_0 \qquad (3)$$

Thus, the index for any day is equal to that of the previous day multiplied by the factor k. If rain occurs on any day, the amount of rain observed is added to the index as is shown in figure 2. Since storm runoff does not, of itself, add to the residual moisture of the basin, it is evident that an antecedent index of "precipitation minus runoff," or basin recharge, should be more satisfactory than precipitation only. This refinement requires con-

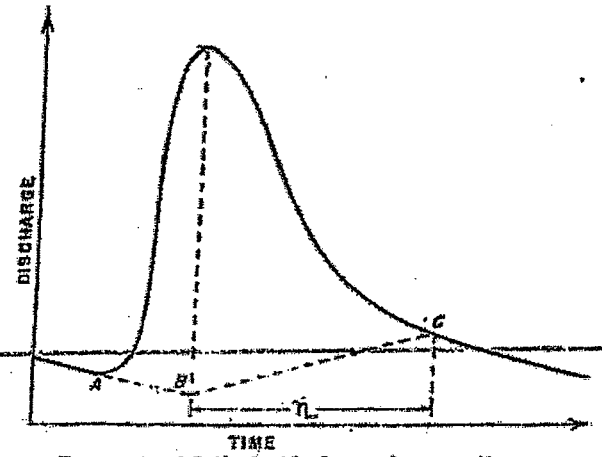

FIGURE 1.—Method of hydrograph separation.

siderably more computations, however, and its use is probably not justified.

The effect of a given amount and distribution of antecedent precipitation upon storm runoff obviously depends upon the extent to which it has been dissipated through evaporation, transpiration, etc. While k could be assumed to vary as a function of pan evaporation, air temperature, dewpoint or vapor pressure deficiency, much of the variation in evapo-transpiration is of a seasonal nature and the introduction of season (or week of year) into the correlation has been found highly satisfactory. There is an added advantage in using season as a parameter in that it reflects variations in surface conditions as related to farming practices, vegetation, etc.

Theoretically, the value of the recession factor k should also be a function of the physiographic characteristics of the basin, but experience has shown that the factor is not critical—values range from 0.85 to 0.90 over most of the eastern and central portions of the United States.

The antecedent precipitation index can be computed either (1) from average daily values over the basin, or (2) from daily precipitation at the various stations, and then averaged.

To utilize the advantages of the logarithmic recession, the computation of the index must be carried forward throughout the period of record being analyzed. The index value for any day theoretically depends upon antecedent precipitation over an infinite period. However, if some reasonable initial value is assumed, the computed index will closely approach the true value within several weeks. It has been the practice either (1) to begin the computations at the end of a dry spell (prior to the first storm analyzed) with an assumed low value of the index, or (2) to begin the computations two or three weeks in advance of the first storm with an assumed value equal to the normal 10-day precipitation for the season (which approximates the average index value for the area).

In computing the data for a particular storm, the index at the beginning of the first day of rain is used. For example, an index value of 1.8 would be used for the storm of the 9th and 10th in figure 2. The computation can be rapidly performed with the aid of a chart (fig. 3), or comparable table. By entering the chart with an initial index, the value t days later (assuming no rainfall) can be read directly.

In any discussion of antecedent precipitation, a question immediately arises regarding snowfall. If the water equivalent of snowfall is added to the index at the time of its occurrence, its effect on a subsequent rain storm will be over-emphasized if removed from the basin through evaporation and underestimated if melted at a later date. In the usual sequence of events, evaporation from the snow surface is not far different from surface evaporation following a rain and, consequently, snowfall can probably best be considered to have been applied to the basin on the day it melted rather than when it fell.

PREPARATION OF DATA

In general, extended complex storms should be broken into as many short, unit storms as can successfully be accomplished through hydrograph

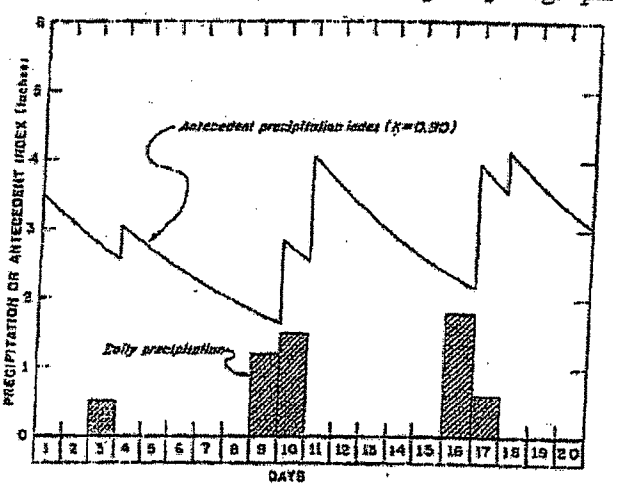

FIGURE 2.—Variation of antecedent index with daily precipitation.

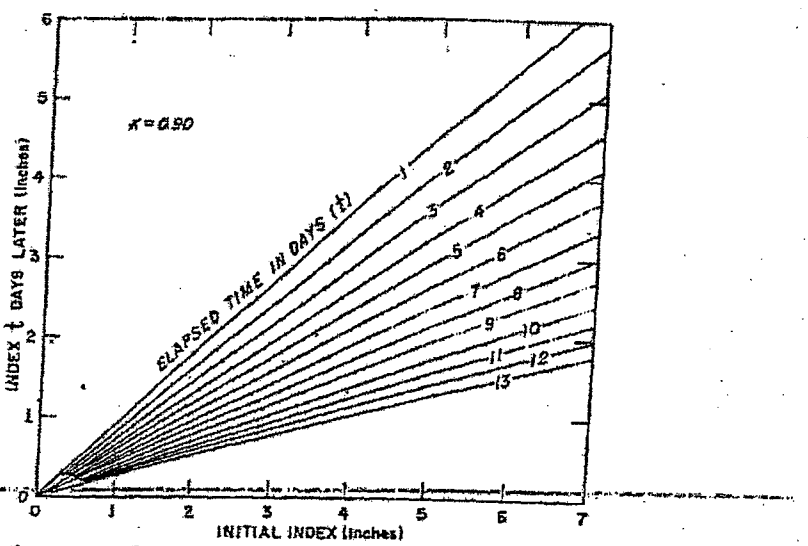

FIGURE 3.—Chart for computing antecedent precipitation index.

analysis. Having decided upon the storm period, the amount and duration of rainfall are computed and tabulated for each storm. While data are generally insufficient to accurately determine the average duration of rainfall over a basin, this factor is not critical and can be adequately derived by examination of available six-hourly rainfall data. In the development of the relations to be described, the duration was defined as the sum of those six-hourly periods with more than 0.2 inch of rain plus one-half the intervening periods with less than 0.2 inch. While experimental infiltration data indicate rates commonly in excess of 0.10 inch per hour after saturation, relations developed to date consistently show that the portion of basin recharge which seems to be correlated with duration takes place at rates in the order of 0.01 inch per hour. The difference between these rates is largely accountable to interflow, intercorrelations, and the method of hydrograph separation.

COAXIAL GRAPHICAL CORRELATION ANALYSIS

In the previous discussion reasons were advanced for the selection of five variables to be included in the correlation—basin recharge, antecedent precipitation index, season or week of year, storm duration, and storm rainfall. While analytical correlation could be used, the existence of joint functions complicates the problem to such an extent that the selection of an appropriate equation is extremely difficult. Ezekiel [4] describes a method of graphical correlation which yields excellent results for some problems, but the coaxial method is more flexible and yields correspondingly better results for runoff correlations because of the joint relations involved.

The coaxial method [2] of graphical correlation is based on the premise that if any important factor is omitted from a relation then the scatter of points in a plotting of observed values of the dependent variable *vs.* those computed by the relation will be at least partially explained by the omitted factor. In other words, if the points of such a plotting are labeled with corresponding values of the omitted factor, a family of curves fitting the data can be used to modify or correct the values computed from the original relation.

In applying the coaxial method to the selected parameters, a three-variable relation is first developed (fig. 4, Chart A) by (1) plotting antecedent precipitation *vs.* basin recharge, (2) labeling the points with week number, and (3) fitting a smooth family of curves representing the various weeks. Chart B, for plotting computed *vs.* observed basin recharge, is placed with horizontal scale (computed) matching that of Chart A to facilitate plotting. Points labeled with duration are then plotted in Chart B at the observed recharge on the vertical scale and at a computed value on the horizontal scale corresponding to that determined by entering Chart A with antecedent index and week number. A smooth family of curves is then drawn which represent the effect of duration upon basin recharge. The combination of Charts A and B constitutes a graphical relation for estimating recharge from antecedent index, week, and storm duration. Storm precipitation is then introduced (Chart C) by (1) plotting computed recharge (from Charts A and B) *vs.* observed recharge (on horizontal scale), (2) labeling the points with rainfall amount, and (3) fitting a family of curves. Charts A, B, and C constitute the first approximation of the relation involving the selected parameters. Chart D, a plotting of observed recharge *vs.* that computed from Charts A, B, and C, is shown to indicate the over-all correlation of the relation.

Since the parameters are intercorrelated and since the first charts were developed independent of factors subsequently introduced, tests should be made to determine if revisions of the charts could improve the relation, i. e., the process is necessarily one of successive approximations. To check the curves of Chart A, the assumption is made that the other charts are correct. Therefore, the horizontal coordinate for an adjusted point (in Chart A) can be determined by entering Charts B and C in reverse order with observed recharge, rainfall amount and duration. The ordinate for the adjusted point corresponds to the observed antecedent precipitation index. In other words, the week-curves must be revised to fit the point adjusted in this manner if the relation is to yield a computed value equal to the observed. The second-approximation curves for duration and storm precipitation and all subsequent approximations are made in a similar manner. In each case the points are plotted by entering the chart sequence from both ends with observed values to determine the adjusted coordinates.

The method of performing the correlation presented in previous paragraphs is of general application and can be used as described. In developing the relation for basin recharge, however, certain modifications simplify the procedure and re-

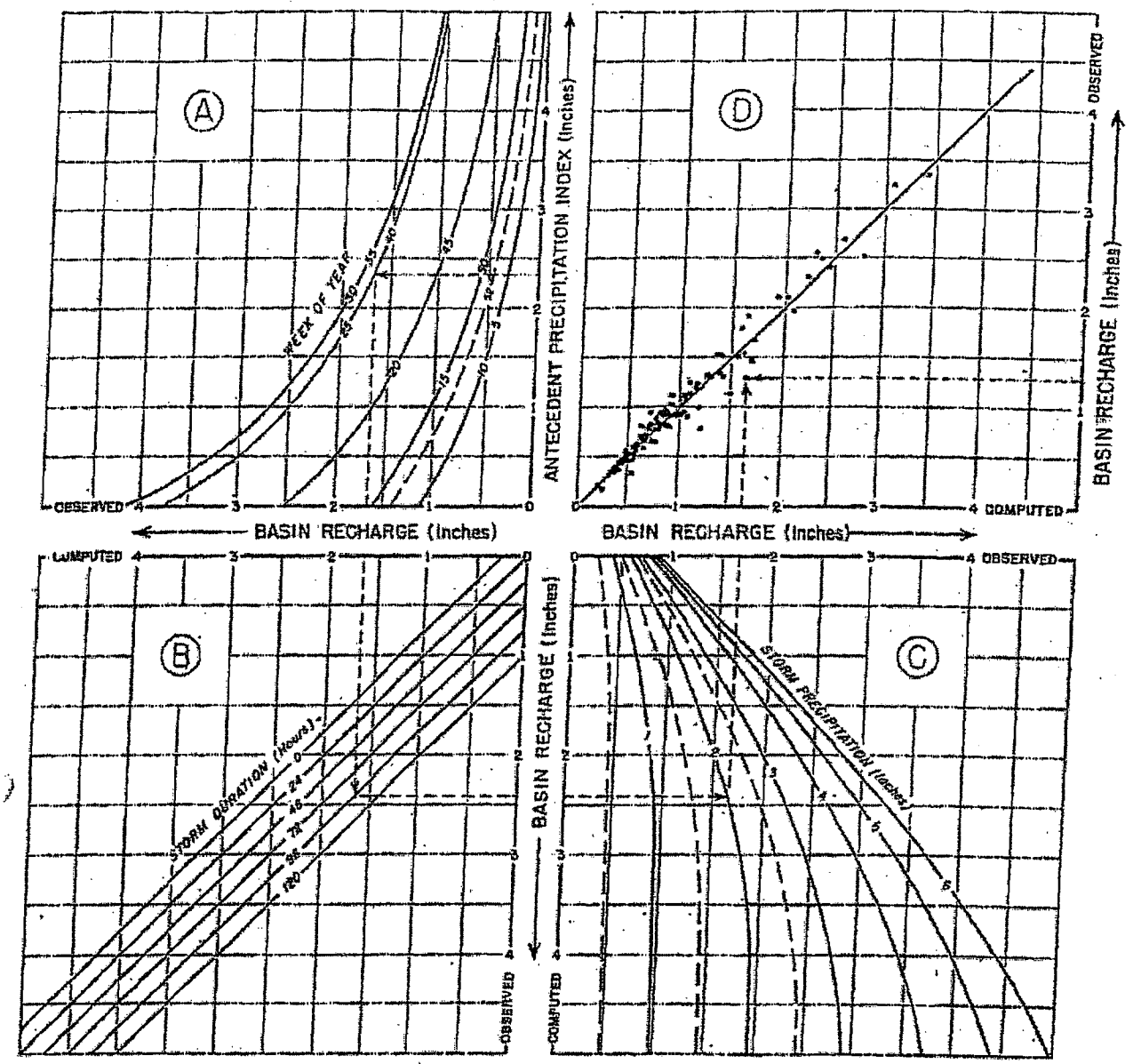

FIGURE 4.--Basin recharge relation for the Monocacy River at Jug Bridge, Md.

sult in the derivation of the final relation with fewer approximations. Since storm precipitation is extremely important, the first plotting of Chart A will show so little correlation that the construction of the curve family is extremely difficult. Introducing storm rainfall in the first plotting would improve the correlation, but there is also an important advantage in having this parameter in the last chart of the sequence—namely, the possibility of computing runoff in excess of rainfall and of computing negative values of runoff is eliminated. Moreover, the arrangement shown in figure 4 results in the determination of a unified index of initial moisture conditions in the first chart—a decided advantage in forecast application.

If the first plotting in Chart A is limited to those storms having an amount of rainfall within a specified class interval (2 to 4 inches, for example), the construction of the curves is simplified provided there are sufficient data. Actually, only limited data are required since the general type of curvature and convergence can be determined from theoretical reasoning. Moreover, the relations are quite similar throughout any general area, and once such a relation is developed, all curve-families but one can be used as the first-

approximation curves for any other basin in the area. In fact, a single relation has been found applicable to as many as six or eight tributary drainages within a river basin.

As stated previously, correlations made to date indicate that storm duration, as determined in an arbitrary manner, is not particularly effective in determining basin recharge. An assumed spacing of one to two hundredths inch per hour generally proves satisfactory, but the assumed curves should be checked by plotting after the curve families of Charts A and C have been finally determined.

Examination of figure 4 will show that the errors of the points with little runoff (recharge approaching precipitation) are considerably magnified when routed back through the chart sequence as described for the development of the second-approximation curves. Therefore, if this approach is used, it will be found that the curves can be more readily determined if low-runoff points are omitted in the plotting. As an alternate approach, the required revisions of the curves can be determined qualitatively by labeling the points of Chart D with weak number or duration to determine if there is any residual correlation. A third approach, also qualitative, is illustrated in figure 5, where the errors of the relation are plotted against antecedent precipitation with weak number as a parameter. Either of these supplementary plottings indicate in which direction the curves should be shifted. For example, figure 5 indicates that weaks numbered about 5 through 8 should be shifted to the right for high antecedent index and to the left for low. The degree of shift indicated by the plottings can be reflected back through the chart sequence to determine approximately how much the curve should be shifted.

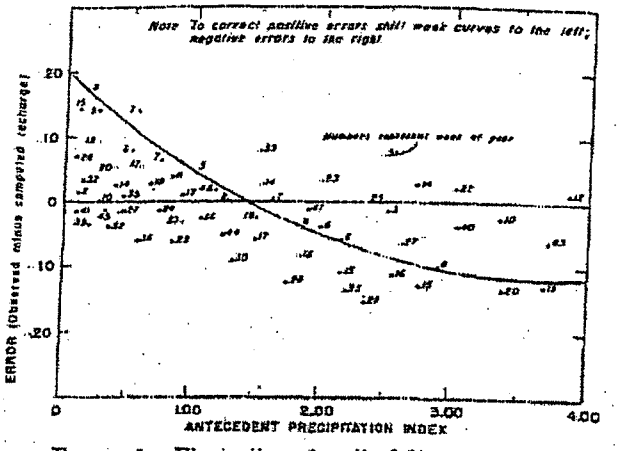

FIGURE 5.—Illustration of method for revision of weak curves.

APPLICATIONS OF DERIVED RELATIONS

In preparing river forecasts, runoff is the controlling factor rather than basin recharge. Since rainfall and recharge determine runoff, however, the curves of Chart C in figure 4 can be converted to read runoff directly as shown in figure 6. Moreover, the charts can be superimposed (fig. 7) to conserve space without reducing the scale.

The proper application of the unit hydrograph requires that runoff increments be estimated for successive time periods throughout an extended storm. This can be accomplished by computing runoff depths from accumulated precipitation up to the termini of the designated periods, and subtracting successive values of runoff. As an alternative, all precipitation prior to the period of interest can be considered to be antecedent precipitation, and the storm rainfall for the period used to compute the corresponding increment of runoff. For forecast purposes, where time is of the essence, the first method may be preferable. The second method, on the other hand, gives more significance to time variations of rainfall intensity and may, therefore, provide for more accurate computations. However, the relative accuracies of the two techniques are also dependent upon the adequacy of the assumed weights for antecedent precipitation, since the first method is in accord with the analysis used in developing the basin relation.

Since it is impossible to segregate the water passing the gaging station according to the portion of the basin in which it fall, statistically derived runoff relations must necessarily be determined from basin averages of the parameters. Unfortunately, because of the higher order and joint functions involved, a relation which is based on storms of uniform areal distribution will yield runoff values which are too low when applied to storms with extremely uneven distribution. This can be demonstrated by computing the runoff for four, six, and eight inches of storm precipitation, assuming all other factors to remain constant. While six is the average of four and eight, the runoff depths computed from these three values of precipitation do not bear a corresponding relation. An uneven distribution of antecedent precipitation produces similar results.

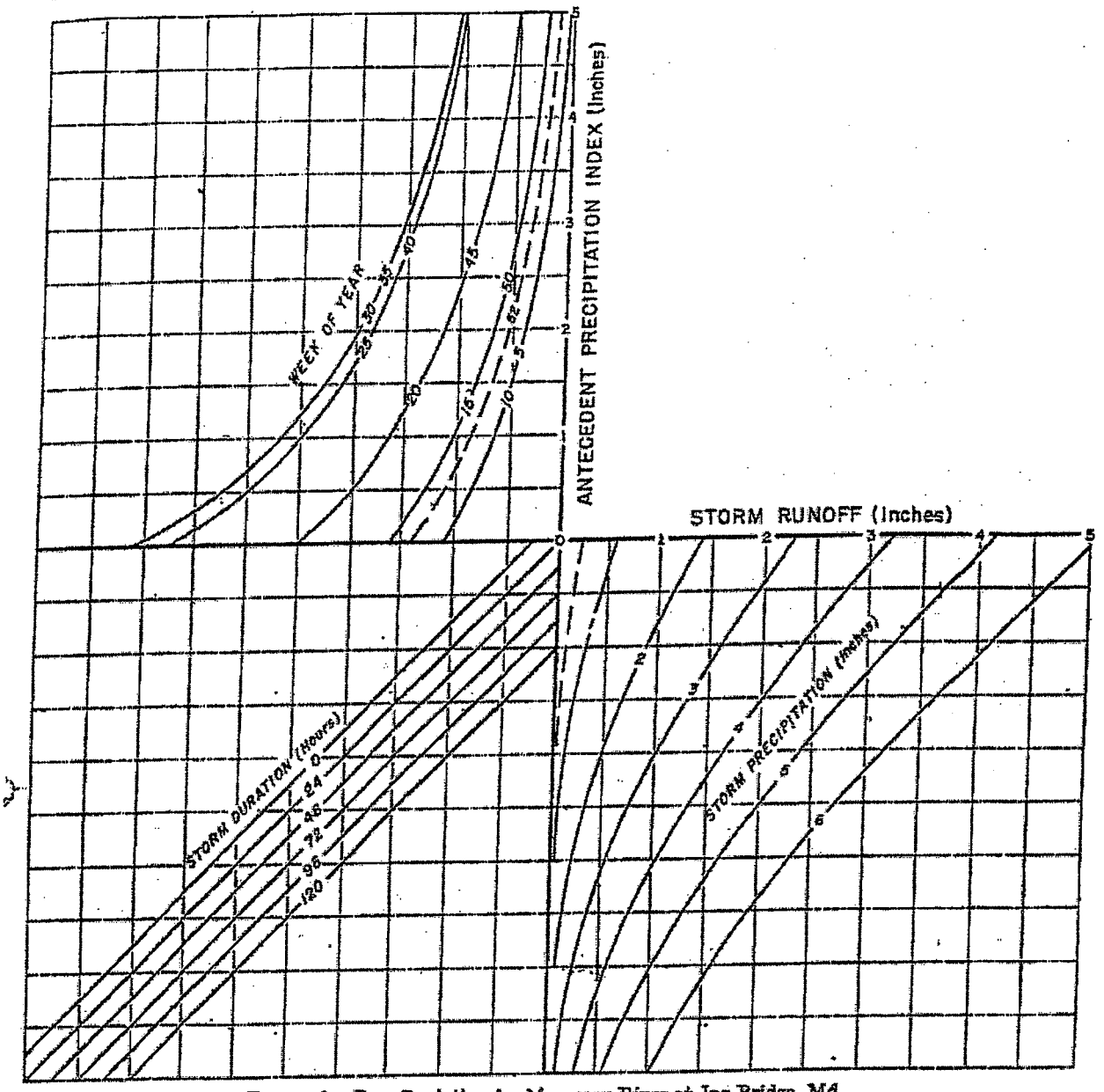

FIGURE 6.—Runoff relation for Monocacy River at Jug Bridge, Md.

If, however, the runoff relations are based on data representing reasonably uniform conditions, they can properly be used to compute the runoff in the vicinity of each of the rainfall stations. The average of such computed values will, in general, more nearly approach the observed runoff. In other words, if either storm or antecedent precipitation is highly variable from one portion of the basin to another, then computed runoff depths, rather than precipitation, should be averaged.

DEFICIENCIES OF DERIVED RELATIONS

Relations of the type described yield high correlation for most basins and provide a simple method of computing runoff, but they, nevertheless, have certain deficiencies which should not be overlooked. First, rainfall intensity is omitted; second, frozen soil obviates their direct use; and third, snowfall has not been considered. Since both rainfall amount and duration are considered, average intensity for the entire storm

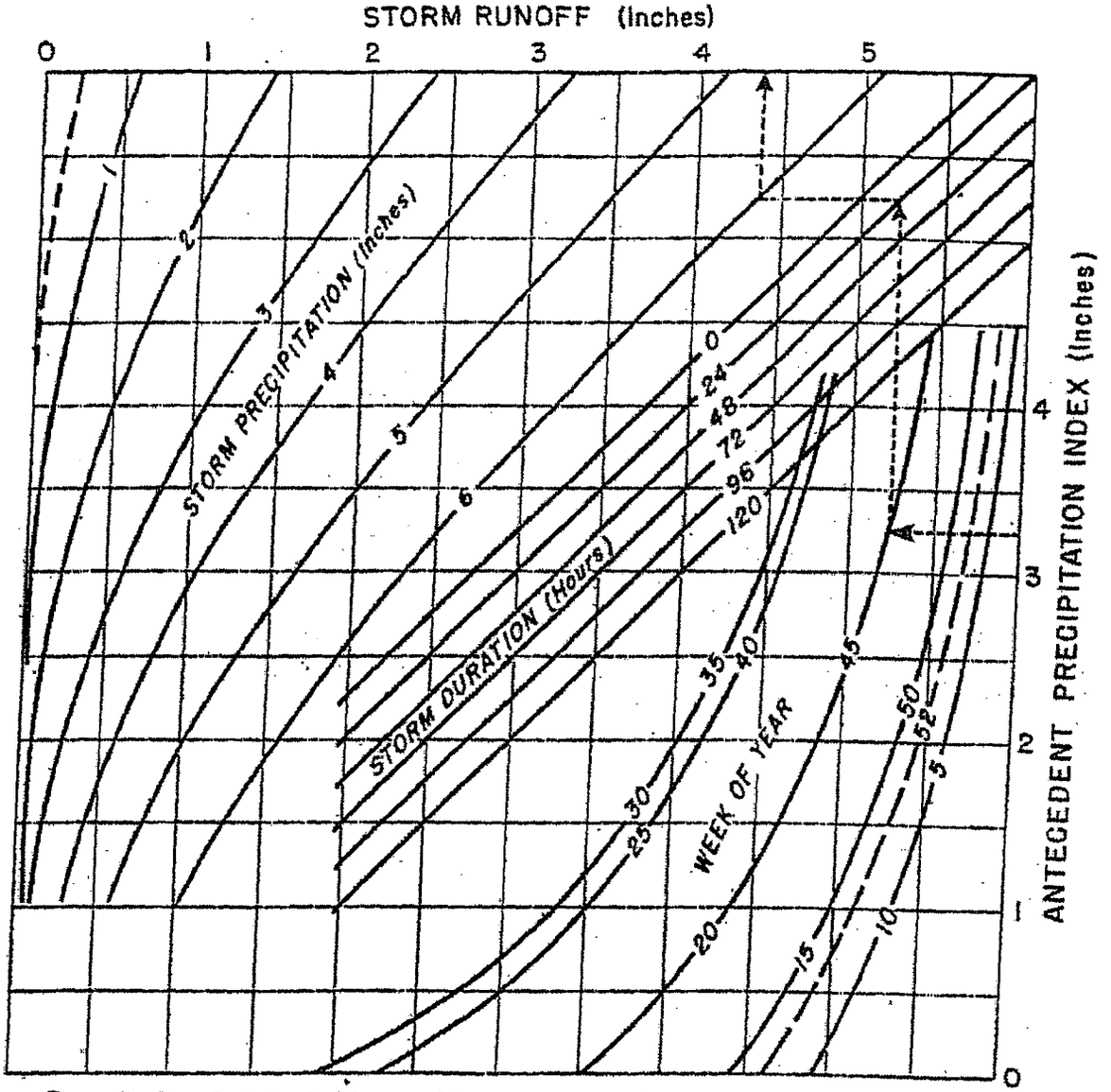

FIGURE 7.—Runoff relation for Monocacy River at Jug Bridge, Md., with curve-families superimposed.

8

period is an integral part of the relations. However, the computed runoff for a 5-inch, 24-hour storm is independent of intensity variations within the period. As mentioned previously, the storm can be treated as several short periods of rainfall, considering all rainfall occurring prior to any specific period as antecedent precipitation. While intensity variations can be given consideration in this manner, neglecting intensity apparently causes serious error in total storm runoff only when intensities are so great throughout the entire storm that rainfall runs off too rapidly to alleviate the moisture deficiency of the basin. Experience has shown that the relations yield fair results during frozen conditions, provided that the weekly curve representing maximum runoff conditions is used, regardless of the date of the storm. Storms which are predominantly snow present an entirely different problem and are not considered here. If only a slight snow cover remains at the end of the storm, the estimated water equivalent can be subtracted from the observed storm precipitation. Snow on the ground at the beginning of the storm should be included in the storm precipitation (rather than antecedent precipitation) if it is dissipated during the storm.

REFERENCES

1. L. K. Sherman, "Streamflow from Rainfall by the Unit-graph Method," *Engineering News-Record*, vol. 108, No. 14, April 7, 1932, pp. 501–505.
2. R. K. Linsley, M. A. Kohler, and J. L. H. Paulhus, *Applied Hydrology*, McGraw-Hill, New York, 1949.
3. H. L. Cook, "The Infiltration Approach to the Calculation of Surface Runoff," *Transactions of the American Geophysical Union*, vol. 27, No. 5, Oct. 1946, pp. 726–747.
4. M. Ezekiel, *Methods of Correlation Analysis*, 2d ed., Wiley, New York, 1941.

WEATHER BUREAU RESEARCH PAPERS

No. 1 **Progress Report on Development of an Electronic Anemometer.* W. R. Thickstun, July 1943.

No. 2 **A Project to Test the Potential Usefulness of Pressure Patterns for Forecasting.* H. W. Norton, G. W. Brier, and R. A. Allen, January 1944.

No. 3 **Preliminary Report on Duration of Stormy Periods at Selected Localities and Intervals Between Periods.* L. L. Weiss, January 1944.

No. 4 **Some Relationships Between Five-Day Mean Surface Maps and Their Component Daily Maps.* C. B. Johnson, January 1944.

No. 5 **Improvement of Trend Methods of Forecasting.* P. F. Clapp, July 1943.

No. 6 (Unassigned)

No. 7 **Formation of New Moving Centers South of Deep Lows.* R. C. Gentry, January 1944.

No. 8 **An Investigation of a Trajectory Method of Forecasting Flow Patterns at the 10,000-Foot Level.* H. G. Dorsey and G. W. Brier, January 1944.

No. 9 **Preliminary Report on Stagnant Highs Over Greenland, Iceland, and England, and Over the Bering Sea and Alaska in July and August.* R. C. Gentry and L. L. Weiss, January 1944.

No. 10 **Persistence in London Temperatures.* H. W. Norton and G. W. Brier, January 1944.

No. 11 **Skill in Selecting the "Best" Forecast.* G. W. Brier, January 1944.

No. 12 *Notes on Interdiurnal Pressure and Temperature Changes in the Upper Air.* R. C. Gentry, January 1944. (Unpublished.)

No. 13 *Investigation and Practical Use of a Method for Constructing Six-Hour Isallobars on Upper Level Charts.* E. M. Cesa and P. F. Clapp, January 1944. (Unpublished.)

No. 14 *Weight Changes for the Atmosphere Divided Into Three Layers.* L. L. Weiss, February 1944. (Unpublished.)

No. 15 **Some Notes on Forecasting for Atlanta and Miami Districts (North and South Carolina, Georgia, and Florida).* Grady Norton, February 1944.

No. 16 **Verification of a Forecaster's Confidence and the Use of Probability Statements in Weather Forecasting.* G. W. Brier, February 1944.

No. 17 **Pressure Patterns Accompanying Cyclonic Activity in the Azores Area.* R. L. Pyle, March 1944.

No. 18 **Normal Mean Virtual Temperatures and Weights of the Air Column Between Sea Level and 10,000 Feet.* Staff, Extended Forecast Section, July 1944.

No. 19 **Temperature Changes During Formation and Dissipation of West Coast Stratus.* Morris Neiburger (University of California at Los Angeles), July 1944.

No. 20 *Empirical Studies of the Motion of Long Waves in the Westerlies.* P. F. Clapp, July 1944. (Unpublished.)

No. 21 **A Collection of Reports on the Preparation of Prognostic Weather Charts.* J. R. Fulks, H. B. Wobus, and S. Teweles, Edited by C. P. Mook, October 1944.

No. 22 **Relationship Between Surface Temperature and Mean Virtual Temperature in the Lower Troposphere.* W. M. Rowe, November 1944.

No. 23 **Forecasting the Time of Formation of Stratus Cloud Ceiling at Oakland, California, Airport.* Edward M. Vernon, April 1945.

No. 24 **Investigation of Polar Anticyclogenesis and Associated Variations of the Zonal Index.* Jerome Namias, September 1945.

No. 25 **Progress Report on Objective Rainfall Forecasting Research Program for the Los Angeles Area.* J. C. Thompson, July 1946.

No. 26 *A Study of Quantitative Precipitation Forecasting in the TVA Basin.* Glen W. Brier, November 1946. $0.25

No. 27 *Objective Methods of Forecasting Winter Minimum Temperatures at Washington, D. C.* C. P. Mook and Saul Price, August 1947. $0.35

No. 28 **Possibility of Long Range Precipitation Forecasting for the Hawaiian Islands.* Samuel B. Solot, January 1948.

No. 29 *An Objective Method of Forecasting Five-Day Precipitation for the Tennessee Valley.* William H. Klein, July 1948 $0.30

No. 30 *First Partial Report on the Artificial Production of Precipitation: Stratiform Clouds—Ohio, 1948.* Richard D. Coons, R. C. Gentry, and Ross Gunn, August 1948. $0.30

(Continued on p. 10)

*Out of print.

Note—Nos. 2, 3, 4, 7, 8, 9, 10, and 11 are included in one publication under the title *A Collection of Reports on Extended Forecasting Research*, Weather Bureau, 1944.

WEATHER BUREAU RESEARCH PAPERS

(Continued from inside self cover)

No. 31 *Second Partial Report on the Artificial Production of Precipitation: Cumuliform Clouds—Ohio, 1948.* Richard D. Coons, Earl L. Jones, and Ross Gunn, January 1949. $0.30

No. 32 *Further Studies in Hawaiian Precipitation.* Samuel B. Solot, January 1950. $0.30

No. 33 *Artificial Production of Precipitation. Third Partial Report: Orographic Stratiform Clouds—California, 1949. Fourth Partial Report: Cumuliform Clouds—Gulf States, 1949.* Richard D. Coons, Earl L. Jones, and Ross Gunn, September 1949.

No. 34 *Predicting the Runoff From Storm Rainfall.* M. A. Kohler and R. K. Linsley, September 1951. $0.40

Weather Bureau Research Papers for sale by Superintendent of Documents, U. S. Government Printing Office, Washington 25, D. C.

U. S. GOVERNMENT PRINTING OFFICE: 1951

STANDARD FORM NO. 64

HYDRAULIC DATA BRANCH

FILE NO. ASF-1173

Office Memorandum • UNITED STATES GOVERNMENT

TO : Albert S. Fry

DATE: June 8, 1950

FROM : L. R. Engstrom and A. J. Cooper

SUBJECT: CONFERENCE WITH U.S.W.B., WASHINGTON, MAY 30 AND JUNE 1 ON FORECASTING PROCEDURES

The writer and A. J. Cooper spent May 30 and June 1 discussing forecasting procedures with U. S. Weather Bureau personnel in Washington. Our principal discussions were on their method of developing rainfall-runoff relations, and on routing procedure with major emphasis on the use of their Electronic Streamflow Analogue. We were impressed enough with their rainfall-runoff procedure to feel that it should be tried out in our own studies. The Electronic Streamflow Analogue in its present form is unable to solve problems of extreme backwater and controlled outflow and it could not be used for reaches such as our Kentucky Reservoir except for special cases of fixed headwater elevation. It does seem probable that a circuit could be devised which would solve more complicated conditions. In its present form it should prove valuable in natural flow computations, predictions of tributary flows, and predictions of inflows to many of our tributary reservoirs. It is our opinion that such a machine would be very valuable in the work of the Forecasting Section both for study and prediction purposes and that it should be available in the Section even if similar equipment is to be provided by the U.S.W.B. for the proposed unit in Knoxville.

Upon arrival, a few minutes were spent with Mr. Bernard, Chief, Division of Climatological and Hydrologic Services, and a somewhat longer time was spent with him before leaving on June 1. Our discussions on procedures were held with his assistant, Mr. Linsley, and with Mr. Kohler and Mr. Nordenson of the Procedures Development Staff.

A considerable amount of time was spent going over their method of developing rainfall-runoff relations. This method is explained in a paper entitled "Predicting the Runoff from Storm Rainfall," by Kohler and Linsley, a copy of which was obtained. This method takes into account four factors: antecedent precipitation, week of the year, duration of rainfall, and amount of rainfall. These factors are correlated in a co-axial relation against "basin recharge" which is the difference between rainfall and surface runoff or is equal to ground-water runoff plus loss. After development it is converted into a direct relation against surface runoff. The Weather Bureau has adopted this procedure as standard. They say that for their purposes it is the most satisfactory relation they have been able to develop, that it seems to work equally well for areas in all parts of the United States, and that it is relatively simple to use, once developed.

NOTED
A. S. FRY

STANDARD FORM NO. 64

Office Memorandum • UNITED STATES GOVERNMENT

TO : Albert S. Fry DATE: June 8, 1950

FROM : L. R. Engstrom and A. J. Cooper

SUBJECT: CONFERENCE WITH U.S.W.B., WASHINGTON, MAY 30 AND JUNE 1 ON FORECASTING PROCEDURES

It is probable that the use of the "antecedent precipitation index" may give a better correlation than our use of ground-water flow. The weekly seasonal index would be a refinement of our method of dividing the year into winter and summer season but defining it may require analysis of a longer period of record than we have used. Their standard procedure is to use 10 years of record if available. Ground-water runoff is not covered in their procedure since they are forecasting crests primarily and in their separation of the hydrograph they assume ground water to recede until crest stage is reached. It seems probable that a similar co-axial relation could be worked out for ground-water runoff based on the same factors.

The Electronic Routing Machine was set up in the office of the Procedures Development Staff and we were given considerable explanation of its use and a demonstration. We also inspected a number of routings made directly from effective rainfall on the ground which showed the accuracy which was obtained. Only one inflow graph could be put into the machine but a third unit, which was almost ready for use, will permit an additional inflow to be introduced which they believe should improve the accuracy of results. In discussing the routing of natural flow on the Tennessee River they thought it might be possible to route Chattanooga in a single step and certainly with a machine which could introduce two inflow graphs. We discussed the possible use of the machine for more complicated routing procedures, such as routing our Kentucky Reservoir. They stated that it was not possible to take care of the additional variables introduced by controlled outflow. They had not attempted to work on design of a more complicated circuit but Linsley states that when he becomes established at Stanford he might try to get the electronic department there to investigate possibilities.

We were also shown a newly set-up procedure for predicting crest stages for points for which the time of concentration is short and the forecast is made by non-technical personnel. A copy of the paper explaining this procedure with accompanying tables was given to us. (Development of Forecasting Tables for the Flood Warning Service.) This procedure, although interesting, would not have any application in our office.

STANDARD FORM NO. 64

Office Memorandum • UNITED STATES GOVERNMENT

TO : Albert S. Fry

DATE: June 8, 1950

FROM : L. R. Engstrom and A. J. Cooper

SUBJECT: CONFERENCE WITH U.S.W.B., WASHINGTON, MAY 30 AND JUNE 1 ON FORECASTING PROCEDURES

Mr. Bernard, in our short talk before leaving, mentioned the tentative plans for the establishment of a river forecasting unit in Knoxville equipped with one of the new electronic machines and stated that one of its expected uses would probably be to compute natural flows on the Tennessee River. He also stated that they felt that in the river basin developments being established throughout the country that the function of forecasting should be handled by the Weather Bureau and he presented us with copies of his talk to the Columbia Basin Inter Agency Committee entitled "The Role of Forecasting in River Basin Management."

L. R. Engstrom

LRE:FNH

TVA 4205 (WCP-10-48)

Number: ASP-1173

Tennessee Valley Authority
Division of Water Control Planning
Hydraulic Data Branch

Date: June 19, 1951

WORK ASSIGNMENT

To: Forecasting Section
Subject: COORDINATION WITH NATURAL FLOW UNIT, U. S. WEATHER BUREAU

In the revised Memorandum of Understanding between the TVA and the United States Weather Bureau, dated June 23, 1951, provision is made for the establishment in Knoxville of a natural flow river stage forecasting unit. Under the Memorandum the Bureau agrees:

To maintain a "natural flow" river stage forecasting unit, based in the City of Knoxville, adequately staffed with competent hydrologic engineers and equipped with electronic flow routing equipment, which unit will

(a) Currently and continuously as required by TVA supply to TVA predicted natural flows on uncontrolled streams at locations requested by TVA to provide information regarding natural flows into reservoirs operated by TVA necessary in TVA's operations.

(b) Where requested, supply TVA with predicted natural stream flows and stages for significant points on the Tennessee River and tributaries, for conditions assuming no TVA projects, to the end that controlled flood stages may be held lower than those which would have been obtained naturally.

(c) Insofar as practicable, prepare flood stage forecasts for those points on uncontrolled streams in the Tennessee Valley which are vulnerable to flood damage and in need of a flood warning service such as First Creek in Knoxville and the cities of Shelbyville, Columbia, and Centerville on the Duck River and Fayetteville on the Elk River.

Under the Memorandum TVA agrees:

To gather precipitation and stream discharge data from stations maintained by TVA and Bureau and to furnish these data to Bureau, including data needed by the "natural flow" unit of Bureau.

To provide all communications facilities which may be required for the exchange of data and information between TVA and the Knoxville Weather Bureau Airport Station and the natural flow forecasting unit.

The Bureau is now in the process of establishing the natural flow unit in Knoxville and preparing to carry out its responsibilities. Mr.

Outline of Procedure: Required _____ Not Required _____

Account Number 321-2b-10 A Project _____

Job Authorizations Issued to _____

Date for Completion Continuing Date Completed _____

Submitted by _____ Approved by _____

Marshall Richards is already in Knoxville and the other two employees contemplated will be here about July 1. At that time it is expected that the electronic routing unit will also be installed.

In order that TVA may obtain the maximum benefit from the new unit, it will be desirable, particularly at the outset, to maintain rather close contact with the head of the unit, Mr. Richards. Confirming our verbal discussions, it is suggested that Mr. Cooper be assigned as TVA contact man. In this capacity, he should provide liaison between the two organizations and should cooperate with Mr. Richards and furnish whatever data and knowledge that we have that would be helpful to the new unit. In this we should not hesitate to take the initiative since Mr. Richards does not know what we have and is not familiar with the Tennessee Valley. We should do everything that we can to help the unit get oriented and give them a knowledge of the problems that we expect them to solve in the Valley and acquaint them with the various parts of the area and the differences which exist in these parts and make them aware of any other matters that would be of value.

We would like to be kept informed as to the progress of the unit and in this connection we would like to have a conference weekly on Monday afternoons at 3:00 p.m. with you and Mr. Cooper to discuss the work. It would be desirable too for Mr. Cooper to make a weekly report to you in writing which you could forward to us for my information, setting forth what is being done and what progress is being made.

Albert S. Ely

ASE:SWH

Tennessee Valley Authority
Division of Water Control Planning
Hydraulic Data Branch

STREAMFLOW FORECASTING AND WATER DISPATCHING FOR TVA RESERVOIR SYSTEM

By

Le Roy Engstrom, M. ASCE
Jackson H. Wilkinson, M. ASCE
and
Alfred Blickensderfer, A.M. ASCE

Presented at
Knoxville Convention
American Society of Civil Engineers
Knoxville, Tennessee
June 8, 1956

STREAMFLOW FORECASTING AND WATER DISPATCHING FOR TVA RESERVOIR SYSTEM

By

Le Roy Engstrom[1], M. ASCE; Jackson H. Wilkinson[2], M. ASCE; and Alfred Blickensderfer[3], A.M. ASCE

INTRODUCTION

The day-to-day operation of the TVA reservoir system is largely dependent upon a knowledge of the streamflow to be expected today, tomorrow, and ten days from now. This is true during the shower periods of spring and summer as well as during periods of flood flows. It is also true during periods of drouth. The dispatching of water for flood control, navigation, power, or other purposes requires accurate estimates of the daily amounts of inflow to each reservoir in the system and of the transit of releases from each reservoir through the system. Estimates of streamflow must be revised daily, or more frequently during storm periods, to adjust for the effects of additional rainfall or to improve estimates on the basis of observed data. This is necessary during periods of high flow to ensure the proper operation of the system for flood control. It is necessary during periods of normal and deficient flow to provide adequate depths for navigation and to ensure the maximum utilization of available water for power purposes.

WATER CONTROL ORGANIZATION

The operation of the reservoir system, shown on Plate 1, is under the direction of the River Control Branch of the Division of Water Control Planning through the Office of the Chief Engineer in Knoxville. The River and Reservoir Forecasting Section of the Hydraulic Data Branch of the

---

[1]Head, River and Reservoir Forecasting Section, Hydraulic Data Branch, TVA, Knoxville, Tenn.

[2]Staff Specialist in Water Dispatching, Hydraulic Data Branch, TVA, Knoxville, Tenn.

[3]Hydraulic Engineer, Hydraulic Data Branch, TVA, Knoxville, Tenn.

Division of Water Control Planning furnishes the current and forecast hydrologic information needed for the operation of the system. It translates the required power load into equivalent water requirements at the various hydro plants and makes adjustments as needed to carry out the current over-all operating plan. It finally routes the resulting releases from the individual plants through the reservoir system and determines the resulting releases and elevations at downstream points.

HYDROLOGY OF THE BASIN

The Tennessee River drains an area of 41,000 square miles. Its headwaters are in the mountains of eastern Tennessee, western Virginia and North Carolina, and northern Georgia where elevations run to over 6000 feet. The drainage basin varies from these mountainous areas to the rolling country of middle Tennessee and the relatively flat reaches of northern Alabama and Mississippi and western Tennessee and Kentucky. The mean annual precipitation over the area is approximately 52 inches, varying from about 38 inches in the driest years to 63 inches in the wettest years. Corresponding runoff is about 22 inches, ranging between extremes of 11 and 33 inches. The mean annual rainfall is relatively uniform over the western half of the basin, but over the eastern half it varies from 40 inches in some sheltered areas up to 80 or 90 inches in the higher mountains as shown on Plate 2. During periods of prolonged drouth, smaller streams in the central and western portion of the basin run dry, whereas substantial areas in the mountains never fall below one-half cubic foot per second per square mile. Rainfall is well distributed throughout the year, mean monthly values ranging between 4 and 5 inches most months, with a maximum of 5.6 inches in March and a minimum of 2.8 inches in October. Although snow cover may accumulate to several feet in the higher mountain areas and to several inches generally over the basin, it usually remains for only short periods and is generally of small importance in the runoff picture.

General flood-producing storms are usually limited to the period from December 15 to April 1. However, maximum storms over more limited areas of the southeastern and eastern portions result from the invasion of occasional West Indian hurricanes in the late summer and fall.

HYDROLOGIC DATA

The forecasting of flows for operation of the system requires reports from an extensive network of rainfall and streamflow stations. Each morning reports are received from 190 rainfall and 41 streamflow stations. Their distribution over the Valley is shown on Plates 3 and 4. In addition, elevations and discharges are received from each hydro plant. During critical periods, additional reports during the day may be arranged for from most stations, and hydro plant elevations and discharges are available every two hours through the power dispatching office in Chattanooga.

Of the 190 rainfall stations reporting daily, 54 are at power plants and substations and are observed by TVA personnel. The remainder are distributed throughout the basin and located as well as communication facilities permit to give an accurate measure of rainfall. The majority are standard nonrecording gages, but 12 recording gages distributed throughout the Valley observe bihourly rainfall. Observers at these stations report by telephone. At certain locations in the Valley from which reports are desired, either communications or observers are not available and 22 automatic radio rain gages are in use which broadcast amounts every two hours, thus adding to the intensity network.

The 41 streamflow stations are located either on principal tributaries or on small areas which are used as an index of flow. At the majority of these, observers abstract stages from the recorder charts and report by telephone. The remaining 19 are automatic radio gages which transmit stages at two-hour intervals. Elevations are received from 10 additional stations on the main river for which daily elevation forecasts are made. Hourly discharges from 33 dams in the system complete the streamflow picture.

THE DATA-COLLECTING SYSTEM

The Hydraulic Data Branch maintains ten area offices covering the Valley. These offices serve as collecting centers for the rainfall and streamflow data for their part of the basin. Observers report to these offices early each morning. Automatic radio receivers in these offices

record the broadcasts from the radio rainfall and streamflow gages in their area. At a fixed time each morning the telephone company completes a reserved call between the area office and the forecasting office in Knoxville. On this call the area engineer transmits all of the data for his area in a period of 5 to 10 minutes. Three engineers in the Knoxville office receive the telephone calls and record them on data forms. Complete information from this part of the data-collecting system is received in a 25-minute period by 8:30 a.m.

The dispatching office of the Division of Power Operations in Chattanooga collects hourly data on elevations and discharge at each reservoir in the system. Twice daily observations of rainfall at 54 dams and substations are received. Each morning, personnel of the Hydraulic Data Branch in Chattanooga transmit this information to Knoxville by teletypewriter. Data to midnight of the preceding day are available in Knoxville by 8:00 a.m. and data for the first 6 hours of the current day are available by 8:30 a.m. During critical periods, current information on the system is obtained by telephone from the Division of Power Operations.

Rainfall reports from U. S. Weather Bureau stations are received by teletypewriter from their Knoxville office and stages on the Ohio River at Paducah and Cairo are received from the U. S. Weather Bureau at Cairo. Rainfall and stage reports from the Cumberland Basin are received from the Corps of Engineers at Nashville.

All data received in the Knoxville office are transcribed in ink on appropriate forms, with most data arranged by areas to facilitate use for forecasting. Each day's data fill eight 11" x 17" sheets. Stream stages are converted to equivalent discharge on these sheets, a rainfall map is prepared, and then a sufficient number of prints are reproduced.

FORECASTING METHODS

Runoff Graphs

The determination of the amount and distribution of runoff to be expected from a storm is based on extensive studies of back records of rainfall and streamflow. Because of the diverse character of the drainage

area, with resultant wide differences in runoff characteristics, it has been necessary to make studies, when data are available, of index areas for each individual drainage for which forecasts are required. Streamflow studies are made at U. S. Geological Survey or TVA gaging stations, at least 10 years of record being used when available. The corresponding rainfall studies are based on all standard and recording rain gages within or adjacent to the area.

The streamflow hydrograph is separated into surface-water runoff and ground-water runoff for both study and forecast purposes. Separation on the recession side is accomplished by the use of ground-water and surface-water recession curves developed from isolated storms. On the rising side, ground water is assumed to increase gradually from the start of runoff to an intersection with the ground-water recession near the point of inflection of the total hydrograph. An idealized separation is shown on Plate 5.

The study of the distribution of surface runoff is made by unit graph methods with correlation against storm duration. If separate forecasts are to be made for the station as part of the inflow to a reservoir, the unit graph ordinates are time-lagged to arrive in the reservoir. In some cases the unit graph developed for a station is used as a guide in developing a total surface-water inflow graph for a reservoir. In developing runoff graphs for large ungaged areas, use is made of a snythetic method. Runoff graphs for studied stations are correlated against the size and shape of their drainage basins. From this correlation, runoff graphs can then be developed for any size and shape of area.

For forecast purposes, ground water is also treated by unit graph methods. An average ground-water runoff graph is developed for an area and is converted into a graph for one inch of runoff.

In forecasting inflows to reservoirs, the instantaneous peak inflow is usually not significant except in the case of extreme floods. What is required is the volume of water arriving in the reservoir by calendar days. Unit graphs for both surface-water and ground-water runoff are therefore converted into daily volumes in 1000 day-second-feet and time-lagged to arrive in the reservoir by calendar days.

Rainfall-runoff Relations

The estimation of the amount of runoff which will result from a given storm or series of storms is the primary problem of forecasting. There are many factors which must be taken into account in any careful analysis of what happens to precipitation after it has fallen. The forecastor for a reservoir system, however, is faced with certain deadlines. His forecasts must be available as early as possible to ensure their maximum usefulness for operation. This is particularly true during flood periods. Information on the flows and stages resulting from the scheduled operation must be made available as early as possible to persons affected. This requires some compromise between accuracy and speed.

TVA is at present changing its method of estimating runoff from rainfall. The original method used correlated runoff with base flow, or the rate of ground-water flow at the beginning of a storm, as an index. In some cases the number of days since the last rain was used as an auxiliary index. This method has proved reasonably satisfactory but it involves current separation of the streamflow hydrograph to determine the rate of ground-water flow. This is time-consuming and quite approximate during complex storms.

The method being adopted is the API, or antecedent precipitation index method, which is now in general use by the U. S. Weather Bureau and others. Rainfall and runoff are correlated against rainfall which has fallen prior to a given storm, weighted in accordance with the number of days since occurrence. In practice, it is a simple index to use since each day's index is 10 percent smaller than that for the day before. When precipitation occurs, its amount is added to the current day's index and the new total is reduced 10 percent for the next day. The other factor in the correlation is season. The amount of runoff from a given rainfall varies considerably between winter and summer for the same index. However, the progression of the seasonal effect is fairly regular from year to year and the introduction of a week number into the correlation makes a reasonably satisfactory adjustment. Additional correlation with intensity has generally not improved results in our studies, and adjustments for extremely high or low rates of precipitation are left to the judgment of the forecastor. Plate 6 illustrates a two-quadrant rainfall-runoff relation in

graphical form. Our studies indicate that the API correlation on the average will give slightly better results than base flow. In addition it is a simpler, faster, and more positive method to use.

FORECASTING PROCEDURES

Since speed is important in the making of a forecast, procedures are set up to make forecasting operations as simple as possible. Forms for incoming data are arranged to facilitate both the receipt and transcription of the data and its use for forecasting. The use of a rapid reproducing machine in the office makes data available quickly in as many copies as needed. Average daily rainfall for a given reservoir drainage is computed on a form which has weighting factors already inserted. Below this average, the computation of the daily API value is made. The runoff relation is set up in tabular form and the forecastor enters with the API value, the week-of-the-year number, and the average rainfall and obtains corresponding values of surface-water and ground-water runoff in inches. The inflow forecasting forms for the reservoirs have daily volume factors corresponding to one inch of runoff for four to eight starting times. The runoff value, previously obtained, is entered opposite the factors for the appropriate time, and slide-rule multiplication gives the volume to be expected from the current storm. Vertical addition of these values for surface water, ground water, and the previous recession gives the total inflow volumes by days to the reservoir. Plate 7 is a copy of the form used in computing inflows to Norris Reservoir. For routing purposes, flows and elevations for the main-river reservoirs are assembled on a single form by days, and in order as they arrive into the system in a downstream sequence. This includes the lagged arrivals from the tributary reservoirs in addition to the local inflows to each main-stream reservoir.

Final figures for all reservoirs are assembled on appropriate forms for transmission to the Division of Power Operations, for preparation of the Daily River Bulletin, and for transmission to the U. S. Weather Bureau and other interested agencies.

Reservoir Routing

TVA's tributary reservoirs are all of such depth compared to rate of flow that for all practical purposes they can be considered flat pools and routing is accomplished by using level storage tables. This is also true of our main-river reservoirs for flows of about turbine capacity or less. For higher flow, however, the amount of storage between level pool and the backwater curve becomes appreciable and must be accounted for. In Wheeler Reservoir, for example, the controlled level storage space between the normal minimum level of elevation 550 and the top of gates at elevation 556.3 is 347,000 acre-feet. With 250,000 cubic feet per second flowing through the reservoir, the volume under the profile above elevation 556.3 is 410,000 acre-feet. This profile condition is illustrated on Plate 8. The routing procedure must allow for this volume as it goes into storage on rising flows and comes out of storage on falling flows.

The method used is dictated in part by the necessity for speed and requires a simple procedure. Storage curves have been developed from observed profiles for past floods. Storages are correlated against headwater elevation at the dam and tailwater elevation at the upstream dam with a correction diagram to adjust for changing stage at the upstream tailwater. These curves are used to determine observed storages. For routing purposes, discharge curves corresponding to the average rating for the upstream tailwater are superimposed on the storage diagram and the outflow from the upstream dam is then used as the parameter to determine volume under the backwater curve. This parameter must be lagged in time to make allowance for the loop in the rating curve. In routing, all quantities are known or estimated except the ending headwater and average outflow. Fixing either of these quantities fixes the other and gives a quick positive solution. Plate 9 is a copy of the storage curves used for routing flows through Wheeler Reservoir.

Routing through the 184 miles of Kentucky Reservoir is a special problem. Treating the reservoir as a simple reach does not give satisfactory accuracy of results. In addition, forecasts at intervening points in the reservoir are desired for navigation and other purposes. For routing purposes, therefore, the reservoir is divided into three reaches using slope ratings at the two intermediate reach ends. Routing is then

accomplished by a cut-and-try procedure until a satisfactory profile and storage are achieved.

Forecasting and Water Dispatching

Forecasts of inflow for 4 to 10 days in advance are needed daily for 31 reservoirs in the TVA-Alcoa system. In addition, inflows to three Corps of Engineers reservoirs in the Cumberland River Basin, which TVA operates for power, are also required. To make these forecasts, to aid in the scheduling of water use at each of these plants, to issue river bulletins and flood warnings, and to perform the operation in a limited time requires a moderate-sized staff and planned scheduling of work. At present, 14 engineers are engaged in the forecasting and water dispatching program.

Reservoirs are grouped by drainage basins and assigned to individual engineers. For instance, part of one engineer's assignment is the Holston River reservoirs. This includes inflow forecasts for South Holston, Watauga, Boone, Fort Patrick Henry, and Cherokee Reservoirs. In addition, he forecasts the effect of scheduled releases from each reservoir at the downstream plants. Similar groups of tributary and main-stream reservoirs are assigned to other engineers. Assignments are rotated from week to week to keep the forecastors familiar with the entire system.

In addition to the dispatching of water, one engineer handles the correlation of the daily power load, which is received from the Division of Power Operations in Chattanooga, with the scheduling of releases from each of the dams. During flood periods, the timing and amounts of spillway discharge necessary to carry out the current water control operation are transmitted to the Division of Power Operations in Chattanooga for execution.

DISSEMINATION OF INFORMATION

Large numbers of persons, both within and without TVA, are directly concerned with, or at least interested in, the observed and predicted elevations and flows at our reservoirs or at other pertinent locations in the Valley. To meet this need, several means of dissemination are utilized. A Daily River Bulletin is issued in cooperation with the U. S. Weather Bureau

which gives observed data for the past 24 hours for 47 points in the Valley and predictions for the following three days for 45 locations. Included are observed temperatures for selected stations and 24-hour weather and temperature forecasts. Plate 10 shows a typical copy of this bulletin. Observed and predicted stages for about 40 locations are also furnished to the U. S. Weather Bureau for publication by newspapers and for radio broadcast. Information on our operations which will affect the Ohio River are also sent by teletypewriter to the U. S. Weather Bureau at Cairo and the Corps of Engineers at Cincinnati.

QUANTITATIVE WEATHER FORECASTS

TVA has an agreement with the U. S. Weather Bureau under which it is furnished quantitative forecasts of precipitation over the various subdivisions of the basin either two or three times daily. A preliminary forecast is received at 8:00 a.m. giving a specific forecast for the next 36 hours plus an outlook for the following 24. The regular forecast based on later data is received about 11:00 a.m. and gives a specific forecast for the next 36 hours and an outlook for the following 3 days. During critical periods, a supplementary forecast is received at 9:00 p.m. covering the next 24 hours. These forecasts are very valuable in setting up water dispatching schedules for the system, particularly in making advance drawdown of main-river reservoirs for either flood control or power. During flood periods, depending upon conditions at the time, the forecast amounts may be used to predict additional runoff. This prediction is then used either to determine its effect upon the operation in progress or possibly to set up the actual operation.

CONCLUSION

The daily sequence of events is much the same throughout the year except that activity is much intensified during storm periods. At 7:30 in the morning, the previous day's system information is received by teletype. At 8:00 comes the first weather forecast. At 8:05 the rainfall and streamflow data collected at area offices begin to come in by telephone. At 8:10, contact is made with the Division of Power Operations in

Chattanooga to obtain hourly discharge schedules and, if it is the beginning of a flood period, instructions are given to them for discharge increases at main-stream dams. Incoming data are entered on forms and a rainfall map is prepared. Copies of data are distributed to the engineers making forecasts and to the River Control Engineer. Pertinent observed information is transmitted to the U. S. Weather Bureau at Knoxville and Cairo and during flood periods to the Corps of Engineers, Cincinnati. The observed data portion of the Daily River Bulletin is prepared for publication. At 9:15 a second contact is made with the Division of Power Operations to discuss the amount and distribution of power requirements for the current and succeeding days. Meanwhile, the incoming data are being analyzed and inflow forecasts are prepared for each reservoir. A tentative schedule of tributary releases is set up to meet power and other requirements. The main-river routing form is prepared showing local inflows to each reservoir and the arrival of water from tributary reservoirs. If it is a period of normal flow, elevations and discharges are set to carry out the current operating plan and tributary releases are adjusted to balance out the over-all hydro power load. If it is a period of excess or flood flows, a routing is made through the reservoirs under the direction of the Chief of the River Control Branch to carry out the desired operation for flood control. The arrival of the regular weather forecast about 11:00 a.m. may require some last-minute adjustments in the operation. Schedules of required discharges at each plant are transmitted to the Division of Power Operations in Chattanooga for execution. The predicted data portion of the Daily River Bulletin is prepared and the bulletin is issued. Pertinent data on the planned operation are transmitted to the U. S. Weather Bureau at Knoxville and Cairo and to the Corps of Engineers at Cincinnati. By this time it is usually noon.

During a flood period, if rain is in progress, a rainfall check at hydro plants and substations is made about noon. This may require an early afternoon revision in the routing of flows through the main river. A complete check of the rainfall and streamflow network may be made around 6:00 p.m. and this, combined with a supplementary weather forecast at 9:00 p.m., may require further revision in inflow estimates and a change in the operation. If it involves a change in the outflow into the Ohio River, the U. S. Weather Bureau at Cairo and the Corps of Engineers at Cincinnati must be notified.

Forecasting and water dispatching for a system such as that of TVA is a continuous process. Complete forecasts for the system are made five days a week. Main-river inflows are revised on Saturdays. A check on main-river inflows is made on Sundays. During flood periods, it becomes a seven-day job with nightly revisions when necessary. Because prompt forecasts are necessary, some accuracy must be sacrificed and accuracy must be regained by subsequent revisions. Streamflow forecasting is not an exact science. It is based on empirical relations which the forecastor must use with some judgment. But reasonably accurate forecasts are a "must" in the operation of a reservoir system.

TENNESSEE VALLEY REGION

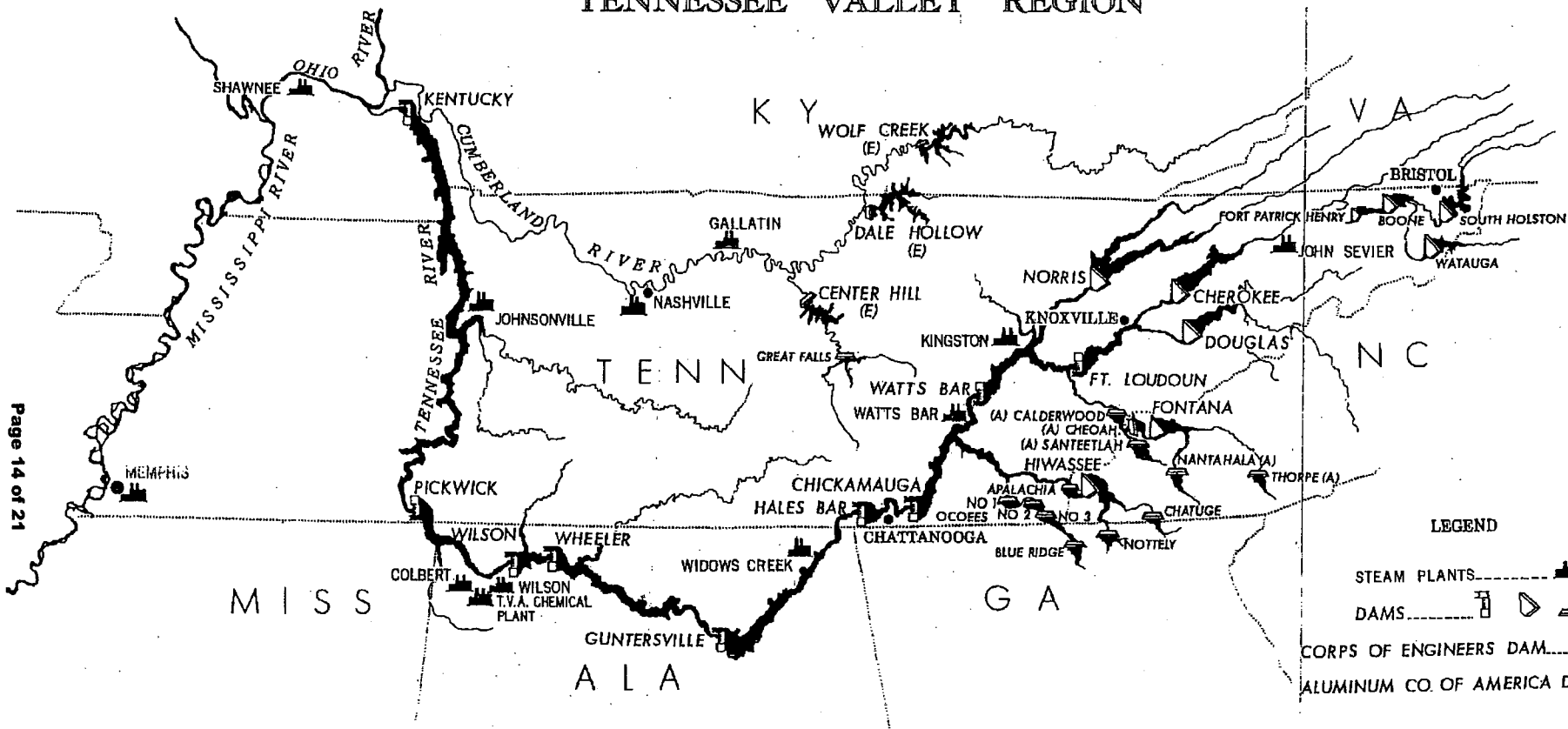

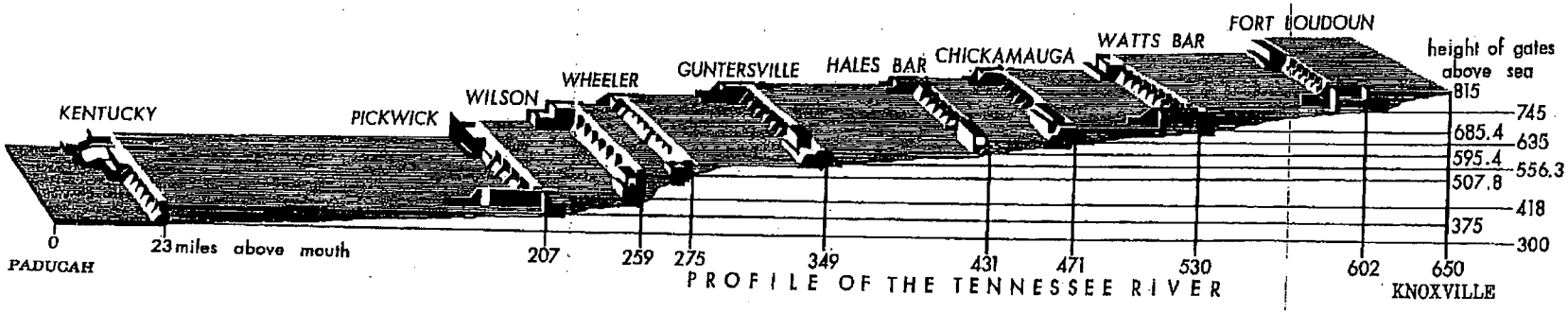

PLATE I

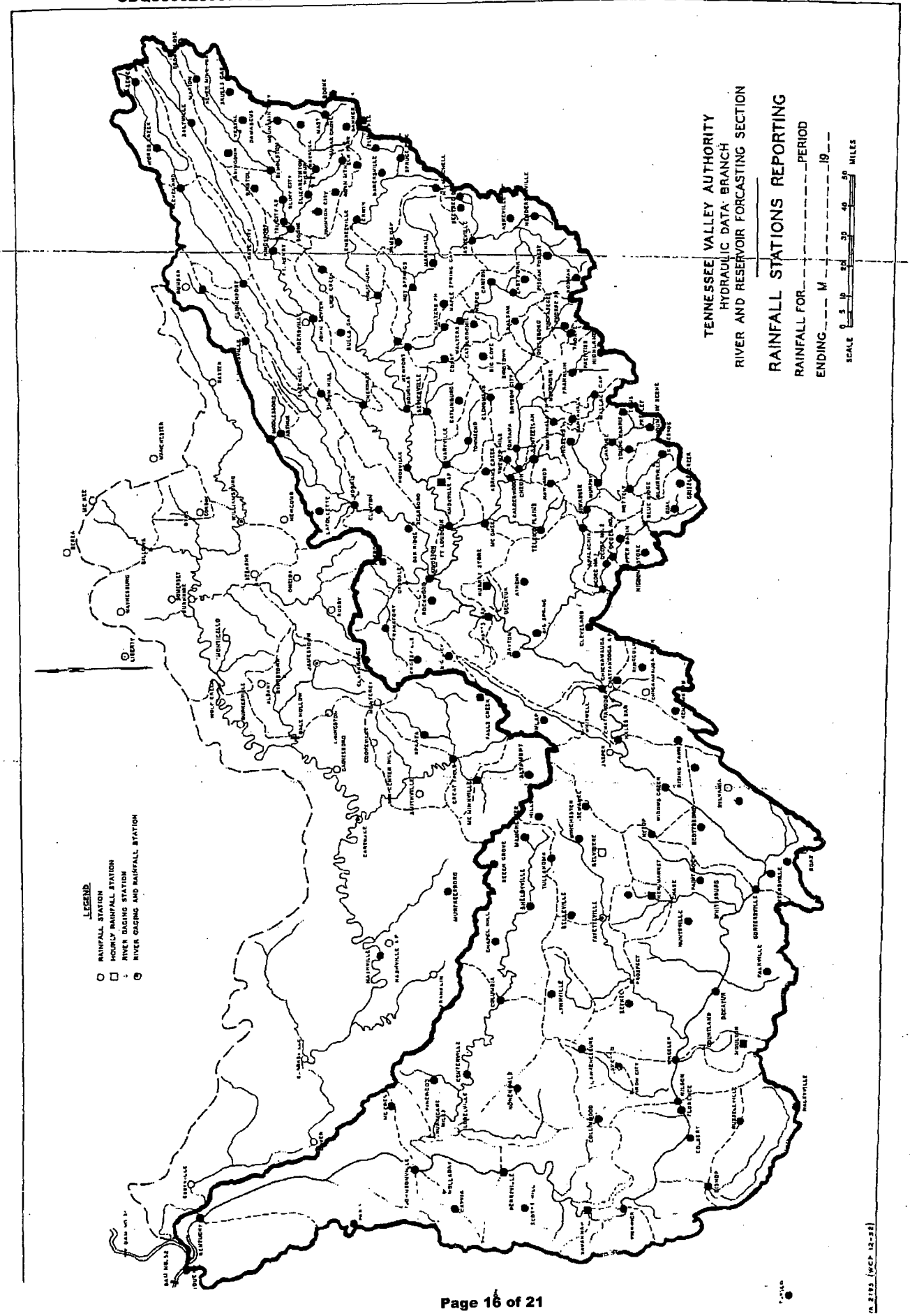
TENNESSEE VALLEY AUTHORITY
HYDRAULIC DATA BRANCH
RIVER AND RESERVOIR FORCASTING SECTION
RAINFALL STATIONS REPORTING
RAINFALL FOR_____PERIOD
ENDING_____M_____19__
SCALE 0 5 10 20 30 40 50 MILES
LEGEND
RAINFALL STATION
HOURLY RAINFALL STATION
RIVER GAGING STATION
RIVER GAGING AND RAINFALL STATION

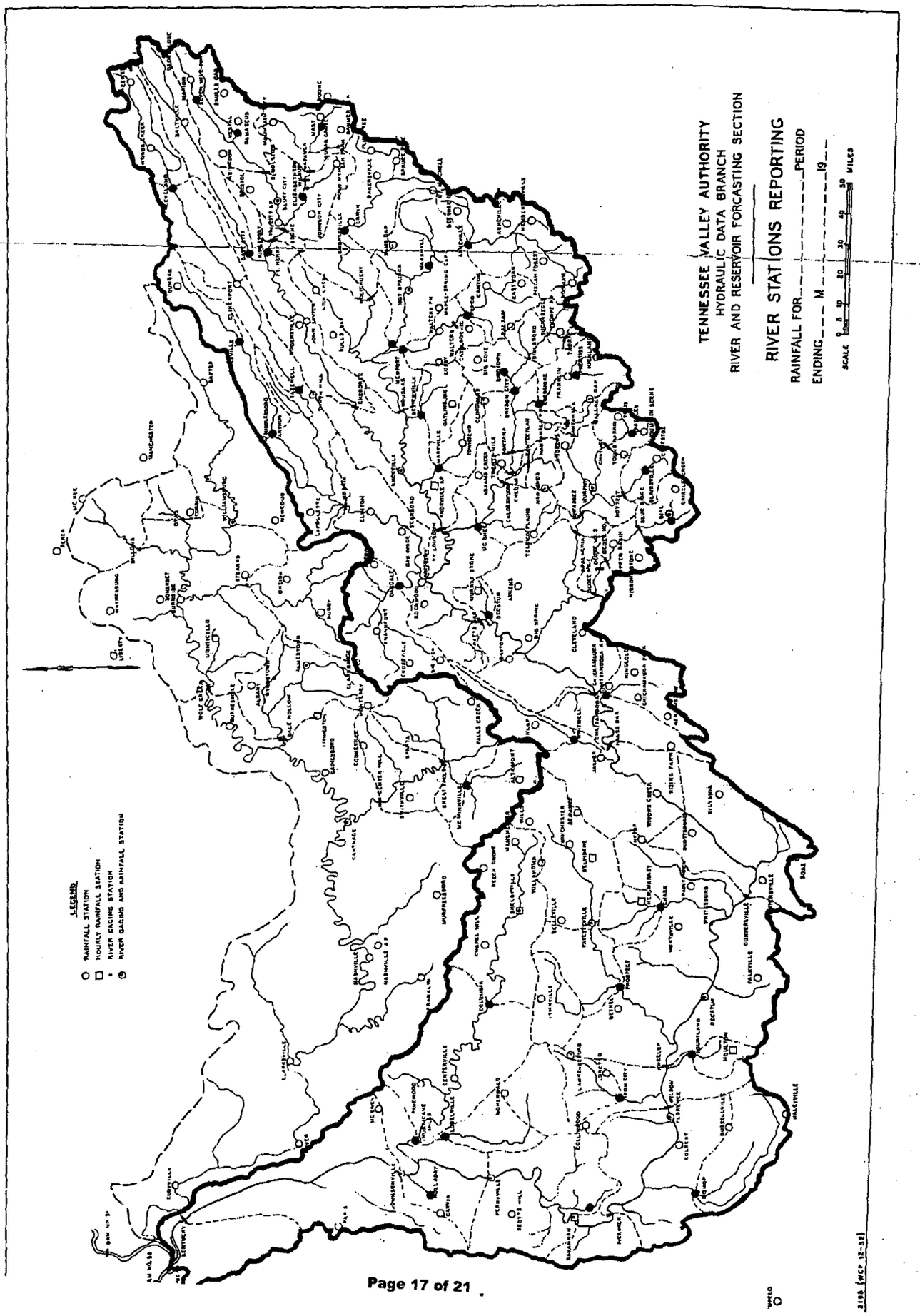
TENNESSEE VALLEY AUTHORITY
HYDRAULIC DATA BRANCH
RIVER AND RESERVOIR FORCASTING SECTION
RIVER STATIONS REPORTING
RAINFALL FOR_____PERIOD
ENDING___M___19__
SCALE 0 5 10 20 30 40 50 MILES
LEGEND
RAINFALL STATION
HOURLY RAINFALL STATION
RIVER GAGING STATION
RIVER GAGING AND RAINFALL STATION

PLATE 5

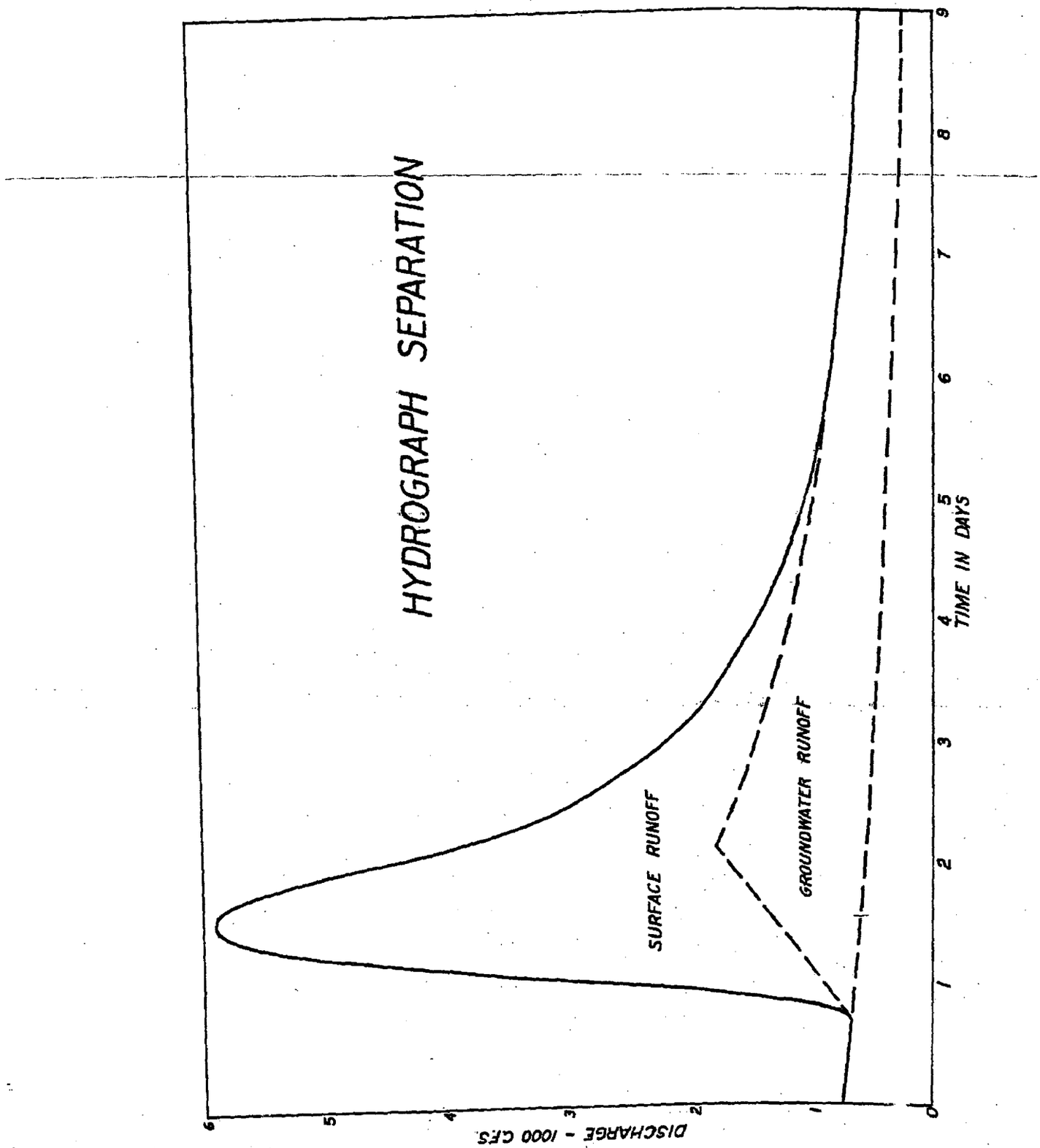
HYDROGRAPH SEPARATION
SURFACE RUNOFF
GROUNDWATER RUNOFF
DISCHARGE - 1000 CFS
TIME IN DAYS
0
1
2
3
4
5
6
7
8
9

PLATE 6

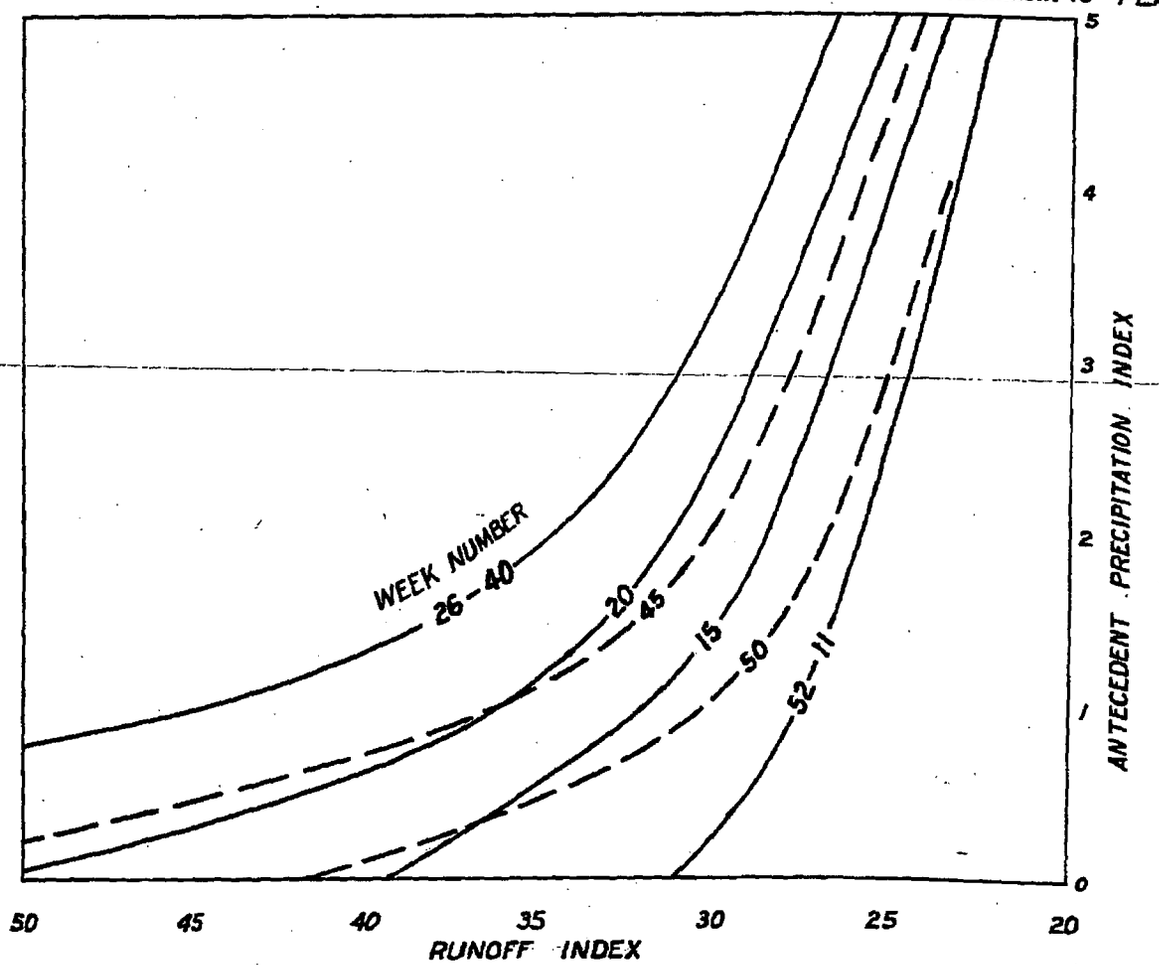

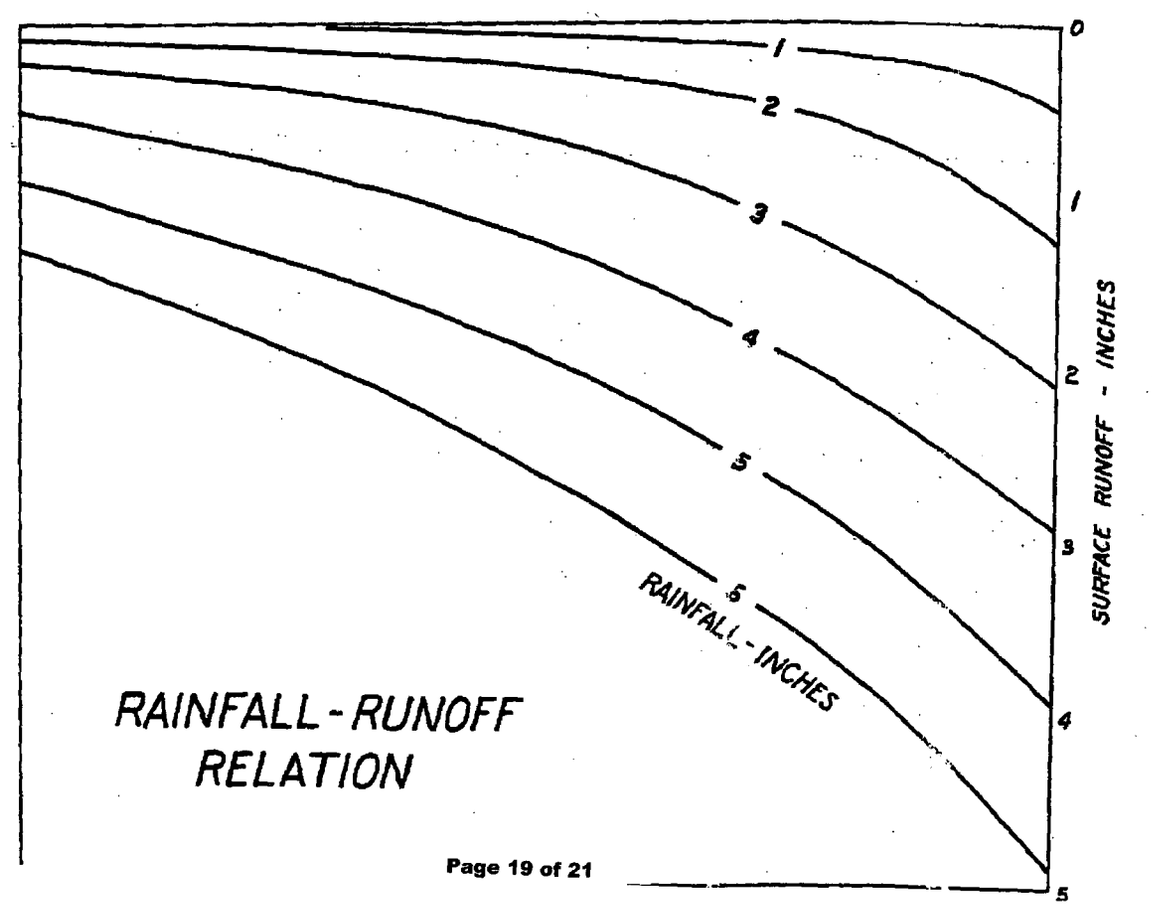

RAINFALL - RUNOFF RELATION

Tennessee Valley Authority — NORRIS RESERVOIR — Hydraulic Data Branch

Basis of Forecast: — FORECAST OF INFLOWS BY DAYS IN 1000 DAY-SECOND-FEET — Computed:

6-HOUR STORM — Date:

DATE										
REACH	Rise Began	Rain (IGW)	Runoff Inches	Fact. Flow	Fact. Flow	Fact. Flow	Fact. Flow	Fact. Flow	Fact. Flow	Fact. Flow
	4a			0	0.2	6.2	4.5	1.7	0.8	0.4
ABOVE CLEVELAND	8a			0	0	5.1	5.3	2.0	0.9	0.5
Surface Runoff	12m			0	0	3.8	6.1	2.4	1.0	0.5
DA-528 Sq. Mi.	4p			0	0	2.4	6.7	2.8	1.1	0.6
Lag-36 Hours	8p			0	0	1.5	7.0	3.3	1.3	0.6
	12p			0	0	0.6	6.8	3.9	1.5	0.7
CLEVELAND TO	4a			1.5	10.5	8.2	2.8	1.2	0.6	0.4
TAZEWELL	8a			0.7	8.9	9.8	3.2	1.4	0.7	0.4
Surface Runoff	12m			0.2	7.0	11.2	3.9	1.6	0.8	0.4
DA-946 Sq. Mi.	4p			0	5.2	12.0	4.6	1.8	0.9	0.5
Lag-4 Hours	8p			0	3.7	12.1	5.6	2.1	1.0	0.5
	12p			0	2.5	11.6	6.8	2.4	1.1	0.6
ABOVE TAZEWELL	12m			0.1	0.9	2.0	2.9	2.8	2.4	2.1
Ground-Water R.O.	12p			0	0.4	1.5	2.6	2.9	2.6	2.3
	4a			0	2.8	3.9	1.2	0.4	0.2	0
ABOVE JONESVILLE	8a			0	1.6	4.8	1.4	0.5	0.2	0.1
Surface Runoff	12m			0	0.8	5.2	1.7	0.6	0.2	0.1
DA-319 Sq. Mi.	4p			0	0.2	5.2	2.1	0.7	0.3	0.1
Lag-24 Hours	8p			0	0	4.7	2.6	0.8	0.3	0.1
	12p			0	0	3.9	3.2	1.0	0.4	0.1
JONESVILLE TO	4a			2.0	4.2	1.9	0.9	0.5	0.3	0.1
ARTHUR	8a			1.1	4.6	2.1	1.1	0.6	0.3	0.1
Surface Runoff	12m			0.4	4.8	2.4	1.2	0.6	0.3	0.1
DA-366 Sq. Mi.	4p			0.1	4.5	2.7	1.3	0.7	0.4	0.2
Lag-4 Hours	8p			0	3.8	3.2	1.5	0.8	0.4	0.2
	12p			0	2.9	3.6	1.6	0.8	0.5	0.2
ABOVE ARTHUR	12m			0	0.5	1.2	1.4	1.2	1.1	0.9
Ground-Water R.O.	12p			0	0.2	0.8	1.4	1.3	1.1	1.0
ARTHUR-TAZEWELL-	4a			11.2	5.1	1.6	0.8	0.4	0.1	0
NORRIS LOCAL AREA	8a			9.3	6.6	1.9	0.9	0.4	0.2	0
Surface Runoff	12m			6.2	9.1	2.2	1.0	0.5	0.2	0
DA-716 Sq. Mi.	4p			2.5	12.2	2.7	1.1	0.5	0.2	0
No Lag	8p			0.4	13.4	3.2	1.3	0.6	0.3	0.1
	12p			0	12.7	4.0	1.4	0.7	0.3	0.1
LOCAL AREA	12m			0.2	1.5	1.5	1.3	1.1	1.0	0.9
Ground-Water R.O.	12p			0	0.8	1.6	1.4	1.2	1.1	1.0
Previous Recession										
Rain on Reservoir										
Total Inflow (12p-12p)										

TVA 5389 (WCP-2-55)

PLATE B

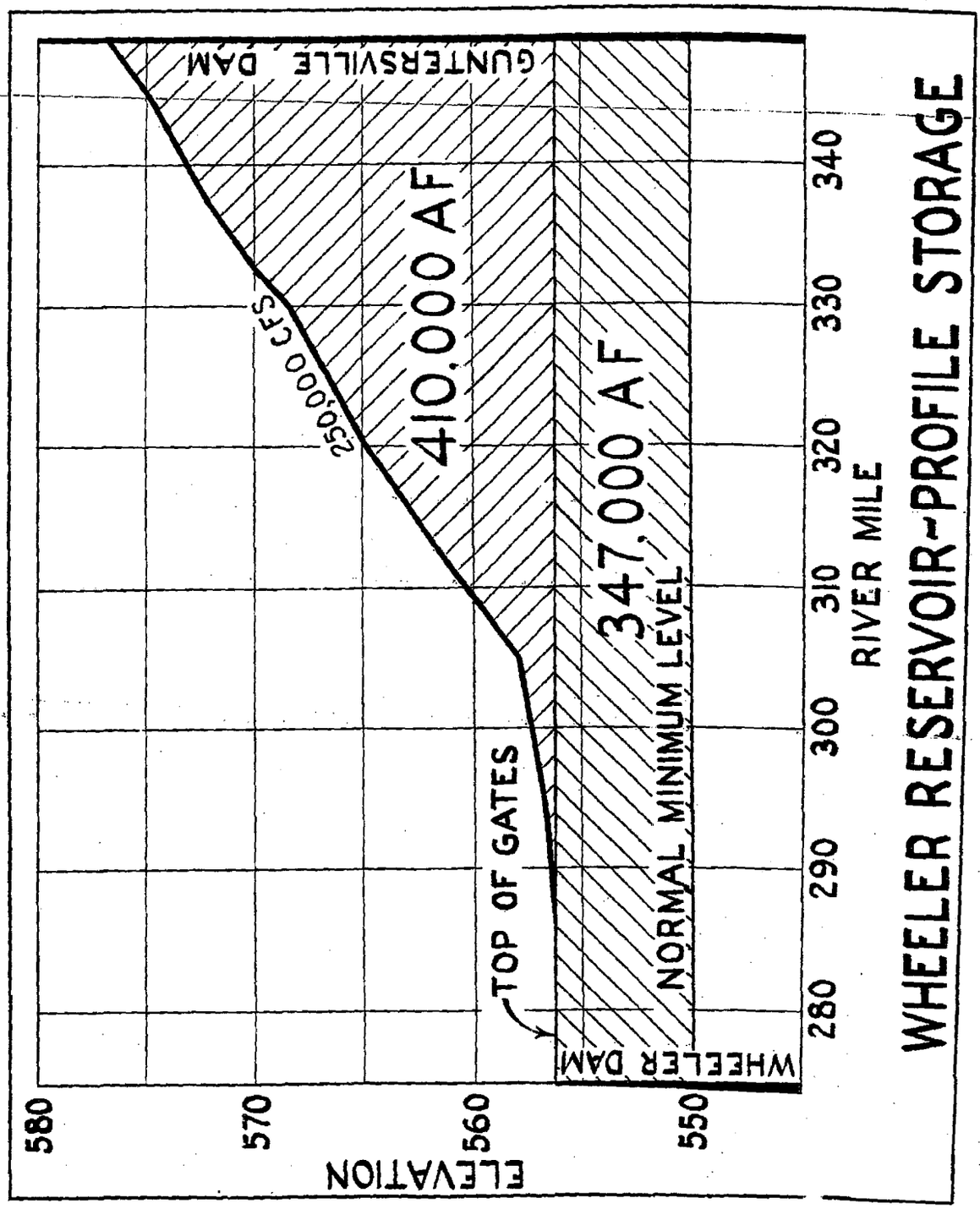
WHEELER RESERVOIR-PROFILE STORAGE
ELEVATION
580
570
560
550
RIVER MILE
340
330
320
310
300
290
280
GUNTERSVILLE DAM
WHEELER DAM
TOP OF GATES
NORMAL MINIMUM LEVEL
347,000 AF
410,000 AF
250,000 CFS

the foregoing description should aid in understanding the relative time variations of hydrologic phenomena which are important in considering the runoff relations discussed later in the chapter.

ESTIMATING THE VOLUME OF STORM RUNOFF

Despite the complex nature of the rainfall-runoff process, the practice of estimating runoff as a fixed percentage of rainfall is the most commonly used method in design of urban storm-drainage facilities, highway culverts, and many small water-control structures. The method can be correct only when dealing with a surface which is completely impervious so that the applicable runoff coefficient is near 1.00.

Computer simulation techniques (Chap. 12) offer the most reliable method of computing runoff from rainfall because they permit a relatively detailed analysis using short time intervals. The type of analysis used in computer simulation would be virtually impossible to carry through by hand because of the detailed computations required. The constraints of hand calculation led to methods using longer time intervals and a correspondingly less rigorous model. The following sections discuss some of the more successful approaches.

8-4 Initial Moisture Conditions

The quantity of runoff from a storm depends on (1) the moisture conditions of the catchment at the onset of the storm and (2) the storm characteristics—rainfall amount, intensity, and duration. The storm characteristics are defined by the data from the precipitation-gage network, but no single observation serves to define the antecedent moisture conditions. Much of the investigation of rainfall-runoff relations was directed at finding a simple index of basin moisture conditions.

In humid areas, where streams flow continuously, groundwater discharge at the beginning of the storm has been found to be a good index to initial moisture conditions. In a study of the Valley River, North Carolina, Linsley and Ackermann [26] found that field-moisture deficiency at any time was approximately equal to 90 percent of the total Class A pan evaporation since the ground was last saturated less any additions made to field moisture by intervening rains. Basin-accounting techniques (Sec. 5-15) applied on a daily basis provide a reasonably accurate estimate of moisture deficiency which can be used as an index to runoff [27].

The most common index is based on antecedent precipitation. The rate at which moisture is depleted from a particular basin under specified meteorological conditions is roughly proportional to the amount in storage (Sec. 5-15). In other words, the soil moisture should decrease logarithmically with time during periods of no precipitation [28],

Soil moisture

$$I_t = I_0 k^t \tag{8-7}$$

where I_0 is the initial value of the *antecedent-precipitation index*, I_t is the reduced value t days later, and k is a recession factor ranging normally between 0.85 and 0.98. Letting t equal one gives

$$I_1 = kI_0 \tag{8-8}$$

Thus, the index for any day is equal to that of the previous day multiplied by the factor k. If rain occurs on any day, the amount of rain is added to the index (Fig. 8-4). Since storm runoff does not add to the residual moisture of the basin, an index of precipitation minus runoff, i.e., *basin recharge*, should be more satisfactory than the precipitation index alone. Commonly, however, the minor improvements gained do not justify the added computation.

Equation (8-7) assumes that the daily depletion of soil moisture (primarily evapotranspiration) is

$$I_0 - I_1 = I_0(1 - k) \tag{8-9}$$

Since actual evapotranspiration is a function of the potential value and the available moisture (I_0), k should be a function of potential evapotranspiration. The variation in potential evapotranspiration is largely seasonal, and Eq. (8-7) has been found to be reasonably satisfactory when used jointly with calendar date (Sec. 8-6). There is an added advantage in using the date as a parameter because it also reflects variations in surface conditions related to farming practices, stage of plant growth, etc.

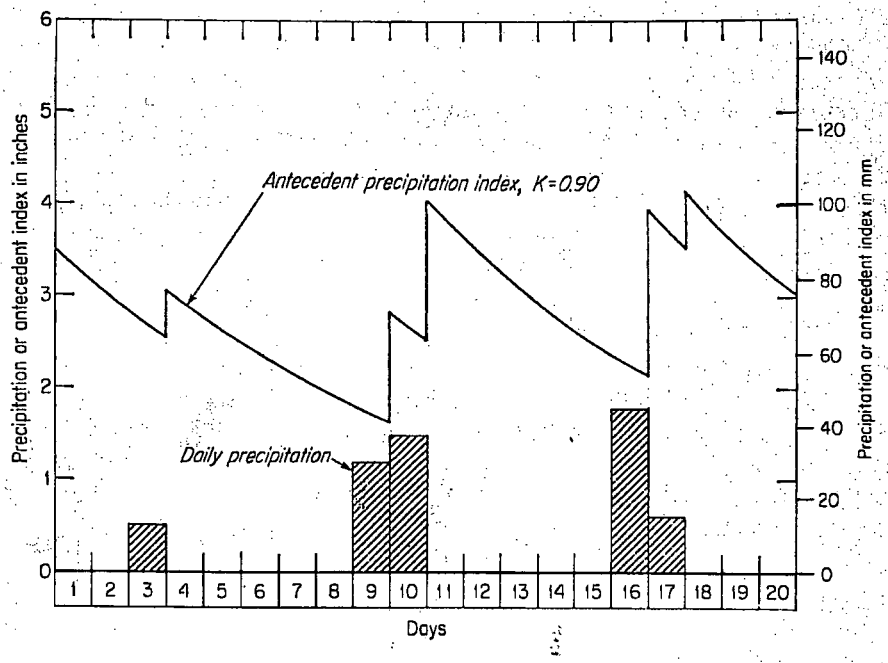

Figure 8-4 Variation of antecedent precipitation index with daily rainfall.

The value of the index on any day theoretically depends on precipitation over an infinite antecedent period, but if a reasonable initial value is assumed, the computed index will closely approach the true value within a few weeks. The index value applicable to a particular storm is taken as that at the beginning of the first day of rain. Thus a value of 1.8 in would be used for the storm of the ninth and tenth in Fig. 8-4.

8-5 Storm Analysis

In any statistical correlation, it is extremely important that the basic data be as consistent and reliable as possible. The consistency tests for precipitation data discussed in Sec. 3-10 should be applied whenever the normal annual precipitation varies appreciably over the catchment. The streamflow records should be carefully reviewed in each case (Sec. 4-16) and adjustments made if necessary.

Methods of storm analysis should be rigorous and objective. Only that storm rainfall which produced the runoff being considered should be included. Small showers occurring after the hydrograph had started to recede should not be included if they had little effect upon the amount of runoff. Similarly, showers occurring before the main storm should be excluded from the storm rainfall and included in the antecedent-precipitation index. Long, complex storms should be separated into as many short storm periods as possible by hydrograph analysis.

Runoff also depends upon rainfall intensity, but for basins of 250 km^2 (100 mi^2) or more, an average intensity as reflected by amount and duration is usually adequate. In this case duration can be estimated with sufficient accuracy from 6-hr rainfall data. An objective rule is preferable, such as "the sum in hours of those 6-hr periods with more than 5 mm (0.2 in) of rain plus one-half the intervening periods with less than 5 mm (0.2 in)." Although experimental infiltration data indicate rates commonly in excess of 2.5 mm/hr (0.1 in/hr), relations such as Fig. 8-5 consistently show the effect of duration on storm runoff to be of the order of 0.25 mm/hr (0.01 in/hr). The difference is largely caused by intercorrelations and the inclusion of interflow with surface runoff.

8-6 Multivariate Relations for Total Storm Runoff

If storm characteristics and basin conditions are to be represented adequately in a runoff relation, a number of independent variables must be included. The relationship is not an additive one, and the usual multivariate linear correlation is not satisfactory. The coaxial graphical method† of correlation was first shown to be particularly useful for this work [28]. Betson et al. [29] subsequently demonstrated an analytical correlation technique.

† Graphical correlation methods were presented in Appendix A of previous editions. Increasing availability of computers has resulted in restricted use of graphical techniques, and the detailed presentation of such methods is now considered unjustified.

To illustrate the coaxial method assume that a relation for estimating storm runoff is desired, using antecedent precipitation, date (or week number), and rainfall amount and duration as variables. Values of these variables are compiled for 50 or more storms. With the exception of rainfall amount, the variables should be more closely related to the fraction of rainfall which does not run off than to the runoff volume. It is therefore convenient to calculate an auxiliary variable equal to the storm rainfall minus the storm runoff. This variable is called the *recharge* in the subsequent discussion. Once a satisfactory relation for estimating recharge is completed, it is a simple matter to revise the precipitation quadrant (chart *C*) so that the final answer is in terms of runoff since rainfall minus recharge should equal runoff. Equations (8-10) and (8-11) show that the correlation can be made to yield runoff, even though the season quadrant is unchanged from that based on recharge.

A three-variable relation is developed first (Fig. 8-5, chart *A*) by (1) plotting antecedent precipitation versus recharge, (2) labeling the points with week

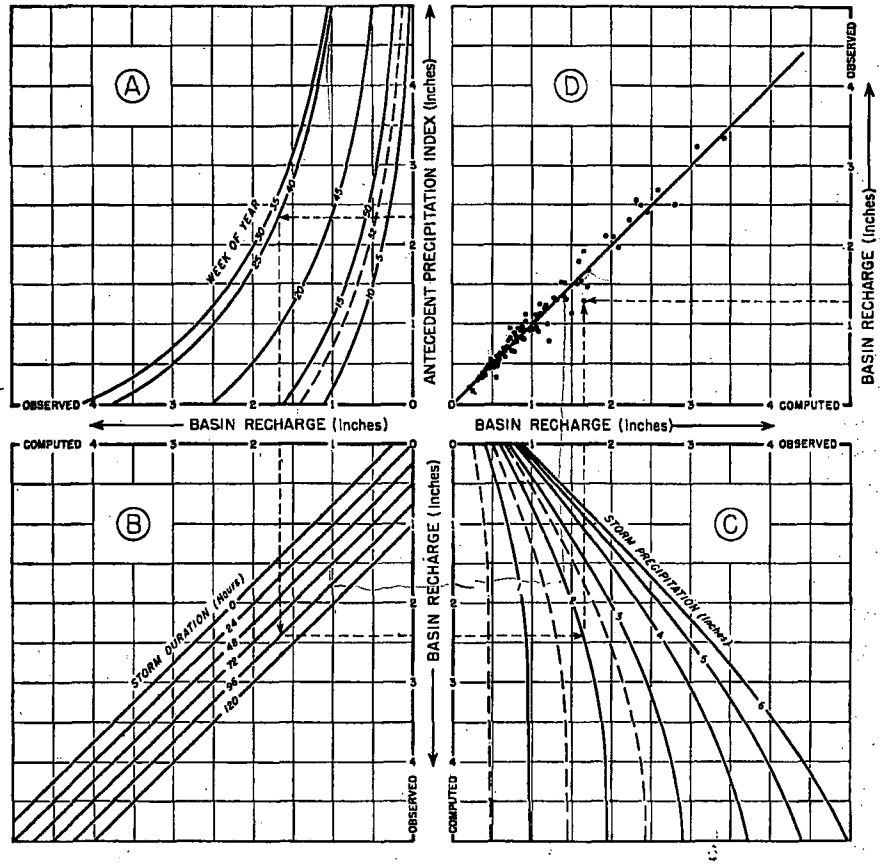

Figure 8-5 Basin-recharge relation for Monocacy River at Jug Bridge, Maryland. (*U.S. National Weather Service.*)

number, and (3) fitting a smooth family of curves representing the various weeks. Chart B is placed with its horizontal scale matching that of chart A to facilitate plotting. Points are plotted in chart B with observed recharge as ordinate and recharge computed from chart A as abscissa, and these points are labeled with duration. A family of smooth curves is drawn to represent the effect of duration on recharge. Charts A and B together are a graphical relation for estimating recharge from antecedent index, week, and duration. Storm precipitation is then introduced (chart C) by (1) plotting recharge computed from charts A and B against observed recharge, (2) labeling the points with rainfall amount, and (3) fitting a family of curves. Charts A, B, and C constitute the *first approximation* to the desired relation. Chart D indicates the overall accuracy of the derived charts.

Since the variables are intercorrelated and the first charts are developed independently of factors subsequently introduced, revision of the charts may improve the overall relation. The process is one of successive approximations. To check the week curves, the other curve families are assumed to be correct and the adjusted abscissa for a point in chart A is determined by entering charts B and C in reverse order with observed recharge, rainfall amount, and duration. The ordinate for the adjusted point is the observed antecedent-precipitation index. In other words, the week curves should be revised to fit this adjusted point if the relation is to yield a computed recharge equal to the observed recharge. The second (and subsequent) approximations for duration and rainfall are made in the same manner. In each case the points are plotted by entering the chart sequence from both ends with observed values to determine the adjusted coordinates.

Although the method presented in the previous paragraphs is general and can be used as described, certain modifications simplify the procedure and require fewer approximations. Since storm rainfall is extremely important, the first plotting of chart A may show little correlation and the construction of the curves will be difficult. However, an important advantage in having the rainfall parameter in the last chart is that the possibility of computing runoff in excess of rainfall or of computing negative values of runoff is eliminated. Moreover, the arrangement of Fig. 8-5 results in the determination of a unified index of moisture conditions in the first chart, which is a decided advantage in river forecasting. If the plotting of chart A is limited to storms having rainfall within a specified class interval (2 to 4 in, for example), the construction of the curves is simplified, provided that there are sufficient data. Only limited data are required since the general curvature and convergence are always as shown in the example. The relations are quite similar throughout a geographic region, and charts A and B for one basin may be used as a first approximation for another basin in the area.

One analytical technique [29] uses the equations

$$I_{ps} = c + (a + dI_s)e^{-bI} \tag{8-10}$$

$$Q = (P^n + I_{ps}^n)^{1/n} - I_{ps} \tag{8-11}$$

where I_{ps} is a runoff index approximating the first quadrant of a coaxial plot, I_s is a fixed function of week number ranging between $+1$ and -1, I is the antecedent-precipitation index, e is the base of napierian logarithms, P is storm rainfall, Q is direct runoff, and a, b, c, d, and n are statistically derived coefficients. With only five constants the functions are quickly derived on a computer but are more constrained in form than the graphical solution. In comparative tests on catchments in the Tennessee River basin, the analytic method gave results generally slightly better than the graphical method. McCallister [30] describes another method of using the computer to develop a runoff relation based on the variables used in the coaxial method.

Since it is impossible to segregate the water passing a gaging station according to the portion of the basin in which it fell, statistical runoff relations must be based on basin averages of the variables. Unfortunately, a relation based on storms of uniform areal distribution will yield runoff values which are too low when applied to storms with extremely uneven distributions. This can be demonstrated by computing the runoff for 4, 6, and 8 in of rainfall, assuming all other factors remain fixed. While 6 is the average of 4 and 8, the average runoff from the 4- and 8-in rainfalls is not equal to that from a 6-in rain. An uneven distribution of antecedent precipitation produces similar results. Runoff relations based on uniform areal conditions can be used to compute the runoff in the vicinity of each rainfall station, and the average of these runoff values will, in general, more nearly approach the observed runoff from the basin when either the storm or the antecedent precipitation is quite variable.

8-7 Relations for Incremental Storm Runoff

In order to determine increments of runoff throughout a storm for application of a unit hydrograph, Fig. 8-5 may be used with accumulated rainfall up to the end of each period and the successive values of runoff subtracted to obtain increments. When applied to small catchments, however, there is a marked tendency to underestimate the peak flows, because the relation does not properly account for the time distribution of rainfall. Some of the errors for larger basins are certainly caused by the same factor.

The principal problem in developing an incremental runoff relation lies in our inability to determine short-period increments of runoff by hydrograph analysis. A process of successive iterations has been proposed [31], and another approach [32] modifies the relation for total storm runoff by introducing a second (short-term) antecedent precipitation index as illustrated in Fig. 8-6. Since duration is constant for an incremental relation (6-hr, for example), this factor can be eliminated by making suitable adjustments in one of the other quadrants. In comparing Fig. 8-6 with Fig. 8-5, it will be seen that the duration quadrant has been replaced by one for the short-term (retention) index, and that the precipitation quadrant has been converted to one yielding runoff instead of recharge. It has been found that the function for the retention quadrant can be assumed as

$$I_{psr} = I_{ps}(B)^{I_r} \tag{8-12}$$

where B is a constant less than unity, I_{ps} is the runoff index from the season quadrant, and I_{psr} is the integrated index reflecting also the retention index I_r.

Two coefficients must be evaluated for the retention index quadrant—the recession factor for computing I_r [corresponding to k in Eq. (8-8)] and B in Eq. (8-12). This is accomplished by a trial-and-error procedure. Using assumed values of B, incremental runoff is computed and summed for each storm event

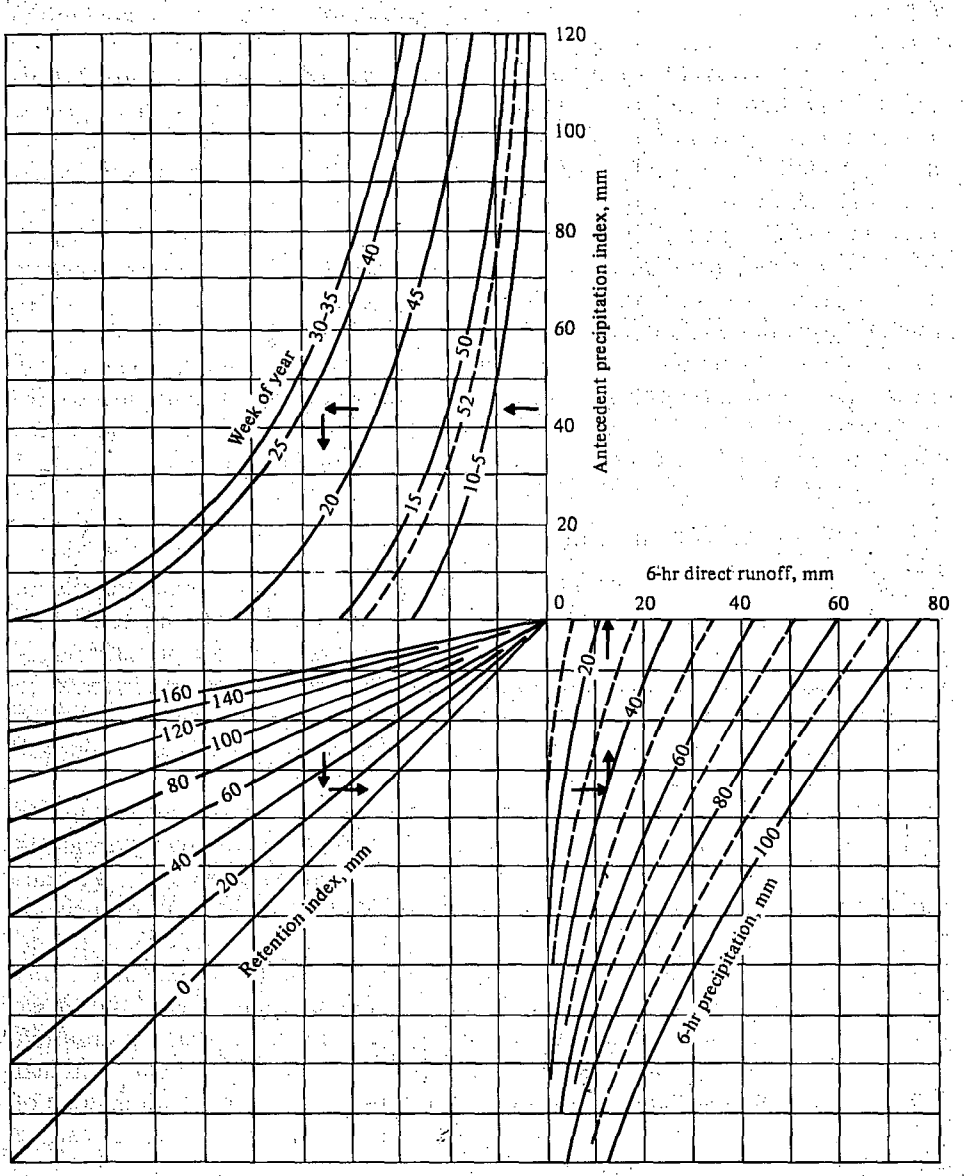

Figure 8-6 Incremental runoff relation using a short-term retention index.

under study. Comparing computed and observed total storm runoff for several assumed values of B leads to a solution for any selected recession factor. Values of the short-term recession factor (daily) are the order of 0.4 to 0.5 and B ranges from 0.6 to 0.8 (0.98 to 0.99 with precipitation in millimeters). The t-hr recession factor is equal to the daily factor to the $t/24$ power.

8-8 Infiltration Approach to Runoff Estimates

The infiltration approach assumes that the surface runoff from a given storm is equal to that portion of the rainfall which is not disposed of through (1) interception and depression storage, (2) evaporation during the storm, and (3) infiltration. If items 1 and 2 are invariable or insignificant or can be assigned reasonable values, one need be concerned only with rainfall, infiltration, and runoff. In the simplest case, where the supply rate i_s is at or in excess of the infiltration capacity, surface runoff is equivalent to the storm rainfall less surface retention and the area under the capacity curve.

The procedure appears to be simple and to offer a solution to the estimation of short period increments of runoff. Experience has shown otherwise. If the rainfall intensity is always above the infiltration-capacity curve (Fig. 8-1) the problem is merely one of defining the infiltration curve which is a function of the antecedent moisture conditions. If rainfall intensities fluctuate above and below the infiltration curve, the matter is confused, since the curve inherently assumes that the infiltration capacity decreases because a fixed amount of water was added to the soil moisture during an interval. If $i_s < f_p$, the increment of soil moisture is less than assumed and the drop in the infiltration curve correspondingly less.

The time-intensity pattern of rainfall is rarely uniform over the catchment, and the applicable infiltration-capacity curve varies from point to point depending on soils, vegetation, and antecedent moisture. Finally, the infiltration approach ignores other storm-flow generation mechanisms (Sec. 8-2) which, in addition to groundwater accretion, must be determined in some other way. For these and other reasons the infiltration approach never proved satisfactory as a tool for hydrograph prediction.

8-9 Infiltration Indexes

Difficulties with the theoretical approach to infiltration led to the use of infiltration indexes [33]. The simplest of these is the Φ *index*, defined as that rate of rainfall above which the rainfall volume equals the runoff volume (Fig. 8-7). The W *index* is the average infiltration rate during the time rainfall intensity exceeds the capacity rate; i.e.,

$$W = \frac{F}{t} = \frac{1}{t}(P - Q_S - S) \tag{8-13}$$

where F is total infiltration, t is time during which rainfall intensity exceeds infiltration capacity, P is total precipitation corresponding to t, Q_S is surface

Continuous Hydrograph Synthesis with an API-Type Hydrologic Model

WALTER T. SITTNER, CHARLES E. SCHAUSS, AND JOHN C. MONRO

U. S. Weather Bureau, Silver Spring, Maryland 20910

Abstract. The U. S. ESSA Weather Bureau Hydrologic Research and Development laboratory has developed a complete hydrologic model utilizing an antecedent precipitation index (*API*) type rainfall–runoff relation to compute surface runoff. With increasing demand for continuous river forecasts as well as flood forecasts, it is necessary to have a model that will predict all components of flow as functions of observable independent parameters on a continuous basis. To formulate the model, existing and proved techniques were used where possible and new techniques developed as necessary. The model consists of four basic parts: a relation for computing ground-water recession, a method of computing the ground-water flow hydrograph as a function of the direct runoff hydrograph, an *API*-type rainfall–runoff relation, and a unit hydrograph. The rainfall–runoff relation is of the incremental type, yielding a runoff computation for each 6-hour period rather than computing the total storm runoff. This has been accomplished through the inclusion of a new parameter, retention index. Two important features of the model are the ease of adjusting parameters to observed flow and the sequential development of the four basic parts with a minimum of interaction.

INTRODUCTION

The U. S. ESSA Weather Bureau has for many years been engaged in a program of continuous river forecasting, utilizing a wide variety of hydrologic techniques to produce various types of forecasts. In large rivers the instantaneous discharge hydrograph is usually predicted by routing observed upstream flows and reservoir releases. Forecasts of total volumes of discharge during extended periods are based on analyses of anticipated precipitation and/or snowmelt. The response of individual headwater basins to storm events is predicted by the use of rainfall–runoff relations and unit hydrographs. Discharge of such basins during fair weather periods is arrived at by extension of ground-water depletion curves. What has been lacking is a purely objective means of predicting the flow from individual basins during periods when it consists of ground-water discharge combined with relatively small amounts of direct runoff.

The demands for river forecasts are continually increasing. These demands are for wider areal coverage as well as for improved precision in the low and medium flow ranges. To accommodate these demands the U.S. Weather Bureau has been evaluating various techniques for making continuous forecasts of the response of individual basins. Such evaluation must include a comparison of forecasts of storm events produced by existing procedures and by the continuous type model under consideration. To facilitate this comparison, the existing techniques were modified to embrace the concept of a continuous streamflow model. This modification, as effected, includes a new method of expressing ground-water discharge as a function of independent parameters. This combination of old and new techniques constitutes a complete hydrologic model that is the subject of this paper.

The results of the test of the model have been very encouraging. Although complete tests have been run on only two basins, the Monocacy River near Frederick, Maryland, and the French Broad River at Rosman, North Carolina, these tests indicate that this model may become a practical forecasting tool.

THEORY OF THE MODEL

General. All flow in any river channel is originally derived from precipitation. Individual particles of water, however, fall in different parts of the basin and reach the channel by a great number of routes. The travel may be above or below ground and may require months

or years or no time at all. Consequently a detailed effort to categorize flow components could yield an almost unlimited number. The flow, however, is usually thought to consist of four components:

1. Channel precipitation: Rain falling directly on the surface of the stream.
2. Surface runoff: Water that falls on the basin surface and finds its way into the stream channel by means of overland flow.
3. Subsurface runoff (also called subsurface flow, interflow, or seepage into the stream): Precipitation that infiltrates the surface soil and moves laterally through the upper soil layers toward the stream channel. This may be pictured as a movement of air and water (unsaturated flow) above the ground-water level.
4. Ground-water runoff or ground-water flow: That part of discharge caused by percolation into the ground-water aquifer (saturated flow).

In runoff analysis there is no rational technique for completely and accurately delineating the various flow components that together define the hydrograph. Further, the decision as to how many components to recognize is somewhat arbitrary. It seems logical to define and treat as few as are necessary to obtain acceptable results. The procedure used in this study is to consider just two components, direct runoff and ground-water flow. Direct runoff consists of items 1, 2, and 3 above. Ground-water flow is defined in item 4.

The direct runoff component of the hydrograph is computed from precipitation by the use of an antecedent precipitation index (*API*) type rainfall–runoff relation and a unit hydrograph. As will be pointed out later, the rainfall–runoff relation has been modified somewhat, but the model computes this component of flow by basically standard techniques. The ground-water discharge hydrograph is represented as a function of the direct runoff hydrograph. The relationship between the two described below involves the use of the ground-water recession coefficient for the basin. The complete model then consists of four parts:

1. Rainfall–runoff relation.
2. Unit hydrograph.

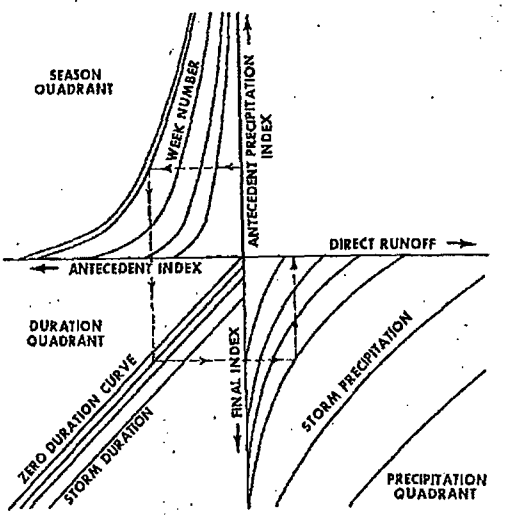

Fig. 1. Standard *API* type rainfall–runoff relation.

3. Relation for expressing ground-water hydrograph as a function of the direct runoff hydrograph.
4. Relation for evaluating the ground-water recession coefficient.

Rainfall–runoff relation. Direct runoff volume is determined within the model by using an *API* type rainfall–runoff relation [*Linsley et al.*, 1949, pp. 418–424]. In this relation (Figure 1) the *API* is used as an index to upper level soil moisture. It is a decay function of precipitation and reflects the precipitation regime for about one month prior to the event. In the season quadrant the *API* is combined with a seasonal parameter, week number, to produce an antecedent index (*AI*), which is intended to represent antecedent conditions completely. The duration quadrant applies a small adjustment based on storm duration to the *AI* and results in a final index (*FI*). The duration quadrant is usually assumed to be standard for all basins and simply applies an adjustment of +0.01 per hour duration. The precipitation quadrant expresses direct runoff as a function of *FI* and storm precipitation.

As described the relation determines the total direct runoff for an event of any duration in terms of total precipitation. In operational forecasting, however, six-hourly increments of runoff are usually required. The most common

method of obtaining these increments is to determine an initial *AI* for the event, using the initial *API* and the week number. At the end of each six-hour period, the *AI* is used with the duration and total accumulated precipitation at that time to compute the total accumulated runoff. Successive figures of accumulated runoff are then subtracted to obtain runoff increments. Although such use of a total storm relation is quite consistent with the concept and with the fact that the relation is developed from total event data, a question occurs when an extended storm period is interrupted by one or more periods of little or no precipitation. Should one continue the computation as described above or break it and start over with new antecedent conditions, considering the subsequent precipitation periods as a separate event? The two methods will not give the same result, and there may be a significant difference. Making the choice always involves a high degree of subjectivity.

In using the *API* type of relation as part of a continuous model, this deficiency becomes of paramount importance. It is virtually necessary to have an incremental type of relation, that is, one in which the precipitation for each unit time period (six hours in this study) is converted to runoff on the basis of its own updated antecedent conditions. The procedure for each six-hour period must be identical to that for every other period and result directly in a six-hour runoff increment. Although the need for such a technique has long been felt, there are two problems connected with it.

The first problem is that the type of relation shown in Figure 1, regardless of the configuration of the curves, cannot be used incrementally as described above. The reason is evident from a discussion of Figure 2, which shows two precipitation regimes and the resultant *API* patterns. The direct runoff resulting from the one inch of precipitation falling in the first period of the fifth day is computed. In both cases the *API*, based on a daily recession factor of 0.9, is equal to 3.91 inches. Since all input parameters to the relation are identical in both cases, the relation must compute the same runoff in both cases. In Figure 2a the precipitation in question occurs after a continuous dry spell of 54 hours. Consequently before runoff starts, interception and depression storage losses must be satisfied. In Figure 2b, however, the subject period is the fifth period of a continuous storm which has already deposited 3.70 inches on the basin. Obviously basin retention capacity is largely satisfied, and the runoff from this inch of precipitation will be greater than from the corresponding inch in the previous case. Since the relation has no way of distinguishing between two such situations, it cannot in this form be used incrementally.

The second problem is one of development. Fitting the relation to a particular basin consists of correlating the independent variables for a number of events with the dependent variable, observed runoff, for each event. While the total runoff resulting from a precipitation event can be easily determined from the observed hydrograph, it is virtually impossible to apportion this quantity among the individual periods of the event. Consequently the development of an incremental relation would be expected to involve correlation with a dependent variable that is not observable.

The method which has been devised overcomes both of these problems. It involves the introduction of a new input parameter, retention index (*RI*). This is similar to the *API* but has a much lower recession factor and is therefore a short-term moisture index reflecting the presence of water in interception and depression storage. In Figure 2 the *RI* (dotted line), based

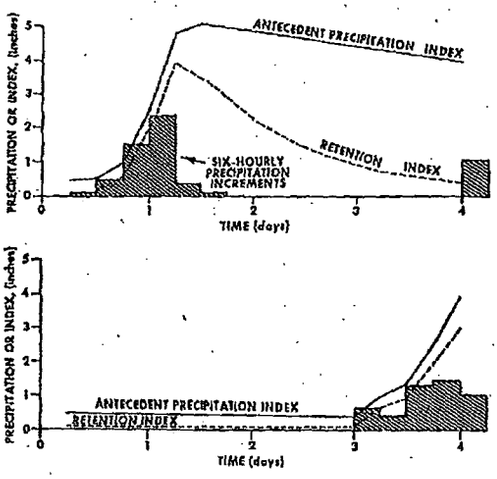

Fig. 2. Variation of antecedent precipitation index and retention index.

on a daily recession factor of 0.4, has a value at the beginning of the fifth day of 0.36 in the first example and 3.00 in the second. Consequently the *RI* can reflect the difference between these two situations, and if properly introduced into the relation, should make it possible to compute the correct runoff in both cases. Figure 3 shows how the *RI* is used. Since all events have been reduced to unit duration, the duration quadrant of Figure 1 is no longer needed and has been replaced by the *RI* quadrant. The total storm relation (Figure 1) is presumably capable of predicting the runoff from any six-hour event or from the first six hours of a longer event. In either case the duration quadrant would modify the *AI* by +0.06. The season quadrant of Figure 3 is identical to that of Figure 1 except that all of the curves have been shifted 0.06 to the left. The configuration of the curves in the precipitation quadrant has not been changed. Thus the relation will correctly predict the first runoff increment of the event if the *RI* quadrant equates the *FI* to the *AI*. If it is assumed that the *RI* at the beginning of any event is zero or close to it, then the zero *RI* curve must be a 45 degree line through the origin as shown. Since all *RI* values greater than zero must act to produce an *FI* smaller than the *AI*, all of the curves must lie above the zero curve. Since small amounts of precipitation can often satisfy retentive capacity and since further rainfall has little additional effect, the curves would be expected to exhibit decreased spacing for higher *RI* values as shown. If the curves are assumed to be straight lines, then the *RI* quadrant can be expressed by the formula

$$FI = AI(RA)^{RI} \qquad (1)$$

where *RA* is a basin constant less than unity.

Since the season and precipitation quadrants can be developed on the basis of storm total parameters, all that is required to define the incremental relation is evaluation of the basin constant *RA*. The technique by which this is accomplished is described in the following section.

All curve families in the rainfall–runoff relation can be expressed analytically. A group of formulas to accomplish this is presented in the appendix.

Groundwater discharge hydrograph.: As noted earlier, this component of channel flow, which originates as infiltrated water, is represented as a function of the direct runoff hydrograph. The close relationship between direct runoff and infiltration suggests such a function. If the ground-water flow hydrograph is considered to represent outflow from the ground-water aquifer, then it is reasonable to think in terms of an 'inflow to ground water' hydrograph, a composite of the inflow taking place throughout the basin. At any time when inflow is zero, the outflow follows a simple depletion pattern; that is

$$G_t = (Kg)^t(G_0) \qquad (2)$$

where G_0 and G_t are the ground-water discharge values at time zero and time t and Kg is the ground-water recession factor. As the direct runoff approaches zero, the total discharge Q approaches the ground-water discharge G. If it is assumed that inflow to ground water I is a function of concurrent direct runoff discharge and that the ground-water and surface water divides coincide, then inflow must become zero at this point and equation 2 will apply. An expedient first assumption is that the relation between inflow to ground-water and direct runoff discharge may be represented by the simplest possible function, a linear one

$$I = Z(Q - G) \qquad (3)$$

where Z is the ratio of the instantaneous value

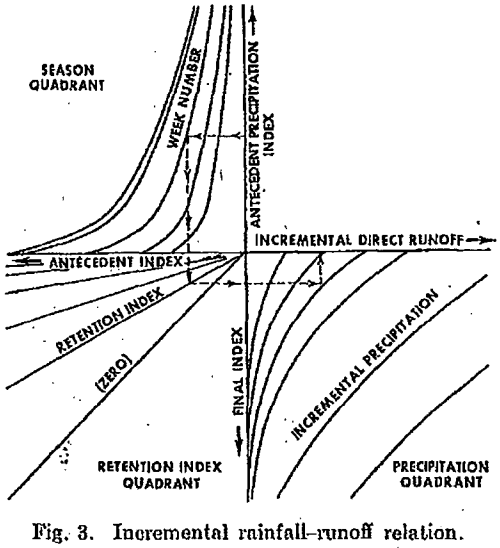

Fig. 3. Incremental rainfall–runoff relation.

of inflow to ground water and the concurrent instantaneous value of direct runoff discharge. Whether or not Z is constant cannot be determined at this time, but the following derivation does not depend on its being so. Later a functional relationship for Z will be determined empirically. If the value of Z is known, however, then the inflow to ground-water hydrograph may be computed with equation 3. This hydrograph, if suitably routed (simulating the movement of water through porous media), will yield the desired ground-water outflow hydrograph. If it is assumed that Muskingum routing [*Linsley et al.*, 1949, 502–503] with zero X (reservoir routing) will accomplish this, then all coefficients in the routing equation may be evaluated if the ground-water recession factor is known.

Referring to Figure 4 which shows a typical storage depletion curve, the discharge at any time t may be expressed as a function of that at a previous time a and the recession factor Kg

$$Q_t = Q_a(Kg)^{(t-a)} \tag{4}$$

During the differential period from time t to time $t + dt$, the change in storage $-dS$ is equal to $Q_t dt$. From this and equation 4

$$-dS = Q_a(Kg)^{(t-a)}\,dt \tag{5}$$

Considering the change in storage from time a to time b

$$\int_a^b -dS = Q_a \int_a^b (Kg)^{(t-a)}\,dt \tag{6}$$

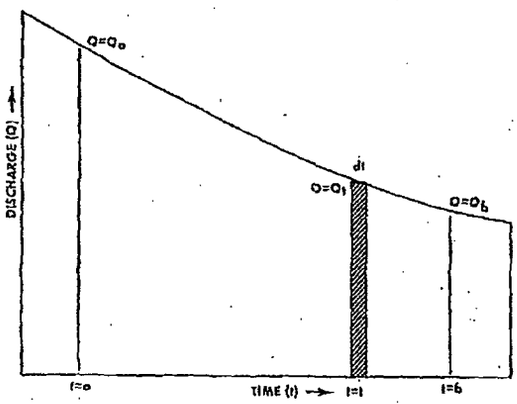

Fig. 4. Ground-water depletion curve.

Integrating

$$S\Big]_a^b = -Q_a \frac{Kg^{(t-a)}}{\ln Kg}\Big]_a^b \tag{7}$$

Applying limits

$$\begin{aligned} S_b - S_a &= -Q_a\left[\frac{Kg^{(b-a)}}{\ln Kg} - \frac{Kg^{(a-a)}}{\ln Kg}\right] \\ &= -\frac{Q_a(Kg)^{(b-a)}}{\ln Kg} + \frac{Q_a}{\ln Kg} \end{aligned} \tag{8}$$

By applying equation 4 at time a and substituting in equation 8

$$S_b - S_a = -\frac{Q_b}{\ln Kg} + \frac{Q_a}{\ln Kg}$$

or

$$Q_b = \left(S_b - S_a - \frac{Q_a}{\ln Kg}\right)(-\ln Kg) \tag{9}$$

The Muskingum storage equation with zero X equates storage with the product of outflow and the storage constant K. Since the outflow in this case is Q_b

$$S = K(Q_b) \tag{10}$$

As the routing involves only increments of storage, absolute storage volumes are not needed and are in fact indeterminate with this type of analysis. All that is required is the value of storage in reference to some arbitrary but constant level. Referring to equation 9, the quantity $(-S_a - Q_a/\ln Kg)$ is constant with respect to time and, although indeterminate, may be considered the datum value. The quantity $(S_b - S_a - Q_a/\ln Kg)$ then becomes the difference between the storage at time b and the datum value. This corresponds to the quantity S in equation 10. Equation 9 then becomes

$$Q_b = (S)(-\ln Kg) \tag{11}$$

Substituting in equation 10

$$S = (K)(S)(-\ln Kg)$$

Solving for K

$$K = -\frac{1}{\ln Kg} \tag{12}$$

For the routing problem at hand, Kg is the ground-water recession factor for the basin.

Having the storage constant K, the routing coefficients for a routing period of six hours (one-fourth day) are computed as follows:

$$C_0 = C_1 = \frac{1}{(8K + 1)} \tag{13}$$

$$C_2 = \frac{(8K - 1)}{(8K + 1)} \tag{14}$$

The routing equation then becomes

$$G_2 = (Z)(C_0)(Q_2 - G_2 + Q_1 - G_1) + (C_2)(G_1) \tag{15}$$

This gives an ordinate on the ground-water flow hydrograph G_2 in terms of the preceding ordinate G_1 and the differential quantity $(Q\text{-}G)$, which is an ordinate on the direct runoff hydrograph. Thus equation 15 may be used to generate the ground-water flow hydrograph if the direct runoff hydrograph is known. The equation may also be written

$$G_2 = \frac{(Z)(C_0)(Q_1 + Q_2) + (G_1)(C_2 - ZC_0)}{(1 + ZC_0)} \tag{16}$$

Equation 16 gives the ground-water hydrograph ordinate in terms of the preceding ordinate G_1, and points Q_1 and Q_2 on the total flow hydrograph. Thus the equation can be used to separate a hydrograph into its two components. While it is not used in this form in the model itself, it is used in the development of both the rainfall-runoff relation and the unit hydrograph.

The above hypothesis does not recognize the condition of depletion of ground-water supply to a point below that corresponding to zero channel inflow and is consequently applicable only to continuous streams. To use this approach with intermittent or ephemeral streams may well require some modification of the basic theory.

Relation for evaluating ground-water recession coefficient. The nature of the computation described above is such that the value of the coefficient Kg is critical. Consequently no attempt is made to use a constant value. Kg is considered to be primarily a function of discharge, having a value of unity at zero discharge and decreasing for higher flows. Since equal discharge values in different seasons probably result from different ground-water level configurations, provision is made for a seasonal variation in Kg.

Figure 5 is a schematic diagram of the complete model. All computations involved in the model can be performed by electronic computer.

DEVELOPMENT OF THE MODEL

Development of the model incorporates independent determination of its four basic relations prior to their combination into the composite model for final verification and adjustment. In this project all computations involved in the development procedure and the operation of the complete model were performed by a small scale electronic computer.

Ground-water recession coefficient. The first part of the model to be evaluated is a relation for expressing the ground-water recession coefficient as a function of ground-water discharge and week number. The daily coefficient is defined by

$$Kg = Q_2/Q_1 \tag{17}$$

where Q_1 and Q_2 are the discharges at some time on two successive days when there is no direct runoff. To derive the relationship a visual inspection of several years of mean daily hydrograph is made to select periods meeting this criterion.

Equation 17 is then solved for a very large number of pairs of discharge values. In practice, for the sake of expedience the mean daily

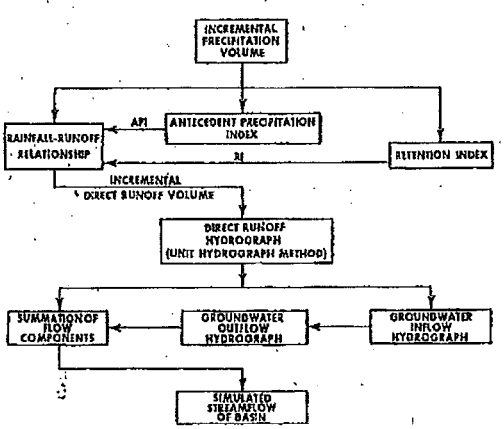

Fig. 5. Schematic diagram of *API* type hydrologic model.

values of discharge are used. Results are virtually identical to those which would be obtained by using instantaneous values. The computed values of Kg are then grouped by discharge and median values of Kg and Q_t computed for each group. For low values of discharge, where Kg approaches unity, group medians give results superior to group averages. A curve through the points so defined represents the average relation between Kg and discharge. The seasonal parameter is then introduced by correlating the deviations of the individual events from the curve with week number. The resultant curve of week number versus deviation is applied as a linear function of discharge in such a way as to simulate a family of curves converging at zero discharge.

Ground-water flow hydrograph. Analyzing several years of mean daily streamflow data and applying equation 16, the ground-water flow hydrograph for the period can be generated, based on any assumed value of or relation for Z. In this application the routing period is one day, and the values of Q used in the equation are mean daily rather than instantaneous. The procedure results directly in a mean daily ground-water flow hydrograph which is virtually identical to that which would be obtained by working with instantaneous values of discharge. The adequacy of the trial value of Z cannot be fully evaluated since the actual ground-water flow hydrograph is not known. However, the manner in which it ties in with the recession of the total flow hydrograph following a rise is a good indication. If the value of Z is too small, the ground-water flow will consistently run below the total after it is obvious that direct runoff has ceased. If Z is too large, ground-water flow values exceeding total flow will result. Although it was found necessary in the study to make some minor revisions to the Z relation based on the output of the complete model, the above technique yielded results that, although tentative, closely approximated the final value.

As noted earlier, there is no theoretic reason for Z to be constant. To obtain a proper ground-water flow hydrograph, it was in fact necessary to adopt a variable ratio. In the one used, Z is a function of total discharge of the form

$$Z = ZA + ZB(Q) \qquad (18)$$

where ZA and ZB are basin constants and Q is the total discharge. A third constant ZC is a limit which Z may not exceed. Some experimentation with other forms of relations took place, but that described gave the best overall results.

Rainfall–runoff relation. The development of the rainfall-runoff part of the model consists of developing a conventional total storm relation and then converting it to the incremental type by evaluating the coefficient RA in equation 1. To accomplish this, several trial values of RA are used. With each value all precipitation events are run through the relation, and the total of all computed increments for each event is compared to the observed total runoff. The errors for individual events are assembled into a summary containing average error, bias, maximum error, or any other meaningful parameter. The several values of RA are then plotted against each of the parameters and the best value of RA selected. It was found that all error analysis parameters tended to minimize at the same value of RA, lending credence to the general approach.

Theory dictates only that the RI recession factor be considerably less than that for the API (usually 0.9). It seems logical to expect that in practice the factor could be standardized, at least geographically, as the API factor has been. In this project, however, it was necessary to optimize both the recession factor and the constant RA, which is unique for a basin. Values of the daily recession factor used were 0.38 for the French Broad basin and 0.50 for the Monocacy.

It was found that in one of the test basins, the Monocacy River near Frederick, Maryland, results could be improved by considering RA a function of week number rather than a constant. To determine the relation for a seasonally variable coefficient, a value of RA is determined for each event such that the error for that event will be zero. These are then correlated graphically with week number. The application of the resulting curve in actual computation is accomplished by table look-up. The determination of the optimum RA for an individual event involves an iterative procedure that is complex but not formidable. During the process a sensitivity figure, the ratio of differential error to differential RA, is computed for each event.

These are used as weights in the correlation with week number.

As stated above, verification is based on the comparison of observed direct runoff for an event with the summation of the computed increments for that event. Such a comparison assumes that if the relation will consistently compute increments adding to the correct total, then the increments themselves must be correct. This assumption is quite logical. Since the incremental relation will compute the runoff from the first increment of any event equal to that resulting from application of the total storm relation, then an acceptably correct total for any two-period storm verifies the second increment. Similarly if the incremental relation correctly predicts the runoff for the first two periods, then the third period of any three-period storm is verified if the correct total is obtained. The reasoning may be extended in this manner to events of any duration. This logic assumes no bias in events of any particular duration category. Correlation of forecast error with duration is one of the tests which should be made in developing any rainfall—runoff relation. This procedure was followed with the relations for each of the test basins, and there was in fact no bias.

An interesting phenomenon was noted during the development process. Because it is possible for an increment of rainfall occurring late in a storm to produce virtually 100% runoff, the precipitation quadrant must be drawn in such a way as to indicate 100% runoff at zero *FI*. Since 100% runoff or any condition closely approaching it is not usually possible on a total storm basis, the season quadrant paired with such a precipitation quadrant will not be capable of producing an *AI* close to zero. The result is that the precipitation quadrant has an area (low *FI*) not used by the total storm relation and hence not defined in its development. The area is used in the incremental relation, however. A revision of the curves in this area, actually the definition of them, must take place during the conversion of the relation to the incremental type. This revision is easily accomplished once the need for it is recognized and understood. The important aspect of this is that the resulting relation more nearly approaches the ideal condition of being defined in all areas of all quadrants than a total storm relation. For this reason such a relation is expected to forecast properly a future event having initial conditions not encountered in the development and test data.

In both basins for which incremental relations were developed, these computed total storm direct runoff at least as well as the total storm relations.

Unit hydrograph. The best fit unit hydrograph for a basin would be one derived from all storms in the period of record. Such an analysis has never been practical because of the great amount of labor involved. In this study, comparable results were achieved by the use of a two-step process. A unit hydrograph was derived in the conventional manner, using several selected events. This was considered a first approximation. Once all model parts were defined, the model itself was used as the tool for adjusting the unit hydrograph. Using either the trial hydrograph referred to above or a subsequent approximation, several years of precipitation data were run through the complete model, and the results compared with the observed streamflow data. Such a comparison involves qualitative inspection of hundreds of storm events, large and small, and indicates unit hydrograph revisions reflecting a truly comprehensive sampling of the data.

Such a trial is fast and easy and can be repeated as many times as necessary to obtain the best fit. The authors do not know of any other technique for unit hydrograph development which permits as complete use of the data.

Sequential development. It will be noted from the foregoing discussion that the four basic parts of the model can be developed individually for a basin in the order specified. In the process the independent and dependent variables involved with each part can be identified and evaluated from hydrometeorologic records. Furthermore the development of each part is dependent upon values assigned to parts previously developed but not upon those to be developed. This permits a direct and definite development procedure. While iterative or trial and error processes are used to optimize some of the parts, there is no iteration among parts. This 'sequential development' capability is one of the model's pronounced advantages.

One minor deviation from this concept is the fact that the Z relation cannot be firmly determined before the complete model has been assembled. In the work so far, it has been found necessary to base some revisions to this formula on the final model output. Although this is coincident with the final revisions to the unit hydrograph, it is fairly easy to associate output errors with one part or the other. Refinements to the Z relation made at this time are small enough not to invalidate the rainfall–runoff relation already developed.

DISCUSSION AND RESULTS

The tests of the model involved two river basins. One is the Monocacy River near Frederick, Maryland. This is an 817 square mile basin located in the foothills of the Appalachians and in the North Central portion of the state. The elevation ranges from 230 to 1900 feet above sea level. The area is largely agricultural, and land cover is principally pasturage and deciduous trees. The mean annual precipitation is 40 to 45 inches, and the mean annual runoff 14.5 inches.

The other basin is the French Broad River at Rosman, North Carolina. The basin covers 68 square miles and is located in the southwest corner of the state, well up on the eastern slope of the Blue Ridge Mountains. The elevation ranges from 2200 to 6000 feet above sea level. Most of the area is unused and covered with stands of deciduous trees. The soil zone is shallow and highly permeable. The mean annual precipitation is 70 to 80 inches, and the mean annual runoff is 43.9 inches.

Instrumentation in the test basins is somewhat better than that usually encountered in operational forecasting. It is felt that for purposes of research and model testing, atypical instrumentation is desirable, although the results of the tests are to some extent superior to those obtained operationally.

During the winter, snow is quite common in the Monocacy basin and falls occasionally in the French Broad basin. This project was not concerned with the computation of snowmelt or with methods of treating the resultant water. Where snow existed, however, it could not be ignored, and it was dealt with in a rational but very rudimentary manner. The procedure was to adjust the precipitation record on the basis of temperature. Each period of precipitation was categorized as liquid or solid. If solid, it was deleted from the record and added to snow cover. This cover was melted on the basis of temperature and the melt figures inserted into the precipitation record. The result was a record which carried solid precipitation at the time it melted rather than at the time it fell. This record was used as model input. The Monocacy record was treated in this manner, but that of the French Broad basin was not. The object was not to reproduce accurately all winter rises but simply to keep the moisture accounting computations from getting badly out of phase.

As noted the model provides acceptable output using only one input parameter, precipitation. This is important since other hydrometeorologic data, such as potential evapotranspiration, are usually not available from sites representative of basins being forecast.

Any hydrologic model contains a great many coefficients and parameters. The concept of the model can be such that these are actual measures of physical quantities, or they may be indices to those quantities. The *API* model is of the latter type. The distinction involves a rather important aspect. Any model, to serve a useful purpose, must be fitted to a basin by determining the values of the various coefficients. There are two basic methods for doing this. One involves use of measured values of the basin input–output quantities and a procedure for adjusting coefficients to fit. The other consists of a theoretic determination of the coefficients based on measurable physical characteristics of the basin itself. With a highly rational model where the coefficients are of the actual measure type, the fitting process usually involves parts of both methods. The index type model, however, is restricted to the first method. The ability to acquire information about the coefficients of a rational model without using hydrometeorologic records is a great advantage in some applications. If significant changes in the physical characteristics of a basin have been made recently or are being anticipated, the manner in which these affect the hydrologic characteristics can be quantitatively estimated. In certain types of planning activities, this capability is needed. The basin changes being referred to are hydrologic (land

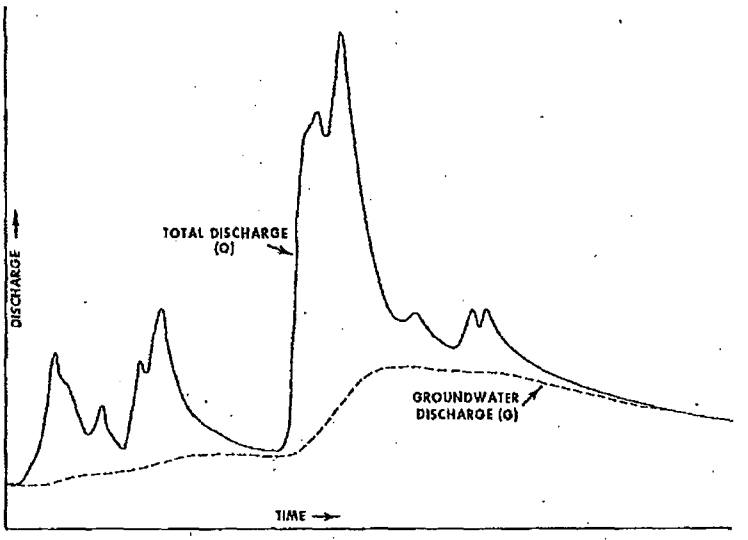

Fig. 6. Typical hydrograph separation.

use and urbanization) as opposed to hydraulic (dams and storage reservoirs).

In operational river forecasting, the ability to alter a model theoretically to reflect such changes is seldom needed. In natural basins of the size commonly forecast, these changes usually come about so slowly that their effect can be gleaned from hydrologic records. The model's ability to make use of existing forecast procedure is a great advantage in adapting it to areas of present forecast responsibility.

A necessary feature of any forecast model is the ability to adjust model parameters at any time to correspond to observed streamflow. In this model, because of the simplicity of its concepts, this adjustment can be made quite easily.

A number of observations made during the study are of interest. The concept of groundwater discharge as a function of direct runoff apparently gives adequate results. Correct evaluation of total discharge verifies the accuracy of the two components of which it consists. In addition, however, the computed ground-water flow hydrograph itself agrees nicely with a logical concept of how this component should appear. Figure 6 shows a portion of the French Broad instantaneous hydrograph separated into the two components. Scales have been left off since what is of interest is the relative shape of the two curves during a typical rise.

The foregoing discussion discloses a number of features of the model which, in a forecasting tool, are distinct advantages. One of the most important qualities in a forecast model, however, is the ability to reproduce accurately an observed hydrograph. In this, the model compares very favorably with all other known methods of stimulating streamflow. Figures 7–10 show one year of discharge record for each of the test basins with both observed and simulated discharge plotted. Here, as in the evaluation data which follow, verification is based on mean daily values of both observed discharge and model output.

Visual examination of plotted hydrographs is a highly reliable method of evaluating the accuracy of model output, although it is almost completely subjective. Consequently an attempt was made to compute some meaningful statistical summaries. Unfortunately, there is no single statistical test or group of tests which is truly comprehensive. Nor are there any standards with which statistical results might be compared. The two tests described below are thought to be informative, but no rigid interpretation of the results can be made.

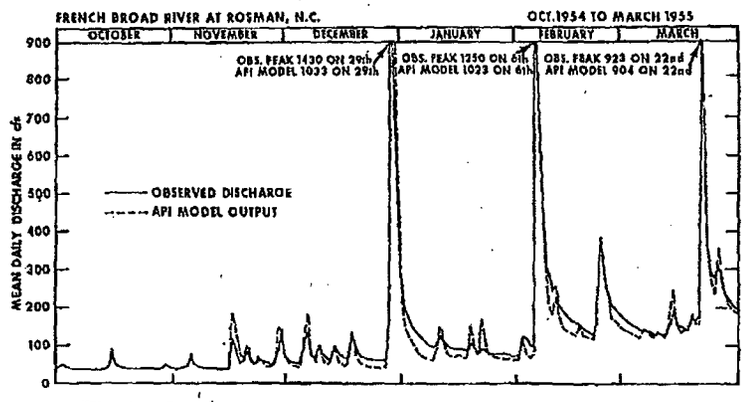

Fig. 7. Sample hydrograph simulation, French Broad River.

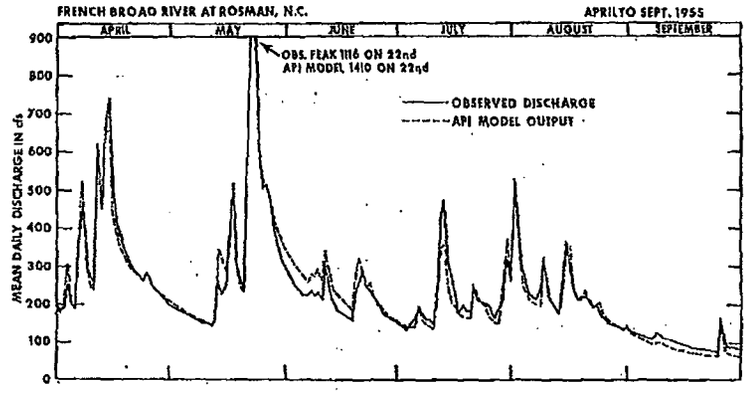

Fig. 8. Sample hydrograph simulation, French Broad River.

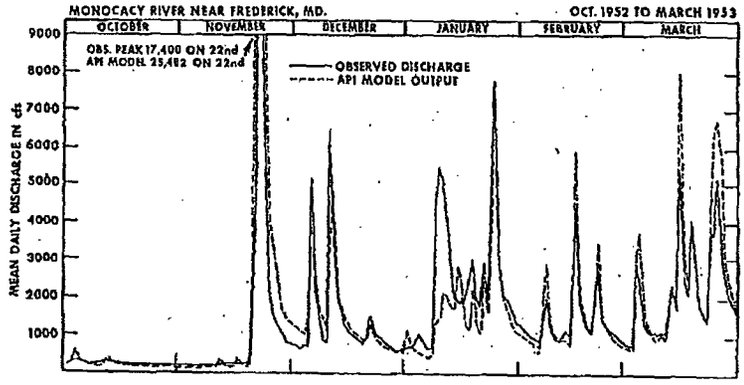

Fig. 9. Sample hydrograph simulation, Monocacy River.

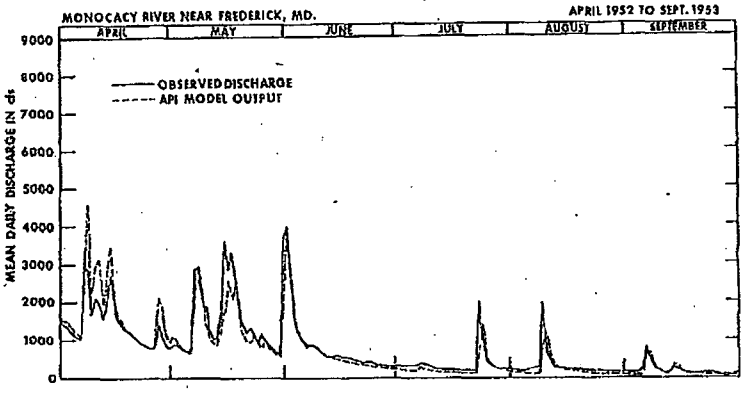

Fig. 10. Sample hydrograph simulation, Monocacy River.

The first test involves computation of the error in the computed mean daily discharge figure for each day in the period of study. The summary of the errors is presented in Figure 11 in the form of a frequency distribution graph. This is a plotting of error as abscissas against the percent of events having less than that error as ordinates.

The second test is designed to simulate actual forecast conditions. The change in discharge from a given date to some date in the future is compared with the change forecast by the model. The difference is the error. It is expressed both in cfs and in percent of the true discharge. All discharge figures are mean daily. The error is computed for periods of 24, 48, and 72 hours. The following example illustrates the method:

Date	Observed discharge	Model Output
10	50	59
11	46	49
12	72	70
13	78	83
14	67	65

To simulate forecasts made on the tenth for 24, 48, and 72 hour periods, the model forecasts changes of −10 cfs, +11 cfs, and +24 cfs. The observed changes are −4 cfs, +22 cfs, and +28 cfs, resulting in errors of −6 cfs, −11 cfs, and −4 cfs. Expressing these errors as percentages of the observed discharge at the end of each forecast period results in −13%, −15%, and −5%. In actual forecasting as opposed to continuous modeling, the discharge at the beginning of the forecast period would be known and the model output adjusted to agree with it. The

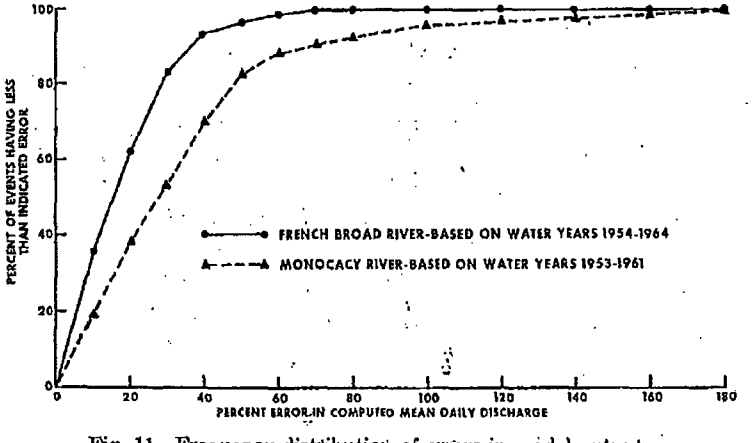

Fig. 11 Frequency distribution of errors in model output.

forecasts therefore would be in error by precisely the amounts shown. Starting on the eleventh, the errors are −5 cfs, +2 cfs, and −5 cfs, or −7%, +3%, and −7%.

Computations of the type described have been made for every day in the period of record for both basins. A summary of the results is presented in Tables 1 and 2. Figure 12 is a frequency distribution plot similar to that of Figure 11 but based on the errors in the 24-hour forecast. The graph is restricted to one forecast period in the interest of clarity. Since basins of the size used in the study reach their crests about one day after the beginning of direct runoff, the most important portion of the hydrograph is the first day following the forecast or a revision to it. Consequently, the 24-hour forecast figures are the most meaningful of the three computed.

Twenty years of streamflow data were simulated in the study, nine in one basin and eleven in the other. At selected times, the model output was adjusted to 'tie' it to observed streamflow. This was done experimentally, and the effect of such a 'tie-in' was found to extend for varying periods into the future, depending on circumstances. The results presented above were obtained by starting with the observed discharge on the first day of the period of record and then running for nine or eleven years with no tie-ins and no input other than precipitation. Interestingly, there was no tendency toward long term divergence from the observed hydrograph. That is, the eleventh year was no better or worse than the fifth or the first, and the quality of each year was not significantly different from what it would have been had there been a tie-in at the beginning of that year. Although it is the nature of the computation to impose upper and lower limits on the output, it was still somewhat surprising to see it faithfully following not only storm peaks but also the long term variation in base flow after ten years of 'free wheeling.'

SUMMARY

A hydrologic model has been devised that simulates basin response on a continuous basis. The model consists of four basic parts: a ground-water recession coefficient relation; a relation for computing Z, which is a coefficient in a formula expressing ground-water flow as a func-

TABLE 1. French Broad River at Rosman, North Carolina. Statistical Summary of Errors in Forecast of Change in Discharge (errors expressed in cfs)

Class Interval			Standard Error			Average Error			Bias		
Range (cfs)	No. of Events	Percent of Total	24-hr.	48-hr.	72-hr.	24-hr.	48-hr.	72-hr.	24-hr.	48-hr.	72-hr.
0–40	42	1	1	1	2	0	1	1	0	0	0
41–80	444	11	6	12	14	3	5	6	0	−1	−1
81–160	1313	33	18	25	29	8	12	14	−1	−2	−3
161–320	1560	39	34	47	51	16	24	27	−1	−1	−1
321–640	550	14	69	89	90	42	57	60	+3	+13	+13
above 640	106	2	221	207	235	153	143	158	+30	0	+18

Errors Expressed in Percent of Observed Discharge at End of Forecast Period

Class Interval			Standard Error			Average Error			Bias		
Range (cfs)	No. of Events	Percent of Total	24-hr.	48-hr.	72-hr.	24-hr.	48-hr.	72-hr.	24-hr.	48-hr.	72-hr.
0–40	42	1	3	4	7	2	3	5	0	0	−1
41–80	444	11	10	17	20	4	8	10	0	−2	−2
81–160	1313	33	15	21	25	7	10	11	−1	−2	−2
161–320	1560	39	14	19	20	7	10	11	0	0	0
321–640	550	14	15	19	20	9	13	14	0	+2	+2
above 640	106	2	22	19	24	16	14	16	+5	+2	+3

TABLE 2. Monocacy River near Frederick, Maryland. Statistical Summary of Errors in Forecast of Change in Discharge (errors expressed in cfs)

Class Interval			Standard Error			Average Error			Bias		
Range (cfs)	No. of Events	Percent of Total	24-hr.	48-hr.	72-hr.	24-hr.	48-hr.	72-hr.	24-hr.	48-hr.	72-hr.
0–100	113	3	24	46	34	8	17	18	2	−1	0
101–200	766	23	59	87	163	25	39	58	1	−2	−12
201–400	812	25	126	220	208	61	105	111	0	−6	+8
401–800	685	21	322	390	441	151	206	228	3	+12	+17
801–1600	510	16	420	711	944	242	390	491	−64	−39	−8
1601–3200	265	8	986	1392	1319	639	880	903	+73	+243	+233
3201–6400	97	3	2321	2695	2761	1791	2010	2102	+99	−35	−141
above 6400	36	1	2926	3199	3674	2320	2524	2839	+25	−1177	−1486

Errors Expressed in Percent of Observed Discharge at End of Forecast Period

Class Interval			Standard Error			Average Error			Bias		
Range (cfs)	No. of Events	Percent of Total	24-hr.	48-hr.	72-hr.	24-hr.	48-hr.	72-hr.	24-hr.	48-hr.	72-hr.
0–100	113	3	26	50	38	10	19	21	+3	0	0
101–200	766	23	37	53	96	16	25	37	0	−1	−8
201–400	812	25	44	76	72	21	36	39	0	−2	+2
401–800	685	21	55	66	74	26	35	39	0	+2	+3
801–1600	510	16	35	59	78	21	33	42	−5	−3	−1
1601–3200	265	8	44	66	61	29	40	41	+1	+10	+10
3201–6400	97	3	57	65	67	42	47	50	+4	+2	0
above 6400	36	1	32	34	38	26	28	30	−1	−13	−17

tion of direct runoff discharge; a rainfall–runoff relation; and a unit hydrograph.

The coefficient Z referred to above enables the ground-water component of channel flow to be computed as a function of the direct runoff hydrograph, using a linear routing procedure that simulates the natural lag characteristics of ground-water movement. During periods of pure ground water, the computation yields a recession curve mathematically identical to the ground-water recession.

The antecedent precipitation index (*API*) type rainfall–runoff relation as used by the U. S. Weather Bureau in operational river forecasting has been modified to operate on an incremental basis. A retention index *RI* has been added to reflect the degree of saturation of interception and depression storage. It decays rapidly in comparison to the antecedent precipitation index.

A unique method for unit hydrograph optimization was used in the study. Using the model itself as a tool, the computation of hundreds of storms on a continuous basis provided the data for evaluation of the trial unit hydrographs.

The model generates two flow components, ground-water flow and direct runoff discharge, and uses only precipitation as an input parameter. Standard types of forecast procedure are used for a portion of the analysis. Although the model was devised for the purpose of comparing this procedure with conceptual models, it appears that it may be a practical forecasting tool itself. Other applications are likely.

The model is completely digital and all computations can be performed by machine.

APPENDIX

U. S. Weather Bureau river forecast centers have for a number of years been using electronic computing equipment for solving *API* type rainfall–runoff relations, and a number of digitizing approaches have been devised. The formulas presented below comprise the method which was used in this study.

To formulate the season quadrant, the two

boundary curves are defined by polynomials 1 and 2, there being differing degree expressions for the segments above and below unity *API*.

If the *API* is equal to or less than unity

$$AX = 1 - API$$

$$AMX = SA_1 + SA_2(AX) + SA_3(AX)^2$$

$$AMN = SB_1 + SB_2(AX) + SB_3(AX)^2 \qquad \text{(A1)}$$

If *API* is greater than unity

$$AX = 6 - API,$$

but is equated to zero if negative.

$$AMX = SC_1 + SC_2(AX) + SC_3(AX)^2 + SC_4(AX)^3 + SC_5(AX)^4$$

$$AMN = SD_1 + SD_2(AX) + SD_3(AX)^2 + SD_4(AX)^3 + SD_5(AX)^4 \qquad \text{(A2)}$$

AMX and *AMN* are the maximum and minimum *AI* values that may result from a particular value of *API*.

A twelve ordinate harmonic equation 3 is then used to express the actual *AI* as a function of the computed boundary values and the date of the event.

$$SE = SG_1 \cos(WK) + SG_2 \cos(2WK) + SG_3 \cos(3WK) + SG_4 \cos(4WK) + SG_5 \cos(5WK) + SG_6 \cos(6WK)$$

$$SF = SH_1 \sin(WK) + SH_2 \sin(2WK) + SH_3 \sin(3WK) + SH_4 \sin(4WK) + SH_5 \sin(5WK)$$

$$SI = SJ + SE + SF \qquad \text{(A3)}$$

WK is the week number divided by $(52/2\pi)$ and is defined by equation 4 below.

$$WK = 0.0172[30.36(M - 1) + D] \qquad \text{(A4)}$$

M and *D* are the month and day corresponding to the event. The adjustment $(52/2\pi)$ causes the parameter *SI* above to exhibit exactly one cycle as the week number varies from 1 to 52 and expresses the position of the particular week curve between the two boundary curves.

AI is computed using equation 5 below

$$AI = AMN + SI(AMX - AMN) \qquad \text{(A5)}$$

The season quadrant is therefore represented by 28 basin constants. They are: $SA_1 - SA_3$, $SB_1 - SB_3$, $SC_1 - SC_5$, $SD_1 - SD_5$, $SG_1 - SG_6$, $SH_1 - SH_5$, and *SJ*.

The *RI* quadrant, as noted in the text, is ex-

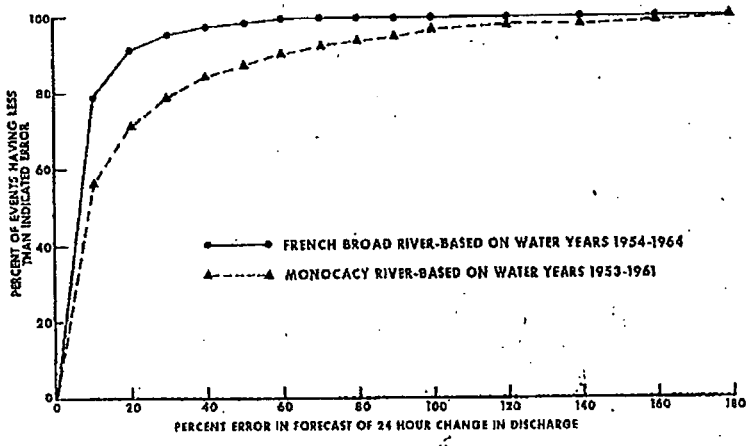

Fig. 12. Frequency distribution of errors in forecast of 24-hour change in discharge.

pressed by equation 6

$$FI = AI(RA)^{RI} \tag{A6}$$

involving one basin constant RA.

In the precipitation quadrant, two intermediate parameters PF and PG are expressed (7) as functions of the FI and five basin constants PA, PB, PC, PD, and PE.

$$\begin{aligned} PF &= PA + PB(FI) \\ PG &= PC + PD(FI)^{PE} \end{aligned} \tag{A7}$$

The incremental runoff RO is then given in terms of the incremental precipitation P by formula 8.

$$RO = [P^{PF} + PG^{PF}]^{1/PF} - PG \tag{A8}$$

REFERENCE

Linsley, R. K., M. A. Kohler, and J. L. H. Paulhus, *Applied Hydrology*, McGraw-Hill, New York, 1949a.

(Manuscript received October 23, 1968; revised May 19, 1969.)

HANDBOOK OF APPLIED HYDROLOGY

A Compendium of Water-resources Technology

VEN TE CHOW, Ph.D., Editor-in-Chief

Professor of Hydraulic Engineering
University of Illinois

McGRAW-HILL BOOK COMPANY

New York *San Francisco* *Toronto* *London*

aries with basin topography and meteorological factors. Areas where precipitation extremely spotty (e.g., where showery-type precipitation predominates) require a reater density than areas where the precipitation is of a more uniform nature.

If possible, rated gaging stations operated by the U.S. Geological Survey and others re selected as the forecast points. Occasionally, it is necessary to issue forecasts or a gage which is not rated.

Reporting Network for River Forecasting

The primary data required operationally are precipitation (rain or snow), snow on he ground (water equivalent, if possible), air temperature, and river stage or discharge. The number of reporting stations depends upon hydrologic need and availability of observers and communications. Criteria for reporting are standardized as much as possible, but may vary somewhat from one area to another. Sample nstructions to observers appear in Fig. 25-IV-1.

The frequency of reports is a function of basin characteristics. In some areas once-daily reports of rainfall and river stages may be adequate. Forecasts for small basins with rapid concentration times may require reports at intervals of 6 hr, or even less, during high-water situations.

It would be desirable to have observers report daily, but economic considerations usually dictate that the observer report only on certain predetermined criteria of precipitation amount or river stage.

In recent years, there has been a significant advance in the hydrologic applications of radar [4, 5]. Information obtained from the radar scope can be used to estimate storm rainfall with a measure of success. Radar indicates the existence of centers of high-intensity rainfall and aids in interpreting the time and areal distribution of rainfall over the basin. Such information is of particular value in dealing with floods over very small watersheds and analyzing thunderstorm-type rainfall. A radar-beacon precipitation gage has been developed which makes it possible to obtain reports from inaccessible areas where there is a lack of observers and communication facilities [6].

III. BASIC RIVER-FORECASTING PROCEDURES

Where adequate data are available and forecasts of the complete hydrograph are required, a reasonably standardized approach to river forecasting has been developed. Rainfall-runoff relations (Fig. 25-IV-2) are used to estimate the amount of water

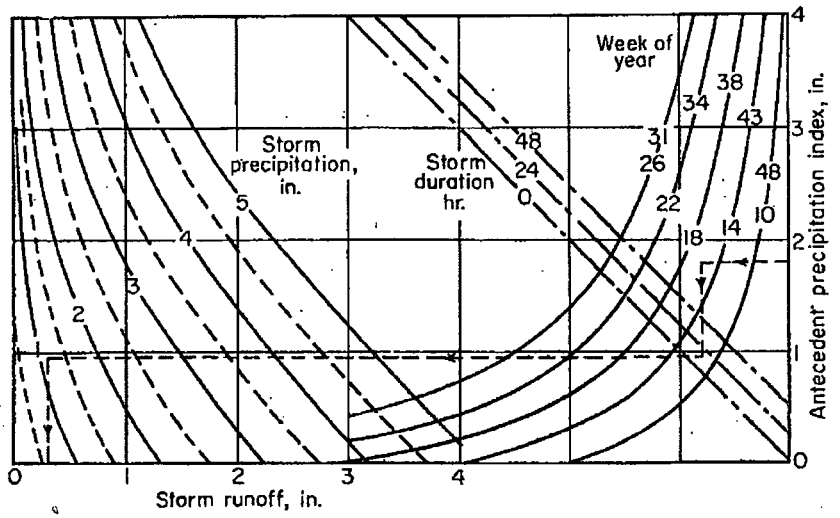

Fig. 25-IV-2. Rainfall-runoff relation.

expected to appear in the streams, while unit hydrographs (Fig. 25-IV-3) and stream flow-routing procedures (Fig. 25-IV-4), in one form or another, are utilized to determine the time distribution of this water at a forecast point. Stage-discharge relations (Fig. 25-IV-5) are then utilized to convert these flows to stages. The basic forecast procedures required are discussed only briefly since they have been described in detail in other sections of the handbook. (See Sec. 25-II.)

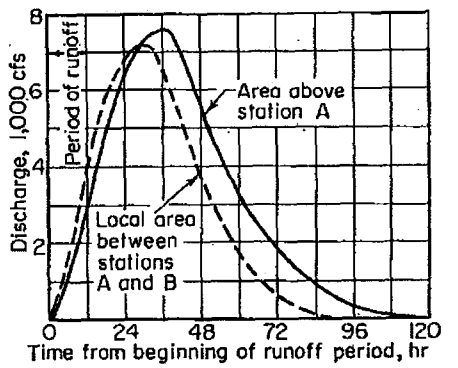

FIG. 25-IV-3. Twelve-hour unit hydrographs.

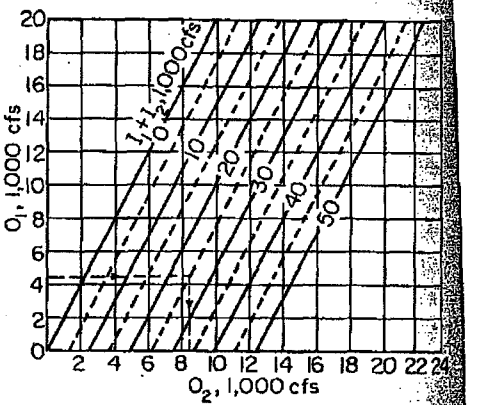

FIG. 25-IV-4. Muskingum routing diagram. $K = 18$ hr; $X = 0$; routing period $\Delta t = 12$ hr.

A. Rainfall-Runoff Relations (see Sec. 14)

The rainfall-runoff relation correlates storm rainfall, antecedent basin conditions, storm duration, and the resulting storm runoff (usually expressed as an average depth in inches, over the basin). The basic technique in use by the U.S. Weather Bureau is the *coaxial graphical method* [7–9] (see also Sec. 8-II). An example is shown in Fig. 25-IV-2. Such a relation is developed using data from one or more headwater areas in the basin for which forecasts are required. Studies must be limited to areas for which the runoff can be evaluated (from the hydrograph) for each individual storm event. In larger basins where more than one area can be analyzed (e.g., the drainage areas above stations A and C in Fig. 25-IV-6), it is necessary to determine which relation is applicable to the downstream areas where detailed studies are usually not practical. Storm runoff can be estimated for the local inflow areas, such as A to B and B and C to D, and tested in the relation. Factors such as soil type, land use, ground cover, etc., are also considered.

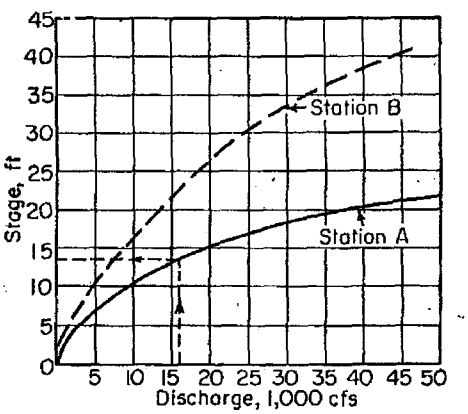

FIG. 25-IV-5. Stage-discharge relations.

In this rainfall-runoff relation the antecedent basin conditions are represented by two variables. The first is an *antecedent precipitation index* (API), which is essentially the summation of the precipitation amounts occurring prior to the storm weighted according to time of occurrence. The API for today is equal to k times the API for yesterday plus the average basin precipitation observed for the intervening day. The value of k used by most Weather Bureau River Forecast Centers is 0.90. An example of the computations is shown in Table 25-IV-1. The second variable is week of the year in which the storm occurs (e.g., the first week in January being 1, etc.). Week of

the year introduces the average interception and evapotranspiration characteristics of each season, which, when combined with the antecedent precipitation index, provides an index of antecedent soil conditions.

Table 25-IV-1. Computation of Antecedent Precipitation Index

		Month April Year _____ Date	10	11	12	13	14	15	16	17	18	19	20	21
Area above *A*	1	Yesterday's API × 0.9	1.93	1.74	1.97	1.77	1.59	1.43	2.01	1.81	1.63	2.55	4.90	
	2	Average basin precipitation		0.45				0.80			1.20	2.90		
	3	API = [(1) + (2)]	1.93	2.19	1.97	1.77	1.59	2.23	2.01	1.81	2.83	5.45		
Area *A* to *B*	4	Yesterday's API × 0.9	1.71	1.54	1.82	1.64	1.48	1.33	1.87	1.68	1.51	2.17	4.74	
	5	Average basin precipitation		0.48				0.75			0.90	3.10		
	6	API = [(4) + (5)]	1.71	2.02	1.82	1.64	1.48	2.08	1.87	1.68	2.41	5.27		

The value of storm duration used in the runoff relation is not critical and can be adequately derived from 6-hourly precipitation records. One method defines the duration as the sum of those 6-hourly periods with more than 0.2 in. of rain plus one-half the periods with less than 0.2 in. (e.g., four periods each with more than 0.2 in. and two periods with less than 0.2 in. would be considered a storm duration of $4 \times 6 + 2 \times 3$, or 30 hr).

The storm precipitation is the average over the basin. If a sufficient number of precipitation stations are available, an arithmetic mean is usually sufficient, although the Thiessen weighting method or isohyetal maps can be used [7, 8].

The storm runoff in most river-forecasting relations is direct runoff. Direct runoff is assumed to be the water which reaches the stream by traveling over the soil surface and through the upper soil horizons and has a rapid time of concentration. It is composed of surface runoff, channel precipitation, and interflow. The groundwater flow is discharged to the stream over a much longer period of time. Any of several methods of hydrograph analysis may be employed, but care must be taken to use the same method operationally as was used in development.

B. Unit Hydrographs (see Sec. 14)

The rainfall-runoff relation provides an estimate of the volume of water which will run off for a given storm situation. It is then necessary to determine the distribution of this water with respect to time at the forecast point. The unit hydrograph is a simple and generally effective method for accomplishing this [10]. In order to deal effectively with uneven distribution of runoff in time, unit hydrographs for short periods are used, very often for 6- or 12-hr durations. The increment of runoff is estimated for each time period, with the contributions from each interval superimposed upon the previous contributions.

C. Streamflow Routing (see Sec. 25-II)

The next basic problem is to predict the movement and change in shape of a flood wave as it moves downstream. Specifically, the river forecaster is interested in deter-

mining the shape of the flood wave from station A as it arrives at station B after being modified by lag and storage in the reach from A to B (Fig. 25-IV-6). Numerous routing methods are available, ranging from very complex storage functions to simple lagging procedures (Sec. 25-II). The Muskingum type of routing was selected for the forecast example [11]. In preparing a forecast for station B it is also necessary to determine the contribution of flow from the local drainage area between A and B.

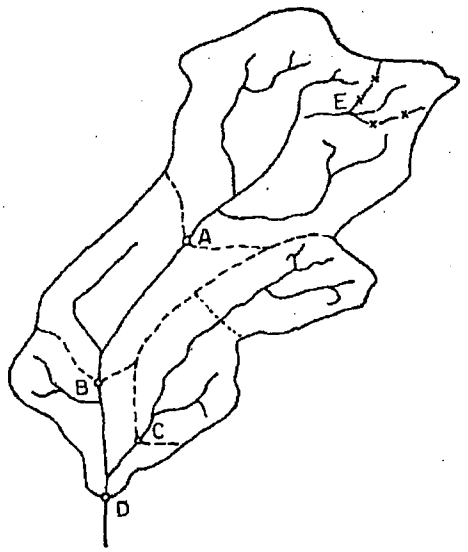

FIG. 25-IV-6. River-basin map.

The procedure for handling the local drainage area is similar to that for a headwater area, i.e., estimate the runoff from the local area and distribute by means of a unit hydrograph.

IV. RIVER-FORECASTING EXAMPLE

An example of a basic river forecast will be described in detail. A hypothetical river basin (Fig. 25-IV-6) has been selected in order to illustrate some of the special forecasting problems (discussed under Subsec. V). The rainfall-runoff relation, unit hydrographs, and routing method are the operational procedures for an actual river basin. However, because of use of a hypothetical basin, the forecast points will be designated as stations A and B.

It is assumed that the storm began about 7:00 P.M. on April 17, and a forecast is being made on the basis of rainfall reported up to 7:00 A.M. on April 19.

A. Computation of Runoff

The computation of storm runoff is shown in Table 25-IV-2. The antecedent precipitation index (API) selected is the value prior to the storm. The week of the year is determined by the date of the beginning of the storm, April 17, which falls in the sixteenth calendar week. The average rainfall amounts above station A and between stations A and B for 12-hr increments are entered on lines 3 and 10.

Dashed lines on the runoff relation (Fig. 25-IV-2) indicate the computation of runoff for station A for 7:00 A.M. on April 18. Enter the relation with API, move left to the week of year, vertically to storm duration, left to storm precipitation, and down to obtain storm runoff. Enter this value on line 6. This process is repeated at the end of each 12-hr period, using precipitation accumulated to that time. The 12-hr increments of runoff (line 7) are determined by subtracting each total storm-runoff value from the previous one and are entered on lines 1 and 12 of the forecast computation sheet (Table 25-IV-3).

Table 25-IV-2. Computation of Storm Runoff
(Using runoff relation in Fig. 25-IV-2)

		Month April Year	17		18		19	
			7 A.M.	7 P.M.	7 A.M.	7 P.M.	7 A.M.	7 P.M.
Drainage area above station A	1	Antecedent precipitation index	1.81					
	2	Week of year	16					
	3	12-hr precipitation increment, in.			1.20	0.80	2.10	
	4	Total storm precipitation, in.			1.20	2.00	4.10	
	5	Duration of storm, hr			12	24	36	
	6	Total storm runoff, in.			0.30	0.70	2.25	
	7	12-hr runoff increment, in.			0.30	0.40	1.55	
Drainage area between stations A and B	8	Antecedent precipitation index	1.68					
	9	Week of year	16					
	10	12-hr precipitation increment, in.			0.90	1.05	2.05	
	11	Total storm precipitation, in.			0.90	1.95	4.00	
	12	Duration of storm, hr			12	24	36	
	13	Total storm runoff, in.			0.15	0.65	2.10	
	14	12-hr runoff increment, in.			0.15	0.50	1.45	

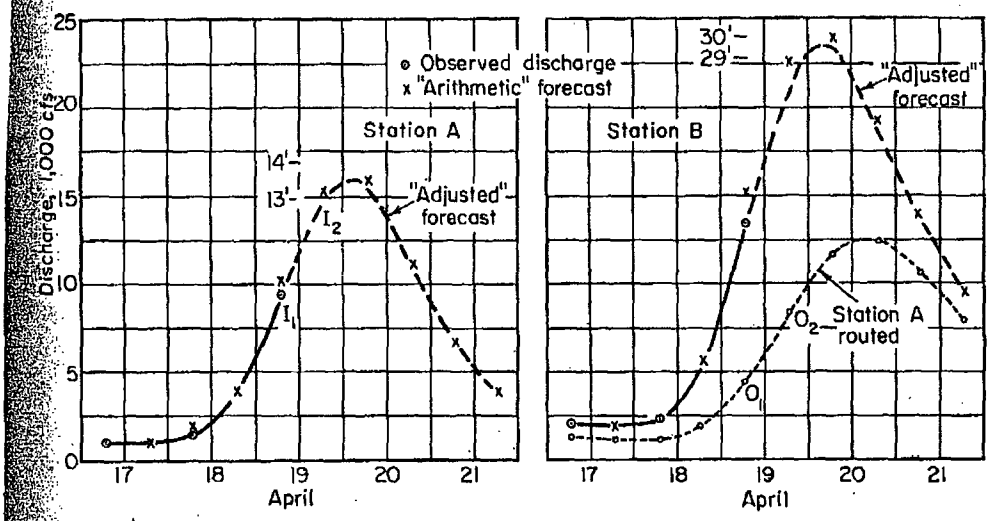

FIG. 25-IV-7. Forecast hydrographs.

Table 25-IV-3. Forecast Computation Sheet
(All discharge values in units of 1,000 cfs)

		Month April	17		18		19		20		21		22		23	
		Year	7 A.M.	7 P.M.	7 A.M.	7 P.M.	7 A.M.	7 P.M.	7 A.M.	7 P.M.	7 A.M.	7 P.M.	7 A.M.	7 P.M.	7 A.M.	7 P.M.
Station *A*	1	Forecast 12-hr RO, in.			0.30	0.40	1.55									
	2	Distribution of RO			0.9	1.9	2.3	1.7	1.0	0.5	0.3	0.1				
	3	" "				1.2	2.5	3.0	2.2	1.3	0.7	0.4	0.1			
	4	" "					4.6	9.8	11.8	8.7	5.1	2.8	1.4	0.5	0.2	
	5	" "														
	6	Total			0.9	3.1	9.4	14.5	15.0	10.5	6.1	3.3	1.5	0.5	0.2	
	7	Base flow	1.0	1.0	0.9	0.9	0.8	0.8	0.7	0.7	0.7	0.7				
	8	Arithmetic forecast	1.0	1.0	1.8	4.0	10.2	15.3	15.7	11.2	6.8	4.0				
	9	Adjusted forecast (*I*)	1.0	1.0	1.5	4.0	9.5	14.7	15.5	10.9	6.8	4.0				
Routing	10	$I_1 + I_2$	2.2	2.0	2.5	5.5	13.5	24.2	30.2	26.4	17.7	10.8				
	11	*A* routed to *B* (O)	1.3	1.2	1.2	2.0	4.4	8.3	11.7	12.4	10.6	8.0				
Station *B*	12	Forecast 12-hr RO, in.			0.15	0.50	1.45									
	13	Distribution of RO			0.6	1.0	1.0	0.6	0.3	0.1						
	14	" "				2.0	3.4	3.3	1.8	0.8	0.3	0.1				
	15	" "					5.8	9.9	9.6	5.4	2.5	0.9	0.1			
	16	" "														
	17	Total			0.6	3.0	10.2	13.8	11.7	6.3	2.8	1.0	0.1			
	18	Base flow	0.8	0.8	0.7	0.7	0.6	0.6	0.6	0.6	0.6	0.6				
	19	Arithmetic forecast	2.1	2.0	2.5	5.7	15.2	22.7	24.0	19.3	14.0	9.6				
	20	Adjusted forecast	2.1	2.0	2.3	5.5	13.5	21.0	23.3	18.7	13.6	9.6				

B. Forecast for Headwater Point (Station *A*)

The 12-hr runoff increments are converted to discharge, using the 12-hr unit hydrograph for station *A* (Fig. 25-IV-3). Each 12-hr ordinate of the unit hydrograph is multiplied by the first runoff (RO) increment (0.30 in.) and entered in line 2 (Table 25-IV-3) with the first value in the same column as the runoff increment (this is the ending time of the 12-hr period when the runoff occurred). This process is repeated on lines 3 and 4 for the other increments of runoff, and the total for each time entered on line 6. Base flow (line 7) includes all flow from events preceding the storm.

The *arithmetic* forecast, the sum of total runoff (line 6) and base flow (line 7), is entered on line 8 and plotted on the hydrograph (Fig. 25-IV-7). This arithmetic forecast is the unadjusted result of the forecasting procedures, and the forecaster must then draw an *adjusted* forecast, reconciling the arithmetic forecast with available observed data. The adjusted forecast is shown as a solid line when based on observed data and as a dashed line in the forecast period. The adjusted values are entered on line 9 for routing to station *B*.

The final step in preparing the forecast is the conversion of forecast discharge to stage using the stage-discharge relation (Fig. 25-IV-5). The forecast for station *A* could be stated as "crest of 13.5 ft at 2:00 A.M. on April 20" or as "crest of 13 to 14 ft early on April 20." Quoting a specific figure, such as 13.5 ft, might give the impression to the recipient of the forecast that it is likely to verify within tenths of a foot, which may not be the case.

C. Forecast for Downstream Point (Station *B*)

The adjusted flows for station *A* (line 9) are routed to station *B*, using the routing diagram (Fig. 25-IV-4). Successive pairs of inflows (line 9) are added to obtain the $I_1 + I_2$ values (line 10). The computation of the routed value for 7:00 P.M. on the 19th (8.3) is indicated by dashed lines on the routing diagram.

The forecast of flow from the local area is made in the same way as for station *A*. The arithmetic forecast is the sum of the routed value (line 11), the total runoff (line 17), and the base flow (line 18). These values are plotted on the hydrograph and adjusted on the basis of observed data.

The forecast for station *B* might be given as "crest of 29.5 ft at 4:00 A.M. on April 20" or as "crest of 29–30 ft early on the morning of April 20." It is a good practice to enter these forecasts on a tabulation sheet (Table 25-IV-4) as soon as completed to minimize the possibility of mistakes in transmitting the forecast to the user.

D. Remarks

It should be clearly understood that the above example demonstrates only one of many ways for deriving forecasts for stations *A* and *B*. Different methods could be used for estimating runoff, distributing runoff, and routing streamflow. The forecaster might also prefer to perform all or part of these computations on the hydrograph. A variety of forecasting techniques are required to handle most effectively the different river conditions encountered in the United States.

V. COMPLICATING FACTORS

The example given describes the basic techniques needed to handle most river-forecasting situations. Operationally there are often some complicating factors; a few of the most common ones will be discussed briefly.

A. Areas Where Unit Hydrographs Are Inadequate

The unit-hydrograph theory assumes uniform areal distribution of runoff. This is rarely the case, but in a fan-shaped basin, as above station *A* (Fig. 25-IV-6), it is usually not critical. In long, narrow basins as that above station *C*, the distribution of runoff may be very important. One solution is the development of special unit hydrographs based on various areal concentrations such as upstream, uniform, and downstream. Another solution is the division of the area into two zones, as indicated by a dotted line in Fig. 25-IV-6, and developing synthetic unit hydrographs for each of the subareas. The unit hydrograph for the upstream area can be prerouted to the forecast point *C* [7]. This approach provides flexibility in the handling of nonuniform areal distributions, but does appreciably increase the time required to prepare the forecast. It is also possible to divide the basin into zones based on estimated travel times and develop a channel inflow which can be routed to the forecast point [8].

In some basins it has been necessary to use a different unit hydrograph, usually cresting earlier and higher, for extreme floods from that for moderate floods [8, 12]. Another solution is to derive a unit hydrograph from moderate floods and develop a correction graph relating the computed peak discharge, using this unit hydrograph against observed peak flow for a number of storms of record [8]. The volume of the hydrograph should be maintained in adjusting the peak flow.

Agriculture

HANDBOOK OF APPLIED HYDROLOGY

 Library of Congress Catalog Card Number 63-13931

10074

PEAKFLOW PREDICTION USING AN ANTECEDENT PRECIPITATION INDEX IN SMALL FORESTED WATERSHEDS OF THE NORTHERN CALIFORNIA COAST RANGE

by

Gregg Bousfield

A Thesis

Presented to

The Faculty of Humboldt State University

In Partial Fulfillment

Of the Requirements for the Degree

Master of Science

In Natural Resources: Watershed Management

April, 2008

ABSTRACT

PEAKFLOW PREDICTION USING AN ANTECEDENT PRECIPITATION INDEX IN SMALL FORESTED WATERSHEDS OF THE NORTHERN CALIFORNIA COAST RANGE

Gregg Bousfield

The vast majority of small watersheds in Northwest California lack stream gage information. Understanding the high flow behavior of these watersheds is crucial for guiding resource managers in project planning. The purpose of this thesis was to develop a predictive relationship between precipitation and peakflow of streams draining small forested watersheds of the Northern California Coast Range. An antecedent precipitation index approach was developed for this purpose.

The five selected watersheds are covered by coastal coniferous forests with drainage areas ranging from 0.4 to 34 km^2. Streamflow and precipitation data from the South Fork of Caspar Creek was used to create the calibration model. Data from the North Fork of Caspar Creek, Hennington Creek, Little Lost Man Creek, and Freshwater Creek were used for independent model testing.

The calibration linear regression model, predicting peakflow as a function of peak antecedent precipitation index, resulted in a r^2 of 0.83 and a residual standard error of 1.20 L s^{-1} ha^{-1}. When peakflow was predicted, using precipitation data from test watersheds, the results were fair to poor with average absolute prediction errors ranging from 28.6 to 66.3 percent. When the ten largest peakflows were predicted separately, the average absolute prediction errors were significantly lower at 10.2 to 44.9 percent. The

model was positively biased at all test watersheds except Freshwater Creek. The root mean square error was within 15 percent of the calibration residual standard error at all test watersheds except Little Lost Man Creek.

The variability in prediction accuracy could be explained by changing unit-discharge relationships, heterogeneous lithologies, different cumulative land management effects, and spatial variation in precipitation intensity. Prediction errors were the greatest for the smallest peakflows, which may be due to greater variation in interception rates during small rainfall events. The antecedent precipitation index approach outlined in this study is best suited for predicting larger rather than smaller peakflow events that may be influenced more by factors other than short-term rainfall history.

ACKNOWLEDGEMENTS

I would like to thank Dr. E. George Robison, Jack Lewis, Dr. Andre Lehre, Dr. Andrew Stubblefield, and Dr. Gary Hendrickson for their extensive and helpful comments during the thesis review process. My committee chair, Dr. E. George Robison, was responsible for the subject and direction of this thesis. A special thanks to Jack Lewis for his statistical expertise and intimate knowledge of Caspar Creek Experimental Watershed. Thanks to Randy Klein for streamflow and precipitation data recorded at the Little Lost Man Creek gaging station. Thanks to Clark Fenton for streamflow and precipitation data recorded at the Freshwater Creek gaging station. I would also like to thank my true love who I met at the beginning of graduate school. She helped me become a better person and was supportive throughout the entire thesis process. My parents were very influential in the continuation of higher education.

TABLE OF CONTENTS

TABLE OF CONTENTS (continued)

LIST OF TABLES

LIST OF FIGURES

LIST OF FIGURES (continued)

LIST OF APPENDICES

INTRODUCTION

The prediction of streamflow in response to precipitation is a recurring theme in watershed management. Methodologies used to create rainfall-runoff models differ in both complexity and data requirements. Modeling strategies range from physically based to empirical. Physically based models use theoretical equations to simulate all runoff generation processes. Empirical models rely on statistical relationships between precipitation inputs and streamflow outputs. Most rainfall-runoff models are not purely physically based or empirical but lie somewhere in-between (Brooks et al. 1997).

Coefficients are required to adjust equations found in physical models due to the stochastic nature of hydrologic processes (Haan 2002). The majority of coefficients are derived using statistical techniques from experimental lab data. For example, infiltration rate coefficients are developed for different soil types by measuring dye wetting front movement rates on soil blocks in a lab. Even cultivated soils will show extreme variability in infiltration rates across the wetting front (Beven 2001). For these reasons, physically based models often have high costs and computational demands.

Empirical or black-box models rely on statistical relationships with little regard to the inherent physical processes. Black-box models require recalibration when applied to different climatic and geologic environments since they are strongly influenced by data. Black-box models are good for re-sizing stream crossing culverts on vast parcels of Federal lands where little data exists and economic incentives are low (Piehl et al. 1988, Cafferata et al. 2004). Simplicity and low cost are the strengths of black-box models.

Rainfall-runoff modeling remains an important tool in watershed management, although there continues to be a lack of simple modeling approaches to estimate peakflows in small forested catchments. Peakflow prediction in these watersheds is crucial for designing bridges, culverts, or channel habitat restoration structures. Unfortunately, natural resource practitioners may only have precipitation data available. Using an antecedent precipitation index (API) as the key variable for streamflow prediction has shown promise in environments with low data availability (Fedora 1987, Beschta 1990).

API was originally conceived to represent current soil moisture conditions in models predicting storm volume (Betson et al 1969, Kohler and Linsley 1951, Lee and Bray 1969, Sittner et al 1969). The universal form of an API equation is as follows:

$$API_t = API_{t-1} C + P_{\Delta t} \qquad (1)$$

where API_t is API at time t, $P_{\Delta t}$ is the precipitation occurring between times t-1 and t, and C is the recession coefficient. The theory of API is that earlier precipitation should have less influence on present streamflow response than recent precipitation. The recession coefficient represents the "memory" of a particular watershed by decaying the effect of accumulated rainfall at each time step.

A long-term API reflects seasonal moisture conditions while a short-term API reflects the most recent rainfall intensity governing peakflow response. The determination of the recession coefficient dictates whether a particular API decays rapidly or slowly. Besides *a priori* estimates, recession coefficients have been determined through optimization techniques (Moreda et al. 2006, Reid and Lewis 2007)

and physical parameters (Beschta 1990, Fedora 1987, Smakhtin and Masse 2000, Ziemer and Albright 1987).

Fedora (1987) developed an API methodology to predict storm hydrographs in small forested catchments of the Oregon Coast Range. His API was assumed to decay at the average rate of storm hydrograph recession. The relatively small watersheds used in the study had steep recession limbs resulting in a short-term API. Fedora's method resulted in average absolute peakflow and storm volume errors of 14.8 and 14.2 percent, respectively.

Beschta (1990) tested Fedora's methodology in tropical environments using data from a small catchment and a large river basin. Peakflow simulation of the four largest storms from the small catchment resulted in an average absolute error of 14 percent compared to 15.4 percent using a physically based model (Shade 1984). Peak stage of the three largest flood events was predicted with an average absolute error of 14.8 percent. Fedora's method may be widely applicable when the model has been locally re-calibrated. However, Beschta's study is the only published independent test of the methodology.

An API model was recently developed to detect changes in peakflows following experimental clearcut harvesting in the North Fork of Caspar Creek (Reid and Lewis 2007). Three different API components were used in a non-linear model ($r^2 = 0.84$) predicting daily peakflow. The components were assumed to represent quick, subsurface, and groundwater flow. Each component had different recession coefficients derived through optimization with quickflow having the fastest decay and groundwater flow the

slowest. When compared with Fedora (1987) and Beschta (1990), the API approach developed by Reid and Lewis (2007) was relatively complex.

The purpose of this study was to develop a simple API approach for modeling peakflow in small forested watersheds located on the Humboldt and Mendocino County Coasts of California. The recession coefficient used in this study was derived following the methodology developed by Fedora (1987). The API model created in this study was solely for peakflow prediction, unlike Fedora's (1987) method of simulating continuous hydrographs for both peakflow and stormflow volume prediction. The research questions were as follows:

1. Can streamflow and precipitation data from the South Fork of Caspar Creek consistently and accurately predict peakflow as a linear function of peak API?
2. Will an antecedent flow rate threshold improve model precision and accuracy?
3. Can the model consistently and accurately predict peakflow elsewhere in the Northern California Coast Range?
4. Does the model predict larger peakflows more accurately than smaller peakflows?

MATERIALS AND METHODS

Data Sources

The following criteria were used to select watersheds for API model development: forested watershed within 25 km of the Pacific Ocean, rain-dominated, drainage area less than 50 km^2, rain gage located within 5 km of the watershed centroid, gaging stations maintained and calibrated on a regular basis, streamflow and precipitation data resolution of one hour or finer, and five or more years of concurrent streamflow and precipitation data.

The distance from the Pacific Ocean was important to keep the analysis focused on coastal watersheds. Rain-dominated watersheds were sought to minimize the influence of snowmelt on streamflow generation. Small watersheds were necessary to study systems with less groundwater and channel routing influences (Gomi et al. 2002). Precipitation gages near the watershed centroid should better estimate average rainfall for the entire watershed. Poor stage-discharge relationships can have an error of 20 percent or more, which makes accurate gages a necessity (Rantz 1982). One hour or finer precipitation data is required since runoff in small watersheds responds rapidly to rainfall inputs (Beven 2001).

Gaging stations on the North and South Forks of Caspar Creek, Little Lost Man Creek, and Freshwater Creek met the criteria. There are other gaged watersheds in the region, but they lack a nearby rain gage or the data are only available at a daily time step. The South Fork of Caspar Creek was chosen as the calibration watershed due to its

moderate size and accurate data set. There was also a lack of forest harvesting at the South Fork of Caspar Creek during the period of concurrent streamflow and precipitation data. Table 1 compares basic gaging station characteristics.

All watersheds are dominated by mixed redwood (*Sequoia sempervirens*) and Douglas-fir (*Pseudotsuga menziesii*) forest. Soils are derived from the Franciscan geologic formation. The Franciscan formation contains a variety of lithologies, creating heterogeneous soils across the landscape (Woiska 1981). The Freshwater Creek watershed also contains the Yager and Wildcat formations, which are more consolidated than the Franciscan (Glass 2003). Figure 1 shows the relative location of the selected watersheds. Individual watershed maps are located in Appendix A through C.

Data Quality

The stream gaging stations have similar equipment, but different control structures. Unlike the other selected watersheds, Caspar Creek Experimental Watershed uses flumes and weirs for artificial control. Artificial control structures have empirically derived stage-discharge relationships that are relatively accurate (5 to 10 percent) and stable. The Freshwater Creek and Little Lost Man Creek gage sites are natural channels that aggrade and degrade though time.

Gage sites without artificial control require routine stage-discharge re-calibration. Randy Klein, the primary hydrologist at Redwood National Park, does not have confidence in peakflows above 3.0 L s^{-1} ha^{-1} at the Little Lost Man Creek gage site after the 1997 water year due to a lack of rating curve measurements and changes in control

Table 1 Gaging station characteristics.

	Calibration Watershed	Test Watersheds			
	South Fork of Caspar Creek	Hennington	North Fork of Caspar Creek	Freshwater Creek	Little Lost Man Creek
Distance from Pacific Ocean, km	6	7	6	15	5
Elevation Range, m	50 - 330	130 - 320	85 -320	25 - 850	60 - 650
Drainage Area, km^2	4.2	0.4	4.7	34	9.1
Rain Gage to Watershed Centroid, km	2	0.8* / 2**	1.5* / 1.5**	5	3
Years of Concurrent Streamflow and Precipitation	18	18	18	6	5

* North Fork Caspar Creek (N408) tipping bucket rain gage.
** North Fork Caspar Creek (N620) tipping bucket rain gage.

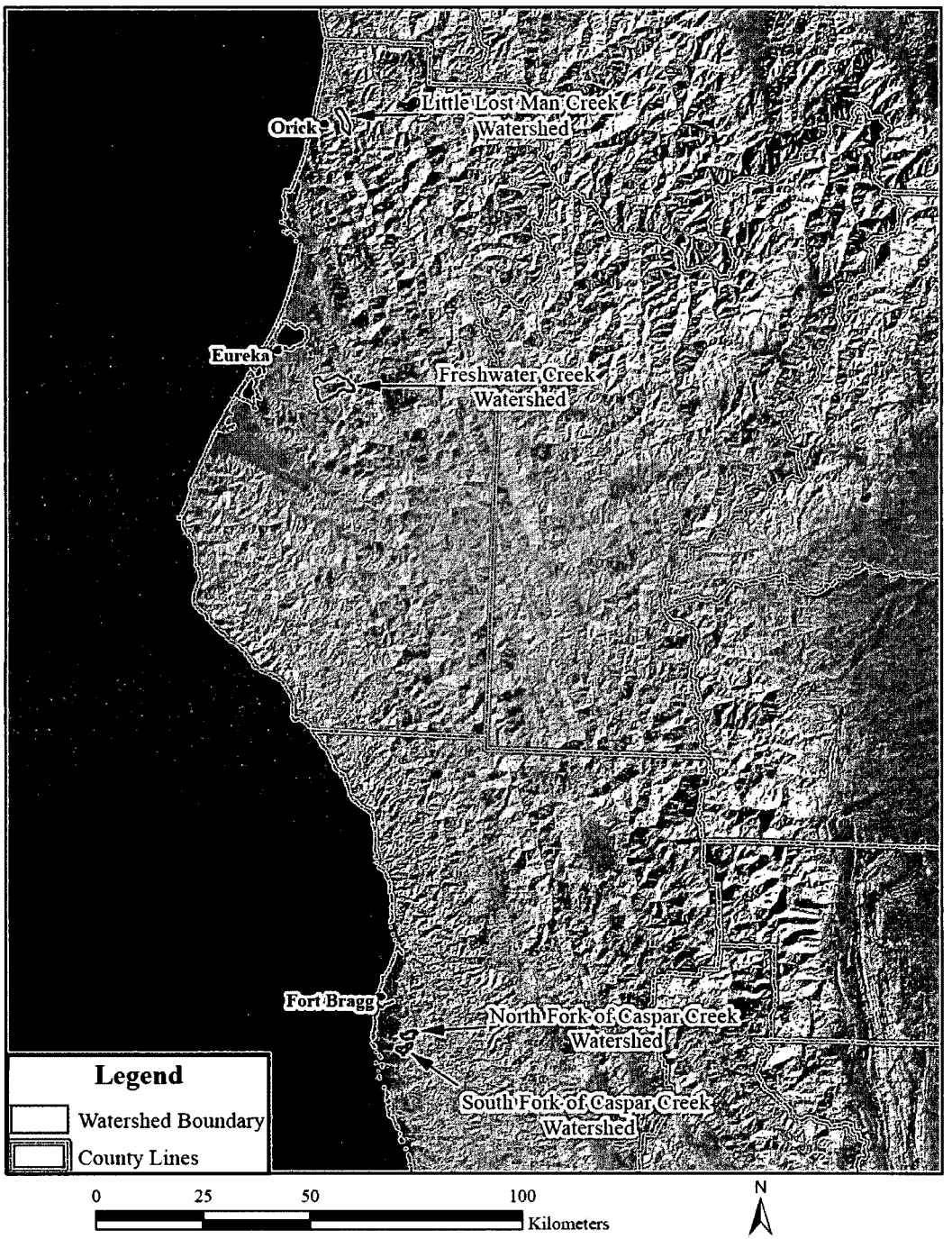

Figure 1 Watershed location map. The Hennington gage is a sub-watershed within the North Fork of Caspar Creek.

section geometry (Klein 2007, personal communication). Therefore, streamflow and precipitation data recorded at the Little Lost Man Creek gage site after 1997 was not used in this study.

Pressure transducers and tipping bucket rain gages have inherent error tolerances. All of the selected watersheds use similar pressure transducers to measure stage with an accuracy of 0.003 meters. Campbell Scientific tipping bucket gages are used at Little Lost Man Creek, Freshwater Creek, and the South Fork of Caspar Creek. The North Fork of Caspar Creek uses a Sierra Misco tipping bucket gage. Rain gage errors are five percent for intensities less than 8.0 cm hr^{-1} (Lewis 2007, personal communication).

API Model Development

The following steps were taken to develop the API model: frequency analysis, hydrograph recession analysis, API calculation, storm event analysis, and least squares regression modeling. Frequency analysis was undertaken to select events with peakflows whose return periods exceed one-year. The analysis used the annual maximum peakflows recorded at the South Fork of Caspar Creek from 1964 to 2004. The one-year peakflow (Q_1) was determined using the Log Pearson III method (Haan 2002). Selective harvesting that occurred during this period did not have a significant effect on annual maximum peakflows (Ziemer 1998).

Corresponding discharge hydrographs and rainfall hyetographs from the South Fork of Caspar Creek (1987 to 2004) were analyzed for their possible use in recession analysis. Recession analysis refers to the systematic observation of hydrograph recession

limbs in order to determine the average rate of discharge decline (Sujona et al. 2004). This analysis used recession limbs of peakflows exceeding Q_1 with data of fair or better quality. Hydrographs were eliminated if additional impulses of rainfall greater than 0.1 cm hr^{-1} or secondary peakflows occurred during the recession limb. These measures were taken to select recession limbs that best represent the recession characteristics of the South Fork of Caspar Creek to discrete rainfall events.

Recession limbs were defined as starting at the peak discharge and ending where Hewlett and Hibbert's (1967) 0.0055 L s^{-1} ha^{-1} baseflow separation line intersected the falling limb. Figure 2 provides an example of the recession limb selection process. Discharge from the selected recession limbs was plotted against discharge lagged by one hour. Following the methodology of Fedora (1987), the slope of the linear regression line was assigned to the recession coefficient in Equation 1.

Hourly time series' of API's were calculated using data from the S620 rain gage in South Fork of Caspar Creek (Equation 1). Calculations ran throughout the water year, since the rapidly decaying API of a prior event should have an insignificant influence after one or two days. For example, after rainfall ceases a recession coefficient of 0.90 will decay API to less than 10 percent of its peak value after 22 hours.

Matching hourly time series' of streamflows and API's from the South Fork of Caspar Creek, (1987 to 2004) were closely investigated. The following storm event attributes were investigated for peakflows exceeding Q_1: peakflow discharge rate, antecedent flow rate, peak API, data quality codes (Figure 3). Successive peakflows occurring on the same hydrograph had to be greater than 24 hours apart and recede by

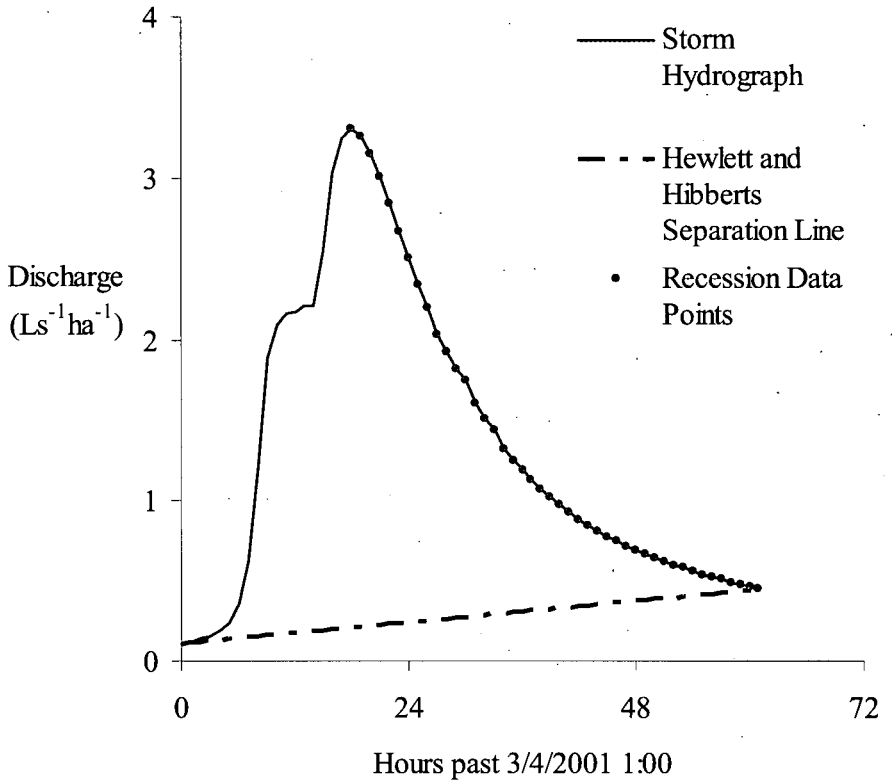

Figure 2 An example of a recession limb from a storm hydrograph recorded at the South Fork of Caspar Creek. Recession limbs began at the peakflow discharge and ended at the point where Hewlett and Hibbert's (1967) baseflow separation line intersects the hydrograph.

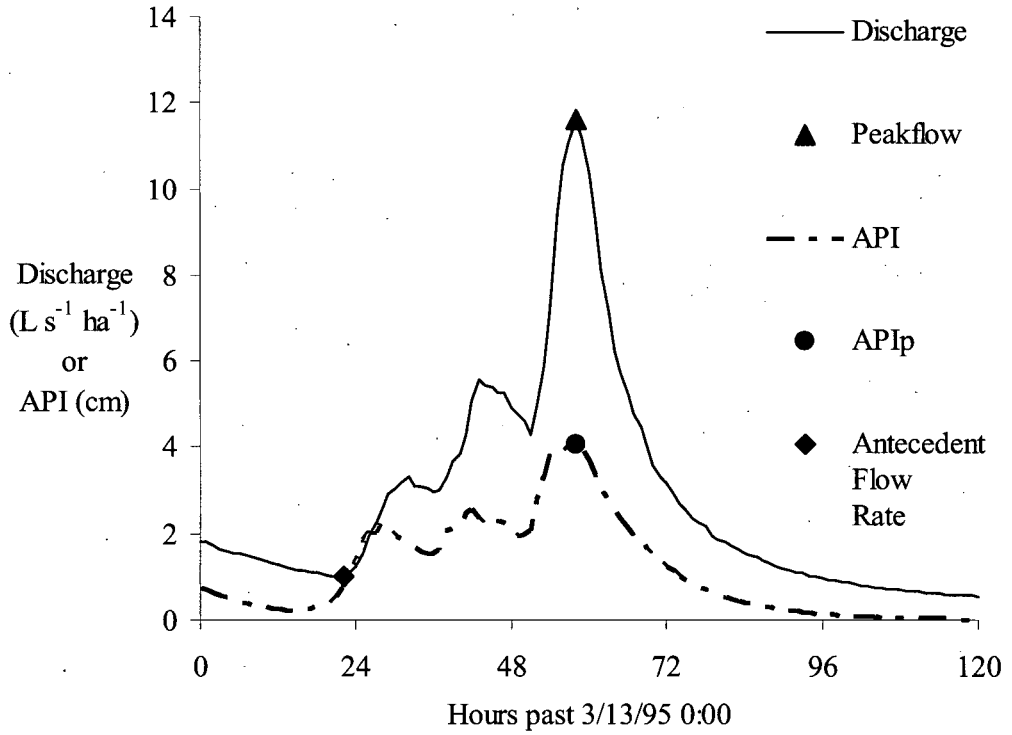

Figure 3 Hourly time series of discharge and API were plotted together to select corresponding peak API (API_p) values and peakflows exceeding Q_1. The previous peaks in the hydrograph were not recorded since they did not recede to less than half of their peak discharge and occurred within 24 hours of the largest peakflow.

50 percent of their peak discharge. Peakflows must rise to double the antecedent flow rate when they occur during hydrograph recession. These restrictions ensure relatively independent peak API values.

Data quality codes for both discharge and rainfall were investigated for each event. Storm events were excluded from this study when the codes indicated poor calibration, large gaps, or data reconstruction of either rainfall or discharge. Data quality codes for discharge were available only for Caspar Creek and Freshwater Creek. Caspar Creek was the only watershed with rain gage quality codes.

Fedora's (1987) API method revealed a different relationship for storm events occurring after extended periods without rain. It was thought that these "dry" events had a lower peakflow response due to a low water table and unsaturated soils. In this study, these conditions were investigated by recording a given storm event's antecedent flow rate. Scatterplots of peakflow as a function of peak API were studied to set an antecedent flow rate threshold that separated "wet" versus "dry" events.

The goal of least squares regression was to create a simple model of peakflow as a function of peak API. A data set must meet a set of assumptions in order to use least squares regression analysis for statistical inference. Since a best fit relationship for peakflow predictions was the main goal of this study, these assumptions were not strictly necessary, but were explored nonetheless. Outliers were first inspected using residual diagnostic techniques, since they can greatly influence the regression modeling results. Outliers could express missing independent variables or multiple populations (Haan 2002). Tests of normality ensured that the residuals were normally distributed.

Autocorrelation was tested using the Durbin-Watson statistic (Hintze 2004).

Independent Model Testing

API calculation and storm event analysis were repeated on the test watersheds. The one-year peakflow, hydrograph recession coefficient, and antecedent flow rate threshold were the same in the test and calibration watersheds. This was necessary to test the method as if rain gages were the only source of data available at the test watersheds. All restrictions applied to the calibration data set were also applied to data sets from the test watersheds for consistent evaluation of model performance.

Bias, precision, and accuracy were used to measure model prediction performance. Statistics used to calculate relative bias, precision, and accuracy were average prediction error, standard deviation of the prediction error, and average absolute prediction error, respectively (Walther and Moore 2005). The prediction error for each observation was calculated using the following equation (Green and Stephenson 1986):

$$E = (Q_p - Q_o / Q_o) * 100 \qquad (2)$$

where E is the prediction error, Q_p is the predicted peakflow in L s^{-1} ha^{-1} and Q_o is the observed peakflow in L s^{-1} ha^{-1}. The average and average absolute prediction error were calculated using the following equations (Green and Stephenson 1986):

$$E_m = (\sum E) / n \qquad (3)$$

$$E_a = (\sum | E |) / n \qquad (4)$$

where E_m is the average prediction error, E_a is the average absolute prediction error, and n is the sample size.

An absolute measure of model accuracy compared the residual standard error (RSE) of the calibration model to the root mean square error (RMSE) of the predicted regression line. The only difference between these two terms is that the sum of the squared residuals is divided by n-2 in the RSE compared to n in the RMSE. The n-2 is used for the calibration model to account for the information used up in estimating the slope and intercept. Model fit was evaluated using the r^2 from the regression of observed versus predicted peakflows. Model fit was also evaluated by testing whether the slope was significantly different from one and the intercept was significantly different from zero (95 percent confidence).

RESULTS

API Model Development

Forty-one annual maximum peakflows were recorded for South Fork Casper Creek with a mean and standard deviation of 10.3 and 5.08 L s^{-1} ha^{-1}, respectively. The largest peakflow on record had a maximum discharge rate of 21.5 L s^{-1} ha^{-1}. All peakflows exceeding Q_1 (2.0 L s^{-1} ha^{-1}) were investigated for their use in hydrograph recession and storm event analysis.

Nineteen recession limbs over the 18 years of record (1987 to 2004) for South Fork of Casper Creek met the stated requirements for hydrograph recession analysis. The associated peakflows had a mean and standard deviation of 6.35 and 5.13 L s^{-1} ha^{-1}, respectively. Segments exceeding 7.5 L s^{-1} ha^{-1} were removed from five recession limbs, since they accounted for 2.5 percent of the discharge observations. This may be explained by an unusually rapid recession following the largest peakflows. Peakflow generation with a greater proportion of saturation overland flow may explain the rapid recession. A regression of discharge lagged by one-hour for 758 discharge observations from the 19 recession limbs is shown in Figure 4. The slope of the linear regression line (0.91) was assigned as the API recession coefficient.

With the estimated recession coefficient of 0.91, API decayed by 90 percent in 26 hours. The time between peakflow events averaged 15 days, but varied from one to 135 days. Only one storm event occurred within 26 hours of a prior event. Peak API would have been reduced by 14 percent if the API time series were reset to zero between these

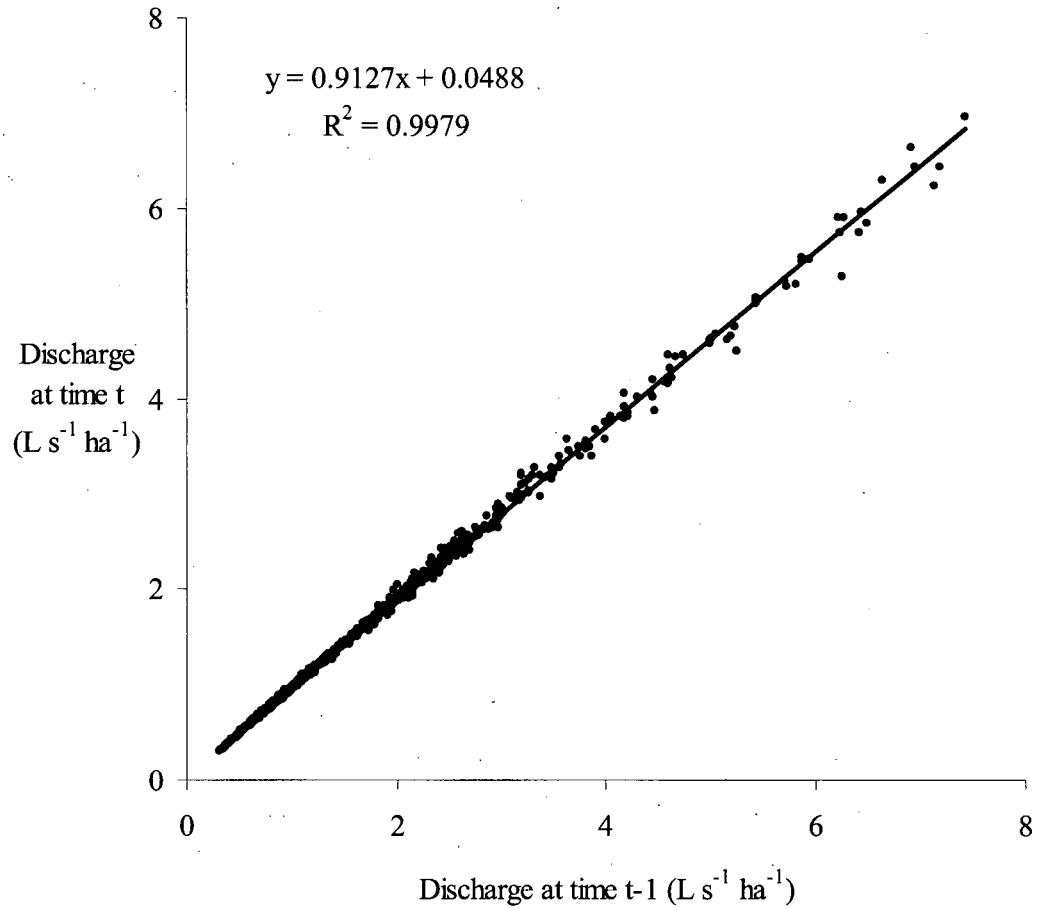

Figure 4 One-hour lag plot of hourly discharge from the South Fork of Caspar Creek.

two events. All peak API's were assumed to be independent since preceding observations had little to no influence on subsequent observations.

A data set of 71 storm events was initially analyzed. A scatterplot of peakflow as a function of peak API had a r^2 equal to 0.60 with a RSE of 2.13 L s^{-1} ha^{-1} (Figure 5). A subset of peakflows, with antecedent flow rates below 0.1 L s^{-1} ha^{-1}, was substantially smaller for a given peak API. Therefore, an antecedent flow rate threshold was set to remove these 12 "dry" events from the original data set. The remaining 59 events had an average peakflow of 5.67 L s^{-1} ha^{-1} and an average peak API of 3.14 cm (Table 2).

A visual inspection of peakflow as a function of peak API reveals a positive relationship. Residual diagnostics indicated that the largest peakflow, which occurred on March 24, 1999, was an outlier (Appendix D through H). Field notes on March 24, 1999 indicate that the V-notch weir was submerged by 0.5 feet (Lewis 2007, personal communication). Average event rainfall agreed to within 10 percent, and one-hour maximum rainfall agreed to within 15 percent at the three Caspar Creek tipping bucket gages. Yet the peakflow recorded at the North Fork of Caspar Creek had a 35 percent lower unit-area discharge rate than that of the South Fork. The March 24 1999 event was removed due to this large deviation in peakflow coupled with the residual diagnostic results.

All residual tests indicated the assumptions of normality were reasonable (alpha = 0.05). The Modified Levene test showed that the residual variance was not constant. Least squares regression analysis was continued regardless of this failure since a best fit for peakflow prediction was the main goal of this study. The Durbin-Watson

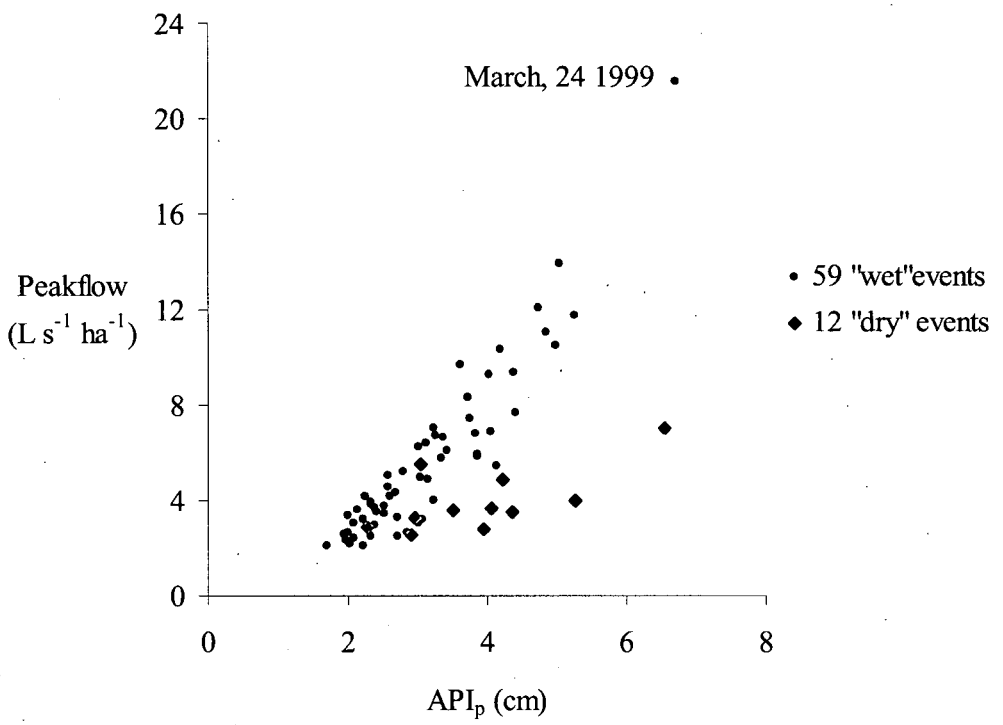

Figure 5 Scatterplot of the 71 selected events with the twelve "dry" events labeled. Storm events were considered "dry" when their antecedent flow rate was below 0.1 L s^{-1} ha^{-1}. The largest event was recorded on March 24 1999.

Table 2 Summary statistics after twelve "dry" storms out of 71 selected events were removed. Storm events were considered "dry" when their antecedent flow rate was below 0.1 L s^{-1} ha^{-1}.

	Peakflow, L s^{-1} ha^{-1}		Antecedent Flow Rate, L s^{-1} ha^{-1}		API_p, cm	
n	Mean	Standard Deviation	Mean	Standard Deviation	Mean	Standard Deviation
59	5.67	3.56	0.54	0.46	3.14	1.02

test for autocorrelation confirmed that peak API values were independent of one another. All tests of regression assumptions are summarized in Appendix I. Summary of the final storm event statistics are listed in Table 3.

The regression model used to predict peakflow as a function of peak API is:

$$Q_p = -3.52 + 2.90 * (API_p) \quad (5)$$

where Q_p is predicted peakflow in L s^{-1} ha^{-1} and API_p is peak API in cm. The r^2 was equal to 0.83 with a RSE of 1.20 L s^{-1} ha^{-1}. The slope term was highly significant ($p < 0.0001$). Figure 6 shows the least squares regression line along with the upper and lower 95 percent Working-Hotelling simultaneous confidence bands (Hintze 2004). These are the confidence bands for all possible values of peak API along the regression line. Additional regression statistics are located in Appendix J. The resulting model may only be applicable for peak API within a range of 1.71 to 5.25 cm. Peak API must be greater than 1.21 cm since lower values will result in negative predicted peakflows.

Independent Model Testing

The results of the API Calculation and Storm Event Analysis on the test watersheds are summarized in Table 4. The North Fork of Caspar Creek had the most observations, while Freshwater Creek had the fewest. The North Fork of Caspar Creek had the largest mean peakflow and peak API, while Freshwater Creek had the smallest.

Peakflow was initially predicted twice at the North Fork of Caspar Creek and Hennington since two rain gages were available. The N408 tipping bucket rain gage was

Table 3 Summary statistics after the March 24, 1999 outlier was removed.

	Peakflow, $L\ s^{-1}\ ha^{-1}$		Antecedent Flow Rate, $L\ s^{-1}\ ha^{-1}$		API_p, cm	
n	Mean	Standard Deviation	Mean	Standard Deviation	Mean	Standard Deviation
58	5.40	2.90	0.54	0.47	3.08	0.91

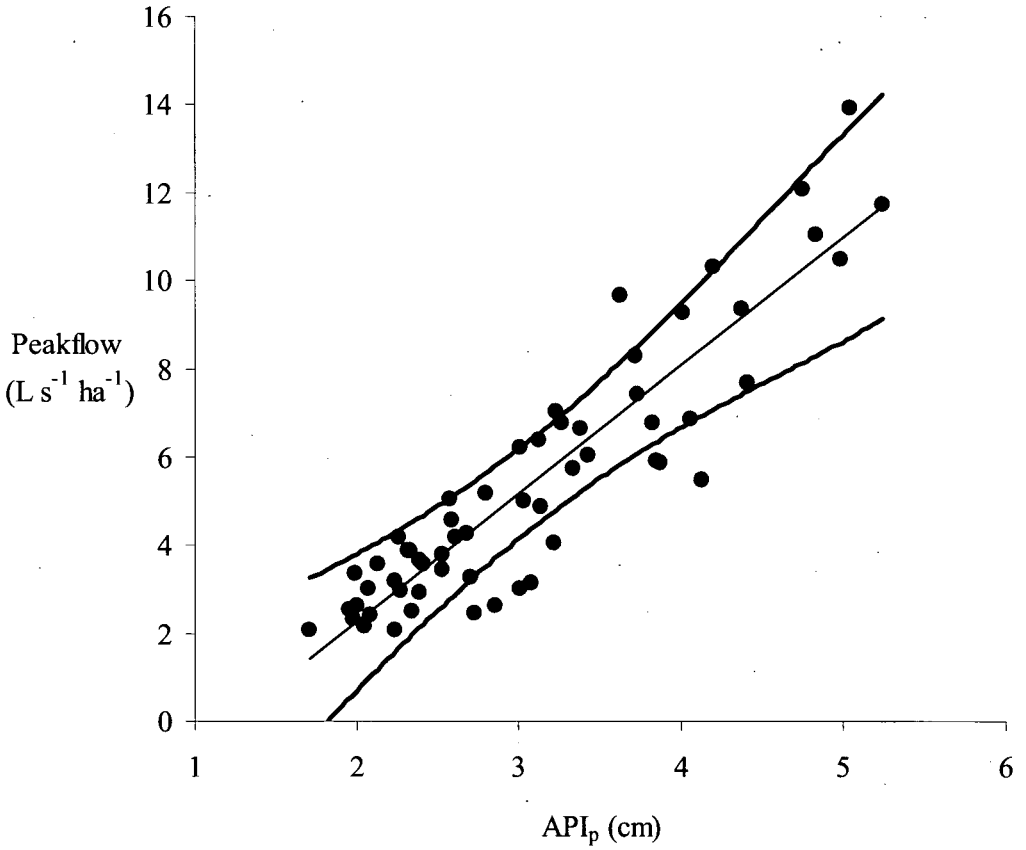

Figure 6 Linear regression line fitted to the 58 selected events along with the upper and lower 95 percent Working-Hotelling confidence bands (bold lines).

Table 4 Summary statistics for selected storm events from the test watersheds.

Test Gaging Station	n	Peakflow, $L\ s^{-1}\ ha^{-1}$		Antecedent Flow Rate, $L\ s^{-1}\ ha^{-1}$		API_p, cm	
		Mean	Standard Deviation	Mean	Standard Deviation	Mean	Standard Deviation
Hennington	39	5.09	2.72	1.22	1.01	3.24	0.98
North Fork of Caspar Creek	49	5.70	2.98	0.79	0.55	3.49	0.97
Little Lost Man Creek	35	4.82	4.95	0.74	0.59	3.46	1.44
Freshwater Creek	32	4.77	3.20	0.69	0.33	2.47	0.89

retained for analysis with Hennington since it produced the best results. Similarly, the N620 tipping bucket rain gage was retained for analysis with the North Fork of Caspar Creek.

Figures 7 through 10 show the prediction error (Equation 2) for each storm event at the test watersheds. All test watersheds showed a decrease in prediction error with increase in peakflow. Unlike the other test watersheds, the majority of the peakflows were under predicted at Freshwater Creek. Little Lost Man Creek had the largest over prediction with almost a third of the errors exceeding 100 percent. Eighty percent of the prediction errors ranged from -50 to 50 percent at all test watersheds, except Little Lost Man Creek.

Bias, precision, and accuracy are summarized in Table 5. The model was positively biased at all test watersheds except Freshwater Creek. Little Lost Man Creek had the lowest precision at 54.2 percent compared to Hennington at 31.5 percent. Little Lost Man Creek had the lowest accuracy at 66.3 percent compared to Hennington at 28.6 percent.

Bias, precision, and accuracy for the ten largest peakflows are summarized in Table 6. The model was positively biased for the ten largest peakflows at all test watersheds except Freshwater Creek. Precision ranged from 12.7 percent at the North Fork of Caspar Creek to 42.8 percent at Little Lost Man Creek. Accuracy ranged from 10.2 percent at the North Fork of Caspar Creek to 44.9 percent at Little Lost Man Creek.

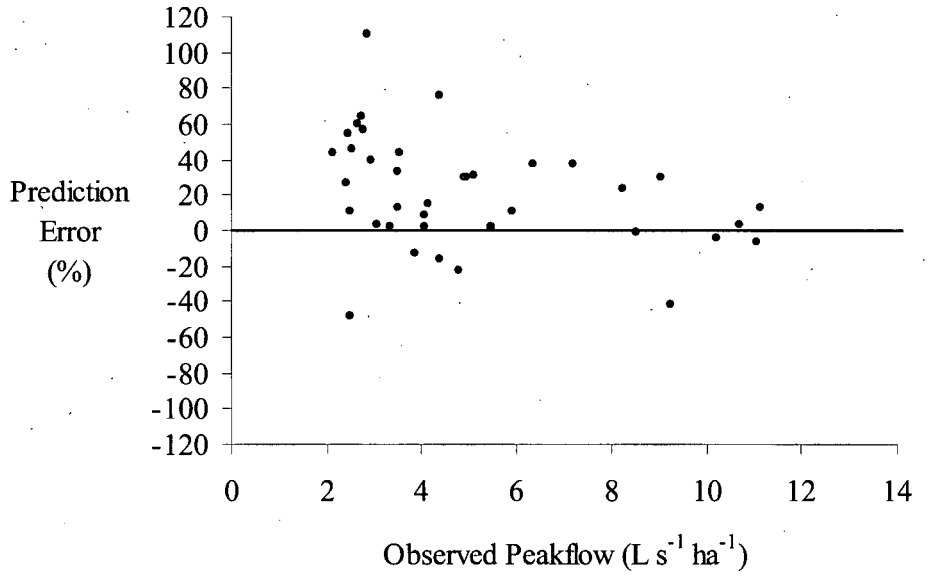

Figure 7 Model prediction errors at the Hennington test watershed show a decrease in variability as peakflows increase in magnitude.

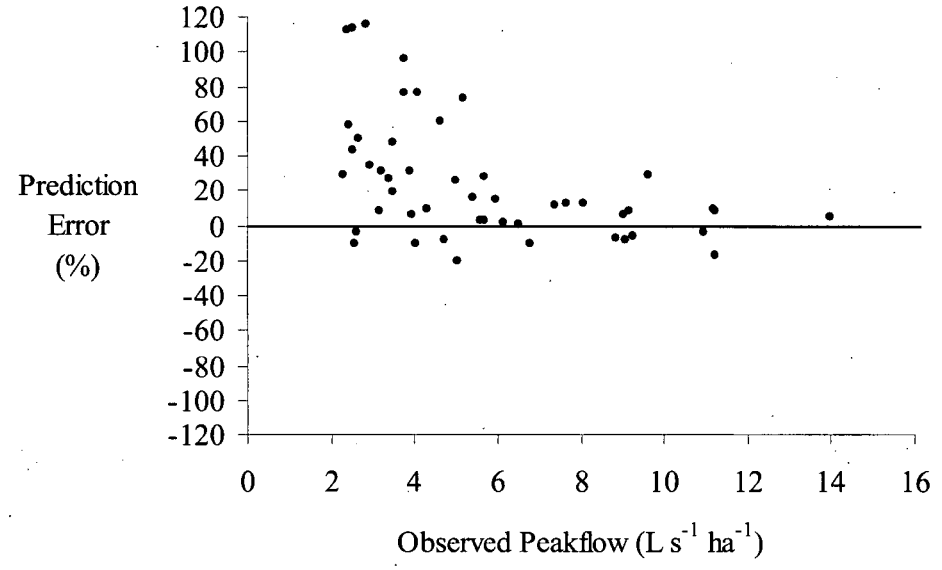

Figure 8 Model prediction errors at the North Fork of Caspar Creek shows a decrease in variability as peakflows increase in magnitude.

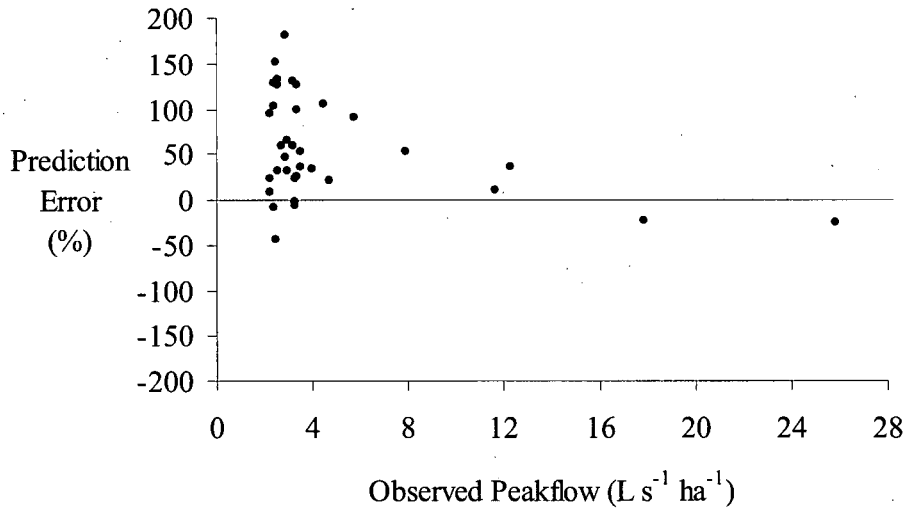

Figure 9 Model prediction errors at Little Lost Man Creek show a decrease in variability as peak flows increase in magnitude.

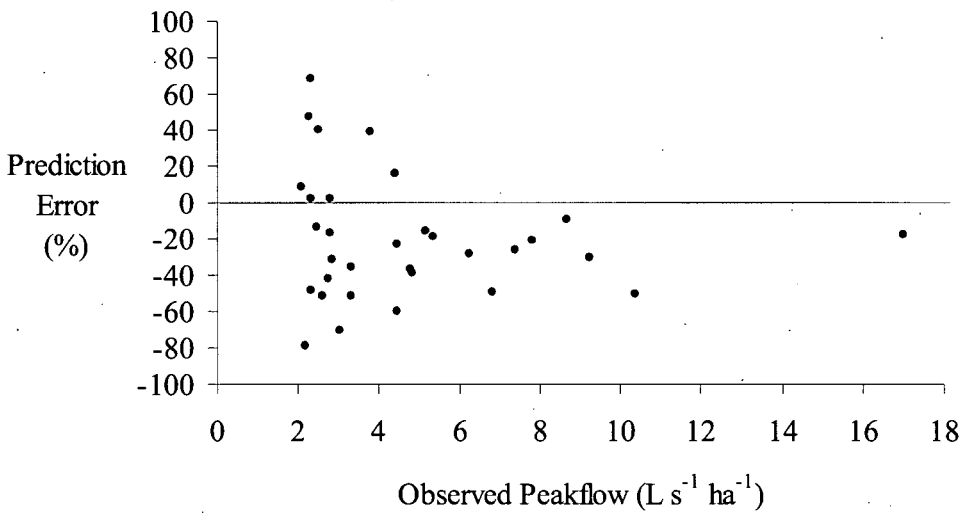

Figure 10 Model prediction errors at Freshwater Creek show a decrease in variability as peakflows increase in magnitude.

Table 5 Bias, precision and accuracy of predicted peakflows at the test watersheds.

		Bias	Precision	Accuracy
		E		
Station	n	Average	Standard Deviation	E_a
		(%)		
Hennington	39	20.7	31.5	28.6
North Fork of Caspar Creek	49	24.5	35.1	29.0
Little Lost Man Creek	35	62.4	54.2	66.3
Freshwater Creek	32	-20.1	34.4	34.0

Table 6 Bias, precision and accuracy for the ten largest peakflows at the test watersheds.

			Bias	Precision	Accuracy
	Observed Peakflow		E		
	Mean	Standard Deviation	Average	Standard Deviation	E_a
Station	L s^{-1} ha^{-1}	L s^{-1} ha^{-1}		(%)	
Hennington	10.2	1.38	4.79	20.2	15.3
North Fork of Caspar Creek	10.5	1.57	3.11	12.7	10.2
Little Lost Man Creek	9.80	7.30	35.5	42.8	44.9
Freshwater Creek	8.50	3.45	-24.6	15.8	24.6

Figure 11 through 14 show regressions of observed versus predicted peakflow at the test watersheds. These contrast with Figures 7 through 10 by showing absolute rather than percentage error. Most peaks were over predicted at the test watersheds except Freshwater Creek. Only the two largest peakflows were under predicted at Little Lost Man Creek. An exponential relationship was observed in Figure 13. This suggests a non-linear relationship between peakflow and peak API at Little Lost Man Creek.

Table 7 lists the least squares regression statistics of the observed versus predicted from the test watersheds. The slope terms were not different from zero and the intercept terms were not different from one (alpha = 0.05). The North Fork of Caspar Creek had the strongest correlation ($r^2 = 0.82$). Hennington and the North Fork of Caspar Creek had the lowest RMSE at 1.27 and 1.26, respectively. Little Lost Man Creek had the lowest r^2 and highest RMSE due to a non-linear relationship.

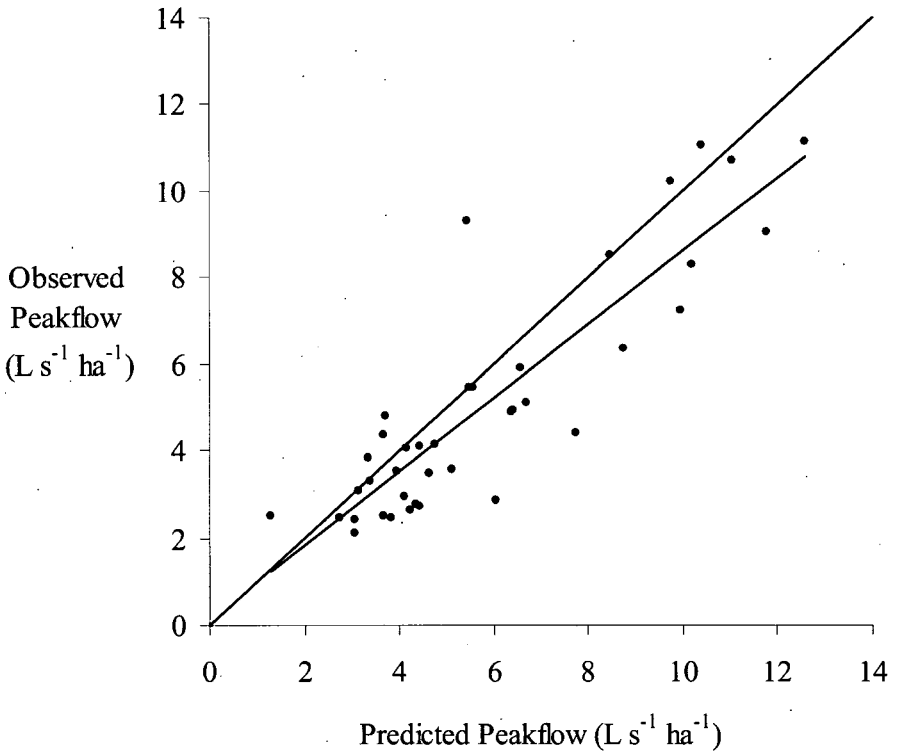

Figure 11 Observed versus predicted peakflow of the 39 events selected from Hennington. The one to one line of perfect agreement is displayed to compare with the linear regression line.

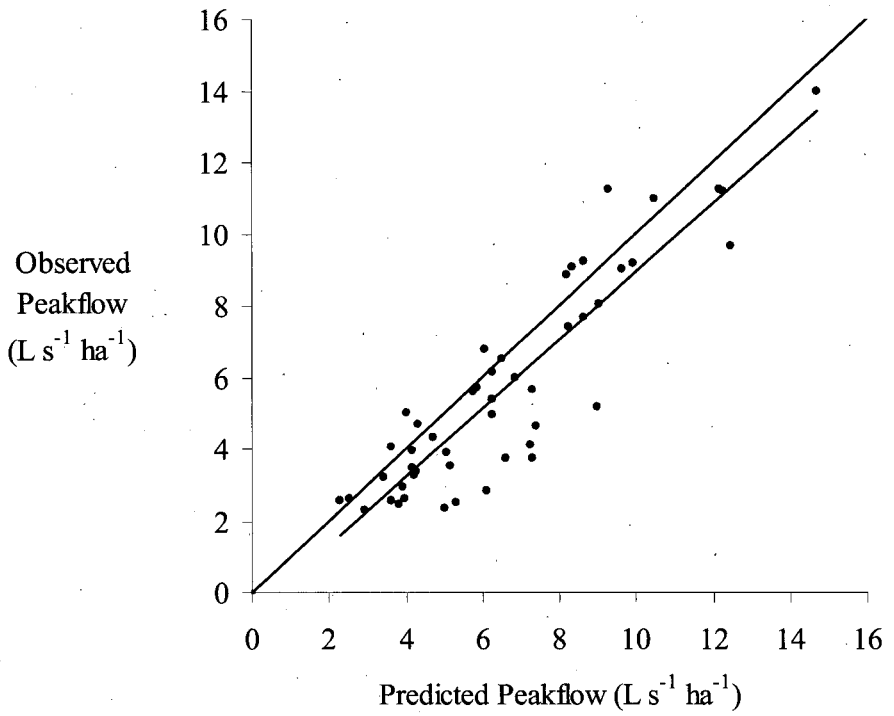

Figure 12 Observed versus predicted peakflow of the 49 events selected from the North Fork Caspar Creek. The one to one line of perfect agreement is displayed to compare with the linear regression line.

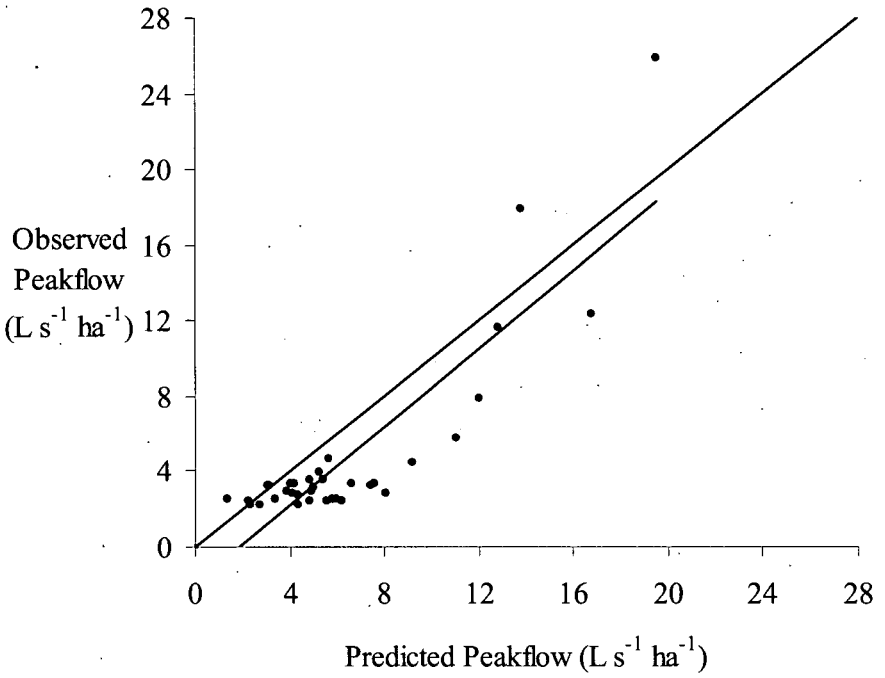

Figure 13 Observed versus predicted peakflow of the 35 events selected from Little Lost Man Creek. The one to one line of perfect agreement is displayed to compare with the linear regression line.

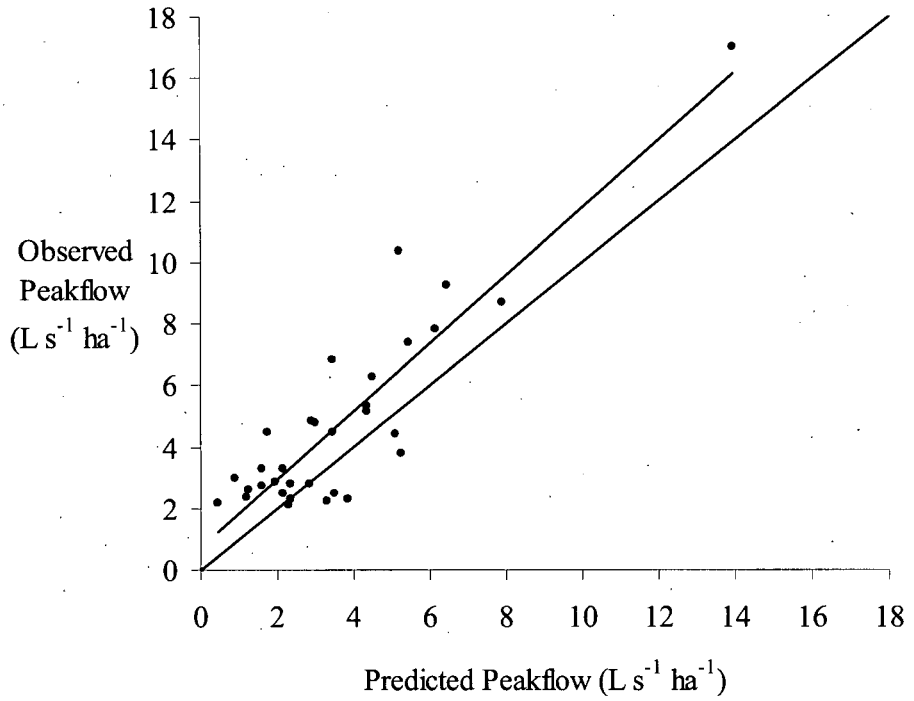

Figure 14 Observed versus predicted peakflow of the 32 events selected from Freshwater Creek. The one to one line of perfect agreement is displayed to compare with the linear regression line.

Table 7 Least squares regression statistics of the observed versus predicted peakflow from the test watersheds.

Station	n	Slope	Intercept	r^2	RMSE
Hennington	39	0.85	0.13	0.78	1.27
North Fork of Caspar Creek	49	0.95	-0.58	0.82	1.26
Little Lost Man Creek	35	1.04	-1.92	0.76	2.38
Freshwater Creek	32	1.11	0.73	0.80	1.42

DISCUSSION

A positive correlation exists between peakflow and peak API at the calibration watershed. The intercept is negative making the model only valid for peak API's above 1.21 cm. Variability in the relationship between peakflow and peak API was characterized by several measures. The r^2 value indicated that peak API explained 83 percent of the variability in peakflow. The residual standard error was 21 percent of the average peakflow. Nineteen percent of the observations fell outside of the confidence bands. Variability can be attributed to a simple linear regression model being used to predict complex non-linear rainfall-runoff processes. These processes, which include rainfall intensity, interception, evapotranspiration, soil hydraulic conductivity, pipeflow, and local saturation overland flow, vary spatially and temporally over a watershed throughout a storm event (Beven 2001).

The relationship between peakflow and peak API showed that "dry" events with antecedent flow rates below 0.1 L s^{-1} ha^{-1} produced substantially smaller peakflows for a given peak API. The calibration model had a 28 percent lower r^2 and a 44 percent higher RSE prior to the removal of the twelve "dry" events. The results are similar to those of Fedora (1987) in that a recession coefficient based on hydrograph recession analysis caused peak API to decay so quickly that long-term antecedent moisture conditions were not properly addressed.

The muted streamflow response with low antecedent flow was most likely due to soil moisture and shallow groundwater deficits occurring after prolonged periods of

drought. Greater antecedent flow indicates higher soil moisture and an elevated water table, creating a larger saturation overland flow response to rain. However, exploratory multiple regression analysis revealed that antecedent flow rate was not a reliable variable throughout the range of peakflows analyzed in this study.

Antecedent flow rate was not related to peakflow or peak API, but proved a reliable threshold indicator of catchment wetness. Lynch and Corbett (1982) explored the relationship between antecedent flow rate, antecedent soil moisture and hydrograph parameters. Antecedent soil moisture was a steep function of antecedent flow rate that flattened to a slope of zero above 0.05 L s^{-1} ha^{-1}, which is relatively close to the threshold set in this study. The small watersheds in this study, like those studied by Lynch and Corbett (1982), have relatively "flashy" and more ephemeral streamflow response than larger watersheds due to less groundwater interaction in holding and releasing flows.

Both consistent under or over prediction at the test watersheds may be due to variability in unit-area discharge relationships. Unit-area discharge had less variability in watersheds larger than 10 km^2 in drainage area (Robinson et al. 1995). Ziemer and Rice (1990) found that mean flow path had a significant positive association with lag-time and an insignificant negative association with unit-area discharge of progressively larger sub-watersheds within the North Fork of Caspar Creek. These results indicate that hillslope processes strongly control streamflow response in the North Fork of Caspar Creek.

Unlike the other test watersheds, the API model was negatively biased for Freshwater Creek. One would expect the API model to be biased to over predict, instead of under predict at Freshwater Creek, since channel roughness and bank storage should

increase lag-time and flatten peakflow response in larger watersheds (Gomi et al. 2002). A combination of clearcut and selective harvesting from 1989 to 1999 removed roughly 82 percent of the timber volume above the stream gage (Glass 2003). Reid and Lewis (2007) indicated a 29 percent increase in rainfall that reaches the forest floor after clearcut timber harvesting. The under prediction of peakflows at Freshwater Creek is most likely due to lower interception and evapotranspiration rates.

The consistent over prediction at the other three watersheds could be due to skid trails in the South Fork of Caspar Creek. Soil compaction due to legacy skid trails could cause overland flow, which artificially extends the natural drainage system. An overland flow component may not have been captured in this API methodology. This phenomenon is less prominent in the North Fork of Caspar Creek since cable yarding produced less soil compaction when compared to selective tractor yarding (Ziemer 1998).

Fedora (1987) analyzed the largest annual events, which resulted in only six to 20 events from his study watersheds. Beschta's (1990) test of Fedora's methodology only looked at four peakflows and three flood events. In contrast, my study looked at every peakflow exceeding Q_1, which resulted in 32 to 58 events from the selected watersheds. Accuracy for peakflow prediction ranged from 10.4 to 30.4 percent in Fedora's (1987) study and 14 to 14.8 percent in Beschta's (1990) study compared to 28.6 to 66.3 percent in my study. Higher variability was expected in my study because the data set represents peakflow response over a wider range of rainfall intensities, amounts, and antecedent soil moisture conditions.

The API model predicted peakflows at Hennington better than the other test watersheds with 28.6 percent accuracy. The North Fork of Caspar Creek was equally accurate at 29.0 percent. Predicted peakflow at Freshwater Creek was 32 percent more accurate than at Little Lost Man Creek. As expected, the RMSE for prediction in the test watersheds exceeded the calibration RSE. Prediction at the North Fork of Caspar Creek (RMSE = 1.26 L s^{-1} ha^{-1}) and Hennington (RMSE = 1.27 L s^{-1} ha^{-1}) was only slightly less accurate than in the calibration watershed, South Fork of Caspar Creek (RSE = 1.20 L s^{-1} ha^{-1}). Little Lost Man Creeks RMSE was 98 percent greater than the calibration RSE. Freshwater Creek had a RMSE 18 percent greater than the calibration RSE, which was surprisingly better than Little Lost Man Creek.

The regression of observed versus predicted peakflow at Little Lost Man Creek revealed a positive exponential transition from larger to smaller peaks. This suggests that the linear relationship used in this study was not adequate for peakflow prediction at Little Lost Man Creek. An exponential relationship between peakflow and peak API should increase the predictive capability at Little Lost Man Creek. Although not explored in this study, an exponential transformation of peak API may be useful to increase prediction power in future applications of this methodology.

The South Fork of Caspar Creek may not truly represent the processes that control streamflow generation at the test watersheds. Errors in peakflow prediction could be due to localized geologic and pedologic variability. The South Fork of Caspar Creek may have greater connectivity in soil macropores and pipes, creating a faster response and generating larger peakflows. Even though the watersheds have relatively similar

geology, heterogeneous lithology could restrict preferential flow paths. The geological formations in the Oregon Coast Range watersheds used by Fedora (1987) may not have as much variability in localized lithology as in the Northern California Coast Range.

Rainfall variability over a given watershed is very hard to quantify unless a dense network of rain gages is present. Rain gages are sparse throughout the Northern California Coast Range, although Caspar Creek Experimental Watershed is an exception. Rainfall intensity can vary significantly within one km (Singh 1997). Individual storms could have errors in rainfall measurements up to 75 percent due to the effects of wind and location (Dingman 2002). Due to orographic influences on rainfall amounts and intensities, rain gages misrepresent a watershed's actual mean rainfall. Erroneous rainfall data may have been used to calculate peak API at the other test watersheds, since only Caspar Creek had rain gage error codes.

The different gaging station control structures could have also influenced model performance. Without artificial control, the location of a gaging station can greatly affect the accuracy and consistency of streamflow measurements. None of the stream gages in this study met all of the criteria for optimal stream gage location (Rantz 1982). It is very hard to find a location in these small watersheds where the stream course is straight for 100 m upstream and downstream. Stage data quality was not available to remove erroneous data at Little Lost Man Creek.

When the ten largest peakflows were analyzed separately, the API model had a higher accuracy of 10.2 to 44.9 percent. The average accuracy of the predicted peakflows at the test watersheds was increased by 40 percent. The test of the API

methodology, like the findings of Fedora (1987) and Beschta (1990), revealed that the largest peakflows on record had the lowest errors. These are promising results for flood prediction since the largest peakflows in this study had return periods which ranged from a 4-year to a 10-year event.

Better prediction of these large events was most likely due to a simplification of physical processes once the soils are saturated and macropores reach their maximum flow rate (Ziemer and Lisle 1998). This may also be explained by decreased variability of interception rates as peakflows increased in magnitude (Link et al. 2004, Pypker et al. 2005, Reid and Lewis 2007). Smaller events could have greater variability in the interactions between the processes that control streamflow generation. These interactions were not addressed in this study.

LITERATURE CITED

Beschta, R.L. 1990. Peakflow estimation using an antecedent precipitation index (API) model in tropical environments. Pages 128-137 in R.R. Ziemer, C.L. O'loughlin, and L.S. Hamilton, editors. Research needs and applications to reduce sedimentation and erosion in tropical steeplands. International Association of Hydrologic Sciences. Publication 192. Washington, D.C.

Betson, R.P., R.L. Tucker, and F.M. Haller. 1969. Using analytical methods to develop a surface runoff model. Water Resources Research 5: 103-111.

Beven, K. J. 2001. Rainfall-runoff modeling: the primer. John Wiley & Sons, Ltd., New York, New York.

Brooks, K.N., P.F. Ffolliott, H.M. Gregersen, and L.F. DeBano. 1997. Hydrology and the management of watersheds. Iowa State University Press, Ames, Iowa.

Cafferata, P., T. Spittler, M. Wopat, G. Bundros, and S. Flanagan. 2004. Designing watercourse crossings for passage of the 100-year flood flows, wood, and sediment. California Department of Forestry and Fire Protection, California Forestry Report No. 1. Sacramento, California

Dingman, S.L. 2002. Physical hydrology. Prentice Hall, Upper Saddle River, New Jersey.

Fedora, M. A. 1987. Simulation of storm runoff in the Oregon Coast Range. Bureau of Land Management Technical Note 378. Denver, Colorado.

Glass, D. 2003. Freshwater Creek watershed analysis cumulative effects assessment. Report of Watershed Professionals Network to Pacific Lumber Company (PALCO), Scotia, California.

Gomi, T., R.C. Sidle, and J.S. Richardson. 2002. Understanding processes and downstream linkages of headwater systems. BioScience 52: 905-916.

Green, I.R.A. and D. Stephenson. 1986. Criteria for comparison of single event models. Hydrological Sciences 31: 395-411.

Haan, C. T. 2002. Statistical methods in hydrology. Iowa State University Press, Ames, Iowa.

Hewlett, J. D. and A. R. Hibbert. 1967. Factors affecting the response of small watersheds to precipitation in humid areas. Pages 275-290, in W.S. Sapper and H.W. Lull, editors. International Symposium on Forest Hydrology. Pergamon Press, New York, New York.

Hintze, J. 2004. NCSS and PASS. Number cruncher statistical systems. Kaysville, Utah. Available at www.ncss.com. Contacted on May 20, 2007.

Kohler, M. A., and R. K. Linsley. 1951. Predicting the runoff from storm rainfall. United States Weather Bureau Research Paper 34. Washington, D.C.

Lee, J. and D. I. Bray. 1969. The estimation of runoff from rainfall for New Brunswick watersheds. Journal of Hydrology 9: 427-437.

Link, T.E., M. Unsworth and D. Marks 2004. The dynamics of rainfall interception by a seasonal temperate rainforest. Agricultural and Forest Meteorology 124: 171-191.

Lynch, J. A. and E. S. Corbett. 1982. Relationship of antecedent flow rate to storm hydrograph components. Pages 73-77, in A.I. Johnson and R.A. Clark, editors. International Symposium on Hydrometeorology June 13-17, 1982, Denver, Colorado. American Water Resources Association.

Moreda, F., V. Koren, Z. Zhang, S. Reed, and M. Smith. 2006. Parameterization of distributed hydrological models: learning from experiences of lumped modeling. Journal of Hydrology 320: 218-237.

Piehl, N.E., M.R. Pyles, and R.L. Beschta. 1988. Flow capacity of culverts of the Oregon Coast Range forest roads. Water Resources Bulletin 24: 631-637.

Pypker, T.G., B.J. Bond T.E. Link, D. Marks, and M.H. Unsworth. 2005. The importance of canopy structure in controlling the interception loss of rainfall: Examples from a young and an old-growth Douglas-fir forest. Agricultural and Forest Meteorology 130: 113-129

Rantz, S.E. 1982. Measurement and computation of streamflow: Vol. 1 Measurement of stage and discharge. United States Geological Survey, Water Supply Paper 2175. Washington, D.C.

Reid, L.M. and J. Lewis. 2007. Rates and implications of rainfall interception in a coastal redwood forest. Pages 107-117 in R.B. Standiford, G.A. Giusti, Y. Valachovic, W.J. Zielinski, and M.J. Furniss, editors. Proceedings of the redwood region forest science symposium: What does the future hold? United States Department of Agriculture, Forest Service, Pacific Southwest Research Station, General Technical Report 194. Albany, California.

Robinson, J. S., M. Sivapalan, and J. D. Snell. 1995. On the relative role of hillslope processes, channel routing, and network geomorphology in the hydrologic response of natural catchments. Water Resources Research 31: 3089-3101.

Shade, P.J. 1984. Hydrology and sediment transport, Moanalua Valley, Hawaii. United States Geological Survey, Water Resources Investigation Report 84-4156. Honolulu, Hawaii.

Singh, V.P. 1997. Effect of spatial and temporal variability in rainfall and watershed characteristics on stream flow hydrograph. Hydrological Processes 11: 1649-1669.

Sittner, W. T., C. E. Schauss, and J. C. Monroe. 1969. Continuous hydrograph synthesis with an API-type model. Water Resources Research 5: 1007-1022.

Smakhtin, V. Y. and B. Masse. 2000. Continuous daily hydrograph simulation using duration curves of a precipitation index. Hydrological Processes 14: 1083-1100.

Sujono, J., S. Shikasho, and H. Hiramatsu. 2004. A comparison of techniques for hydrograph recession analysis. Hydrological Processes 18: 403-413.

Velleman, P.F. and R.E. Welsch. 1981. Efficient computing of regression diagnostics. The American Statistician 35: 234-242.

Walther, B.A. and J.L. Moore. 2005. The concepts of bias, precision and accuracy, and their use in testing the performance of species richness estimators, with a literature review of estimator performance. Ecography 28: 815-829.

Woiska, E. P. 1981. Hydrologic properties of one major and two minor soil series of the Coast Ranges of Northern California. Master of Science Thesis, Natural Resources, Humboldt State University, Arcata, California.

Ziemer, R. R. 1998. Flooding and Stormflows. Pages 15-24, in R. R. Ziemer, editor. Proceedings of the conference on coastal watersheds: The Caspar Creek story. United States Department of Agriculture, Forest Service, Pacific Southwest Research Station, General Technical Report 168. Albany, California.

Ziemer, R. R. and J.S. Albright. 1987. Subsurface pipeflow dynamics of north-coastal California swale systems. Pages 71-80, in R. L. Beschta, T. Blinn, G. E. Grant, G. G. Ice, and F. J. Swanson, editors. Erosion and sedimentation in the Pacific Rim. International Association of Hydrological Sciences. Publication 165. Washington, D.C.

Ziemer, R.R. and T. E. Lisle. 1998. Hydrology. Pages 43-68, in R.J. Naiman and R.E. Bilby, editors. River ecology and management: lessons from the Pacific Coastal Ecoregion. Springer-Verlag, New York, New York.

Ziemer, R. R. and R. M. Rice. 1990. Tracking rainfall impulses through progressively larger drainage basins in steep forested terrain. Pages 413-420, in H. Lang and A. Musy, editors. Hydrology in mountainous regions. 1 – Hydrological measurements; the water cycle. International Association of Hydrological Sciences. Publication 193. Washington, D.C.

PERSONAL COMMUNICATIONS

Klein, R. 2007. Personal Communications. Redwood National and State Parks, 1655 Heindon Road, Arcata, CA 95521

Lewis, J. 2007. Personal Communications. Redwood Sciences Laboratory, Pacific Southwest Research Station, USDA Forest Service, 1700 Bayview Drive, Arcata, CA 95521

LIST OF VARIABLES AND ACRONYMS

API = Antecedent precipitation index, cm

API_p = Peak API, cm

C = Recession coefficient, dimensionless

E = Prediction error for each observation, (%)

E_a = Average absolute prediction error, (%)

E_m = Average prediction error, (%)

$P_{\Delta t}$ = Precipitation occurring between times t-1 and t, cm

RMSE = Root mean square error, L s^{-1} ha^{-1}

RSE = Residual standard error, L s^{-1} ha^{-1}

Q_1 = Peakflow with a return period of one-year equal to 2.0 L s^{-1} ha^{-1}

Q_o = Observed peakflow, L s^{-1} ha^{-1}

Q_p = Predicted peakflow, L s^{-1} ha^{-1}

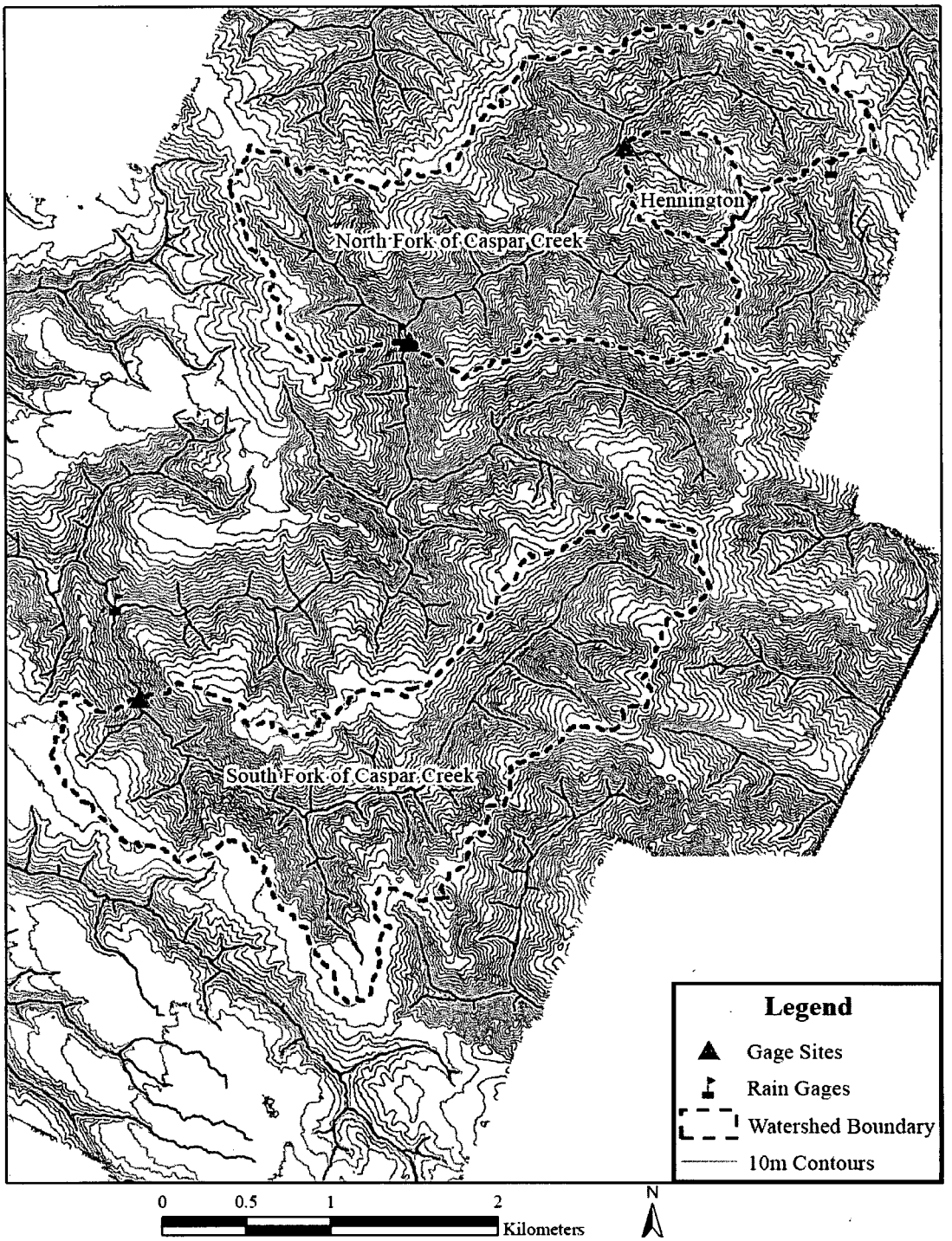

Appendix A. South Fork of Caspar Creek, North Fork of Caspar Creek, and Hennington watershed boundaries with gage sites and rain gage locations

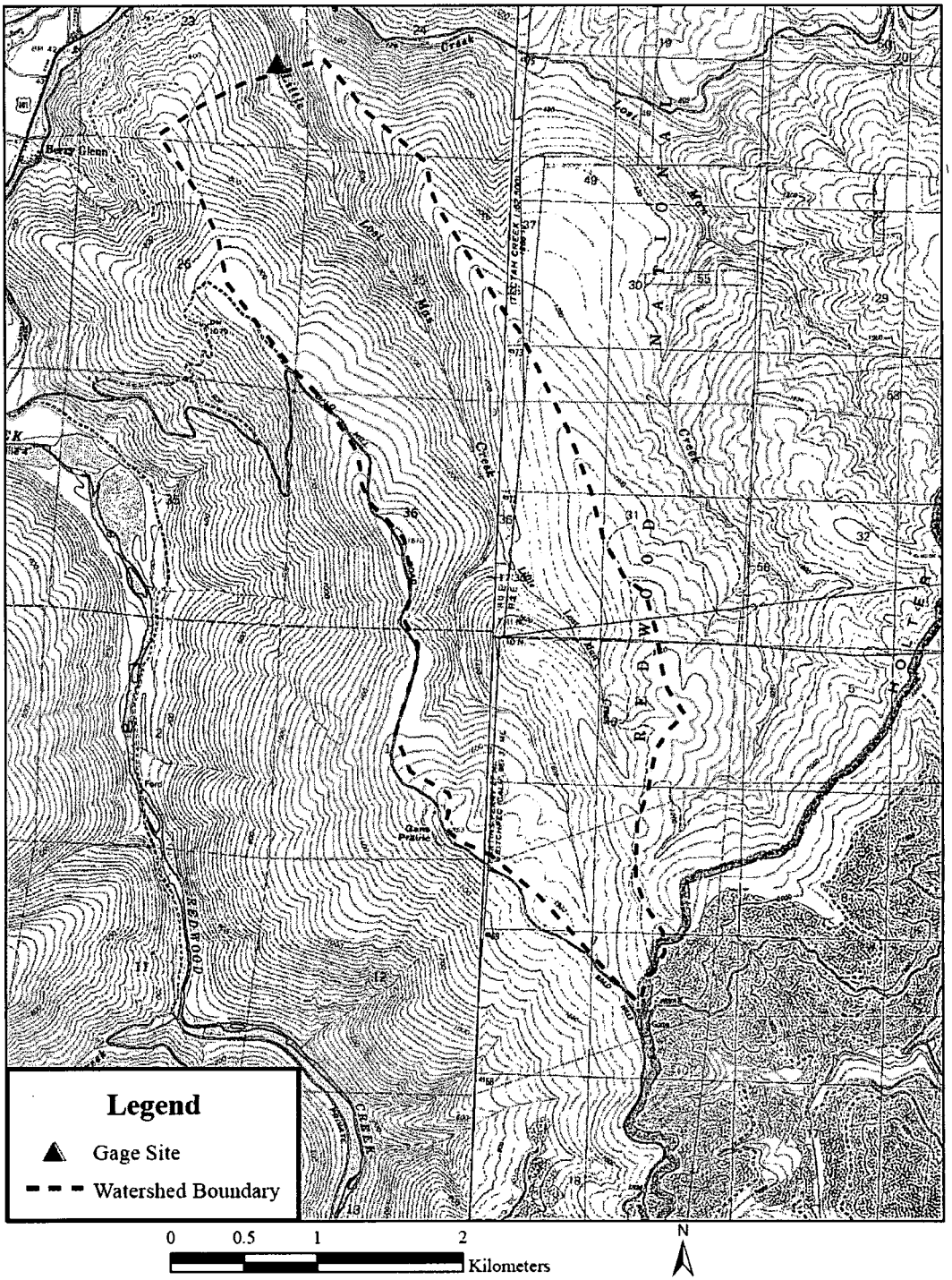

Appendix B. Little Lost Man Creek watershed boundary and gage site location.

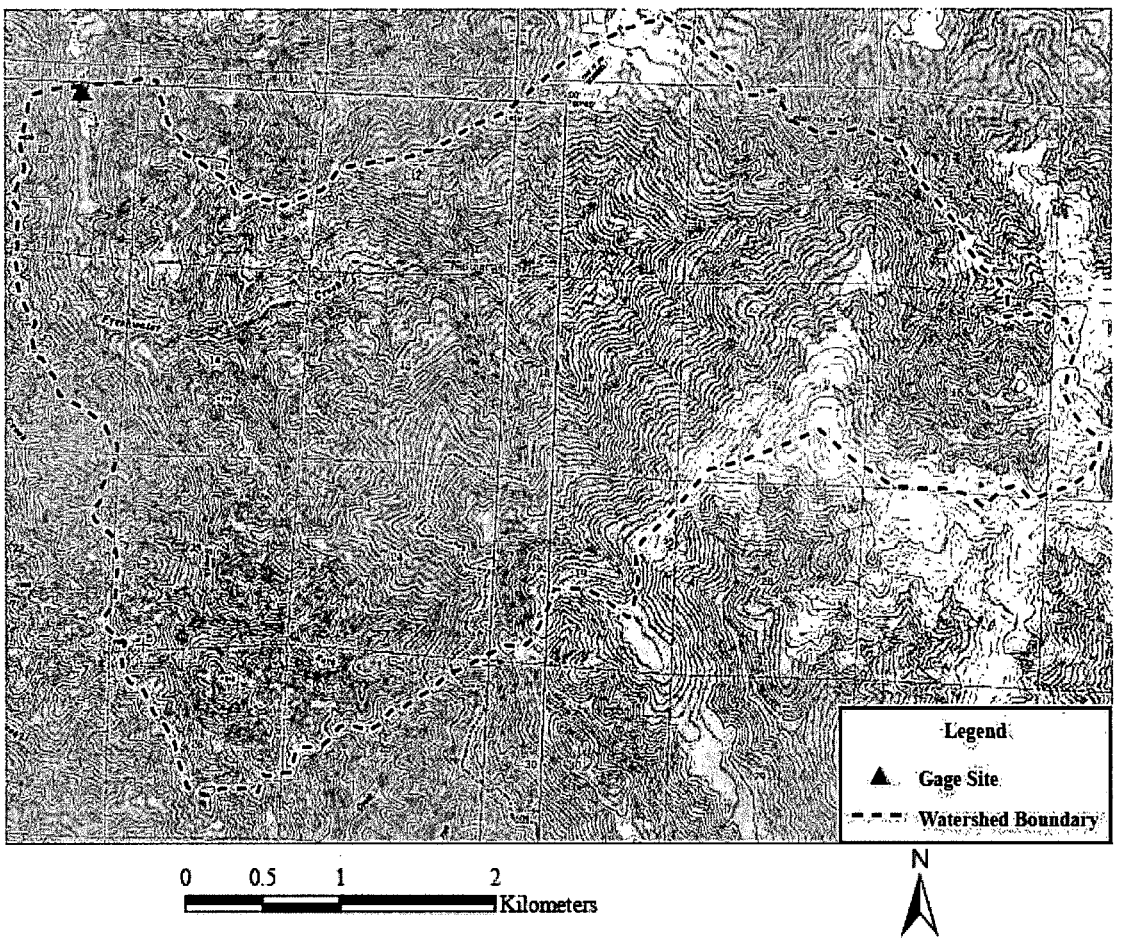

Appendix C. Freshwater Creek watershed boundary and gage site location.

Appendix D. Outlier detection statistics from residual diagnostics before and after the March 24, 1999 event was removed. The March 24, 1999 event failed all four tests. The three remaining observations passed the DFFITS and Cook's D tests. Two out of the three were considered high leverage outliers based on Rstudent and Hat Diagonal, the other failed the Rstudent test. All statistics were calculated using NCSS (Hintze 2004).

	Initial Outlier Detection Statistics				
API_p	Residual	Rstudent*	DFFITS**	Cook's D***	Hat Diagonal****
4.13	-3.3886	-2.5746	-0.476	0.1016	0.0331
6.72	3.8943	3.5637	2.1085	1.7944	0.2593
	Outlier Detection Statistics after March 24, 1999 event removal				
API_p	Residual	Rstudent	DFFITS	Cook's D	Hat Diagonal
5.05	2.7111	2.3672	0.8255	0.3109	0.1084
3.63	2.684	2.2259	0.3476	0.0558	0.0238
4.13	-2.987	-2.5342	-0.5235	0.1231	0.0409

* An observation is considered an outlier if the absolute value of Rstudent (also known as the studentized deleted residuals) is greater than two (Hintze 2004).

** An observation is considered influential concerning prediction if the absolute value of DFFITS is greater than one. DFFITS measures the influence of a single observation on its fitted value (Velleman and Welsch 1981).

*** Cook's D values greater than one indicate that the observations have a large influence. It measures the influence of each observation on all fitted values (Velleman and Welsch 1981).

**** Hat Diagonal measures the remoteness of the observations in the X-space. Hat Diagonals greater than 2*degrees of freedom / n (2*2/59 = 0.068) are considered high-leverage observations. Leverage refers to the amount of influence a given observation has on the trend of the least squares regression estimate (Velleman and Welsch 1981).

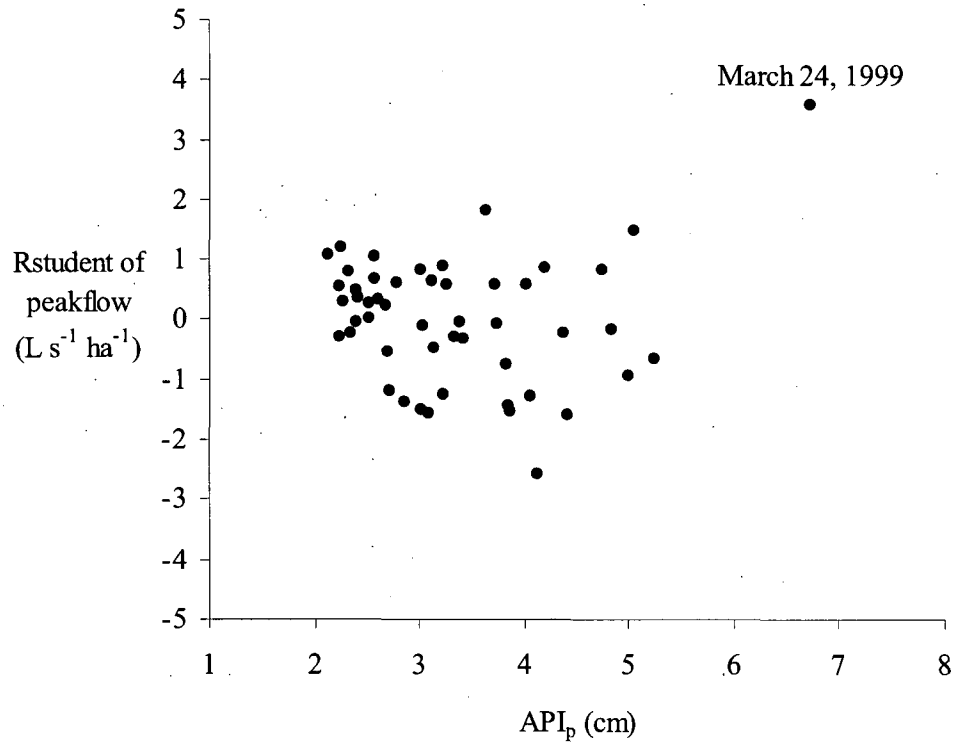

Appendix E. Rstudent as a function of peak API shows the March 24, 1999 event as an outlier.

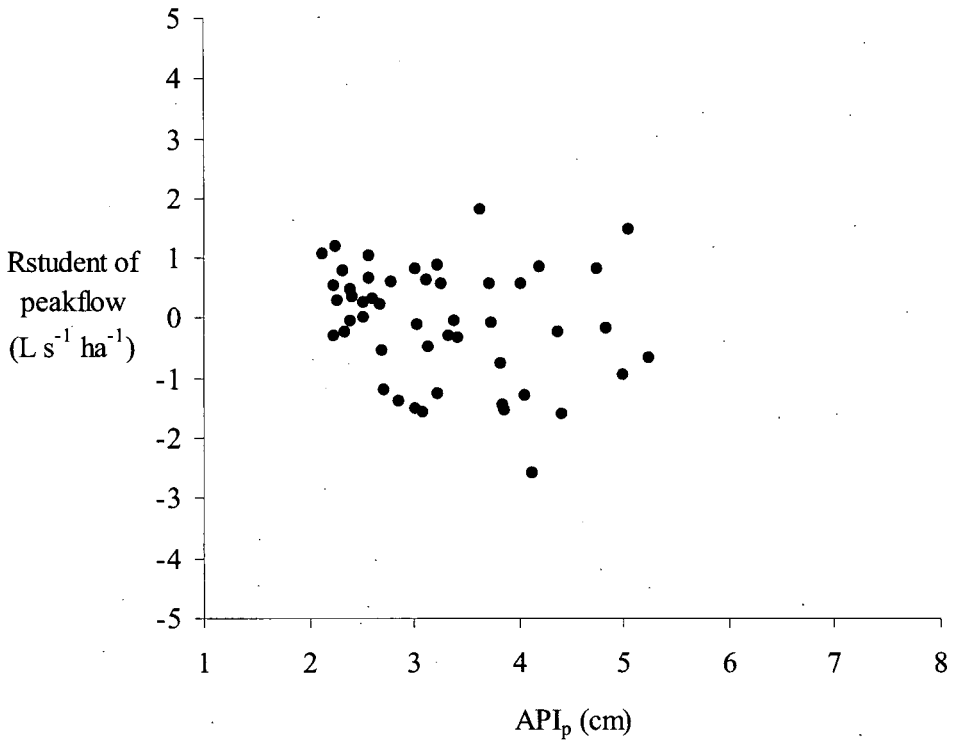

Appendix F. Rstudent as a function of peak API with the March 24, 1999 event removed. Two observations with an absolute value of Rstudent greater than two remain. These observations were retained because they did not deviate significantly from the cloud.

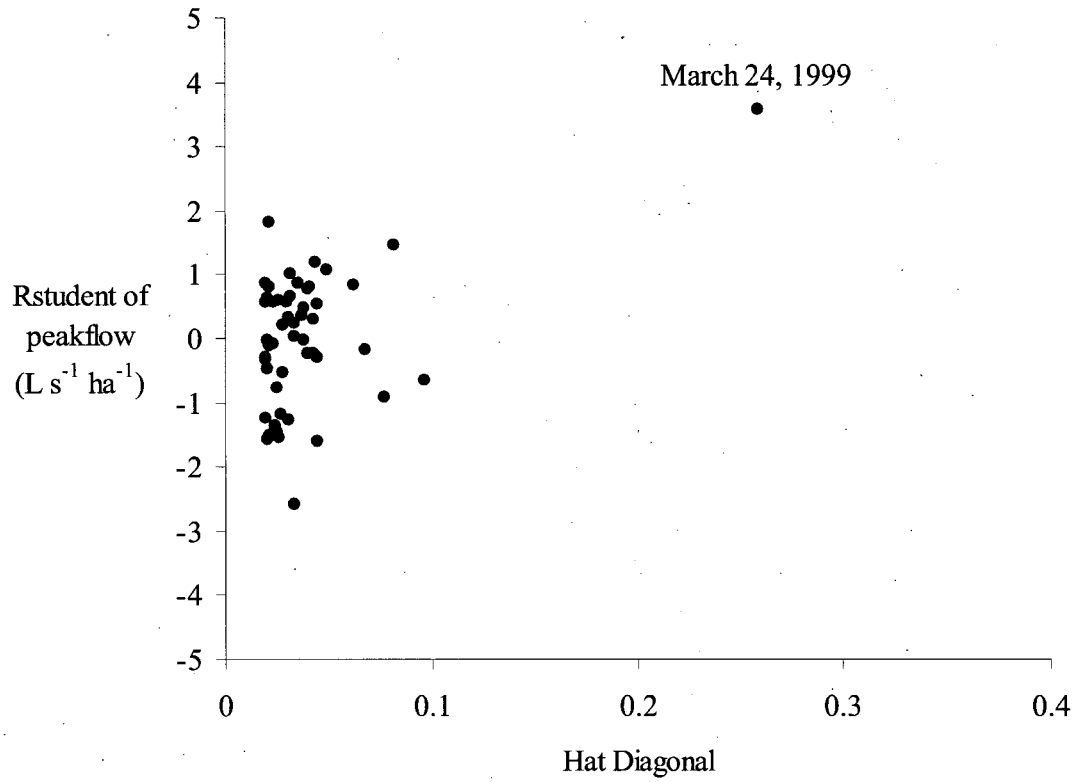

Appendix G. Rstudent as a function of Hat diagonal indicates that the March 24, 1999 event was a high leverage observation.

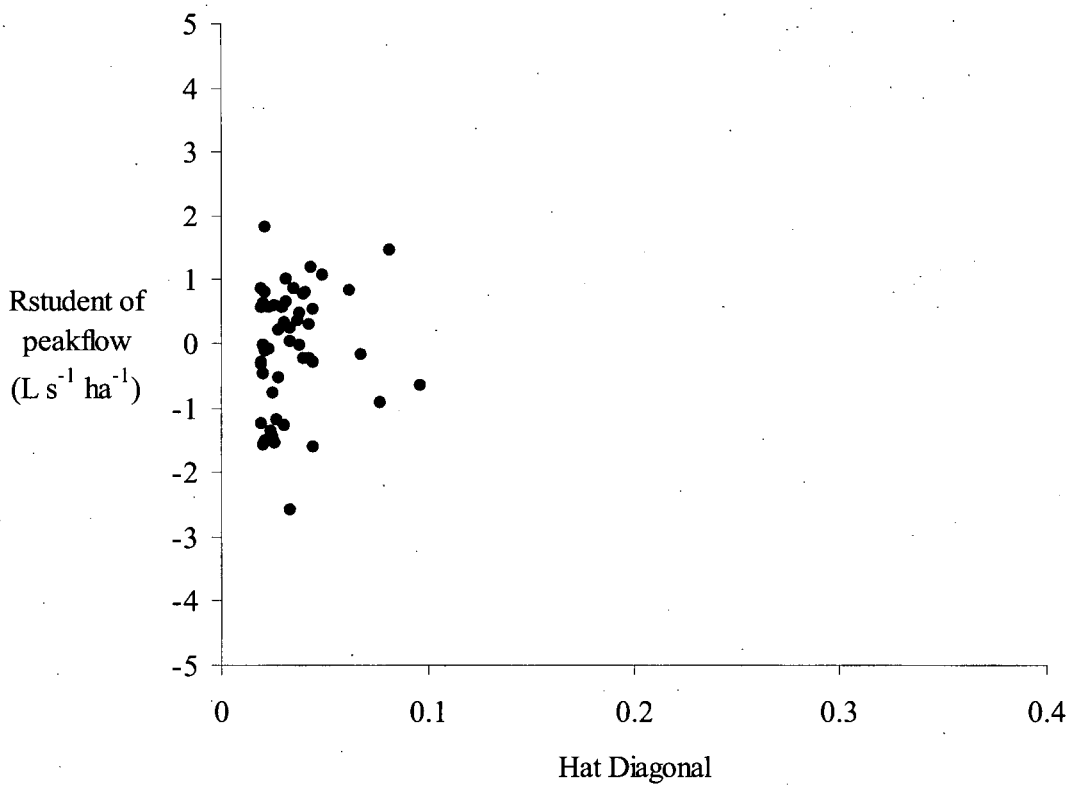

Appendix H. Rstudent as a function of Hat diagonal with the March 24, 1999 event removed. One of the observations remaining was considered an outlier, four were considered high leverage, and one was considered a high leverage outlier. However, they all passed the DFFITS and Cook's D test unlike the March 24, 1999 event.

Appendix I. Tests of regression assumptions after the March 24, 1999 outlier was removed. The Modified Levene Test indicates a lack of constant residual variance. The other null hypotheses were not rejected at the 0.05 alpha level. The Durbin-Watson test indicated a lack of positive and negative autocorrelation (alpha = 0.05). All statistics were calculated using NCSS (Hintze 2004).

Do the residuals follow a normal distribution?	Test Value	Probability Level	Assumption Reasonable ($\alpha = 0.05$)
Shapiro Wilk	0.9736	0.235103	Yes
Anderson Darling	0.6689	0.080721	Yes
D'agnostino Skewness	-0.8441	0.398635	Yes
D'agnostino Kurtosis	0.572	0.5673	Yes
D'agnostino Omnibus	1.0397	0.594621	Yes
Constant residual variance?			
Modified Levene	10.7631	0.001785	No
Durbin-Watson test for lack of autocorrelation			
Positive	1.60	0.0626	Yes
Negative	1.60	0.9378	Yes

Appendix J. API model coefficients and related statistics.

Parameter	Intercept B(0)	Slope B(1)
Coefficients	-3.5222	2.8963
Lower 95% Confidence Limit	-4.6398	2.5482
Upper 95% Confidence Limit	-2.4046	3.2444
Standard Error	0.5579	0.1738
Standardized Coefficient	0.0000	0.9123
T statistic	-6.3134*	16.6668*

* Significant at 0.05 alpha ($p < 0.0001$)

Research Needs and Applications to Reduce Erosion and Sedimentation in Tropical Steeplands (Proceedings of the Fiji Symposium, June 1990): IAHS-AISH Publ. No.192, 1990.

Peakflow estimation using an antecedent precipitation index (API) model in tropical environments

R.L. BESCHTA
Oregon State University, Corvallis, Oregon 97330, USA

ABSTRACT An antecedent precipitation index (API) model is presented which utilizes a hydrograph recession coefficient in conjunction with precipitation amounts and timing to simulate streamflow during large storm events. Application of the methodology is illustrated for estimating peakflows on a 865 ha watershed in Hawaii, USA, and simulating stream levels of the Wainganga River in India.

INTRODUCTION

The prediction of peakflows associated with tropical catchments represents an important problem in applied hydrology. Historical rainfall and runoff data often forms the basis for undertaking empirical frequency analyses or to develop and calibrate hydrologic models which may be used for flow simulations and predictions. In most countries, precipitation data is generally more commonly available (both the number of stations and length of record) than is streamflow data. Thus, there is a need for methodologies that utilize existing precipitation-runoff information as a basis for estimating peakflows and associated return periods.

A variety of hydrologic models exist for simulating catchment hydrology and streamflow. These models range from complex physically-based process models to simple regression models that require little hydrologic understanding of processes. Three general categories of rainfall-runoff models are often identified (Wood & O'Connell, 1985): (1) distributed physically-based models which attempt to simulate the vast array of hydrologic process and physical laws that govern runoff on natural and disturbed watersheds (e.g., Beven, 1985), (2) lumped parameter models which are quasi-physical in nature and offer a simplified conceptual representation of the various hydrologic processes (e.g., Blackie & Eeles, 1985), and (3) input-output or "black-box" models which focus on relationships between rainfall and runoff without necessarily identifying any of the internal mechanisms whereby this transformation takes place.

A linear regression of total storm runoff as a function of rainfall amount would represent a black-box model in perhaps its simplest form. Incorporating hydrologic concepts into an input-output model might

allow one to characterize such a formulation as a "grey-box" model. For example, a unit hydrograph approach which postulates a linear relationship between effective rainfall and storm runoff fits this category. A rainfall-runoff model that utilizes antecedent precipitation to adjust runoff responses could similarly be categorized as a grey-box model. In comparison to other modeling strategies for rainfall-runoff simulations, input-output models are of simple construction and tend to have minimal data and computational requirements.

The purpose of this paper is to present an input-output model for peakflow simulation that is based on antecedent precipitation concepts. Application of the methodology in the coastal mountains of the Pacific Northwest, USA, indicated the methodology provided reasonable estimates of peakflows (Fedora & Beschta, In press). Similarly, Ziemer & Albright (1987) found that an API approach was useful for evaluating pipe-flow hydrology in steep mountainous terrain of the Pacific Northwest, USA.

THE ANTECEDENT PRECIPITATION INDEX METHODOLOGY

High flows at the mouth of a catchment are primarily dependent upon the occurrence of large amounts of rainfall over a relatively short period of time. The API model presented in this paper can be used to simulate storm runoff and requires essentially three steps: (1) recession analysis of storm hydrographs, (2) calculation of API values, and (3) correlation of API values with stream discharge.

Recession analysis

An underlying assumption of an API modeling approach is that antecedent precipitation influences the runoff efficiency from precipitation occurring at time **t**. Precipitation that occurs several days prior to time **t** has less effect on rainfall-runoff relationships than precipitation that has occurred more recently. Thus, the capability of antecedent precipitation to influence rainfall-runoff relationships decreases or decays with time.

For the API model presented herein, the temporal decay of antecedent precipitation amounts is indexed by a storm hydrograph recession coefficient **C**. The recession coefficient integrates various effects of a catchment's soils, geology, topography, vegetation, etc. In general, catchments that are relatively small, and which have steep topography and shallow soils, tend to have larger recession coefficients than catchments which are large or have gentle terrain and deep soils.

Rainfall hyetographs and storm hydrographs are required to undertake recession analysis. After peak discharge occurs during a given storm, and flows continue to recede, the recession coefficient is determined. This coefficient is obtained by deriving the slope of the line formed from plotting stream discharge at time **t** against the discharge at time **t-Δt** (Figure 1). Information regarding rainfall patterns is also needed because the recession analysis is only undertaken for those periods during which no rainfall was occurring. The recession coefficient can also be approximated by the slope of the recession hydrograph when plotted on semilogarithmic paper (Linsley et al., 1982).

If the time interval for precipitation observations and the time interval used to derive the recession coefficient are not they same, the recession coefficient needs to be adjusted to a time interval that is consistent with that of the precipitation data. The coefficient derived from recession analysis can be easily adjusted to the time interval of precipitation observations by the following relation:

$$C = C'^{(\Delta t/\Delta t')} \quad (1)$$

where **C** = recession coefficient for time interval **Δt** ($0 \le C \le 1$), **C'** = recession coefficient derived from time interval **Δt'** ($0 \le C' \le 1$), **Δt** = time interval of precipitation observations (in hours), and **Δt'** = time interval used to derive recession coefficient **C'** (in hours).

Calculation of the antecedent precipitation index (API)

The API model is mathematically formulated as follows:

$$API_t = (API_{T-\Delta t} \times C) + P_t \quad (2)$$

where API_t = antecedent precipitation index at time **t** (mm), **Δt** = time interval of precipitation observations (h), **C** = storm hydrograph recession coefficient (dimensionless), and P_t = precipitation that occurs from **t-Dt** to **t** (mm). Although calculated values of API_t are theoretically dependent upon all precipitation occurring prior to time **t**, precipitation that occurs during the most recent time interval has a greater effect on API_t than an equivalent amount of rainfall that fell during any previous period. Precipitation during the time interval immediately prior to time **t** contributes fully to API_t, while the effect of previously fallen precipitation (i.e., prior to **t-Δt**) is decayed through time. A simple computer program can be used to calculate API_t values; spreadsheet programs can also be used.

For a particular gaging station, several of the largest runoff events of record are selected.

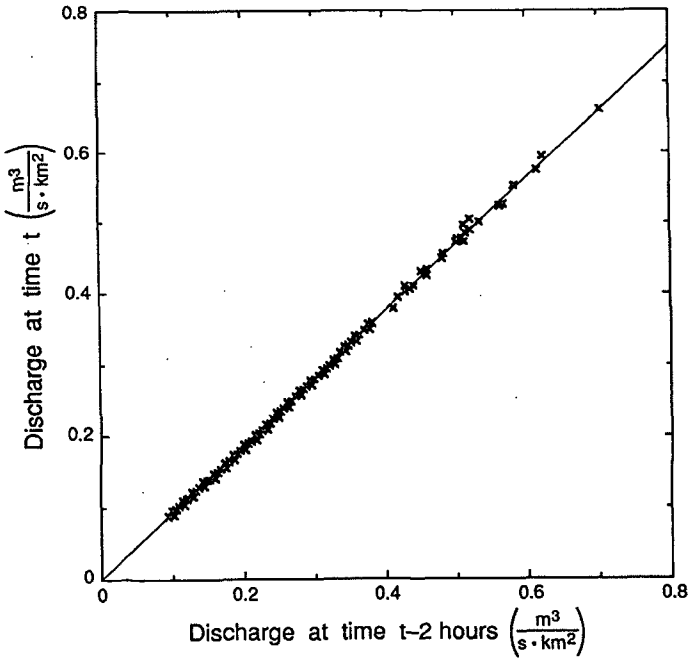

FIG.1 Comparison of flows at time **t** and **t-2** hours for an Oregon Coast Range stream, USA. The slope of the regression line is 0.929 for data collected at 2-hour intervals, hence **C** = 0.96 on an hourly basis.

Corresponding precipitation data for the catchment are also needed for each period of high flow and for several days prior to each event. Hopefully, the precipitation records will provide reasonably accurate indications of catchment amounts and temporal distributions. Runoff events used for analysis can be defined to begin and end using the baseflow separation technique described by Hewlett & Hibbert (1967). Precipitation amounts associated with these runoff events are then used in conjunction with Equation (2) to calculate $\mathbf{API_t}$ values during the period of high flow.

Even though peakflow may be of primary interest, simulations need to begin several days prior to the occurrence of peak discharge. This is because the effects of antecedent precipitation amounts upon $\mathbf{API_t}$ decay through time and generally become insignificant after a period of several days. For example, the effect of precipitation which occurred 4 days prior to the time **t** upon $\mathbf{API_t}$ will have decreased by 99%, assuming an hourly recession coefficient of 0.95. In this manner, the cumulative effectiveness of previous precipitation

amounts for influencing API_t is decayed through time. Determining the length of time prior to the occurrence of peak discharge that API_t calculations should be undertaken is somewhat arbitrary, but it should be sufficiently long so that at least 90% of the relative effectiveness of the earliest precipitation amount has "decayed".

Correlation of API with stream discharge

Once API values have been calculated for each storm, corresponding values of the antecedent precipitation index API_t and stream discharge Q_t are then correlated. The coefficient of determination (i.e., r^2) for this line will provide an initial indication of the goodness-of-fit between the two variables. It may be desirable to transform either variable to obtain a straight-line relationship. For example, in western Oregon, USA, Fedora & Beschta (In press) found that the square root of discharge provided a linear relationship with API_t (Figure 2).

The slope **S** of the regression line in Figure 2 represents the rate of change in discharge with a unit change in precipitation. The y-axis intercept **I** represents the average base flow immediately before and after high flow events.

For large catchments, precipitation that falls on a distant portion of the catchment may require a significant period of time for it to be routed to the catchment outlet, even during high flow conditions. The API methodology, as currently formulated, does not specifically adjust for time-of-travel. Thus, rising limbs of storm hydrographs tend to be over-predicted by the model and recession limbs under-predicted. Although visually disconcerting, this effect may not greatly influence peakflow estimates. A relatively simple approach for overcoming this problem is to undertake cross-correlation analyses of API_t and Q_t values to determine an appropriate timing offset for precipitation amounts to account for time-of-travel effects.

Regionalization of coefficients

To use the API methodology for a specific catchment, three coefficients (**C**, **S**, and **I**) need to be established. Because storm hydrographs are generally less "flashy" as catchment size increases, recession coefficients tend to increase with catchment size. Thus, it may be possible to develop a relation between **C** and catchment area (e.g., Fedora & Beschta, In press). Similarly, **S** and **I** may be associated with watershed characteristics such as soil depth, geologic rock type or depth of weathering, terrain steepness, drainage density, etc. If regional estimates of recession coefficients can be developed (or predicted

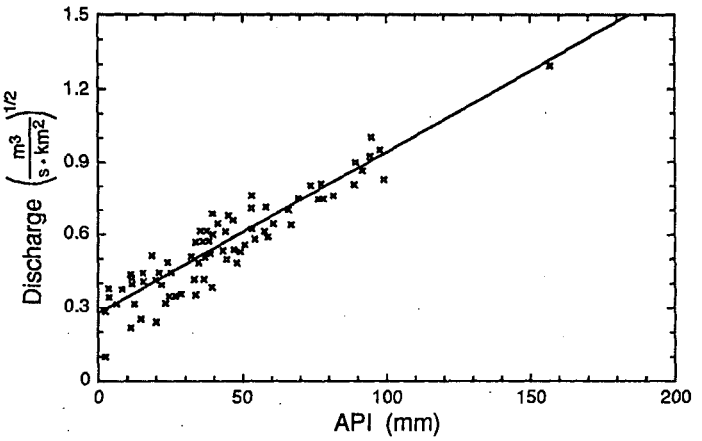

FIG.2 Relationship of stream discharge and $\mathbf{API_t}$ during high flow conditions for an Oregon Coast Range stream, USA.

from regression analysis with other factors), the API methodology could be used for predicting peakflows from ungaged watersheds where precipitation records are available. Furthermore, if regionalized characterizations of large rainfall events (i.e., storm amounts and temporal distributions) were developed from historical precipitation records, peakflows could be estimated using an API model for ungaged catchments. Although initial results in western Oregon indicate that the API coefficients can be regionalized (Fedora & Beschta, In press), the API methodology has not been widely applied or tested.

APPLICATION AND DISCUSSION

Peak flow estimation in tropical areas

A preliminary analysis of rainfall-runoff data was undertaken for an 865 ha catchment in the Moanalua Valley, on the Hawaiian island of Oahu, to evaluate the potential applicability of the API procedure for tropical catchments which experience high intensity rainfall events. The four largest flow events within an eight-year period of record were analyzed. $\mathbf{API_t}$ values were calculated at five-minute intervals for each of three precipitation gages on the catchment. Based on hydrograph analysis, an hourly recession coefficient of 0.24 (i.e., $\mathbf{C'}$= 0.888 for five-minute intervals) was used for all $\mathbf{API_t}$ calculations. To account for time-of-travel, the calculated values of $\mathbf{API_t}$ for each precipitation gage were delayed in relation to distance

from the streamgage (e.g., a 30-minute delay was used for the farthestmost precipitation gage) and an aerially weighted API_t was calculated at each time t. A relationship between the $Q_t^{0.5}$ and API_t was then established by regression. The resulting C, S, and I coefficients were then used as a basis to simulate peakflow hydrographs.

The average absolute error of the four largest storms was 14 percent (Table 1). In a more comprehensive analysis of rainfall-runoff patterns on this catchment, Shade (1984) obtained an average absolute error of 15.4% for these same five events using the distributed routing rainfall-runoff model of Dawdy, Schaake, and Alley (DSA).

Flood hazard forecasting in real time

The potential usefulness of API as a flood-stage forecasting methodology is illustrated with stage data for the Wainganga River in India. Data for three periods of flooding (Chander et al., 1981) provide the basis for this example. Recession curve analysis of stage hydrographs indicated a hourly recession coefficient of approximately 0.87. Regression analysis of stage versus API_t was then undertaken to find the line of best fit. The plotting of stage vs. API_t values indicated a pronounced hysteresis effect whereby API_t greatly overpredicted stage on the rising limb of the flood-stage hydrograph and similarly underpredicted stage on the recession limb of the flood-stage hydrograph. Cross-correlation analysis between stage and API_t values indicated that "delaying" the occurrence of precipitation by 9 hours would tend to minimize this effect. Thus, precipitation amounts were lagged by 9 hours and API_t values calculated for the floods illustrated by Chander

TABLE 1 Observed and simulated peak discharges for the four largest events, 1968-75, Moanalua Valley, Hawaii

Storm No.	Date of storm	Observed peak	Simulated peak	Error[a]
		($m^3\ s^{-1}$)	($m^3\ s^{-1}$)	(%)
1	2/1/69	84.4	79.3	-6
2	7/25-26/70	77.6	70.8	-9
3	11/25-26/70	61.7	42.8	-31
4	4/5-6/71	51.5	56.6	10

[a] Error = ((Simulated - Observed) / Observed) x 100%

et al. (1981). The following relationship between stage (m) and $\mathbf{API}_t$ was then obtained by regression ($r^2 = 0.83$):

$$\text{Stage}_t = 2.04 + (0.219 \times \mathbf{API}_t)$$

In this example, river stage is linearly related to $\mathbf{API}_t$ so that each additional five millimeters of rainfall causes, on average, a one-meter increase in the stage of the Wainganga River.

Hydrographs of the observed and synthesized stages for three storms are shown in Figure 3. Even though precipitation was lagged 9 hours for these examples, the predicted stage overpredicts the rising limb stages for the 1st flood. This overprediction could be the result of significant storm precipitation going into retention storage. For the remaining floods, the API methodology replicates the general shape and magnitude of the flood-stage hydrographs reasonably well. Absolute errors in peak discharges for the three floods illustrated in Figure 3 averaged 0.4 meters. With each incremental amount of precipitation, predicted flood-stage hydrographs can be simulated up to 9 hours in advance. Thus, API provides a relatively simple technique for flood prediction that can be easily used in real time.

General comments

The API methodology implicitly assumes that abstractions from rainfall amounts, such as increased soil moisture storage, and evaporation or transpiration, are relatively insignificant for large rainfall events. Perhaps the inclusion of a long-term or seasonal antecedent factor might be useful in areas where seasonal changes in soil moisture levels have an important effect on storm discharges.

The API model is based on the concept that the relative efficiency of precipitation for generating storm runoff depends on both the amount and the time distribution of storm precipitation. Because the model attempts to account for antecedent precipitation effects on rainfall-runoff relationships, the method does not require a priori assumptions about the temporal distribution of storm precipitation. The utilization of a storm hydrograph recession coefficient provides the basis for "decaying" the hydrologic significance of antecedent precipitation amounts through time. This feature of the model provides a mechanism for linking the model against a single, integrative catchment characteristic that is easily and systematically derived.

The widely used SCS runoff curve model (e.g., US Department of Agriculture, 1972) assumes a systematic increase in runoff efficiency as a storm progresses. In contrast, the basic premise of the API model and the results of API simulations indicate that the relative

efficiency of a catchment to produce streamflow from a given unit of precipitation continuously varies. Hence, the API method appears to have potential application for geographical areas where the temporal distribution of storm precipitation amounts is highly variable.

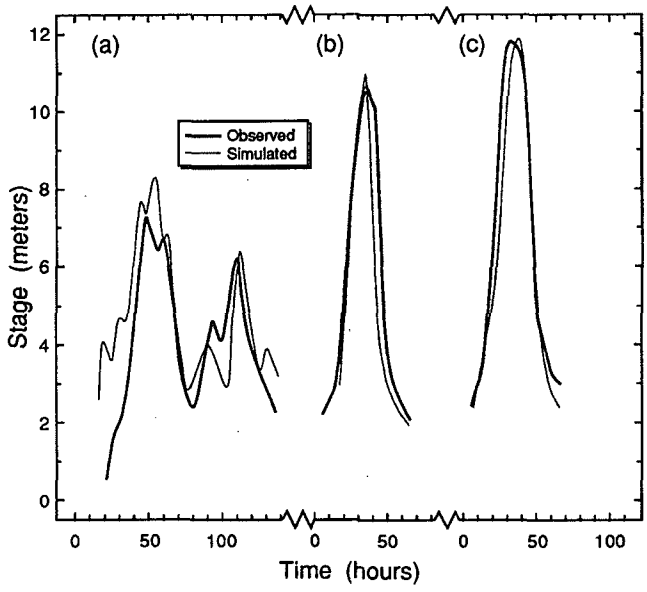

FIG.3 Comparison of observed and simulated flood-stage hydrographs for the Wainganga River in India: (a) 30 July to 6 August 1969, (b) 28 August 1972, and (c) 28 August 1973.

Although the slope **S** and intercept **I** of the relation between Q_t and API_t may have a hydrologic interpretation, little is known about how these parameters vary with different catchments, or how they are affected by topography or catchment characteristics.

Because of its relative simplicity and reasonably accurate simulations, the API methodology may have widespread application in tropical regions for simulating storm discharges from large rainfall events. Once calculated API_t values have been developed from existing rainfall-runoff records, theoretically storms of any temporal distribution can then be used to synthesize storm discharge. However, additional simulations over a wide range of hydrologic conditions in tropical catchments are needed to further evaluate the potential applicability and accuracy of the API method.

REFERENCES

Beven, K. (1985) Chapter 13; distributed models. In: Hydrological Forecasting (ed. by M.G. Anderson & T.P. Burt), John Wiley, New York, 405-436.

Blackie, J.R., & Eeles, C.W.O. (1985) Chapter 11; Lumped catchment models. In: Hydrological Forecasting (ed by M.G. Anderson & T.P. Burt), John Wiley, New York, 311-346.

Chander, S., Spolia, S.K., & Kumar, A. (1981) Chapter 46; flood stage forecasting in rivers. In: Monsoon Dynamics (ed. by J. Lighthall & R.P. Pearce), Cambridge Univ. Press, U.K., 707-717.

Fedora, M.A., & Beschta, R.L. (In press) Storm runoff simulation using an antecedent precipitation index (API) model. J. Hydrol.

Hewlett, J.D., & Hibbert, S.R. (1967) Factors affecting the response of small watershed to precipitation in humid areas. In: International Symposium on Forest Hydrology. (ed. by W.E. Sopper & H.W. Lull), Pergamon Press, New York, 275-290.

Linsley, R.K., Kohler, M.A., & Paulhus, J.L.H. (1982) Chapter 7; streamflow hydrographs. In: Hydrology for Engineers. McGraw-Hill, New York.

Shade, P.J. (1984) Hydrology and sediment transport, Moanalua Valley, Hawaii. U.S. Geological Survey, Water-Resources Invest. Rep. 84-4156.

US Department of Agriculture. (1972) Hydrology. Soil Conservation Service, Natl. Eng. Handb., Sect. 4, Washington, D.C.

Wood, E.F., & P.E. O'Connell. (1985) Chapter 15; Real-time forecasting. In: Hydrological Forecasting. John Wiley, New York, 505-558.

Ziemer, R.R., and J.S. Albright. (1987) Subsurface pipeflow dynamics of north-coast swale systems. Pp. 71-80. In: Erosion and Sedimentation in the Pacific Rim. (ed. by R.L. Beschta, T. Blinn, G.E. Grant, G.G. Ice, & F.J. Swanson). Proc. Corvallis Symp., Int. Assoc. of Hydrol. Sci., Publ. No. 165.

II.3-API-SLC SALT LAKE CITY (CBRFC) API-RUNOFF OPERATION

Introduction

This Chapter describes the Antecedent Precipitation Index (API) runoff Operation (API-SLC) developed by the Colorado Basin River Forecast Center (CBRFC) River Forecast Center.

API procedures were first defined in the 1940's by M. A. Kohler (Reference 1). During this period of hydrology, scientists were seeking techniques which would simplify the relationships of rainfall and runoff. Various techniques which tried to conceptualize soil characteristics, through the application of infiltration theory and other models, were too complex especially when trying to apply them to a very large basin. A more important consideration in forecasting is the time required to produce the product. Without computers alternate less time-consuming methods were needed (References 5 and 6).

Availability of input parameters was another consideration in model selection. Generally storm characteristics can be determined from an adequate network of precipitation stations but determining soil moisture conditions throughout the basin is difficult. Variations in soil and surface characteristics, vegetation differences and land use add to the complexity. Many factors have been used to index the moisture conditions such as:

- days since last rain
- discharge at the beginning of the storm
- antecedent precipitation

The first index is obviously insensitive because it only accounts for the duration of the drought and does not take into effect recharge to the basin. The second is seasonally sensitive and does not reflect changes by previous rains. Antecedent precipitation generally provides good results, provided it is properly derived and uses a seasonal index or temperature.

The variable API, for which the procedure is named, is a rough representation of the initial soil-moisture condition and can also be easily determined. It tries to utilize the accumulated precipitation and, at the same time, take into account evaporation and infiltration.

By using API, week of the year and storm precipitation and duration as parameters, Kohler and Linsley (Reference 2) developed a relationship between storm runoff and precipitation by a graphical method of coaxial relations. It is based on the premise that if any important factor is omitted from a relation, then the scatter of points in a plotting of observed values of the dependent variable versus those computed by the relation will be at least partially explained. The API procedure is really a set of three-variable relations arranged with common axes to facilitate computation.

The Colorado Basin River Forecast Center (CBRFC) has adapted these procedures and applied them to basins in Arizona. Modifications were

made to alter the lower limit of the API index, adjust the API recession based on simulated percent areal snow cover and allow duration to be affected by differing 6 hour significant precipitation levels.

API Model (Reference 3)

The API model consists of 3 three-variable relations (Figure 1), relating basin recharge as the dependent variable to the antecedent precipitation (API), date (week number), the rainfall amount and the rainfall duration as the independent variables. Basin recharge is defined as the loss due to interception, infiltration and depression storage or basically the difference between precipitation and runoff.

Chart A in Figure 1 is the API versus basin recharge, with the points labeled with the week numbers. A family of curves is fitted to the points with one curve for each week. Chart B is the observed recharge versus the computed recharge with the points labeled for rainfall storm duration (hours). Again a family of curves is drawn defining the effect of duration on recharge. Chart C is observed basin recharge versus computed recharge with the points labeled with rainfall amounts. Chart D displays the accuracy of the procedure of the other three charts. It is a plot of observed recharge versus computed recharge.

The calibration process is successive approximations of curve selection to converge to the best graphical solution. The methods for adjusting the relationships are made by alternating the entrance into the procedure from Chart A through D and then D through A.

The API as used in the CBRFC model (Reference 4) is slightly modified to facilitate its usage in computer applications (Figure 2). The precipitation curves have been swapped with duration curves. The duration quadrant has re-introduced the antecedent precipitation and season indices as a parameter for effective duration. Also the output has been changed to display runoff directly reducing the need to subtract basin recharge from precipitation.

First Quadrant (Season) (Reference 4)

The first quadrant is a relation of API versus basin recharge. The points are labeled with the week number and a family of curves drawn to represent the date or seasonal effect on basin recharge. The following equation defines these curves:

```
RI1 = (A + B*Y) * (C)**API

B  = (I-A)/2
G1 = (E2 - E1)/2
G2 = (E1 - E2)/2

For weeks between WN and WX:
   Y = 1 - (COS((W-WN)(Pi/(WX-WN))))**CP
```

```
    C = E1 + G1*(((W-WN)/(WX-WN))/2)

For weeks between WX and 52:
    Y = 1 + (COS((W-WX)(Pi/(52 + WN-WX))))**CP
    C = E2 + G2 * (((W-WX)/(52 + WN-WX))/2)

For weeks between 52 and WN:
    Y = 1 + (COS(W+52 - WX)(Pi/(52 + WN-WX))))**CP
    C = E2 + G2 * (((52 + W-WX)/(52 + WN-WX))/2)

where  A   is the intercept of WN in the RI axis
       I   is the intercept of WX in the RI axis
       WN  is the wettest week number
       WX  is the driest week number
       W   is the week number of the current storm
       E1  is the curvature constant for WN
       E2  is the curvature constant for WX
       G1  determines the rate at which E1 approaches E2
       G2  determines the rate at which E2 approaches E1
       CP  determines the distribution of week curves
       API is the Antecedent Precipitation Index
```

A CP value of 1.0 distributes the week curves evenly between WX and WN. As CP approaches zero, the week curves tend to pack around WX and WN. When CP increases above 1, the week curves cluster midway between WX and WN. See Figures 3 and 4 for relationship of parameters.

The antecedent precipitation index is generally defined by the equation:

$$API = b_1P_1 + b_2P_2 + b_3P_3 + \ldots + b_iP_i$$

where P_i is the amount of precipitation i day prior to storm
b_i is a constant as function of time 1/i

For this model the decrease with time has been assumed to follow a logarithmic decay rather than a reciprocal. Thus during periods of no precipitation:

$$API_i = k * API_{i-1}$$

For periods with precipitation:

$$API_i = (API_{i-1} + Precip) * k$$

The API index for any day is equal to that of the previous day multiplied by the factor K. If any rain occurs it is added to the index (Figure 5). The value k varies with physiographic basin characteristics, evaporation, temperature and humidity. However through the use of other factors, such as the week or seasonal term, most variation has been accounted. Through experimentation (Reference 3), k is important, though not critical and ranges in value from 0.85 to 0.90 over most of the eastern and central portions of the United States.

The antecedent precipitation index is computed from mean areal precipitation (MAP) provided as output from the snow accumulation and ablation model. In areas of snowfall, the precipitation is applied to the model on days it melts rather than when it falls. This prevents over forecasting of events by applying water-equivalent of the snow at occurrence.

Snow cover provides for a modification to the API calculation. As percent areal snow cover approaches 100 percent, moisture loss is reduced. The term k is modified by a snow term to reduce the API reduction from day to day:

$API_1 = API_0 - API_0 * (1.-k)*(1.-\text{fraction of snow cover})$

For areas in Arizona with long periods of drought, API is allowed to decease below zero to minimum of -0.99 inches. If the lower limit of API is selected to be negative, the method of reducing API changes. Once API reaches .05 inches, a constant increment of .01 inches per day is subtracted until the API value reaches the lower limit. The value of API used in the model is set at .01 until API reaches a positive value. This process simulates an increased soil moisture capacity which must be satisfied before API is allowed to increase.

Second Quadrant (Storm Precipitation) (Reference 4)

This quadrant gives the relation of observed basin recharge versus computed recharge. Points are labeled with precipitation in inches and a family of curves of storm totals is drawn. This represents the effect of precipitation on recharge under the conditions calculated in the first quadrant. The following equation defines this curve:

$RI2 = P * (P/(P+1))^{**}RI1$

where P is observed precipitation

Precipitation is obtained from mean areal precipitation calculated directly from one of the precipitation models. The MAP could be modified by the snow accumulation and ablation model before being used as input to the API model.

Third Quadrant (Storm Duration) (Reference 4)

This relation is observed basin recharge versus runoff with points labeled on the basis of storm duration. Basin recharge as explained through the first quadrant relationship is re-introduced as a parameter of effective duration. The equation of the curves is defined as follows:

$RO = RI2 * (K)^{**}FD$

$FD = (DUR*(RI1 + 1))/(6 + M * (RI1)^{**}POW$

where DUR is storm duration in hours

M, POW and K are constants (K is less than 1)

Average duration over the entire basin is difficult to determine but it is not critical when limited to 6 hourly rainfall data. This model keeps track of duration based on 6 hourly significant rainfall. Results from experimental infiltration data show a value of 0.10 inches is a good default for significant rainfall level but the significant level can be altered to take into account variations across the United States.

Runoff

Runoff is produced through a series of equations approximating the curves of the API coaxial graphical method. This runoff represents surface flow for a specific period. For this operation, the period is fixed at 24 hours in the 12Z to 12Z time frame.

In order to provide an output, runoff time series with a 6 hour data time interval, 24 hour runoff is distributed in the same percentage as precipitation for the same 24 hour period. Thus it is assumed that each 6 hour period of precipitation is an antecedent precipitation index.

An alternative to this method would be computing runoff depths from accumulated precipitation up to the end of a 6 hour period and subtracting successive values of runoff.

The relative accuracies of the two techniques are dependent upon the adequacy of the assumed weights for antecedent precipitation. The first method is preferred because it gives more significance to time variations of rainfall intensity and may, therefore, provide for more accurate computations.

Conclusions

The effect amount and distribution of antecedent precipitation has upon storm runoff depends upon the extent to which it has been dissipated through evaporation, transpiration, etc. Through the API coaxial relationships, a generally high correlating procedure can provide a simple method of computing runoff.

There are some limitations which directly effect reliability or use of such models. Most problems can be overcome utilizing input from the professional hydrologist. The following difficulties are considered to be some of the major deficiencies:

- a relation based on storms of uniform areal distribution will yield runoff values which are too low when applied to storms of extremely uneven distribution
- rainfall intensity is omitted or is generally smoothed into 6 hour periods
- the procedure does not model frozen ground

References

1. M. A. Kohler, 'The Use of Crest Stage Relations in Forecasting the Rise and Fall of the Flood Hydrograph', U.S. Weather Bureau, 1944 (mimeo).

2. Linsley, Kohler and Paulhus, 'Hydrology for Engineers', McGraw-Hill, 1958.

3. M. A. Kohler and R. K. Linsley, 'Predicting the Runoff from Storm Rainfall', U.S. Weather Bureau Research Paper No. 34, 1951.

4. J. P. McCallister, 'Role of Digital Computers in Hydrological Forecasting and Analyses', U. S. Geological Survey Publication No. 63, 1963.

5. M. A. Kohler and M. M. Richards, 'Multicapacity Basin Accounting for Predicting Runoff from Storm Precipitation', Journal of Geophysical Research, Dec. 1962.

6. R. P. Betson, R. L. Tucker and F. M. Haller, 'Using Analytical Methods to Develop a Surface-Runoff Model', Water Resources Research, Feb. 1969.

Figure 1. Coaxial relationship - Antecedent Precipitation Index (Chart A, Chart B, Chart C and Chart D)

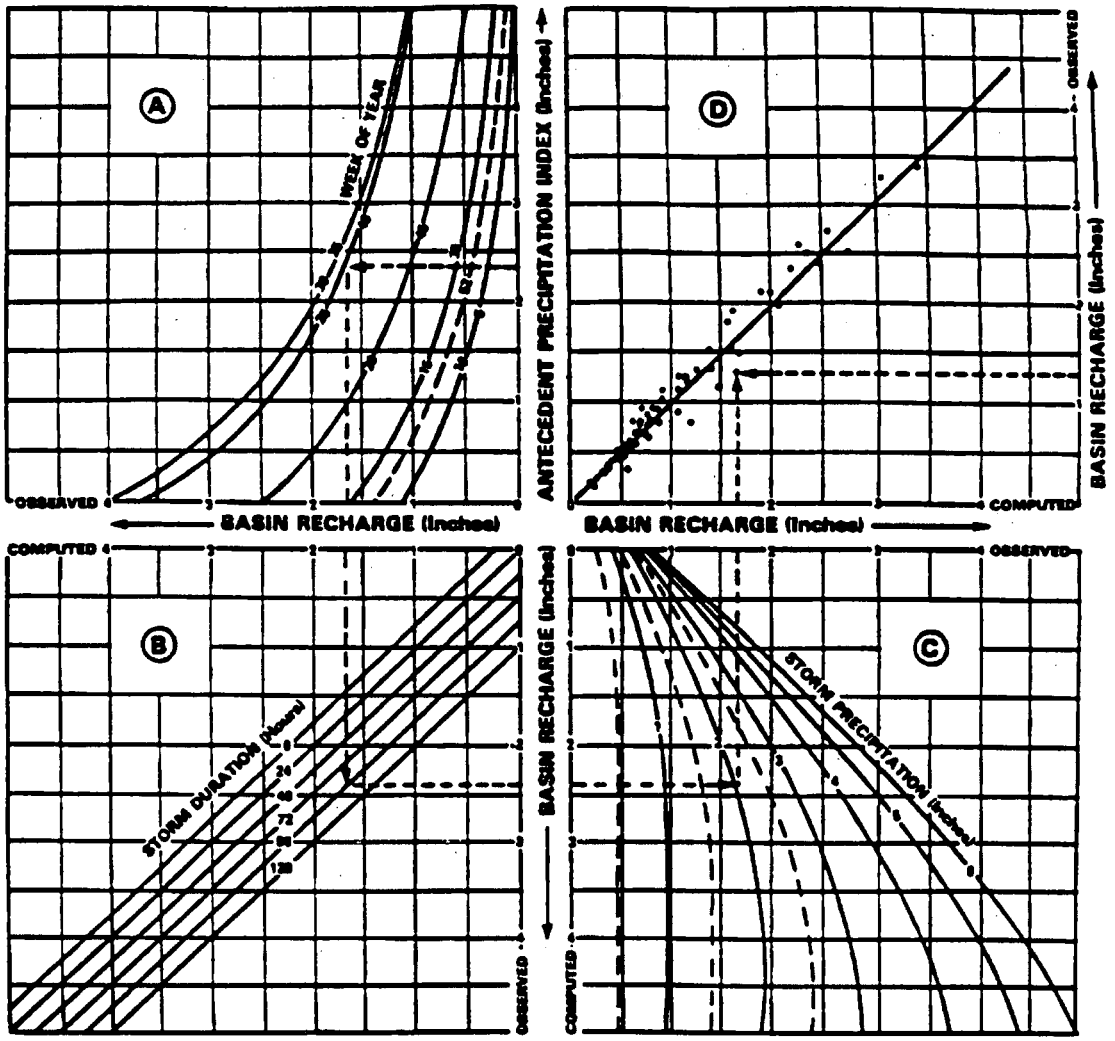

Figure 1. Coaxial relation -- Antecedent Precipitation Index

Figure 2. Modified API - Salt Lake City RFC

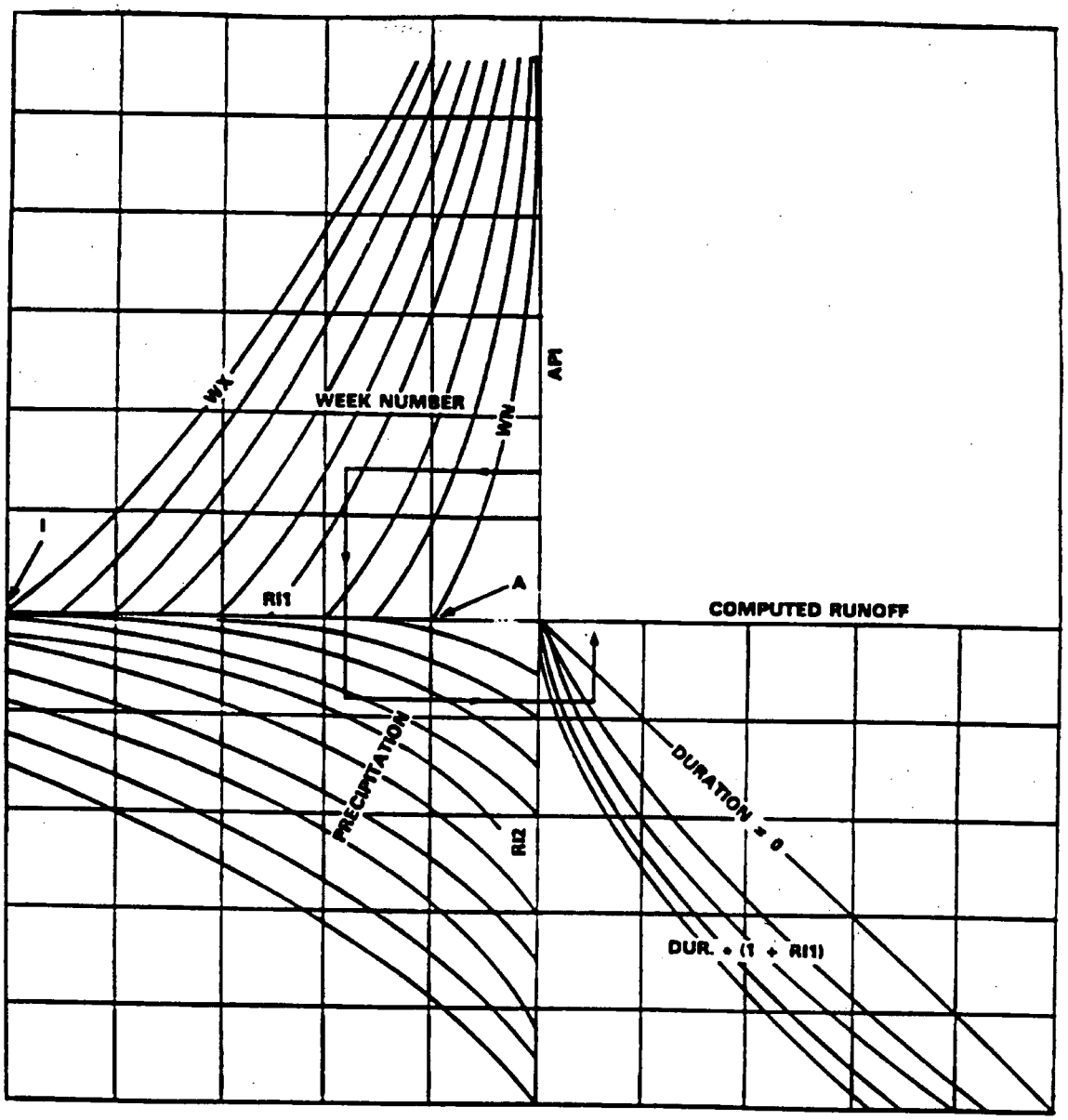

Figure 2. Modified API -- Salt Lake City RFC

Figure 3. First quadrant (seasonal relation)

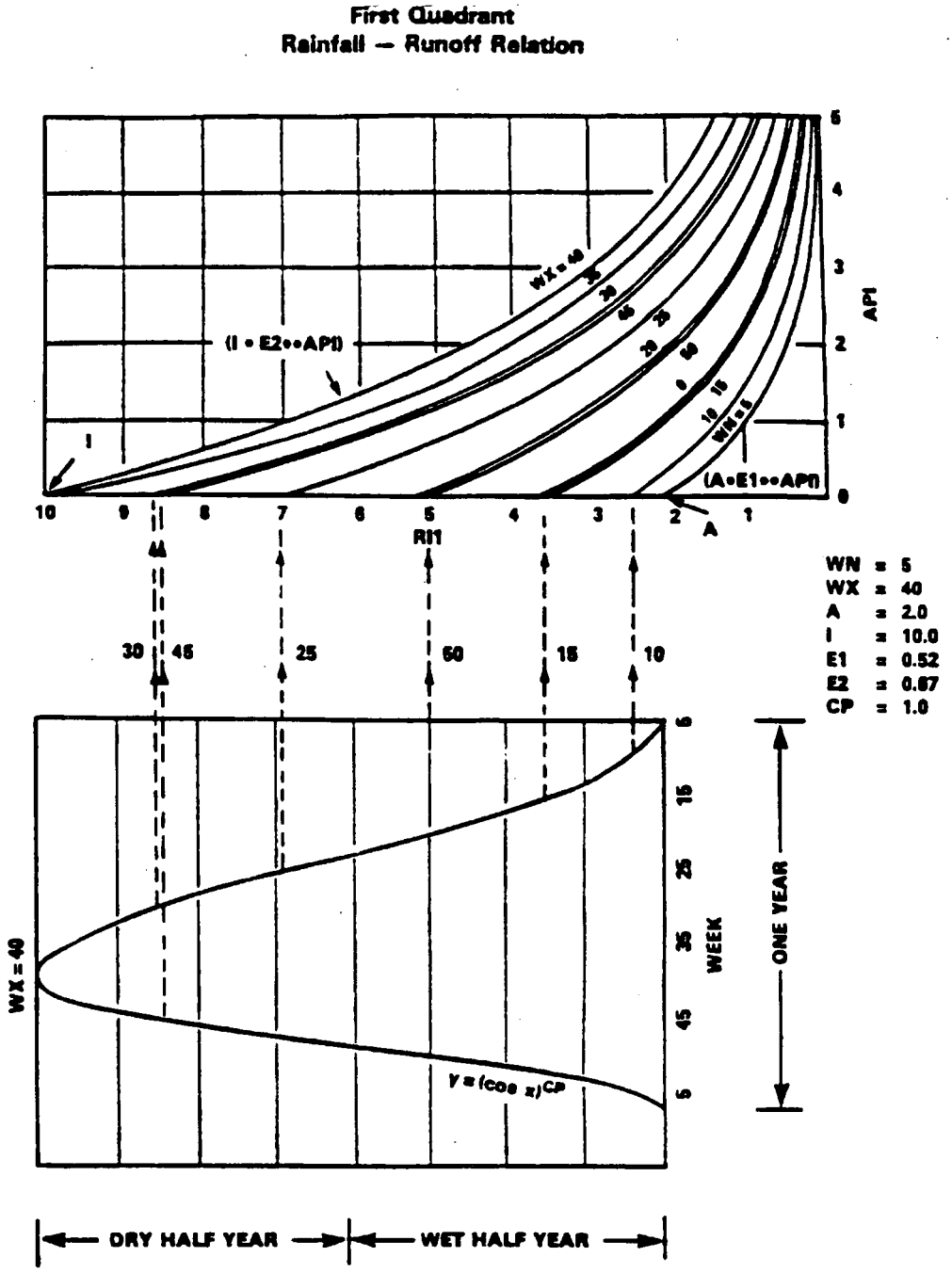

The Cosine Function Determines the Intercept of Each Week with the ABSCISSA of the First Quadrant Curve (API = 0)

Figure 3. First quadrant (seasonal relation)[7]

Figure 4. First quadrant intercept function

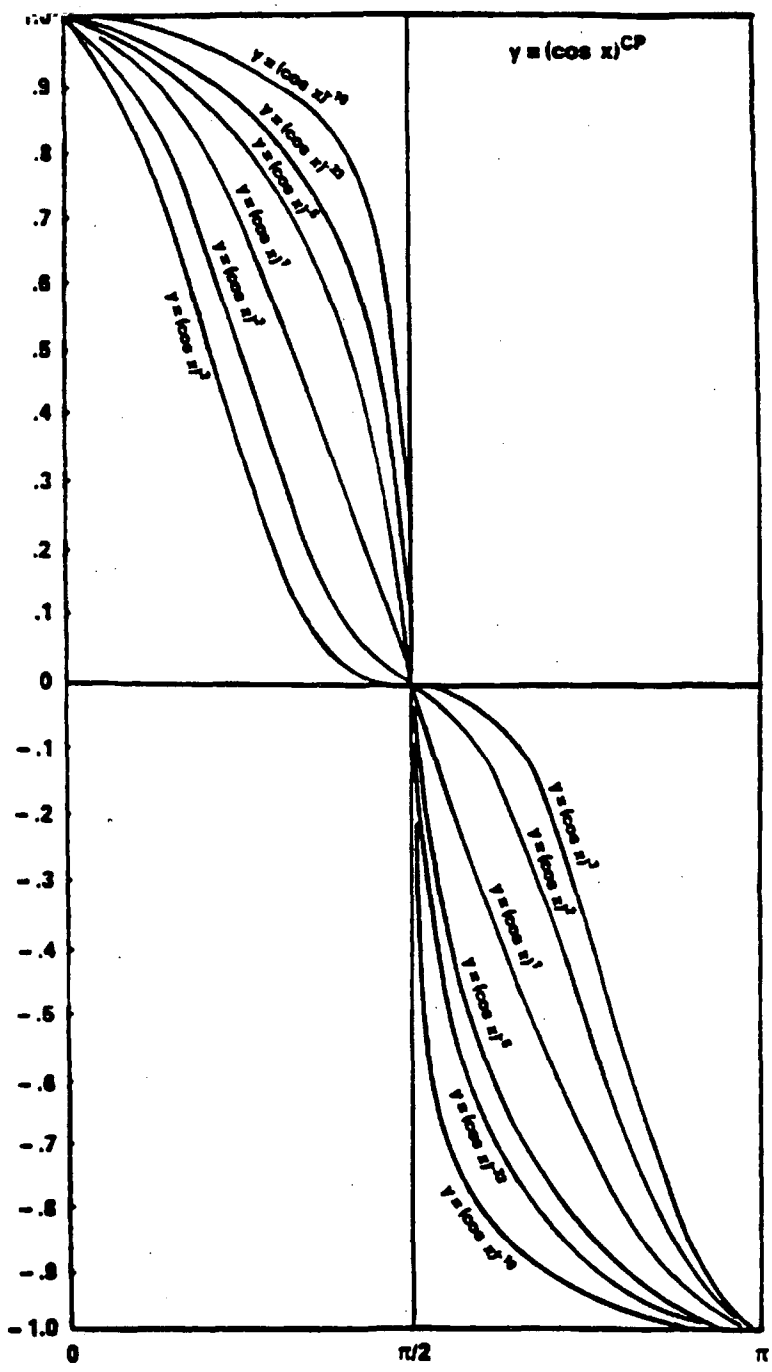

Figure 4. First quadrant intercept function[7]

Figure 5. API relation

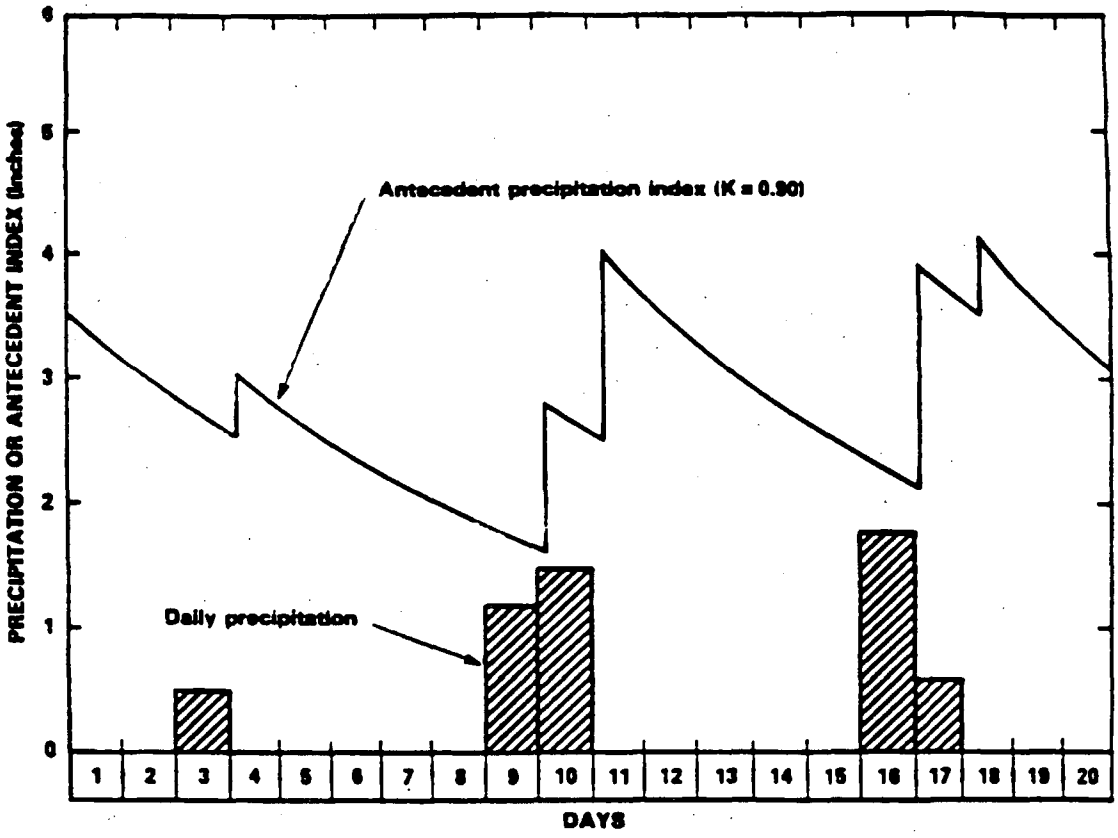

Figure 5. API relation

II.3-API-CONT CONTINUOUS API MODEL

Introduction

Antecedent Precipitation Index (API) based procedures have been used for many years by River Forecast Centers (RFCs) for producing flood forecasts (Linsley et al, 1949). The API procedures developed by the RFCs are applied on a storm basis. The API value at the beginning of the storm is typically related to time of the year, storm duration and storm rainfall to compute storm runoff (see Figure 1a). Incremental runoff is computed by subtracting the total storm runoff at the end of a period from that at the beginning. A unit hydrograph is then applied to the incremental runoff values to produce a discharge hydrograph. Since storm or event API procedures only compute surface or storm runoff, baseflow needs to be added to the surface runoff hydrograph to produce the total discharge. For short-term river or flood forecasts (hours or days into the future) satisfactory estimates of baseflow can usually be determined. During floods, errors in baseflow estimates have a minimal impact. During recessions it is relatively easy to make a several day projection of discharge. Many RFCs have continued to use API based rainfall-runoff models because they are simple to understand, easy to update when observed values differ from computed estimates and generally do a good job forecasting floods when properly applied.

In recent years two problems have arisen related to the use of API based rainfall-runoff models by the RFCs.

First, the need for water management forecasts is increasing dramatically. For water management purposes predictions are often needed for weeks or months into the future, plus in many cases low flow values are of interest. Within NWSRFS, the Extended Streamflow Prediction (ESP) System is used to generate such forecasts. For general ESP purposes, a model must be able to accurately simulate all flow levels for extended periods. Event API models cannot do this, thus the RFC is faced with switching to a different type of model or using one model for flood forecasting and another for ESP applications. Neither of these options is appealing to some of the RFCs.

Second, it is very difficult to calibrate event API models in conjunction with other hydrologic models for a watershed. The data used for calibration of an event API model typically includes the API value at the beginning of the event and the storm rainfall, both computed from precipitation data; the date and duration of the storm; and the total surface runoff for the event. Total runoff is computed by separating surface runoff from baseflow using one of the standard techniques for baseflow separation. The calibration is then done by either manually deriving the coaxial graphical relationship between the variables (see Figure 1a) and/or using computer techniques to minimize the error between computed and observed storm runoff. A unit hydrograph to be used in conjunction with an event API model can be derived based on events when all surface runoff is generated in a single time period or when uniform runoff can be assumed for several

periods. Unit hydrographs derived from other storms are not directly compatible with the event API model because the distribution of runoff used to derive the unit hydrograph is not the same as would be produced by the API model if it was applied to the same event. For other hydrologic models, such as a snowmelt model, that might be used in conjunction with an API model, the output variables of the model rarely can be isolated by analyzing a hydrograph. Thus, these other models cannot be calibrated for the watershed. Currently when a snow model is used with an event API model by the RFCs, the snow model parameters are based on calibrations done somewhere in the area in conjunction with a conceptual rainfall-runoff model or on point calibrations of the snow model using observed water-equivalent data. The calibration procedures provided within NWSRFS generally cannot be used for an event API model.

Since several RFCs prefer to use an API based rainfall-runoff model for flood forecasting, the Continuous API Model was developed so that an API based model that could be used with the ESP and calibration systems would be available within NWSRFS. The Continuous API Model computes runoff on an incremental, not on a storm, basis and generates both surface and baseflow runoff amounts.

Background

In the 1960's a continuous API-type model was developed for use within the Office of Hydrology in order to compare emerging conceptual models with API based rainfall-runoff procedures (Sittner et al, 1969). The original model has since been revised to simplify some of the equations and reduce the number of parameters (Nemec and Sittner, 1982). This continuous API model was developed on the premise that an event API rainfall-runoff relationship could be converted to an incremental relationship by replacing the duration quadrant with a retention index (RI) quadrant. RI reflects whether surface conditions are dry (typical state at the beginning of an event) or wet (condition during an event when interception, depression and upper zone moisture storages have been satisfied). The difference between surface runoff computations in an event API model and Sittner's continuous model can be described by using Figure 1b. An event API model basically uses one curve for the entire event based on antecedent conditions at the beginning of the event. Sittner's model moves from curve to curve as the API and retention index change during the event (typically moves to curves reflecting wetter conditions as the event progresses). However, incremental rather than storm precipitation is used to enter the relationship so that only the beginning portion of the curves, where the most curvature exists, are typically used. It is not clear whether this curvature should exist for every time period during an event. This creates some doubt as to whether the same precipitation-runoff relationship or even the same form of equations, should be used for an incremental API-type model as is used for an event model.

Rather than using the Sittner continuous API model the model this model was developed because of:

- Doubt that the same equational form of the precipitation-runoff

relationship can be used in both an incremental and event API model.

- The belief that some of the model components could be simplified and thus required fewer parameters and be more easily visualized by the user.
- Personal preference.

Description of the Model

The Continuous API Model consists of 4 quadrants (see Figure 2), equations to compute baseflow runoff and a few additional features including an option to account for the effect of frozen ground on runoff. The four quadrants perform the following functions:

- The first quadrant accounts for the seasonal relationship between API and current soil-moisture conditions,
- The second quadrant accounts for surface moisture conditions,
- The third quadrant computes the incremental surface runoff based on surface and overall soil-moisture conditions and
- The fourth quadrant computes what portion of the precipitation that does not become surface runoff enters groundwater storage.

Baseflow runoff is computed based on the total water in groundwater storage and the amount that has entered the storage in the recent past. The model also allows for impervious area runoff and riparian vegetation losses.

1st quadrant

The first quadrant serves the same function in all API based models. This quadrant accounts for the seasonal variations between API and an index to soil-moisture conditions. The index is usually referred to as the Antecedent Index (AI).

Computation of AI: The equations used to compute AI from API are basically the same as used in the West Gulf RFC API model (McCallister, 1963) and are the same as currently used by Sittner for his continuous API model. The only differences are: 1) the variation between wet and dry curves is represented differently and 2) optional ways to express the seasonal variation are included. The equations are:

$$AI_w = AIXW * CW^{API} \quad (1)$$

$$AI_d = AIXD * CD^{API} \quad (2)$$

$$AI = AI_w + y*(AI_d - AI_w) \quad (3)$$

where AI is the Antecedent Index (inches)
AIXW is the intercept of wet curve (i.e. AI value when API = 0 and y = 0) (inches)
CW is the wet curve curvature constant (0.0 < CW < 1.0)
AIXD is the intercept of dry curve (i.e. AI value when API = 0 and y = 1) (inches)
CD is the dry curve curvature constant (0.0 < CD < 1.0)
y is the fractional distance between wet and dry conditions
(y = 0 is wet, y = 1 is dry)

Computation of API: The equations use to compute API are:

$$API_2 = K_p * API_1 + P \quad (4)$$

$$K_p = APIK^{(\Delta t/24)} \quad (5)$$

$$API_2 \leq APIX \quad (6)$$

where API is the Antecedent Precipitation Index (inches), (subscripts refer to beginning and end of the time period)
P is the precipitation or rain + melt (inches)
APIK is the daily API recession rate (0 < APIK < 1.0- normally assumed to be 0.9)
Δt is the length of the time period (hours)
K_p is the API recession rate for the time period
APIX is the Maximum value that API can attain.

An upper limit is provided for API because with sufficient rainfall or rain + melt, the soil will become saturated and any additional water goes to runoff, not to increasing the level of soil saturation. The maximum API value is only attained during major flood events.

When a snow cover exists, the API recession rate may need to be reduced. The reduction in API and the subsequent increase in AI is due to both evaporation from the soil and drainage of water in excess of field capacity. AI is an index to the total wetness of the soil. Since a snow cover will inhibit evaporation, the APIK recession rate should be reduced. The amount of reduction is a function of the typical climate conditions of the basin to which the model is being applied. For example, in the upper Midwest a snow cover may exist for most of the winter. If fall soil-moisture conditions are to influence spring runoff, the API recession rate must be reduced to 1.0 or nearly that amount to retain a memory of fall conditions. On the other hand, in a more temperate area where periodic rain or melt periods may occur when a snow cover exists, the snow cover may reduce evaporation, but does not affect water draining through the soil. In such an area, a much smaller reduction in the API recession rate is warranted when snow exists. If the API recession rate were set to 1.0, very large API values could build up during rain-on-snow or melt periods and cause even small amounts of rain + melt to produce a large percent surface runoff.

When the areal extent of the snow cover is known, APIK becomes:

$$APIK_s = APIK + (APIKS-APIK)*S_c \quad (7)$$

where $APIK_s$ is the daily API recession rate when snow exists
S_c is the areal extent of snow cover (decimal fraction)
APIKS is the daily API recession rate with 100 percent snow cover ($APIK \leq APIKS \leq 1.0$)

When only the water-equivalent and not the areal extent of the snow cover is known, S_c is set to 1.0 whenever the water-equivalent exceeds 0.1 inches (S_c = 0.0 otherwise).

Seasonal variation: The most common method to account for seasonal variation is to use time of the year. Time of the year is specified by week number which is computed as:

$$W_n = D_j/7.0 \quad (8)$$

where W_n is the week number
D_j is the Julian day (January 1 = 1, December 31 = 365; February 29 and March 1 have same value)

In order to use week number in the 1st quadrant, the week numbers when the wettest and driest conditions typically exist need to be specified. The seasonal variation between wet and dry conditions is expressed as:

$$y = \left[0.5 + \frac{\cos[\pi * (1-f)]}{2}\right]^{cs} \quad (9)$$

where f is the fractional distance between WKD and WKW (f = 1 when W_n= WKD and f = 0 when W_n = WKW)
WKW is the week number when the wettest conditions typically exist
WKD is the week number when the driest conditions typically exist
CS is the seasonal curvature exponent (CS > 0.0)

When going from wet to dry conditions (typically early spring to late summer), the value of CS is fixed at 1.0, thus resulting in a sinusoidal variation. When going from dry to wet conditions, the parameter CS controls the shape of the seasonal variation. A value of CS considerably greater than 1.0 is typically needed in areas where there is a rapid transition from dry to wet conditions in the fall. Rapid transitions from dry to wet conditions occur in basins where a large soil moisture deficit typically develops over the summer due to evapotranspiration significantly exceeding rainfall and the deficit is reduced to zero over a relatively short period in the fall due to increased rainfall and decreased evapotranspiration. In areas where the trees lose their leaves over a relatively short period in the fall, the decrease in evapotranspiration is accentuated. The seasonal variation in y is shown in Figure 3.

One alternative method of accounting for the seasonal variation is the use of an Antecedent Evaporation Index (AEI). This method has been used by the Middle Atlantic RFC. AEI is computed on a daily basis as:

$$AEI_2 = AEIK * AEI_1 + PE \quad (10)$$

where AEI is the Antecedent Evaporation Index (inches)
AEIK is the daily AEI recession rate (0.0 < AEIK < 1.0)
PE is the daily potential evaporation or ET-demand (inches); when snow exists PE is adjusted using Equation 18

The minimum AEI value typically occurs a month or so after the time when minimum PE values occur and the maximum AEI a month or so after when maximum PE values occur. When using AEI, the seasonal variation is expressed as:

$$y = \frac{AEI-AEIN}{AEIX-AEIN} \quad (11)$$

where AEIN is the minimum allowed AEI value (inches)-corresponds to wettest time of year (if AEI < AEIN, AEI = AEIN)
AEIX is the maximum allowed AEI value (inches) - corresponds to driest time of year (if AEI > AEIX, AEI = AEIX).

The sinusoidal variation explicitly built into Equation 9 (CS = 1.0) occurs naturally in Equation 11 because PE and thus AEI exhibits a sinusoidal pattern.

The second alternative method of accounting for the seasonal variation is through the use of an Antecedent Temperature Index (ATI). The ATI is a weighted mean temperature and is computed as:

$$ATI_2 = ATI_1 + ATIR*(Tm-ATI_1) \quad (12)$$

where ATI is the Antecedent Temperature Index (DEGF)
ATIR is the temperature weighing factor ($0.0 < ATIR \leq 1.0$)
Tm is the mean daily air temperature (DEGF)

When using ATI the seasonal variation is expressed as:

$$y = \frac{ATI-ATIN}{ATIX-ATIN} \quad (13)$$

where ATIN is the minimum allowed ATI value (DEGF) - corresponds to wettest time of year (if ATI < ATIN, ATI = ATIN)
ATIX is the maximum allowed ATI value (DEGF) - corresponds to driest time of year (if ATI > ATIX, ATI = ATIX)

Similarly to AEI, ATI naturally exhibits a sinusoidal variation.

The possible advantage of using AEI or ATI rather than week number is to better account for abnormal conditions. AEI or ATI should indicate a abnormally cold spring or an abnormally warm fall which should cause a shift in the API vs AI relationship for that time of year.

2nd quadrant

The 2nd quadrant of the Continuous API Model adjusts the AI value computed in the 1st quadrant for the effect of surface moisture. The result is an adjusted or final AI value (AI_f). It is assumed that when surface moisture conditions are wet that AI_f = AI. When surface moisture is dry, AI_f needs to be increased. This causes surface runoff to be decreased in the 3rd quadrant to reflect interception, depression storage and upper zone moisture losses that occur when the surface is dry. The 2nd quadrant accounts for the initial abstraction loss that occurs at the beginning of an event.

Computation of AI_f: The form of the equation used to compute AI_f as a function of AI and the surface moisture conditions is similar to the form of the equations used in the 1st quadrant except that the curvature constant is fixed. The equation is expressed as:

$$\frac{SMI}{SMIX} = 0.9^{\left[\frac{AI_f}{AI}-1\right]} \qquad (14)$$

where SMI is the Surface Moisture Index (inches)
SMIX is the maximum value of SMI (inches)
AI_f is the Final Antecedent Index (inches)

When the ratio SMI/SMIX = 1, the surface is saturated (i.e. interception, depression and surface moisture storages are full).

Solving Equation 14 for AI_f gives:

$$AI_f = AI * \left[\frac{\ln\left(\frac{SMI}{SMIX}\right)}{\ln(0.9)}+1\right] \qquad (15)$$

Equation 15 plots as a straight line for each SMI/SMIX ratio (see Figure 2) The constant 0.9 causes the 2nd quadrant to act almost as a threshold storage (i.e. very little surface runoff can be generated until SMI = SMIX).

Computation of SMI: Surface moisture conditions dry out much faster in the summer than in the winter because evaporation rates are much higher in the summer. This needs to be reflected in the computation of SMI. SMI is computed by the equation:

$$SMI_2 = SMI_1 - E*(SMI_1/SMIX) + P \qquad (16)$$

where E is the evaporation (inches)

If the AEI option is used in the first quadrant, then actual evaporation values are used in Equation 16. When week number or ATI are used to express seasonal variation, daily evaporation is computed as:

$$E_d = 0.5*(PEX+PEN) + 0.5*(PEX-PEN) *\sin\left[\frac{2*\pi*(D_j-105)}{365}\right] \qquad (17)$$

where E_d is the daily evaporation estimate (inches)
PEX is the maximum daily evaporation rate, assumed to occur on July 15th (inches)
PEN is the minimum daily evaporation rate, assumed to occur on January 15th (inches)

E is obtained from E_d by assuming uniform evaporation during the day. Values for PEX and PEN can be obtained from an evaporation atlas such as those produced by Farnsworth et al, 1982. In some cases the values derived from the atlas should be adjusted for the effect of vegetation (e.g. January values should be reduced in areas with deciduous forests or cold climates). When a snow cover exists, the evaporation is reduced by:

$$E_s = E*(1-S_c) + E*S_c*EFC \quad (18)$$

where E_s is the evaporation when a snow cover exists (inches)
EFC is the effective forest cover (decimal fraction)

The effective forest cover can be estimated by taking the portion of the area covered by conifers times the average canopy density.

When actual evaporation data are used (i.e., AEI defines seasonal variation), the values in Equation 17 take on a different meaning. PEX and PEN become adjustment factors for July and January 15th and E_d becomes the vegetation adjustment for the current day.

It should be noted that Equation 16 has the same form as the equation used to compute upper zone tension water contents in the Sacramento soil-moisture accounting model (Burnash et al, 1973). Also Equation 16 gives the same results as if it was written in the form of Equation 4 with the daily recession rate equal to 1.0 minus (E_d /SMIX). Thus, SMI could be calculated in the same way that API is computed only with a seasonally varying recession rate. The form of Equation 16 and the use of evaporation data makes it easier for the user to estimate the parameter values.

3rd Quadrant

The 3rd quadrant of the Continuous API Model computes surface runoff knowing AI_f and the amount of precipitation. Earlier it was indicated that some doubt exists as to whether the same relationship can be used for this quadrant in a continuous API model as is used in an event model. Also the typical equations used for this quadrant in previous API models involve 4 or 5 parameters which are not easy to visualize. Thus in this model a much simpler approach was taken.

Computation of Surface Runoff: The model assumes that the fraction of the precipitation that becomes surface runoff increases as AI_f decreases and reaches a maximum when $AI_f = 0$. This is expressed as:

$$F_s = FRSX*0.7^{AI_f} \quad (19)$$

where F_s is the fraction of precipitation that becomes surface runoff (decimal fraction)

FRSX is the maximum percent runoff (decimal fraction)

The curvature constant in Equation 19 has been fixed at 0.7. Because of the common functional form of equations in the model (Equations 1, 2, 19 and 23) and because the second quadrant is linear, a curvature parameter is not needed in Equation 19. If a different curvature constant is selected, new values of AIXW, AIXD, AICR, CG and RVAI can be computed such that the model will produce exactly the same results. The value of 0.7 was selected so that F_s does not vary too quickly or too slowly as a function of AI_f.

The amount of surface runoff is then computed as:

$$R_s = F_s * P \qquad (20)$$

where R_s is the surface runoff (inches)

Some would think that the maximum fraction of surface runoff should be 1.0 (i.e. F_s should equal 1.0 when $AI_f = 0.0$). While this is the case for many watersheds there are also many watersheds that never reach 100 percent surface runoff. Watersheds with high saturated soil permeability never reach 100 percent runoff even near the end of a very large event. For example, at the French Broad River at Rosman, North Carolina from September 28 to 30, 1964 the remnants of a hurricane dropped over 12 inches of rain on the watershed. An additional 1.5 inches occurred over the next 3 days. On October 4th and 5th, 9.8 inches of rain from another hurricane produced the flood of record. The percent surface runoff for this record event was only 32 percent. For this reason the parameter FRSX is needed.

4th Quadrant

The 4th quadrant is used to compute what portion of the precipitation that does not become surface runoff (i.e. $P-R_s$) enters groundwater storage and eventually becomes baseflow runoff. The water that does not become surface runoff or groundwater inflow enters soil-moisture storage or becomes recharge to deep aquifers. No accounting of this water is made in an API model.

Computation of Groundwater Inflow: Based on soil-moisture conditions either none, some or all of the $P-R_s$ quantity enters groundwater storage. It is first assumed that when SMI is less than SMIX (i.e. surface storages not full), that groundwater inflow (G_i) is zero. Second it is assumed that when SMI = SMIX and the soil is wet enough, that $G_i = P-R_s$. Since AI_f is the available index to soil conditions, there is a value of AI_f below which all of the remaining water enters groundwater storage. This value is referred to as the critical AI_f value (AICR). When AI_f is greater than AICR, the fraction of $P-R_s$ entering groundwater storage is reduced and approaches zero as AI_f approaches infinity (see Figure 2). The equations used to compute G_i are:

When SMI < SMIX:

$$F_g = 0.0 \qquad (21)$$

where F_g is the fraction of $P-R_s$ that enters groundwater storage (decimal fraction)

When SMI = SMIX and $AI_f \leq AICR$:

$$F_g = 1.0 \quad (22)$$

where AICR is the critical AI_f value (i.e. AI_f value below which $F_g = 1.0$) (inches)

When SMI = SMIX and $AI_f > AICR$:

$$F_g = CG^{(AI_f - AICR)} \quad (23)$$

where CG is the curvature constant for groundwater inflow ($0.0 < CG < 1.0$)

The actual amount of groundwater inflow is then:

$$G_i = F_g * (P-R_s) \quad (24)$$

where Gi is the groundwater inflow (inches)

Baseflow Runoff

The baseflow runoff equations of the Stanford Watershed Model (Crawford and Linsley, 1966) are used to compute runoff from groundwater storage in the Continuous API Model. The Stanford Model baseflow component is simple, but yet has proven to adequately represent baseflow runoff in a wide variety of basins. The Stanford and Sacramento Models represent baseflow runoff in a very similar manner. Both models assume that there are two baseflow runoff components. First, there are the aquifers that feed the stream during long periods with no groundwater recharge. In the Sacramento Model this is termed primary baseflow runoff. Second, there are aquifers that drain more rapidly and only feed the stream for weeks or months after a period of recharge. The Sacramento Model refers to this drainage as supplemental baseflow runoff. When both sets of aquifers are contributing, the resulting baseflow recession rate is a weighted average of the individual recession rates for each aquifer.

Baseflow Runoff Computations: A baseflow index (which is analogous to API) is used to indicate the amount of groundwater inflow that has occurred in the recent past. This index is computed as:

$$BFI_2 = K_g * BFI_1 + G_i \quad (25)$$

$$K_g = BFIK^{(\Delta t/24)} \quad (26)$$

where BFI is the Baseflow Index (inches)
K_g is the BFI recession rate for the time period.
BFIK is the daily BFI recession rate

BFIK is similar to the supplemental baseflow recession rate in the Sacramento Model (i.e. BFIK ≈ 1.0 - LZSK where LZSK is the daily lower zone supplemental withdrawal rate in the Sacramento Model).

Baseflow runoff is then computed as:

$$R_g = (1.0-K_b)*(1.0+BFIM*BFI)*G_s \quad (27)$$

$$K_b = BFPK^{(\Delta t/24)} \quad (28)$$

where R_g is the baseflow or groundwater runoff (inches)
K_b is the primary baseflow recession rate for the time period
BFPK is the daily primary baseflow recession rate
BFIM is the weighing factor (BFIM $\geq$ 0.0)
G_s is the groundwater storage contents (inches)

BFPK is the same as the primary baseflow recession rate in the Sacramento Model (i.e. BFPK = 1.0 - LZPK where LZPK is the daily lower zone primary withdrawal rate in the Sacramento Model). BFIM determines the relative magnitude of supplemental versus primary baseflow runoff. If BFIM = 0.0 only primary runoff occurs.

The change in the groundwater storage contents are then computed as:

$$G_{s_2} = G_{s_1} + G_i - R_g \quad (29)$$

Additional Features

The Continuous API Model can account for constant impervious area runoff and riparian vegetation losses. Also the computational method used by the model needs to be described.

Impervious Runoff: The model computes impervious runoff as:

$$R_i = PIMPV*P \quad (30)$$

where R_i is the impervious area runoff (inches)
PIMPV is the fraction of the watershed that acts as an impervious area (decimal fraction)

Riparian Vegetation Loss: When the soil is quite dry, riparian vegetation will withdraw water from groundwater seeping into the stream. The antecedent index (AI) is used to reflect moisture conditions. Riparian losses can occur when AI exceeds a specified value (RVAI). Riparian losses are computed as:

When AI $\leq$ RVAI:

$$L_r = 0.0 \quad (31)$$

where RVAI is the AI value above which riparian vegetation losses can occur (inches)

L_r is the amount of riparian vegetation loss (inches)

When AI > RVAI:

$$L_r = RIVA*E*\left(1.0-\frac{SMI}{SMIX}\right)*\left(\frac{AI-RVAI}{AIX-RVAI}\right) \quad (32)$$

where RIVA is the fraction of the watershed covered by riparian vegetation (decimal fraction)

AIX is the maximum AI value for the current day [AIX = AIXW + y*(AIXD-AIXW)] (inches)

The term E*(1.0-SMI/SMIX) represents the residual evaporation demand from the surface layers and ((AI-RVAI)/(AIX-RVAI)) crudely represents that the residual evaporation demand from the rest of the soil increases as AI increases.

Computation Method: The Continuous API Model uses an explicit solution to the equations where the value of the variables at the start of the time interval represent the conditions during the interval. To avoid significant errors during periods with large amounts of precipitation, no time interval is allowed to contain more than 0.2 inches of precipitation. Thus, during periods with large amounts of precipitation, the model increments along the curves by subdividing the period into shorter intervals.

Total Runoff: The total runoff generated by the Continuous API Model is computed as:

$$R = R_i + (R_s+R_g)*(1-PIMPV) - L_r \quad (33)$$

where R is the total runoff (inches)

Frozen Ground Effects

Frozen ground can have a significant effect on the amount of runoff that results from rain or snowmelt. When the ground freezes, the water that is in the soil pores will freeze causing a blockage and thus a reduction in the infiltration rate. Unless the soil is quite saturated when freezing occurs, there is initially very little reduction in the rate of infiltration. This is because there is not enough water in the pore spaces, especially in the larger spaces. The infiltration rate is not reduced significantly until enough rain or snowmelt enters the soil and freezes to restrict the entry of water into the ground. As thawing occurs, the water frozen in the pores melts allowing for water to again infiltrate at a rate unrestricted by ice. The Continuous API Model attempts to account for the effect of frozen ground by using a frost index and a frost efficiency index. The frost index indicates the extent of frost in the soil (Anderson and Neuman, 1984). The frost efficiency index indicates the degree to which the soil pores have been filled with ice.

The frost index and frost efficiency index are intended to be representative of the portion of the basin that can exhibit

significant frozen ground effects on runoff. In general, open agricultural areas experience much more significant frozen ground effects than conifer forests with a thick litter layer. If a watershed contains a mixture of open and forested areas, the indices should be used to estimate frozen ground conditions in the open areas. The overall effect of frozen ground on runoff for the basin is computed using an effective frost area parameter.

Frost Index

The empirical frost index is computed as:

$$FI_2 = FI_1 + \Delta FI \quad (34)$$

where FI is the frost index (DEGF), (subscripts refer to the beginning and end of the time period)

FI is always $\leq$ 32 DEGF. The change in FI is computed differently depending on whether the air temperature is above or below freezing. When the air temperature is below freezing (i.e. frost is typically growing):

$$\Delta FI = -C*\sqrt{(T_a-32)^2+(FI_1-32)^2} - C*(FI_1-32) + GHC*(24/\Delta t) \quad (35)$$

where C is the frost coefficient for the time interval
T_a is the air temperature (DEGF)
GHC is the daily thaw rate due to ground heat (DEGF)

When the air temperature is above freezing (i.e. the frost is thawing):

$$\Delta FI = C*(T_a-32) + GHC*(24/\Delta t) \quad (36)$$

Thawing can also occur due to heat transfer from rainwater, however, since the amount of heat transferred is generally much less than from the atmosphere, this factor is neglected.

Figure 4 depicts the change in the frost index when GHC is zero. The frost index grows most rapidly when the air temperature is considerably below the current FI value. The frost index will continue to grow whenever the temperature is below freezing unless the change due to temperature is less than GHC.

The frost coefficient that primarily controls the change in the frost index is dependant on the heat transfer characteristics of the upper soil layers. Frost will develop faster in an area with bare ground than in an area covered by litter. When snow is on the ground, the frost coefficient needs to be reduced due to the insulating effect of the snow cover. The frost coefficient is computed as:

$$C = CSOIL*(\Delta t/6)*(1-S_c) + CSOIL*(\Delta t/6)*S_c*(1-CSNOW)^{W_e} \quad (37)$$

where CSOIL is the frost coefficient for non-snow covered soil (6 HR^{-1})
CSNOW is the reduction in CSOIL per inch of snow water-

equivalent (decimal fraction)
W_e is the snow water-equivalent (inches)

Figure 5 shows the reduction in the frost coefficient as a function of snow water-equivalent for typical values of the CSNOW parameter.

Frost Efficiency Index

The frost efficiency index varies between zero (frost has no effect on runoff) and 1.0 (concrete frost exists over the entire area, thus there is a 100 percent runoff rate). When there is insufficient frost in the soil to freeze the water in the pore spaces, the frost efficiency index becomes zero.

The frost efficiency index is computed as:

$$FEI_2 = FEI_1 + \Delta FEI \quad (38)$$

where FEI is the frost efficiency index (subscripts refer to the beginning and end of the time period)

Frozen ground has no effect on runoff when FI is greater than or equal to a specified value, thus:

When FI $\geq$ FICR:

$$FEI = 0.0 \quad (39)$$

where FICR is the critical frost index (DEGF)

FEI can change due to water within the soil freezing when the frost index grows, rain or melt water freezing when it enters frozen soil and thawing when the air temperature is above freezing.

The change in FEI due to water in the soil freezing as frost develops is computed as:

When FI $\geq$ FICR or $FI_2 > FI_1$:

$$\Delta FEI_f = 0.0 \quad (40)$$

When FI < FICR and $FI_2 < FI_1$:

$$\Delta FEI_f = (1-FEI_1)*CF*(1-AI_r)^2*(FI_1-FI_2) \quad (41)$$

where ΔFEI_f is the change in FEI due to freezing
CF is the FEI freezing coefficient ($DEGF^{-1}$)
AI_r is the ratio of current AI to AIX, the maximum value for the date

The value of AI_r is an indicator to the soil-moisture conditions. Equation 40 indicates that the soil must be quite wet (i.e. most pore spaces filled with water) before freezing temperatures will significantly reduce infiltration and that the rate of water freezing is reduced as more pores are filled with ice. The insulating effect

of a snow cover is built into the computation of the FI values.

The change in FEI due to rain or meltwater freezing when it enters frozen soil is computed as:

When FI $\geq$ FICR or P = 0.0:

$$\Delta FEI_p = 0.0 \quad (42)$$

When FI < FICR and P > 0.0:

$$\Delta FEI_p = \frac{1}{CP} * R * (1 - AI_r) * P \quad (43)$$

$$R = 0.5 + \frac{COS[\pi * (1 - FI_r)]}{2} \quad (44)$$

where ΔFEI_p is the change in FEI due to precipitation freezing in the soil
CP is the FEI precipitation coefficient (inches)
FI_r is the frost index ratio ((FICR-FI)/70.0); when (FICR-FI) > 70, FI_r = 1.0

CP is the amount of precipitation needed to raise FEI from 0.0 to 1.0 with wet soil and maximum frost conditions. Equation 43 indicates that more of the precipitation will freeze and clog the pores when the soil is wet (precipitation is held in the soil and allowed to freeze) and when there is significant frost (more chance of freezing before water percolates below the frost level).

The change in FEI due to thawing is computed as:

When $T_a \leq 32$:

$$\Delta FEI_t = 0.0 \quad (45)$$

When $T_a > 32$:

$$\Delta FEI_t = -C_t * (T_a - 32) \quad (46)$$

$$C_t = CT * (\Delta t/6) * (1 - S_c) + CT * (\Delta t/6) * S_c * (1 - CSNOW)^{W_e} \quad (47)$$

where ΔFEI_t is the change in FEI due to thawing
CT is the FEI thaw coefficient for non-snow covered ground ($DEGF^{-1} * 6HR^{-1}$)

Just as with the frost coefficient used in FI computations, the FEI thaw coefficient is reduced when snow covers the ground.

The total change in the frost efficiency index is:

$$\Delta FEI = \Delta FEI_f + \Delta FEI_p + \Delta FEI_t \quad (48)$$

The frost efficiency index is used to compute the additional surface runoff that occurs due to ice filled soil pores. It is assumed that the rate of increase of additional surface runoff increases as FEI increases (i.e. the relationship between FEI and additional surface runoff is not linear). The frost efficiency, as noted earlier, is only applied to the portion of the watershed where frozen ground has a significant effect on runoff. The fraction of surface runoff when frozen ground exists is computed as:

$$F_s' = F_s + (1-F_s)*FEI^2*EFA \quad (49)$$

where F_s' is the fraction of precipitation that becomes surface runoff when frozen ground exists (decimal fraction
EFA is the effective frost area (decimal fraction)

F_s' is then used in place of F_s in Equation 20. Figure 6 shows what the 3rd quadrant of the model looks like for an effective frost area of 1.0.

Additional Frozen Ground Modifications

In addition to modifying the fraction of the precipitation that becomes surface runoff, the computation of API and SMI need to be modified when frozen ground exists. The API recession rate is assumed to be 1.0 and the evaporation amount used to compute SMI is assumed to be zero over the EFA when frozen ground is present. When significant frozen ground exists (FI < FICR), the API recession rate becomes:

$$APIK_f = 1.0*EFA + (1-EFA)*APIK_s \quad (50)$$

where $APIK_f$ = daily API recession rate when frozen ground exists

When frozen ground exists, the evaporation value used in SMI computations (Equation 16) becomes:

$$E_f = (1.0-EFA)*E_s \quad (51)$$

where E_f is the evaporation when frozen ground exists (inches)

In addition to reducing the API recession rate, the precipitation value used in computing API (Equation 4) is modified when frozen ground exists. As the soil pores fill with ice (i.e. FEI increases), more of the subsequent precipitation becomes surface runoff and less goes to increasing soil moisture. Thus, the API value should not increase by the full amount of new precipitation. If no reduction is applied to the precipitation amount used to compute the change in API, the soil will be too wet after the frost is gone. Thus, when frozen ground exists, Equation 4 becomes:

$$API_2 = K_p*API_1 + (1-(FEI*EFA))*P \quad (52)$$

The recession rate, K_p, is computed from $APIK_f$ using Equation 5.

Parameter Summary

The parameters of the basic Continuous API Model and the parameters associated with the frozen ground option are summarized in this section.

Basic Model Parameters

The parameters of the basic Continuous API Model can be divided into 3 categories.

Category 1: This category contains the parameters that need to be determined through trial-an-error and automatic calibration procedures. These parameters typically can't be determined based on a hydrograph analysis or physiographic factors. The category 1 parameters are:

- AIXW, CW, AIXD, CD - These 1st quadrant parameters define the wet and dry curves relating API to AI and are probably the most critical parameters to be determined by the calibration process.

- CS - Seasonal curvature exponent used to control the transition from dry to wet curves in the 1st quadrant. A value of 1.0 results in a sinusoidal transition from late summer to winter conditions. Values considerably greater than 1.0 (e.g. 2.5-4) cause a rapid change in the fall and are indicative of watersheds where the soil-moisture deficit built-up during the summer is reduced to zero over a relatively short period of a month or so in the fall.

- AICR and CG - These 4th quadrant parameters control how much of the precipitation that does not become surface runoff enters groundwater storage. The parameters control the magnitude of baseflow. Changes to 1st quadrant parameters will affect groundwater inflow because the AI values will change, however, changes to AICR and CG will not affect surface runoff computations.

- BFIM - This weighing factor controls the magnitude of faster responding or supplemental baseflow relative to slower responding or primary baseflow. BFIM thus controls the timing of baseflow runoff assuming the two recession rates are reasonably correct.

Category 2: This category contains the parameters that can generally be derived from a hydrograph analysis or from physiographic information about the watersheds. These parameters should require little if any adjustment as part of the calibration process.

- WKW and WKD - The week number of the wettest and driest times of the year can usually be obtained from a general knowledge of the area. WKW generally occurs from late February through early May with the later dates being associated with northern or mountain basins with considerable snowmelt runoff. WKD usually occurs in August or early September.

- APIKS - The daily API recession rate when the ground is completely covered by snow. In areas with long periods of snow cover with little rain or melt, use an APIKS of 1.0 so that soil moisture conditions prior to the snow cover are remembered when snowmelt

occurs in the spring. In temperate zones where significant rain or melt can occur when a snow cover exists, APIKS should only be slightly greater than APIK.

- SMIX - The maximum value of the surface moisture index represents, the size of interception, depression and surface moisture storage. In general, significant surface runoff does not occur until SMI = SMIX. The correct general magnitude of this parameter is important, but the results do not appear to be sensitive to small changes in the value of SMIX. A reasonable estimate of SMIX can usually be determined by finding the amount of precipitation needed to cause surface runoff after a dry period in the summer.

- FRSX - This parameter represents the maximum percent surface runoff that can ever occur. In many watersheds a good approximation of FRSX can be derived by computing the percent surface runoff for a very large event that occurs when the soil is wet. The value of FRSX is somewhat greater than the percent runoff for the event since the percent runoff at the end of the event is greater than for the event as a whole. In the case of basins where the maximum percent runoff occurs near the end of extended snowmelt periods, an initial estimate of FRSX is much more difficult to derive.

- PEX and PEN - These are the maximum and minimum daily evaporation rates and are assumed to occur on July 15th and January 15th, respectively. These values are obtained from historical evaporation data. Sometimes the values should be adjusted for the effect of vegetation (e.g. in areas with deciduous forests, the value of PEN should be adjusted downward or even set to zero in northern climates).

- EFC - The effective forest cover is used to adjust evaporation rates when snow exists. It is equal to the fraction of the area covered by conifer forests times the average cover density.

- BFIK and BFPK - These are the daily recession rates for short-term or supplemental baseflow and for long-term or primary baseflow. These values can usually be derived from historical streamflow data.

- PIMPV - The percent impervious area also can usually be estimated from historical data. Streamflow and concurrent precipitation data are required.

- RVAI and RIVA - The values of these riparian vegetation parameters can not be derived in advance, but the presence of riparian losses can be detected. Sharp baseflow recessions during dry summer months indicate that riparian losses exist. Sometimes the flow will go to zero during these periods, but then recover in the fall without the occurrence of significant recharge. When these losses exist, the calibration is normally done with RVAI and RIVA set to zero and then as a final step the riparian loss is included. At this point estimates of RVAI and RIVA can be made by comparing the simulated hydrograph without riparian losses with the observed hydrograph.

Category 3: This category contains the parameters that generally have

the same or a similar value for all watersheds. Very seldom are different values required.

- APIK - The daily API recession is normally set to 0.9.

- APIX - The maximum allowed API value is generally in the range of 8-10 inches.

The parameters for the special seasonal variation options involving AEI and ATI are not included in the parameter summary.

Frozen Ground Parameters

The Continuous API Model parameters involved in frozen ground computations can be divided into those used to compute the frost index and those used in calculating the frost efficiency index and its effect on runoff.

Frost Index: There are 3 parameters used to compute the frost index. These parameters are:

- CSOIL - The frost coefficient for bare ground conditions controls both the growth of the frost index (freezing) and the decay of the frost index (thawing). This is the most important parameter in the calculation of the frost index. Open areas with bare soils should exhibit the greatest amount of frost and the highest CSOIL values, while areas with a litter layer will have less frost and the lower values of the parameter.

- CSNOW - Accounts for the insulating effect of a snow cover. Even a few inches of snow depth can reduce the frost coefficient by 80-90 percent.

- GHC - This parameter controls how the frost index is affected by heat transfer from below the frost layer. Ground heat provides a small, but steady reduction in the frost index. The primary need for GHC is to reproduce the thawing of frozen ground that occurs under a deep snow cover.

Frost Efficiency Index: There are 5 parameters used in computing the frost efficiency index and its effect on runoff. In addition, the CSOIL parameter is also used during FEI calculations. The parameters are:

- FICR - The value of the frost index above which soil frost has no effect on infiltration and the generation of runoff. A small amount of soil frost will essentially have no effect.

- CP - The amount of precipitation that must freeze in order to fill the soil pores with ice. Even when there is deep frost penetration, there will not be much effect on runoff until there is sufficient rain or snowmelt to fill the soil pores and freeze.

- CF - The FEI freezing coefficient controls the increase in FEI during cold periods. Rain or snowmelt does not occur during these

periods. The frost efficiency index will increase slowly due to freezing of existing water in the soil pores. CF has a minor effect on the increase in FEI unless there are very high soil-moisture conditions when frost is formed.

- CT - The FEI thaw coefficient controls the decrease in FEI when thawing of the soil occurs. CT will determine how long it will take, once warm weather occurs and the snow melts, for the effect of soil frost on runoff to disappear.

- EFA - The effective frost area controls the portion of the watershed that runoff generation can be significantly affected by frozen ground. The frost index and frost efficiency index values are intended to be representative of this portion of the basin.

References

Anderson, E. and Neuman, P., 1984, 'Inclusion of Frozen Ground Effects in a Flood Forecasting Model', Proceedings of the Fifth Northern Research Basins Symposium held March 19-23, 1984 at Vierumaki, Finland, pp 5.1-5.14.

Burnash, R., Ferral, R. and McGuire, R., 1973, 'A Generalized Streamflow Simulation System, Conceptual Modeling for Digital Computers', California-Nevada River Forecast Center, Sacramento, CA (also see Section II.3.1).

Crawford, N. and Linsley R., 1966, 'Digital Simulation in Hydrology: Stanford Watershed Model IV', Dept. of Civil Engineering, Stanford University, Stanford, CA.

Farnsworth, R., Thompson, E. and Peck, E., 1982, 'Evaporation Atlas for the Contiguous 48 United States, NOAA Technical Report NWS 33, U.S. Dept. of Commerce.

Farnsworth, R., Thompson, E., 1982, Mean Monthly, 'Seasonal and Annual Pan Evaporation for the United States, NOAA Technical Report NWS 34, U.S. Dept. of Commerce.

Linsley, R., Koler, M. and Paulhus, J., 1948: 'Runoff Relations', Applied Hydrology, chapter 16, McGraw-Hill, pp 405-443.

McCallister, J.P., 1963, 'Role of Digital Computers in Hydrological Forecasting and Analyses, U.S. Geological Survey Publication No.63 (also see section II.3-API-SLC).

Nemec, J. and Sittner, W., 1982, 'Application of the Continuous API Catchment Model in the Indus River Forecasting System in Pakistan', Applied Modeling in Catchment Hydrology, Water Resources Publications, pp 313-322 (part of the Proceedings of the International Symposium on Rainfall-Runoff Modeling held May 13-21, 1981 at Mississippi State University)

Sittner, W., Schauss, C. and Monro, J., 1969, 'Continuous Hydrograph

Synthesis with an API-Type Hydrologic Model', Water Resources Research, Vol.5, No.5, pp 1007-1022.

Figure 1a. Typical event API Rainfall-runoff relationship: graphical coaxial relationship

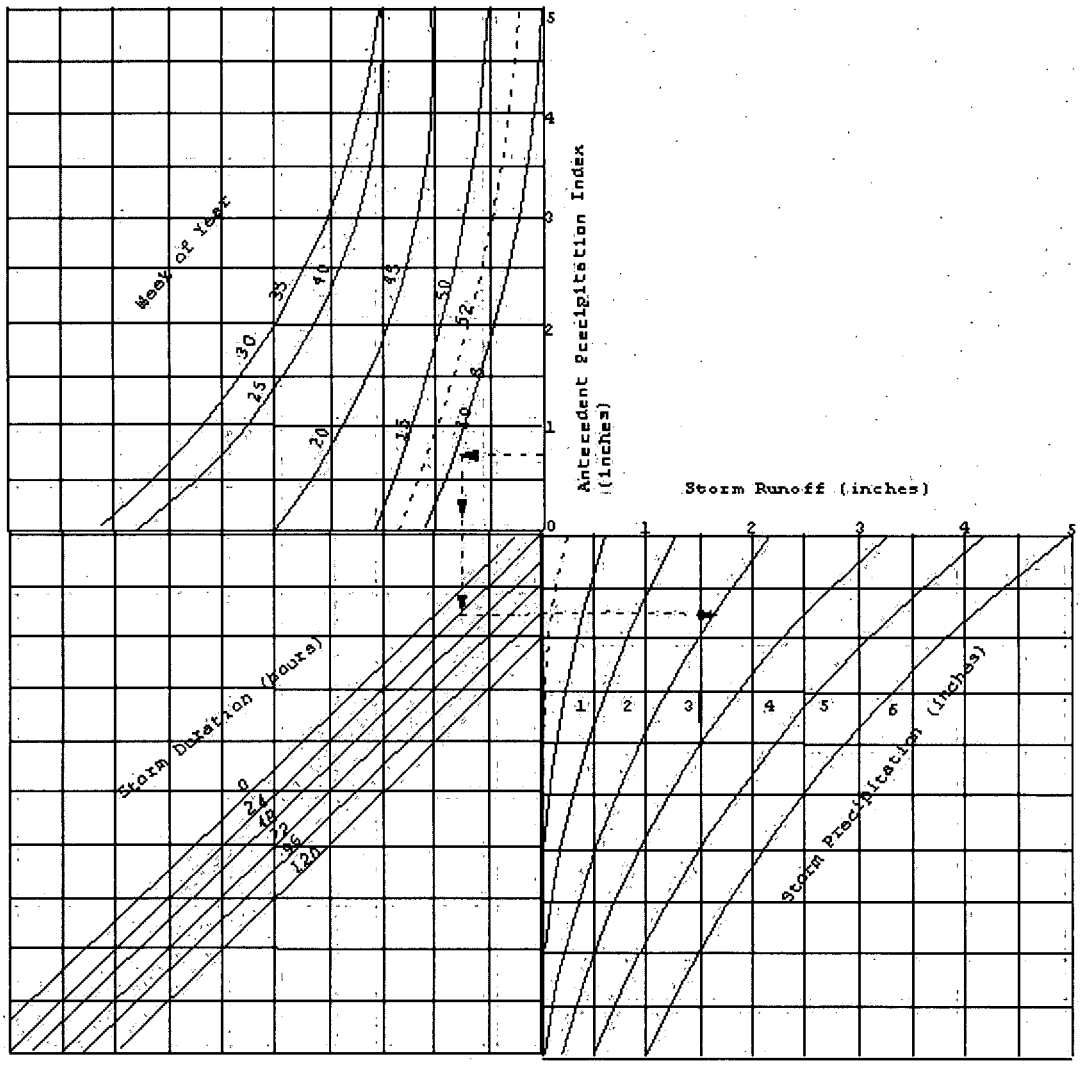

Figure 1b. Typical event API rainfall-runoff relationship: precipitation versus runoff as a function of antecedent conditions

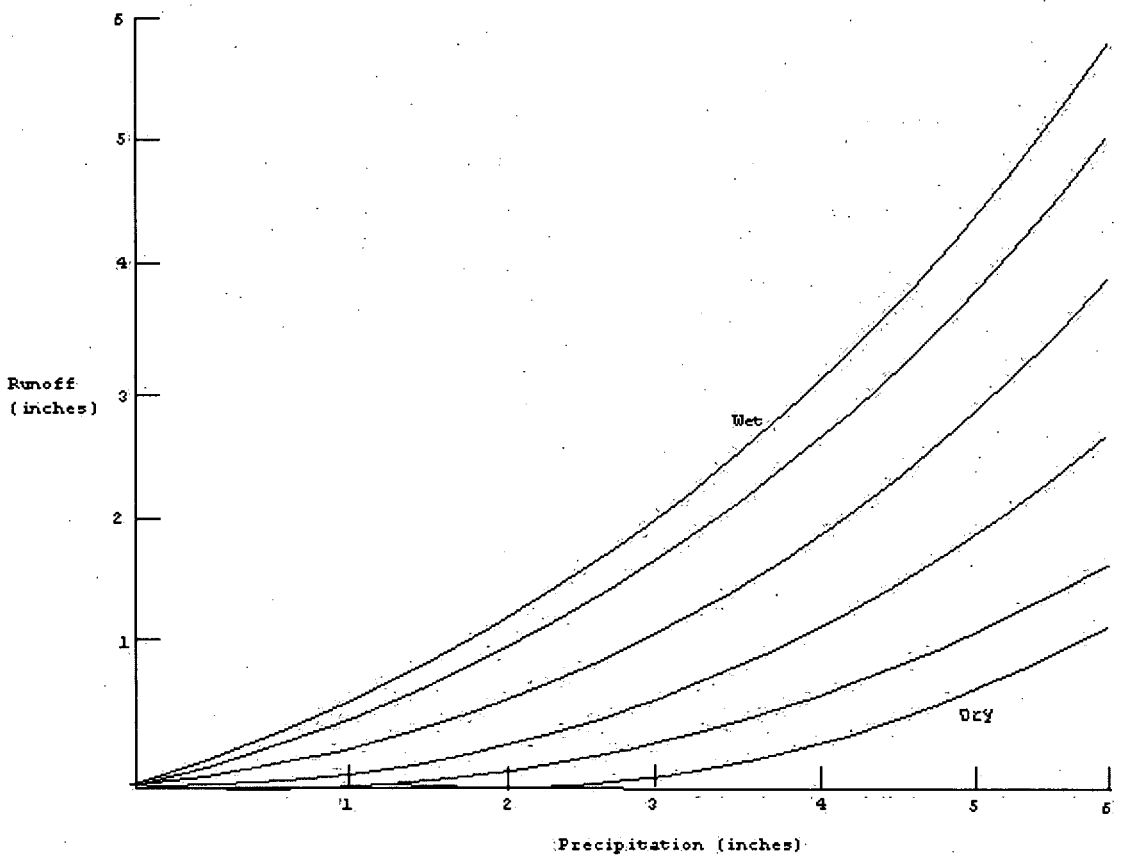

Figure 2. Graph of the 4 quadrants of the Continuous API Model

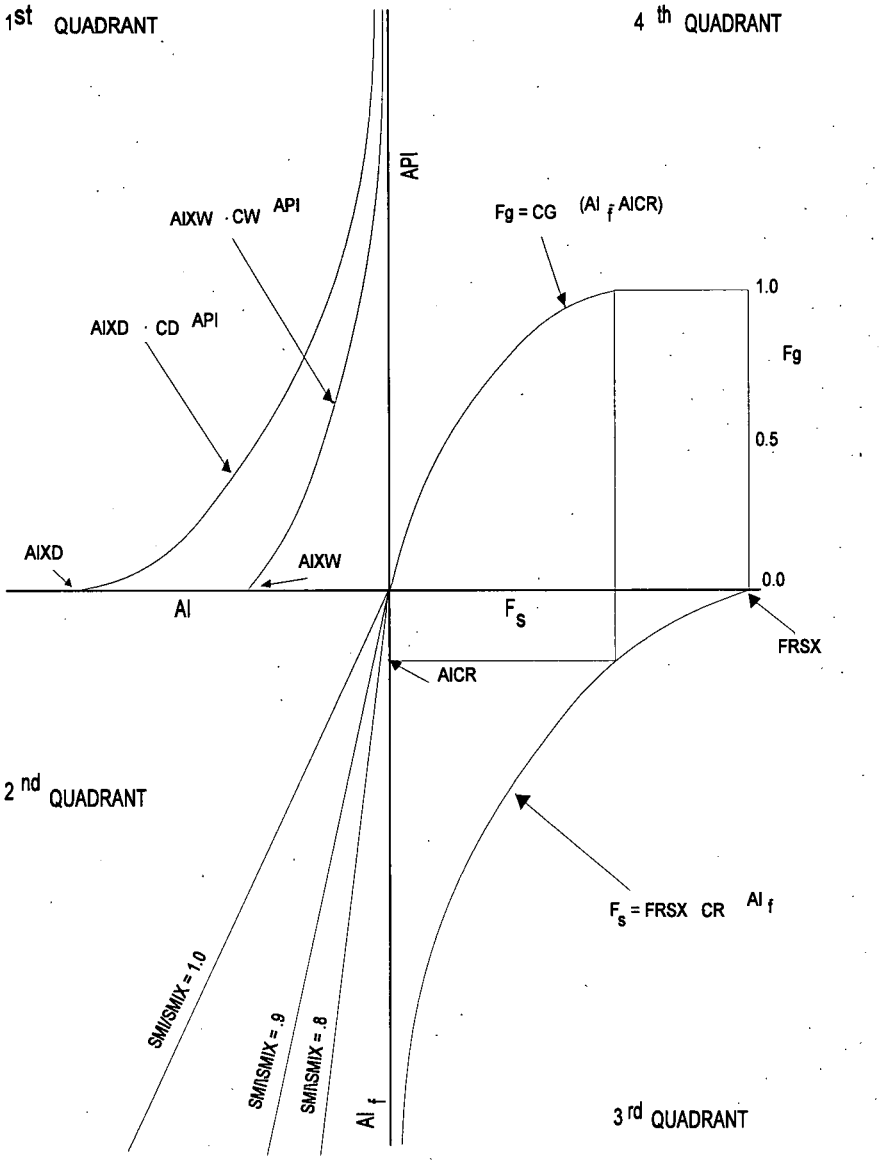

Figure 3. Seasonal variation of y for typical values of WKW and WKD

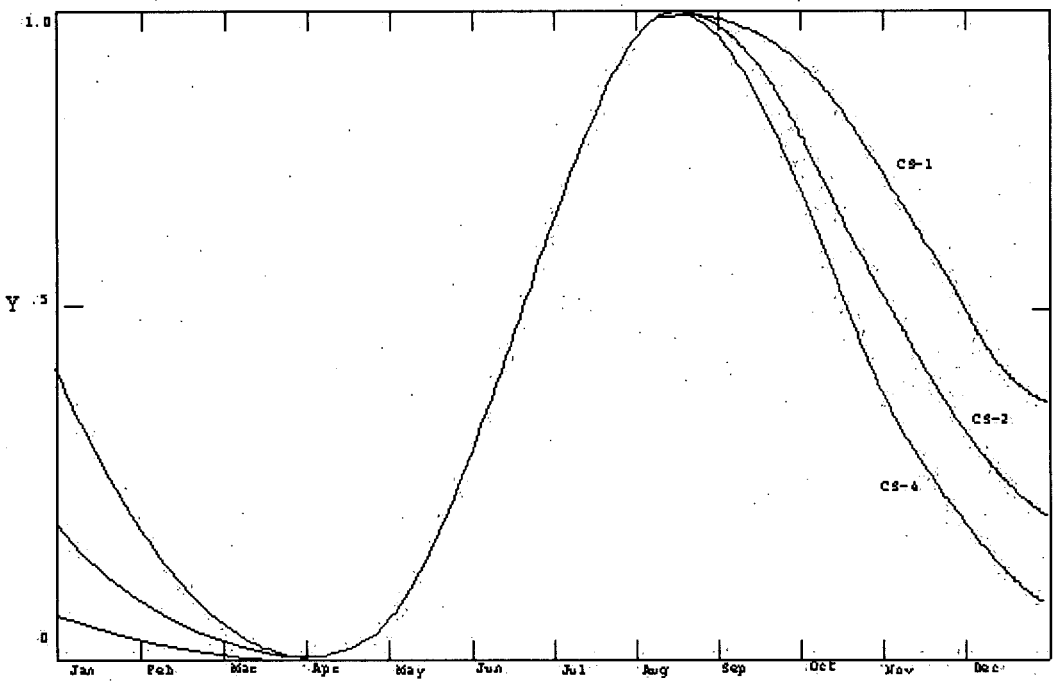

Figure 4. Graphical depiction of the change in the frost index (ΔFI) versus air temperature (T_a) with no ground heat

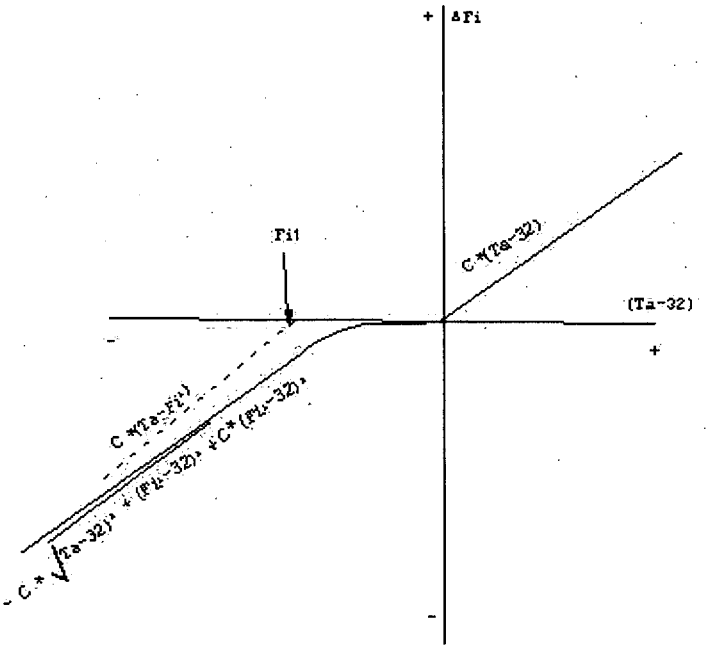

Figure 5. The reduction in the frost coefficient as a function of the amount of snow for typical values of CSNOW

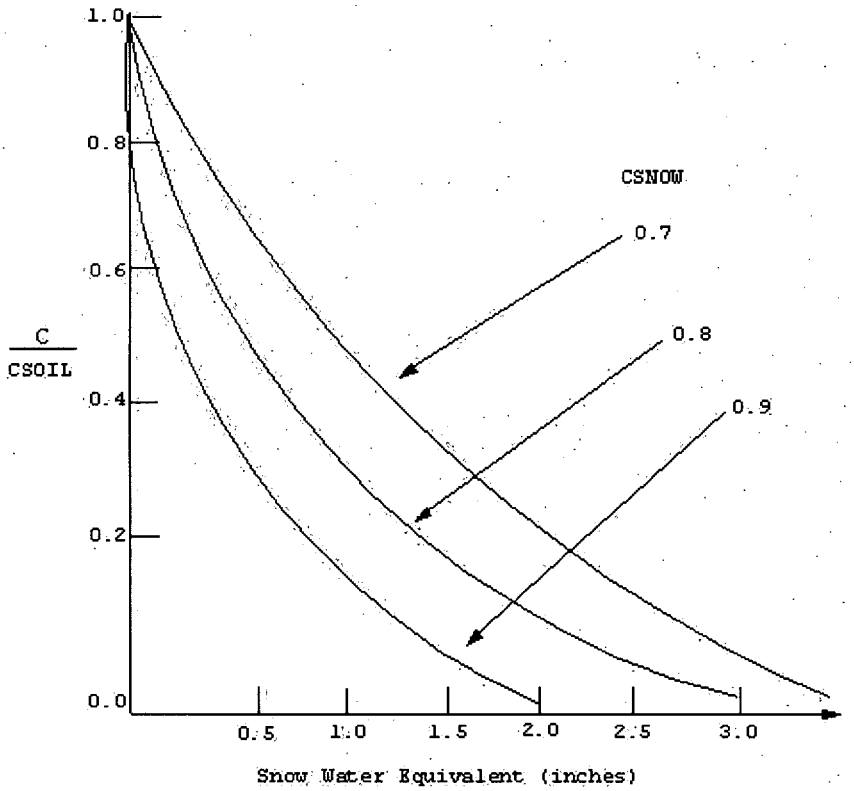

Figure 6. 3rd quadrant of the model when frozen ground is included (assumes an effective frost area of 1.0)

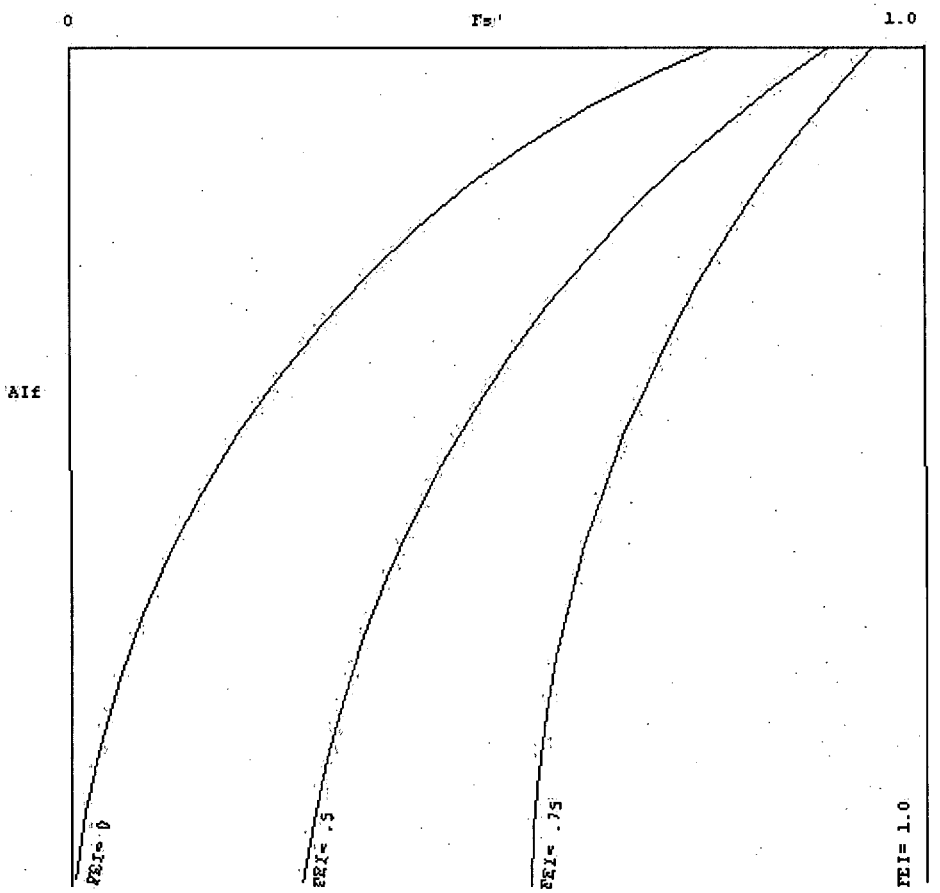

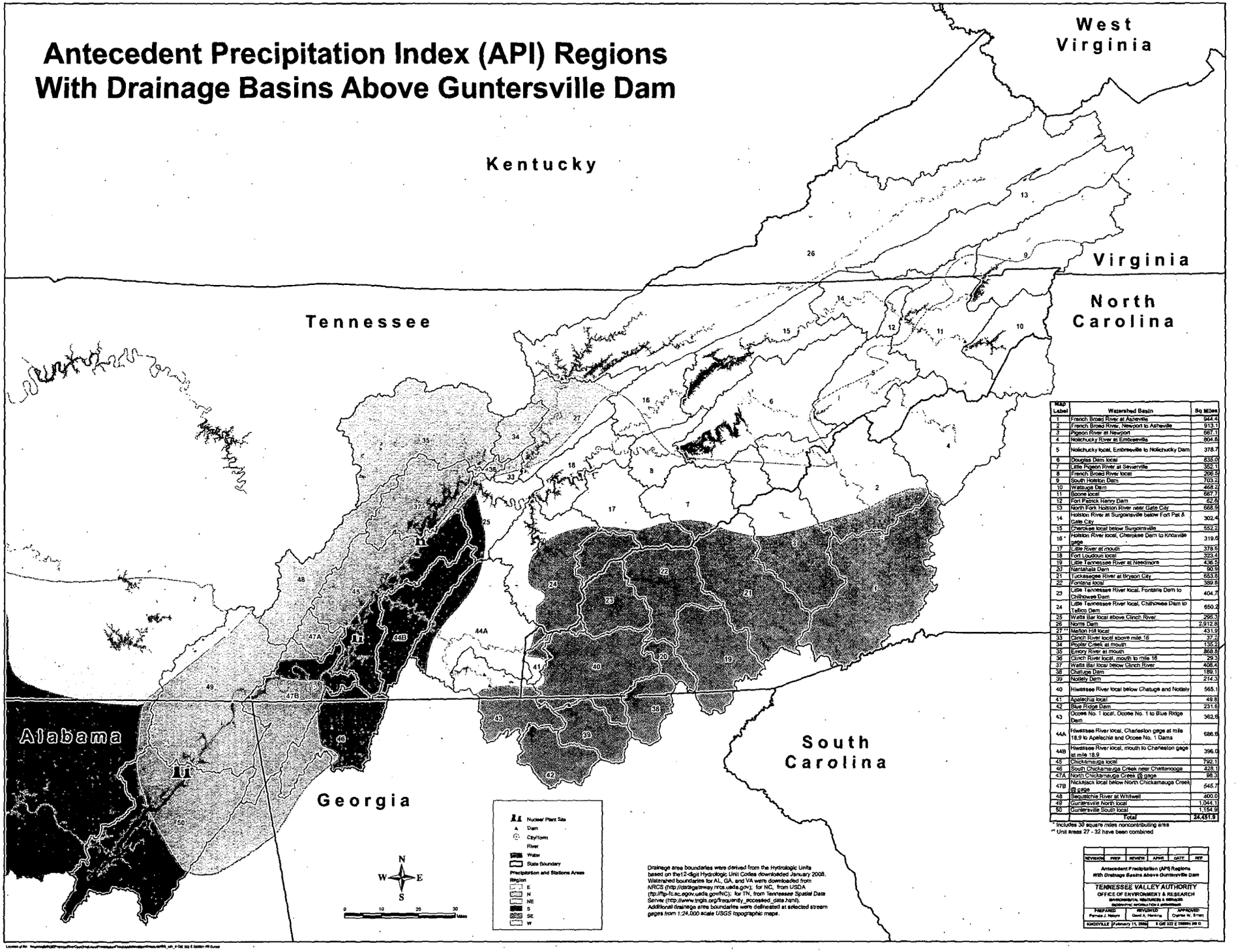

Map Label	Watershed Basin	Sq Miles
1	French Broad River at Asheville	944.4
2	French Broad River, Newport to Asheville	913.1
3	Pigeon River at Newport	667.1
4	Nolichucky River at Embreeville	804.8
5	Nolichucky local, Embreeville to Nolichucky Dam	378.7
6	Douglas Dam local	635.0
7	Little Pigeon River at Sevierville	362.1
8	French Broad River local	296.5
9	South Holston Dam	703.2
10	Watauga Dam	468.2
11	Boone local	587.7
12	Fort Patrick Henry Dam	62.8
13	North Fork Holston River near Gate City	668.9
14	Holston River at Surgoinsville below Fort Pat & Gate City	302.4
15	Cherokee local below Surgoinsville	552.2
16 *	Holston River local, Cherokee Dam to Knoxville gage	319.6
17	Little River at mouth	378.6
18	Fort Loudoun local	323.4
19	Little Tennessee River at Needmore	436.5
20	Nantahala Dam	90.9
21	Tuckasegee River at Bryson City	553.6
22	Fontana local	389.8
23	Little Tennessee River local, Fontana Dam to Chilhowee Dam	404.7
24	Little Tennessee River local, Chilhowee Dam to Tellico Dam	650.2
25	Watts Bar local above Clinch River	296.3
26	Norris Dam	2,912.8
27 **	Melton Hill local	431.9
33	Clinch River local above mile 16	37.2
34	Poplar Creek at mouth	135.2
35	Emory River at mouth	868.8
36	Clinch River local, mouth to mile 16	29.3
37	Watts Bar local below Clinch River	408.4
38	Chatuge Dam	189.1
39	Nottely Dam	214.3
40	Hiwassee River local below Chatuge and Nottely	565.1
41	Apalachia local	49.8
42	Blue Ridge Dam	231.6
43	Ocoee No. 1 local, Ocoee No. 1 to Blue Ridge Dam	362.6
44A	Hiwassee River local, Charleston gage at mile 18.9 to Apalachia and Ocoee No. 1 Dams	686.8
44B	Hiwassee River local, mouth to Charleston gage at mile 18.9	396.0
45	Chickamauga local	792.1
46	South Chickamauga Creek near Chattanooga	428.1
47A	North Chickamauga Creek @ gage	98.3
47B	Nickajack local below North Chickamauga Creek @ gage	545.7
48	Sequatchie River at Whitwell	400.0
49	Guntersville North local	1,044.1
50	Guntersville South local	1,164.5
	Total	24,451.8

* Includes 30 square miles noncontributing area
** Unit areas 27 - 32 have been combined

REVISION	PREP	REVIEW	APPR	DATE	REF
Antecedent Precipitation (API) Regions With Drainage Basins Above Guntersville Dam					

TENNESSEE VALLEY AUTHORITY
OFFICE OF ENVIRONMENT & RESEARCH
ENVIRONMENTAL RESOURCES & REMEDIES
GEOSPATIAL INFORMATION & APPLICATIONS

PREPARED	REVIEWED	APPROVED
Pamela J. Nelson	David A. Hamilton	Charles W. Smith

KNOXVILLE February 11, 2008

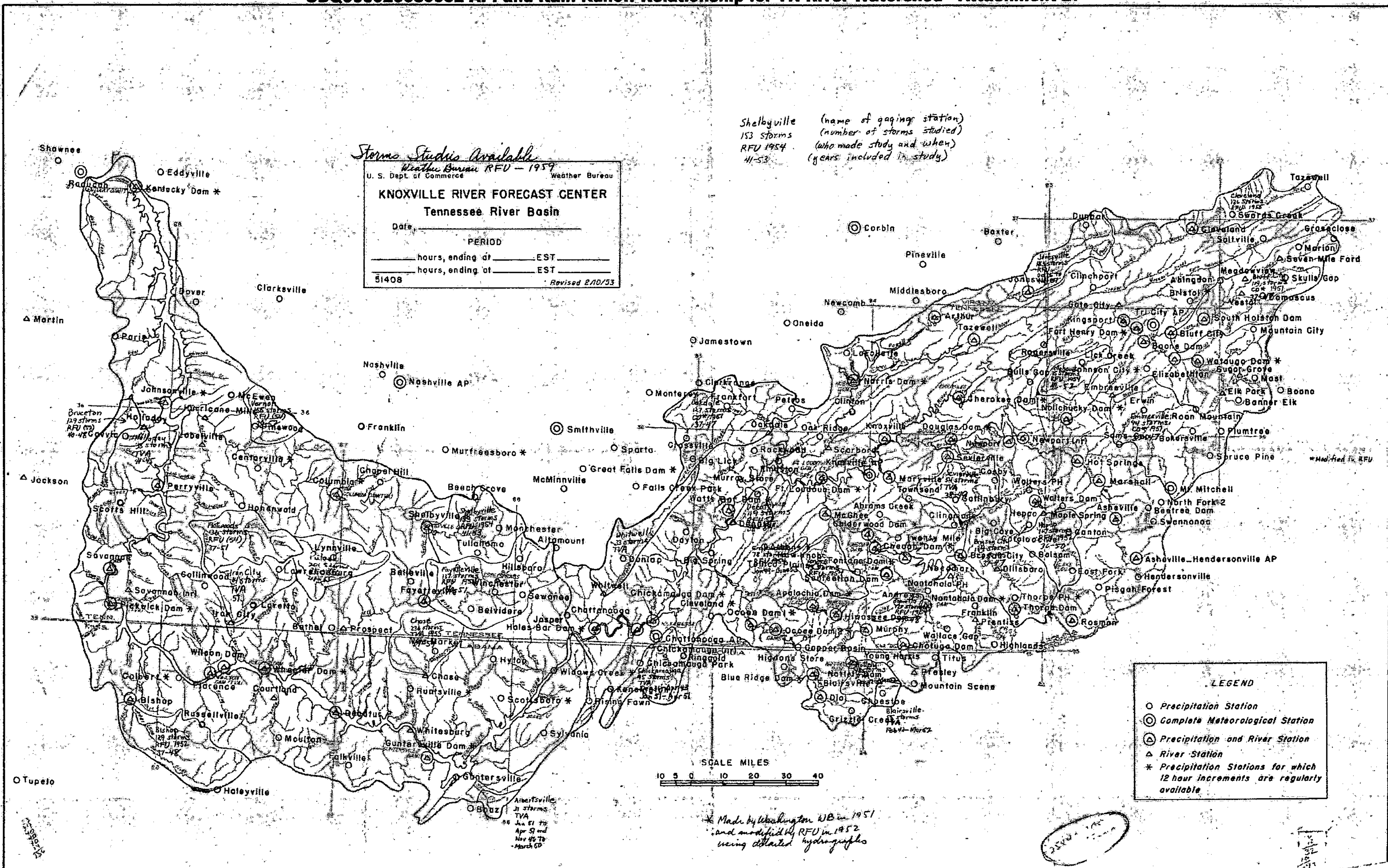
Storms Studies Available
Weather Bureau RFU – 1959
U. S. Dept. of Commerce
Weather Bureau
KNOXVILLE RIVER FORECAST CENTER
Tennessee River Basin
Date
PERIOD
hours, ending at EST
hours, ending at EST
51408
Revised 2/10/53
Shelbyville (name of gaging station)
153 storms (number of storms studied)
RFU 1954 (who made study and when)
41-53 (years included in study)
LEGEND
Precipitation Station
Complete Meteorological Station
Precipitation and River Station
River Station
Precipitation Stations for which 12 hour increments are regularly available
SCALE MILES
10 5 0 10 20 30 40
* Made by Washington WB in 1951 and modified by RFU in 1952 using detailed hydrographs
*Modified by RFU
Shawnee
Paducah
Eddyville
Kentucky Dam
Dover
Clarksville
Martin
Paris
Nashville
Nashville AP
Johnsonville
McEwen
Franklin
Smithville
Murfreesboro
Sparta
Great Falls Dam
McMinnville
Falls Creek Park
Centerville
Perryville
Jackson
Scotts Hill
Hohenwald
Columbia
Chapel Hill
Beech Grove
Shelbyville
Manchester
Tullahoma
Altamount
Savannah
Collinwood
Lawrenceburg
Belleville
Fayetteville
Winchester
Sewanee
Savannah (nr)
Pickwick Dam
Iron City
Loretto
Bethel
Prospect
Belvidere
Jasper
Hales Bar Dam
Chattanooga
Colbert
Florence
Wilson Dam
Wheeler Dam
Courtland
Decatur
Bishop
Russellville
Huntsville
Chase
Hytop
Scottsboro
Widows Creek
Whitesburg
Moulton
Guntersville Dam
Falkville
Guntersville
Sylvania
Rising Fawn
Boaz
Haleyville
Tupelo
Corbin
Baxter
Dunbar
Pineville
Middlesboro
Newcomb
Oneida
Jamestown
Arthur
Tazewell
LaFollette
Norris Dam
Clarkrange
Monterey
Frankfort
Petros
Clinton
Oakdale
Oak Ridge
Knoxville
Douglas Dam
Crossville
Rockwood
Big Lick
Scarboro
Newport
Sevierville
Morristown
Dayton
Dunlap
Big Spring
Chickamauga Dam
Cleveland
Ocoee Dam
Chattanooga AP
Blue Ridge Dam
Copper Basin
Murphy
Hiwassee Dam
Chatuge Dam
Mountain Scene
Highlands
Franklin
Nantahala Dam
Fontana Dam
Bryson City
Cherokee Dam
Kingsport
Fort Henry Dam
Bristol
South Holston Dam
Watauga Dam
Boone Dam
Elizabethton
Johnson City
Erwin
Nolichucky Dam
Greeneville
Hot Springs
Marshall
Asheville
Mt. Mitchell
North Fork 2
Swannanoa
Asheville-Hendersonville AP
Hendersonville
Pisgah Forest
Rosman
Canton
Waynesville
Tazewell
Cleveland
Saltville
Marion
Seven Mile Ford
Abingdon
Damascus
Mountain City
Boone
Banner Elk
Roan Mountain
Plumtree
Spruce Pine
Clinchport
Tri City AP
Bluff City

WB FORM 830-1 (Formerly 6008)

U. S. DEPARTMENT OF COMMERCE, WEATHER BUREAU

COMPUTATION AND TABULATION SHEET

Storm Studies made in RFV

* made in CO but modified at RFV using dist. Sheet hydrographs

Computed by ____ Date ____ Checked by ____ Date ____

Station	Date Completed		Total Storms Studied	Period Studied: Beginning		Period Studied: End		Unit Hydrograph
Oakdale *	Sept	51	152	Dec	37	May	47	TVA
Ashville *	Oct	51	50	Feb	40	Nov	47	RFU
Oregon City *	Oct	51	165	Oct	37	Sept	47	
✓ Embreeville *	Nov	51	101	Oct	37	Sept	47	TVA
✓ Bluff City *	Nov	51	116	Oct	37	Sept	47	
Tomotla	Feb	52	118	Dec	39	July	48	
Hepco	May	52	167	Oct	36	Dec	50	TVA
Jonesville	May	52	183	Oct	36	Nov	51	TVA
✓ Rockhof	July	52	130	Oct	37	Feb	48	TVA
✓ Bruston	Aug	52	129	Jan	40	Dec	48	
Mohawk	Jan	54	75	Aug	46	May	52	
✓ Vernon	Feb	54	119	June	38	May	52	
✓ Vonore	Feb	54						
Shelbyville	Apr	54	153	Apr	41	Feb	53	RFU
✓ Flatwoods	May	54	140	Oct	37	July	51	
✓ Fayetteville	June	54	136	Mar	40	Aug	51	
✓ Englewood	June	54	78					
Pulaski	Jy	56	201	Apr	41	Feb	55	RFU
Cleveland		55						TVA

(Formerly 5008)

U.S. DEPARTMENT OF COMMERCE, WEATHER BUREAU

COMPUTATION AND TABULATION SHEET

Land and Rain Runoff Relationship for TN River Wate

Sheet of

Computed by		Date		Checked by		Date		
Whitwell	old		33					TVA
Chickamauga		51	95	Dec	36	Apr	51	TVA
Decatur	Mar	52	119	Jan	38	Apr	54	
Chase	Nov	54	215	Jan	44	June	54	
Holladay			33	Mar	40	May	45	TVA
Sevierville	about	1950	55	May	38	Jan	49	TVA
Knoxville	old		few					
Blaineville		54	50	Feb	42	Nov	52	TVA
Mottley		54	23	"	"	"	"	
								TVA
								TVA
								TVA
								TVA

Commerce-Weather Bureau, Washington, D. C.

REPORT NO. 107

STRATEGIES FOR WATER QUALITY MONITORING

By

JABBAR K. SHERWANI
Department of Environmental Sciences and Engineering

and

DAVID H. MOREAU
Department of City and Regional Planning
and
Department of Environmental Sciences and Engineering
University of North Carolina at Chapel Hill

June 1975

Water Resources Research Institute
OF THE UNIVERSITY OF NORTH CAROLINA

UNC-WRRI-75-1Ø7

STRATEGIES FOR WATER QUALITY MONITORING

By

Jabbar K. Sherwani
Department of Environmental Sciences and Engineering

and

David H. Moreau
Department of City and Regional Planning
and
Department of Environmental Sciences and Engineering
University of North Carolina at Chapel Hill

The work upon which this publication is based was supported in part by funds provided by the Office of Water Research and Technology, Department of the Interior, through the Water Resources Research Institute of The University of North Carolina as authorized under the Water Resources Research Act of 1964, as amended.

Project No. A-065-NC
Agreement No. 14-31-0001-4033

June 1975

E.S.E. Pub. No. 398

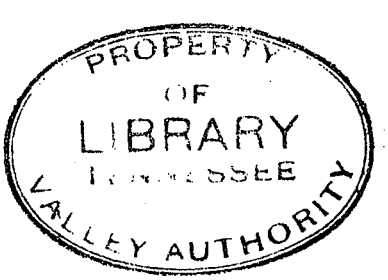

for different S.I.C. categories. An accuracy of ±10 to ±20 percent should easily be attainable. The accuracy requirements will depend on the ratio of the mass rate of flow of a constituent in the source to its mass flow in the receiving waters.

The spatial and temporal resolution of a constituent depends on the half-life of the constituent, variability of the source, response time of the stream, and the averaging period. For D.O. it has been suggested that (13)

diurnal variation	±0.5 mg/1
seasonal variation	±1-2
mean annual change	±1

The same reference gives the ability of a network to detect the long-term trend as ±20 percent.

The desired precision of estimate is also related to the extrapolation desired. The longer the extrapolation period used in predictive models, the more stringent are the accuracy requirements of the rate of change.

The adequacy of error is also related to the desired confidence level for defining the instream water quality.

3.8 Sample Size

In monitoring design, a decision must be made as to the size of the sample. Too large a sample results in wasteful use of resources, and too small a sample diminishes the utility of results. The uncertainty inherent in an estimate is related to the sample size. The larger the sample size, the more closely would the sample statistics agree with population values. However, the standard error does not decrease proportionately with the increase in sample size. One has to balance the conflicting demands of cost and accuracy.

If the sample size is increased, a more precise estimate of the population mean will be obtained for the same confidence level or the same precision will be achieved with increased confidence.

Often the population variance is not known; this must somehow be estimated. One cannot say for sure how good the selected sample size is.

The sample size will depend on the water quality parameter to be sampled. In a multi-parameter monitoring network some method for reconciling these values must be found. The chosen sample size should be evaluated to see whether it is consistent with the resources available for the monitoring program.

The sample size for a specified degree of confidence and allowable error is given by

$$n = \frac{t^2 S^2}{(\mu - \bar{x})^2} = \frac{t^2 (CV)^2}{P^2}$$

where

t is the "Student's" value for the desired confidence level,
P is the allowable departure from true mean expressed as a fraction,
$\mu - \bar{x}$ is the allowable error,
S is an estimate of the standard deviation of the population, and
CV is the coefficient of variation of the parameter.

The coefficient of variation can be estimated if the sample population distribution is known. For a normal distribution, $CV = \frac{S}{m}$ where m is the mean. For a log-normal probability distribution

$$CV = \text{Antilog } Sg - 1$$

where Sg is the geometric standard deviation.

3.9 Seasonal Variation of Parameters

The first requirement for the validity of any statistical analysis is that the data being analyzed come from a homogeneous population. An analysis of Weiss' data (6) for Haw and New Hope Rivers shows that there are significant seasonal differences in the concentration values of different parameters. The mean and standard deviation of concentration values for winter season at station HAW-5 are given in Table 15 and those for summer months in Table 16. The t-test for the difference between sample means was used for significance. The t-values show that there are significant differences for flow, temperature, pH, D.O., total carbon, total soluble carbon, ammonia-nitrogen, nitrite-nitrate nitrogen. The difference was not significant at 5 percent level for turbidity, suspended solids, conductivity, BOD, inorganic carbon, chlorophyll, orthophosphate, total phosphorus, and kjeldahl nitrogen.

The variance-ratio test to investigate whether the summer and winter sample variances are sufficiently alike showed that there were significant differences for flow, temperature, conductivity, D.O., inorganic carbon, chlorophyll, ammonia-nitrogen, nitrite-nitrate nitrogen, orthophosphorus, and total phosphorus. So the only parameters for which there is no significant

10133 Sherrill Boulevard, Suite 200
Knoxville, TN 37932
(865) 637-2810
(865) 673-8554 Fax

BWSC BARGE WAGGONER SUMNER & CANNON, INC.

MEETING NOTES

Date of Meeting: 02/11/09
Project: TVA Hydrology, BLN Units 3&4, API Calculation CDQ000020080052
Location of Meeting: TVA
Subject: RI values below 20

BWSC File No.: 3410702

PARTICIPANTS:

cc: Gary Hauser (TVA Retired), Ramon Lee (contractor), Greg Lowe (contractor), David Hunt (NSAI), Stu Henry (BWSC)

ITEMS DISCUSSED:

1. RI values below 20 are included in the FLDHYDRO code, but no values in the API lookup tables reference these values. In searching for the genesis of these values, a copy of tables showing RI values below 20 was found in TVA files dated 10-7-76 and marked 'preliminary' (see attachment). The initials of the author indicated that Gary Hauser, a TVA retiree, had produced this document.

   Discussions during a meeting with Mr. Hauser at the TVA Knoxville offices indicated that he remembered extrapolating the tables down to RI = 16 based on the delta surface runoff factor (SRF) between RI = 20 and RI = 21. Mr. Hauser was able to retrieve a copy of extrapolated tables from his personal files (see attachment). He also had a sheet labeled 10-27-76 that showed that the SRO = f(RI,SRF) curves had subsequently been curve fit using a polynomial regression equation.

2. Mr. Hauser could not remember the specific reasons for extending the curves down to RI = 16, but believed it was done to incorporate the extension of the RI and runoff values through equations instead of the look up tables into a computer code (NARFE) which was the predecessor to FLDHYDRO.

3. A review of the values in Mr. Hauser's preliminary table and the FLDHYDRO lookup table showed that the values in FLDHYDRO did not match those in the preliminary table. Apparently the values were adjusted or re-extrapolated prior to inclusion in the FLDHYDRO code.

4. Mr. Hauser did not assist in writing the FLDHYDRO code and had no knowledge about the preliminary RI extrapolation below 20 being subsequently used or adjusted.

After the meeting, a review of tables used currently by TVA River Operations showed a maximum API of 5 and minimum RI of 20 confirming that RI values below 20 are not currently in use.

Signed: _____ **Date:** 02/18/09
Ramon Lee

Signed: _____ **Date:** 02/18/09
Greg Lowe, P.E.

Signed: _____ **Date:** 02/18/09
David B. Hunt.

Signed: _____ **Date:** 02/18/09
Stuart N. Henry, P.E.

cc: Gary Hauser (via e-mail)

Extension of RAINFALL - SRO TABLES

— PRELIMINARY —

COMPUTED GEH DATE 10-7-76

CHECKED DATE

SRO (RI)	TV 16	17	18	19		SE 16	17	18	19	
0	0	7	13	18	2	42	44	46	48	2
05	05	12	19	26	2	53	56	59	62	3
10	11	19	27	35	3	60	65	70	75	5
15	17	27	35	43	3	71	77	83	89	6
20	21	31	41	51	10	81	88	95	102	7
25	27	39	50	61	11	91	99	107	115	10
30	30	42	54	66	12	105	113	121	129	9
35	38	50	62	74	12	114	123	132	141	9
40	46	58	70	82	12	123	133	143	153	10
45	54	66	78	90	12	136	146	156	166	10
50	58	72	85	98	13	144	155	166	177	11
55	65	78	91	104	13	156	167	178	189	11
60	72	85	98	111	13	164	176	188	200	12
65	75	89	103	117	14	176	188	200	212	12
70	82	96	110	124	14	187	199	211	223	12
75	89	103	117	131	14	194	207	220	233	3
80	96	110	124	138	14	~~205~~	~~218~~	231	244	
85	103	117	131	145	14	216	229	242	255	
90	110	124	138	152	14	226	239	252	265	13
95	112	127	142	157	15	232	246	260	274	14
100	123	138	153	167	15	242	256	270	284	14
105	125	140	155	170	15	251	265	279	293	
110	132	147	162	177	15	260	274	288	302	
115	138	153	168	183	15	269	283	297	311	
120	144	159	174	189	15	278	292	306	320	
125	150	165	180	195	15	286	300	314	328	14
130	157	172	187	202	15	294	308	322	336	14
135	163	178	193	208	15	297	312	327	342	15
140	169	184	199	214	15	304	319	334	349	
145	175	190	205	220	15	311	326	341	356	15
150	181	196	211	226	15	313	329	345	361	16
155	187	202	217	232	15	320	336	352	368	
160	192	207	222	237	15	327	343	359	375	
165	198	213	228	243	15	333	349	365	381	
170	204	219	234	249	15	339	355	371	387	
175	210	225	240	255	15	345	361	377	393	16
180	216	231	246	261	15	351	367	383	399	

COMPUTED GEH DATE

TV

CHECKED DATE

SRO RI	16	17	18	19		16	17	18	19	
185	222	237	252	267	15	356	372	388	404	16
190	227	242	257	272	15	357	374	391	408	17
195	233	248	263	278	15	362	379	396	413	17
200	239	254	269	284		367	384	401	418	17
205	240	256	272	288	16	372	389	406	423	
210	246	262	278	294	16	377	394	411	428	
215	252	268	284	300		382	399	416	433	
220	258	274	290	306		387	404	421	438	
223 2.78 2.94 3.10 225	264	280	296	312		391	408	425	442	17
230	269	285	301	317		393	411	429	447	18
235	275	291	307	323		398	416	434	452	
240	281	297	313	329		403	421	439	457	
245	287	303	319	335		408	426	444	462	19
250	293	309	325	341		412	430	448	466	18
255	299	315	331	347		418	436	454	472	
260	304	320	336	352		423	441	459	477	
265	309	325	341	357		428	446	464	482	
270	314	330	346	362		433	451	469	487	
275	320	336	352	368		438	456	474	492	15
280	326	342	358	374		443	461	479	497	
285	331	347	363	379		448	466	484	502	
290	337	353	369	385		453	471	489	507	
295	342	358	374	390		458	476	494	512	
300	349	365	381	397		463	481	499	517	18
305	353	369	385	401		468	486	504	522	
310	358	374	390	406		473	491	509	527	
315	363	379	395	411		478	496	514	532	
320	369	385	401	417		483	501	519	537	
325	374	390	406	422	16	488	506	524	542	18
330	375	392	409	426	17	493	511	529	547	
335	381	398	415	432		498	516	534	552	
340	386	403	420	437		503	521	539	557	
345	392	409	426	443		508	526	544	562	
350	397	414	431	448		513	531	549	567	18
355	402	419	436	453		518	536	554	572	
360	408	425	442	459		523	541	559	577	

COMPUTED GEH DATE

CHECKED DATE

TV

SF

RI / SRO	TV 16	TV 17	TV 18	TV 19	SF 16	SF 17	SF 18	SF 19
365	413	430	447	464	528	546	564	582
370	419	436	453	470	533	551	569	587
375	420	438	456	474	538	556	574	592
380	425	443	461	479	543	561	579	597
385	430	448	466	484	548	566	584	602
390	436	454	472	490	553	571	589	607
395	441	459	477	495	558	576	594	612
400	446	464	482	500	563	581	599	617
405	451	469	487	505	568	586	604	622
410	456	474	492	510	573	591	609	627
415	461	479	497	515	578	596	614	632
420	467	485	503	521	583	601	619	637
425	472	490	508	526	588	606	624	642
430	477	495	513	531	593	611	629	647
435	482	500	518	536	598	616	634	652
440	487	505	523	541	603	621	639	657
445	493	511	529	547	608	626	644	662
450	498	516	534	552	613	631	649	667
455	503	521	539	557	618	636	654	672
460	508	526	544	562	623	641	659	677
465	509	528	547	566	628	646	664	682
470	514	533	552	571	633	651	669	687
475	519	538	557	576	638	656	674	692
480	524	543	562	581	643	661	679	697
485	529	548	567	586	648	666	684	702
490	534	553	572	591	653	671	689	707
495	540	559	578	597	658	676	694	712
500	545	564	583	602	663	681	699	717
505	550	569	588	607	668	686	704	722
510	556	575	594	613	673	691	709	727
515	561	580	599	618	678	696	714	732
520	566	585	604	623	683	701	719	737
525	571	590	609	628	688	706	724	742
530	576	595	614	633	693	711	729	747
535	581	600	619	638	698	716	734	752
540	585	605	624	643	703	721	739	757

COMPUTED GEH DATE

TV

SF CKED DATE

SRO RI	16	17	18	19		16	17	18	19	
545	591	610	629	648		708	726	744	762	
550	596	615	634	653	19	713	731	749	767	
555	601	620	639	658		718	736	754	772	
560	606	625	644	663		723	741	759	777	
565	611	630	649	668		728	746	764	782	
570	616	635	654	673		733	751	769	787	
575	621	640	659	678		738	756	774	792	
580	626	645	664	683		743	761	779	797	
585	631	650	669	688		748	766	784	802	
590	636	655	674	693		753	771	789	807	
595	641	660	679	698		758	776	794	812	
600	646	665	684	703	19	763	781	799	817	18
Max Basin Recharge	47	66	85	103						

SHEET ____ OF ____

EAST API vs RI Tables

Equation Coefficients : $RI = a_0 + a_1(API) + a_2(API)^2 + a_3(API)^3 + a_4(API)^4 + a_5(API)^5$

COMPUTED GEH DATE 10-28-76

CHECKED DATE

	1	2-11	12	13	14	15	16	17	18	19	20	21	22	23
a_0	31.373291	31.373291	32.395020	33.575439	36.353271	39.961182	41.426270	43.725342	46.501953	49.488770	51.639160	54.066406	57.616943	60.775391
a_1	-4.481201	-4.481201	-4.854736	-4.715410	-7.507813	-10.968750	-11.550781	-14.058594	-17.230461	-21.191406	-23.542969	-22.699219	-24.335938	-26.307813
a_2	1.140625	1.140625	1.200928	.988281	2.296875	3.781250	3.773438	5.132813	6.757813	9.066406	10.382813	8.265625	7.796875	8.410156
a_3	-.123596	-.123596	-.127655	-.090515	-.376221	-.637939	-.594971	-0.926758	-1.286621	-1.857646	-2.162109	-1.399170	-1.090557	-1.153588
a_4	0	0	0	0	.022034	.037598	.031677	.060944	.088226	.134338	.163788	.085022	.044632	.049973
a_5	0	0	0	0	0	0	0	0	0	0	0	0	0	0

	24	25	26	27	28	29	30-40	41 (Initial Guess from Curve entry plot)	42	43	44	45	46	47
a_0	65.585400	68.777852	71.697266				71.697266	69.818115	66.406782	62.542236	59.277588	56.316650	53.613867	50.073013
a_1	-30.722656	-34.500000	-36.722656				-36.722656	-37.128906	-36.66045	-33.624219	-31.227051	-29.790039	-27.198975	-24.210938
a_2	11.597656	11.597656	12.082031	same	same	same	12.082031	12.370625	14.500000	13.667969	12.665283	12.500000	11.601563	10.046875
a_3	-1.650685	-1.694336	-1.681152				-1.681152	-2.159912	-2.617676	-2.536865	-2.374512	-2.410645	-2.306152	-1.929199
a_4	.085663	.091604	.073425				.073425	.123601	.171875	.170792	.163315	.169006	.168610	.135254
a_5	0	0	0	0	0	0	0	0	0	0	0	0	0	0

	48	49	50	51	52
a_0	47.811635	45.255127	42.59032	36.999512	31.373291
a_1	-23.203125	-21.468714	-18.968750	-12.156250	-4.481201
a_2	10.235039	9.762451	8.607375	5.171875	1.140625
a_3	-2.107178	-2.076172	-1.801025	-1.029297	-.123596
a_4	.158569	.161224	.135406	.072418	0
a_5	0	0	0	0	0

TV RI Tables

Equation Coefficients : $\Sigma SRO = a_0 + a_1(\Sigma RF) + a_2(\Sigma RF)^2 + a_3(\Sigma RF)^3$

COMPUTED GEH DATE 10-27-76

	16	17	18	19	20	21	22	23	24	25	26	27	28	29
a_0	.048874	-.021988	-.076589	-.111084	-.164063	-.197021	-.226563	-.226318	-.225342	-.221680	-.220947	-.223877	-.229736	-.230957
a_1	.730713	.693848	.642311	.573242	.546631	.499268	.458984	.404053	.359387	.312012	.278564	.251709	.229248	.206543
a_2	.043747	.048065	.056229	.069855	.069214	.073685	.075500	.082169	.086166	.090195	.091003	.090057	.088303	.086607
a_3	-.002127	-.002378	-.002976	-.003784	-.003736	-.003844	-.003752	-.004066	-.004215	-.004341	-.004224	-.004032	-.003752	-.003547

	30	31	32	33	34	35	36	37	38	39	40	41	42	43
a_0	-.231445	-.235348	-.232412	-.217041	-.207520	-.200195	-.169678	-.156738	-.129150	-.119873	-.085449	-.085693	-.078857	-.078125
a_1	.186035	.164307	.146729	.127197	.108154	.094238	.061523	.045410	.018555	.007568	-.019531	-.018066	-.024170	-.023193
a_2	.085526	.083968	.081680	.079910	.078430	.076431	.077057	.074783	.074639	.071777	.071899	.067764	.065185	.064117
a_3	-.003256	-.003136	-.002893	-.002679	-.002526	-.002343	-.002287	-.002073	-.002006	-.001722	-.001728	-.001463	-.001301	-.001097

	44	45	46	47	48	49	50	51	52	53	54	55	56	57
							→ Begin use of 2nd order equation. Judged better fit by plotting.							
a_0	-.082520	-.084229	-.086182	-.088379	-.105713	-.102295	-.107651	-.087280	-.070053	-.051453	-.023193	-.002197	.023193	.043701
a_1	-.020264	-.019287	-.016357	-.014893	-.003662	-.004639	-.000427	-.012192	-.023178	-.033447	-.046829	-.057114	-.068619	-.079117
a_2	.057692	.054276	.050827	.047928	.043488	.041275	.038714	.038510	.038312	.038054	.038016	.037780	.037636	.037440
a_3	-.000678	-.000718	-.000544	-.000411	-.000207	-.000119	0	0	0	0	0	0	0	0

	58	59	60	61	62	63	64	65	66	67	68	69	70
a_0	.063477	.089158	.107910	.132813	.159668	.190918	.215088	.244141	.273682	.308105	.334717	.373779	.406982
a_1	-.086960	-.096512	-.105347	-.115479	-.125763	-.136902	-.145554	-.155533	-.164703	-.175369	-.183182	-.194000	-.203110
a_2	.037079	.036857	.036619	.036427	.036259	.036157	.035918	.035755	.035548	.035454	.035197	.035109	.034952
a_3	0	0	0	0	0	0	0	0	0	0	0	0	

SHEET ____ OF ____

SE Tables

Equation Coefficients: $\Sigma SRO = a_0 + a_1(\Sigma RF) + a_2(\Sigma RF)^2 + a_3(\Sigma RF)^3$

COMPUTED GEH DATE 10-27-76

CHECKED DATE

	16	17	18	RUNOFF 19	20	21	22	INDEX 23	24	25	26	27	28	29
a_0	.100586	.131592	.155518	.186035	.205322	.223877	.260254	.288574	.290293	.289063	.282227	.261230	.240723	.187256
a_1	-.034912	-.090820	-.132324	-.175049	-.199707	-.221436	-.266357	-.289795	-.273809	-.274414	-.257568	-.229492	-.199951	-.143799
a_2	.196396	.195999	.192444	.189301	.182617	.175751	.176300	.170502	.156555	.145569	.133820	.118820	.105209	.087112
a_3	-.011926	-.011361	-.010566	-.009909	-.009057	-.008207	-.007977	-.007305	-.006149	-.005268	-.004439	-.003432	-.002555	-.001524

	30	31	32	33	34	35	36	37	38	39	40	41	42	43
a_0														
a_1														
a_2														
a_3														

	44	45	46	47	48	49	50
a_0							
a_1							
a_2							
a_3							

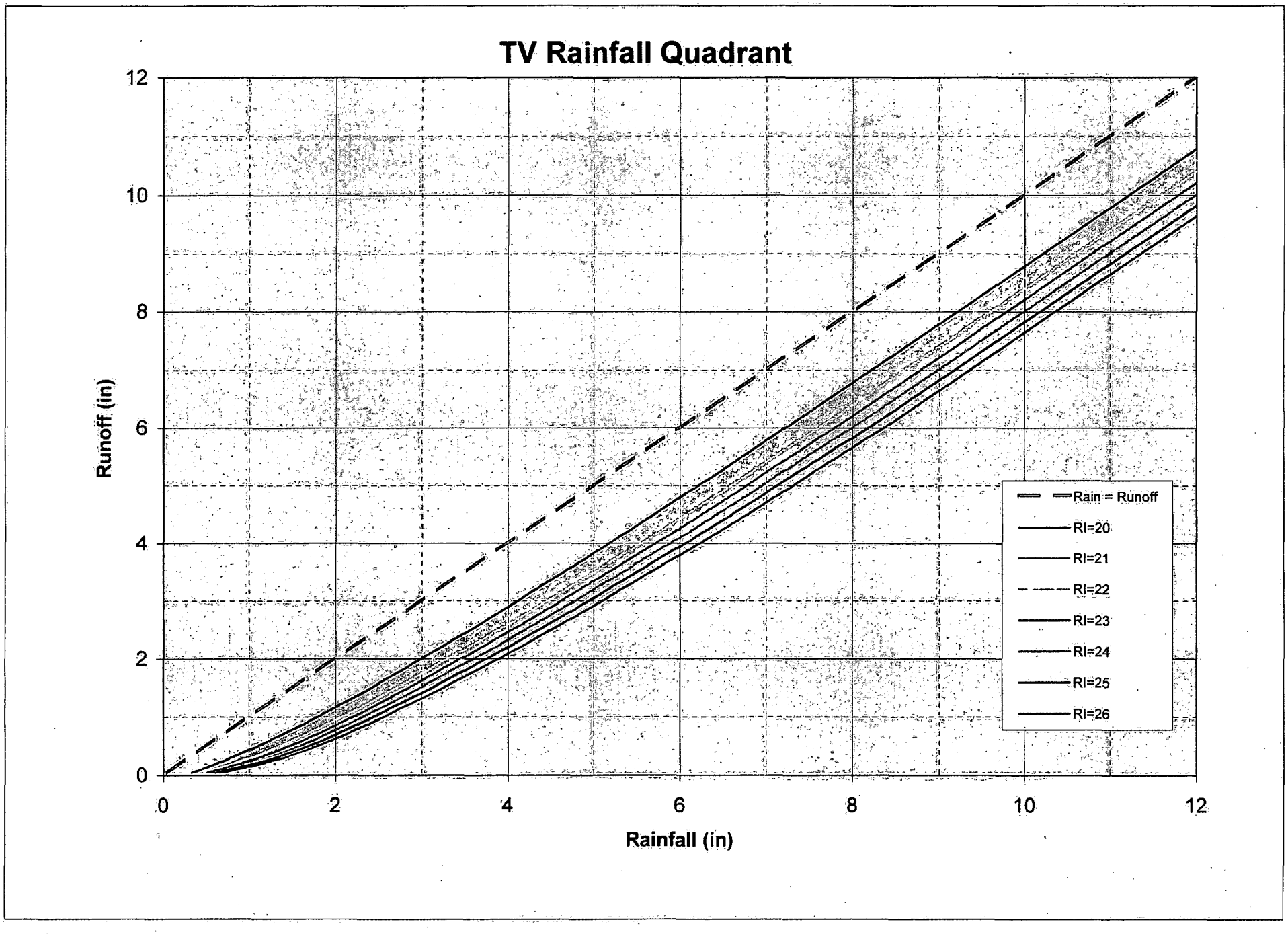
TV Rainfall Quadrant
Runoff (in)
Rainfall (in)
0
2
4
6
8
10
12
Rain = Runoff
RI=20
RI=21
RI=22
RI=23
RI=24
RI=25
RI=26

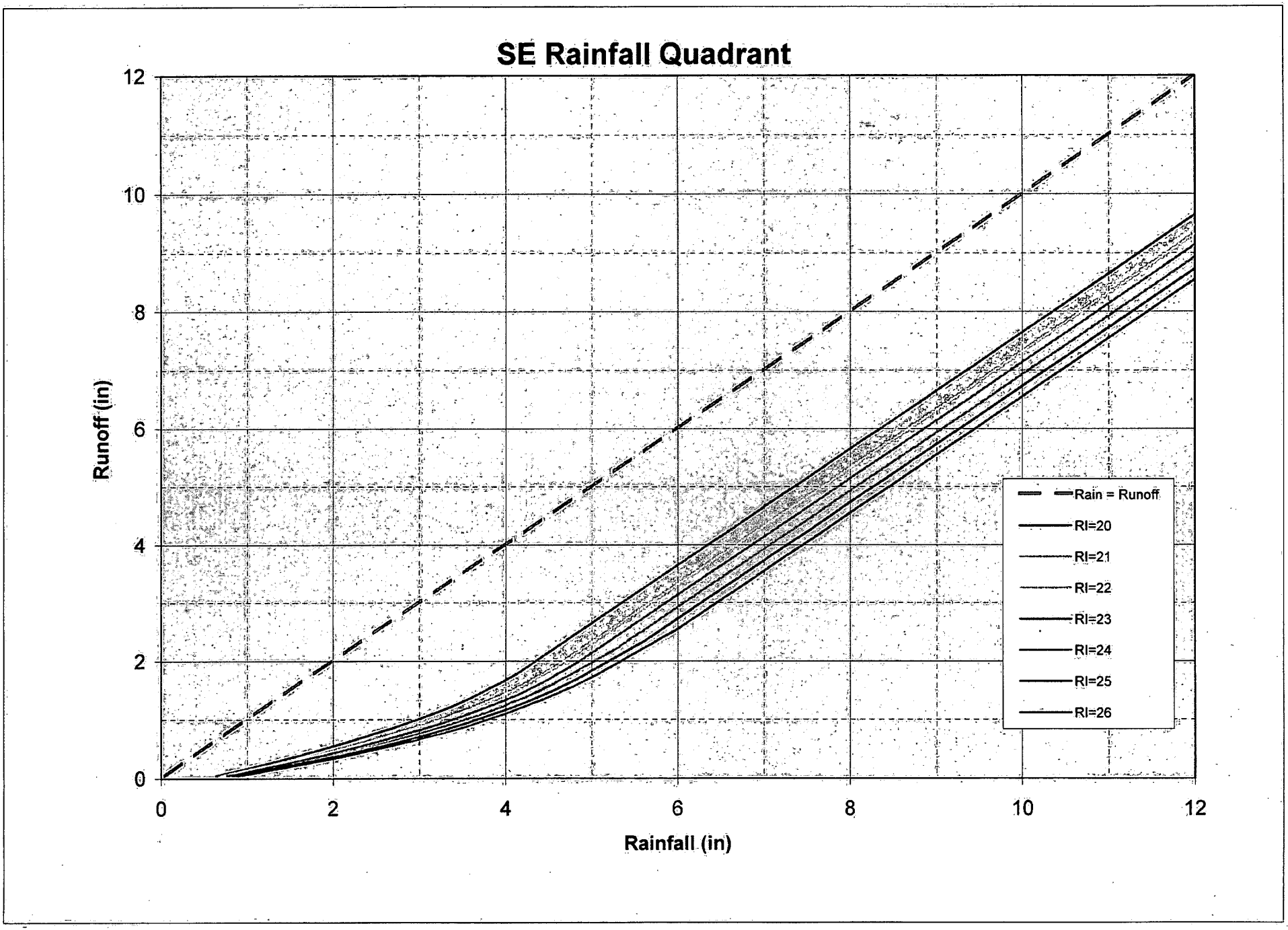
SE Rainfall Quadrant
Runoff (in)
Rainfall (in)
0
2
4
6
8
10
12
Rain = Runoff
RI=20
RI=21
RI=22
RI=23
RI=24
RI=25
RI=26

L58 090325 800

Bellefonte Units 3 and 4
Hydrology Project
Request For Information (RFI)
Response Information Continuation Sheet

RFI Number:	BE21146056B028	Rev. 0	Page 1 of 2

This provides initial PMP data for the 5 subbasins (French Broad River at Asheville, unit area 1; Nolichucky River at Embreeville, unit area 4; Norris Dam, unit area 26; South Chickamauga Creek near Chattanooga, unit area 46; and Sequatchie River at Whitwell, unit area 48) used in the comparison of different rainfall runoff methods. This initial PMP data was used in the original BLN study and was manually determined by planimetering. For the current BLN study the PMP is being determined using GIS procedures and minor differences are expected.

The PMP rainfall defined in HMR-41 is a nine-day event consisting of a 3-day antecedent storm, a three-day dry period, and a 3-day main storm. The 3-day antecedent storm is 40 percent of the main storm and is postulated to occur evenly over the watershed above Guntersville.

The attached table provides the antecedent and main storm rainfall for the 5 subbasins together with the adopted time distribution.

References:	TVA calculation CDQ000020080052 Data Source – TVA file book 254-10 2, Book 1, Bellefonte Design Floods, March 21,400 Square Mile PMF located in Chattanooga, Nuclear Power Group (NPG) - Document Control Records Management (DCRM).
Prepared By / Date:	Thomas A Fee 3/24/09
Checked By / Date:	Susan Barksdale 3/25/09
Approved For Use TVA Project Engineer	03/25/2009

Bellefonte Units 3 and 4
Hydrology Project
Request For Information (RFI)
Response Information Continuation Sheet

RFI Number:	BE21146056B028	Rev. 0	Page 2 of 2

6-Hour Period	Rainfall, Inches Antecedent Storm	Unit Area 1	Unit Area 4	Unit Area 26	Unit Area 46	Unit Area 48
1	.16	→ Antecedent rainfall distributed evenly over the total watershed above Guntersville				
2	.18					
3	.21					
4	.22					
5	1.05					
6	2.02					
7	.69					
8	.56					
9	.43					
10	.36					
11	.29					
12	.27					
13-24	3-day dry period					
25	Main Storm →	.40	.40	.40	.40	.30
26		.40	.40	.40	.40	.30
27		.60	.50	.50	.40	.40
28		.60	.60	.50	.50	.40
29		2.80	2.60	2.40	2.20	1.70
30		5.40	4.20	3.80	3.00	1.80
31		1.90	1.70	1.60	1.50	1.30
32		1.50	1.30	1.20	1.10	1.00
33		1.20	1.10	1.00	.90	.80
34		1.00	.80	.80	.80	.70
35		.80	.80	.60	.60	.50
36		.80	.70	.60	.50	.60

REQUEST FOR INFORMATION (RFI)

BLN Hydrology Support

RFI NUMBER: BE21146056B028		**DATE:** 19 March 2009
PREPARED BY: Stuart Henry/BWSC		**PHONE/FAX:**
TO: Perry Maddux, TVA	**cc:** Greg Lowe, Ramon Lee	
REFERENCE DRAWING(S):		**REV.:**
PROJECT DOCUMENTS:		**REV.:**

INFORMATION REQUESTED:

Please provide the following for development of the API and Rain Runoff Relationship for the Tennessee River Watershed (CDQ00020080052):

- Preliminary PMP rainfall data for use in rainfall runoff calculation comparison. Data is not for use in final controlling calculations Data shall include time step and rainfall in inches for the HMR-41 9-day event.

RESPONSE REQUIRED BY: 25 March 2009

ASSUMPTIONS:

IMPACTS: Information is input to API calc Cannot release revised calc until resolved.

WORK STATUS: **CONTINUING:** ☒ **STOP:** ☐

APPROVED FOR ISSUANCE TO TVA:

Carried Stokes **DATE:** 03-19-2009

United States
Department of
Agriculture

**Natural
Resources
Conservation
Service**

Part 630 Hydrology
National Engineering Handbook

Chapter 10 Estimation of Direct Runoff from Storm Rainfall

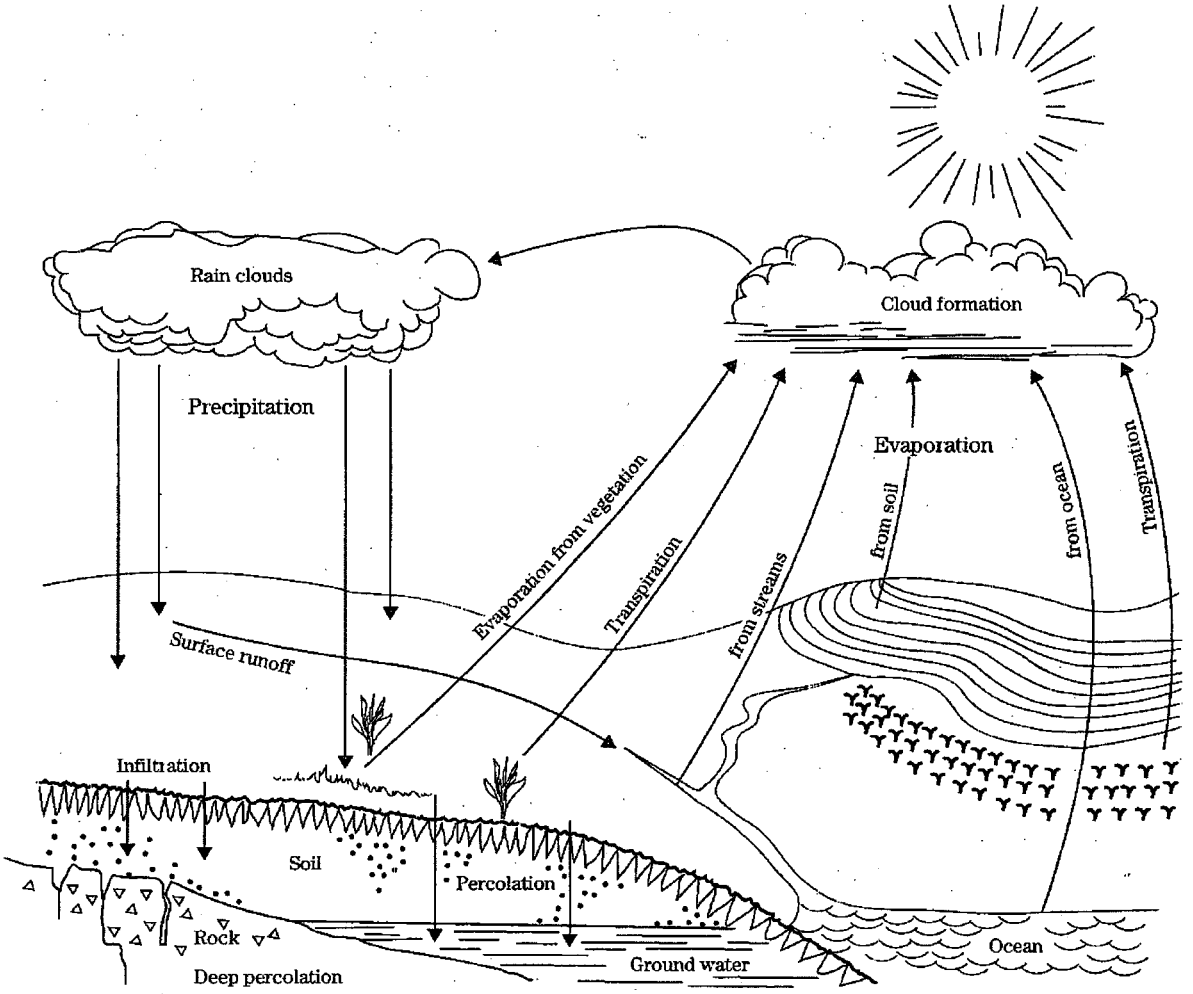

Table 10–1 Curve numbers (CN) and constants for the case $I_a = 0.2S$

1	2	3	4	5	1	2	3	4	5
CN for ARC II	--CN for ARC-- I	III	S values* (in)	Curve* starts where P = (in)	CN for ARC II	--CN for ARC-- I	III	S values* (in)	Curve* starts where P = (in)
100	100	100	0	0	60	40	78	6.67	1.33
99	97	100	.101	.02	59	39	77	6.95	1.39
98	94	99	.204	.04	58	38	76	7.24	1.45
97	91	99	.309	.06	57	37	75	7.54	1.51
96	89	99	.417	.08	56	36	75	7.86	1.57
95	87	98	.526	.11	55	35	74	8.18	1.64
94	85	98	.638	.13	54	34	73	8.52	1.70
93	83	98	.753	.15	53	33	72	8.87	1.77
92	81	97	.870	.17	52	32	71	9.23	1.85
91	80	97	.989	.20	51	31	70	9.61	1.92
90	78	96	1.11	.22	50	31	70	10.0	2.00
89	76	96	1.24	.25	49	30	69	10.4	2.08
88	75	95	1.36	.27	48	29	68	10.8	2.16
87	73	95	1.49	.30	47	28	67	11.3	2.26
86	72	94	1.63	.33	46	27	66	11.7	2.34
85	70	94	1.76	.35	45	26	65	12.2	2.44
84	68	93	1.90	.38	44	25	64	12.7	2.54
83	67	93	2.05	.41	43	25	63	13.2	2.64
82	66	92	2.20	.44	42	24	62	13.8	2.76
81	64	92	2.34	.47	41	23	61	14.4	2.88
80	63	91	2.50	.50	40	22	60	15.0	3.00
79	62	91	2.66	.53	39	21	59	15.6	3.12
78	60	90	2.82	.56	38	21	58	16.3	3.26
77	59	89	2.99	.60	37	20	57	17.0	3.40
76	58	89	3.16	.63	36	19	56	17.8	3.56
75	57	88	3.33	.67	35	18	55	18.6	3.72
74	55	88	3.51	.70	34	18	54	19.4	3.88
73	54	87	3.70	.74	33	17	53	20.3	4.06
72	53	86	3.89	.78	32	16	52	21.2	4.24
71	52	86	4.08	.82	31	16	51	22.2	4.44
70	51	85	4.28	.86	30	15	50	23.3	4.66
69	50	84	4.49	.90	25	12	43	30.0	6.00
68	48	84	4.70	.94	20	9	37	40.0	8.00
67	47	83	4.92	.98	15	6	30	56.7	11.34
66	46	82	5.15	1.03	10	4	22	90.0	18.00
65	45	82	5.38	1.08	5	2	13	190.0	38.00
64	44	81	5.62	1.12	0	0	0	infinity	infinity
63	43	80	5.87	1.17					
62	42	79	6.13	1.23					
61	41	78	6.39	1.28					

* For CN in column 1